Iowa Research Online
The University of Iowa's Institutional Repository

University of Iowa
Iowa Research Online

Theses and Dissertations

Summer 2016

Reactivation of Organophosphorus agent inhibited-human acetylcholinesterase

Sumana Nilahthi Yasapala
University of Iowa

Copyright 2016 Sumana Nilanthi Yasapala

This dissertation is available at Iowa Research Online: http://ir.uiowa.edu/etd/2169

Recommended Citation
Yasapala, Sumana Nilahthi. "Reactivation of Organophosphorus agent inhibited-human acetylcholinesterase." PhD (Doctor of Philosophy) thesis, University of Iowa, 2016.
http://ir.uiowa.edu/etd/2169.

Follow this and additional works at: http://ir.uiowa.edu/etd

Part of the Chemistry Commons

REACTIVATION OF ORGANOPHOSPHORUS AGENT INHIBITED-HUMAN ACETYLCHOLINESTERASE

by

Sumana Nilanthi Yasapala

A thesis submitted in partial fulfillment
of the requirements for the Doctor of Philosophy
degree in Chemistry in the
Graduate College of
The University of Iowa

August 2016

Thesis Supervisor: Professor Daniel M. Quinn

Copyright by

Sumana Nilanthi Yasapala

2016

All Rights Reserved

Graduate College
The University of Iowa
Iowa City, Iowa

CERTIFICATE OF APPROVAL

PH.D. THESIS

This is to certify that the Ph.D. thesis of

Sumana Nilanthi Yasapala

has been approved by the Examining Committee for
the thesis requirement for the Doctor of Philosophy degree
in Chemistry at the August 2016 graduation.

Thesis Committee: _____
Daniel M. Quinn, Thesis Supervisor

_____
Amnon Kohen

_____
Alexei V. Tivanski

_____
Mishtu Dey

_____
Robert J. Kerns

To my loving family…….

ACKNOWLEDGEMENTS

First and foremost I would like to thank my research advisor Professor Daniel M. Quinn for his kind and invaluable guidance throughout my graduate carrier in University of Iowa. Next my thanks should go to the past and present Quinn group members for their numerous help and creating a pleasant working environment. Special thanks should go to Dr. Joseph Topczewski who gave me a solid foundation in research.

I would like to convey my thanks to all technical and administrative staff at the department of chemistry, University of Iowa for their support and encouragement during this journey Further, I would like to thank to faculty and staff at University of Kelaniya, and Central colege, Anuradhapura for giving me a solid start to my education career.

My heartiest gratitude should go to my loving parents, sister, brothers and all my friends for their numerous help, giving me courage and strength. I would like to convey my special thanks to my beloved husband, Sanjeewa Rasika Karunathilaka who encouraged me to start my graduate studies and giving his blessings to make it success. Finally, I would like to thank my loving little daughter Dinali Adhya Karunathilaka, for her sacrifice.

ABSTRACT

Organophosphorus compounds (OPs) are used as pesticides, e.g. parathion, which is converted in the body to paraoxon, and chemical warfare nerve agents, such as sarin, soman, cyclosarin, VX, and tabun. Even small amounts of OP exposure can be fatal, depending on the toxicity of the compound. Great stocks of highly toxic chemical warfare nerve agents exit around the world and are considered a serious threat to national security and international stability.

OPs exert their toxicity by covalent irreversible inhibition of acetylcholinesterase (AChE) that prevents the enzyme from hydrolyzing acetylcholine (ACh), a neurotransmitter in the central and peripheral nervous systems (CNS and PNS). Therefore, ACh accumulates in the cholinergic synapses throughout the body, which results in overstimulation of the ACh receptors. Removal of the phosphyl moiety from the OP-bound AChE active site has been a promising method to restore AChE's catalytic activity. However, a secondary process called aging also occurs in the OP-AChE complex. Once aging occurs, currently available oximes are ineffective in removing the phosphyl moiety from the enzyme's active site, and hence are ineffective as antidotes against the aged enzyme.

Several families of alkylating and acylating agents including several classes of agents that combine alkylating moieties with known active site or peripheral cite (PAS) binding motifs were synthesized and evaluated. The general aim of the research was that successful alkylation or acylation of the phosphonate monoanion of aged AChE would produce neutral phosphyl complexes that would either spontaneously reactivate or would be reactivatable in the presence of oxime antidotes.

Methoxylamine analogs of the oxime antidote 2-PAM were synthesized with the aim that methyl transfer to the aged AChE adduct would produce a neutral phosphyl AChE adduct

simultaneously with 2-PAM *in situ*, and subsequent 2-PAM nucleophilic attack would reactivate the newly formed neutral phosphyl-AChE adduct. However, none of these 2-PAM analogs resurrected the activity of aged AChE.

Another strategy for resurrecting the activity of aged AChE utilizes N-methylpyridiniums that are substituted at the 2-position with a beta-lactam moiety. For these compounds, opening of the electrophilic beta-lactam unmasks a nucleophilic amidine function which could putatively attack at phosphorus to expel the free enzyme. For this class of agents, only the active site directed compound that possessed the 5-CF_3 substituent showed possible resurrection of the activity of aged AChE, though activities in both the control and treated samples were low.

Methyl transfers are common in Nature, and the natural transfer agent is S-adenosylmethionine, a sulfonium methyl donor. Consequently, the array of sulfonium compounds were evaluated on the expectation that they would bind to the AChE active site and transfer a methyl group to the phosphonate monoanion of the aged enzyme. Though high-affinity binding was noted for these compounds, none of these resurrected the activity of the aged AChE complex.

Finally, several selected agents were evaluated on reactivating the initial OP-AChE complex before aging has occurred. It was observed that degraded samples of selected inhibitors are capable of reactivating initial complexes of sarin and soman inhibited AChE at low concentration that is an important character of efficient reactivators. However, the structure of reactivator is still unknown.

Two major challenges still face researchers in the quest to design effective medicinal agents for counteracting poisoning by AChE-inhibiting nerve agents. The first is that there is no universal oxime antidote. Oximes that are effective against certain nerve agents are ineffective against

others. The second is that, despite extensive efforts that span two generations, aged phosphyl-AChE adducts have never been reactivated. However, given the powerful tools of modern structural biology, medicinal chemistry and molecular biology, there is still hope that these considerable challenges can be met.

PUBLIC ABSTRACT

Organophosphorus compounds (OPs) are used as pesticides, e.g. parathion, which is converted in the body to paraoxon, and chemical warfare nerve agents, such as sarin, soman, cyclosarin, VX, and tabun. Even small amounts of OP exposure can be fatal, depending on the toxicity of the compound. Great stocks of highly toxic chemical warfare nerve agents exit around the world and are considered a serious threat to national security and international stability.

OPs exert their toxicity by covalent irreversible inhibition of acetylcholinesterase (AChE) that prevents the enzyme from hydrolyzing acetylcholine (ACh), a neurotransmitter in the central and peripheral nervous systems (CNS and PNS). Therefore, ACh accumulates in the cholinergic synapses throughout the body, which results in overstimulation of the ACh receptors. Removal of the phosphyl moiety from the OP-bound AChE active site has been a promising method to restore AChE's catalytic activity. However, a secondary process called aging also occurs in the OP-AChE complex. Once aging occurs, currently available oximes are ineffective in removing the phosphyl moiety from the enzyme's active site, and hence are ineffective as antidotes against the aged enzyme.

Herein, several families of inhibitors to resurrect the aged enzyme were synthesized and kinetically evaluated. None of the inhibitors were able to resurrect the aged AChE. However, some inhibitors in these families were able to reactivate the initial complex of the sarin and soman inhibited AChE.

TABLE OF CONTENTS

LIST OF TABLES…….....x

LIST OF FIGURES…….....xi

LIST OF SCHEMES…….....xviii

LIST OF EQUATIONS……xix

CHAPTER 1: REACTIVATION OF ORGANOPHOSPHORUS NERVE AGENT INHIBITED ACETYLCHOLINESTERASE 1

Introduction ..... ……..1

Importance of Acetylcholinesterase 2

AChE Structure 4

AChE Catalytic Mechanism 8

CHAPTER 2: SYNTHESIS AND KINETIC EVALUATION OF 2-PYRIDINE ALDOXIME METHYL HALIDE (2-PAM) ANALOGS AS NOVEL ALKYLATING AGENTS OF AGED HUMAN ACETYLCHOLINESTERASE 44

Chemical Mechanism and Significance 44

Objective of the Study 48

Materials and Methods 49

Results and Discussion 59

Conclution 1…….....……69

Conclusion 2 73

CHAPTER 3: EVALUATION OF N-METHYL PYRIDINIUM β-LACTAM COMPOUNDS AS SUICIDE INHIBITORS OF HUMAN ACETYLCHOLINESTERASE 74

Chemical Mechanism and Significance 74

Objectives of the Study 75

Materials and Methods 76

Results and Discussion 80

Conclusion 92

CHAPTER 4: SULFONIUM SPECIES AS REVERSIBLE INHIBITORS OF HUMAN ACETYLCHOLINESTERASE 93

Chemical Mechanism and Significance 93

Objectives of the Study 94

Materials and Methods 94

Results and Discussion 98

Conclusion 103

CHAPTER 5: UNKNOWN REACTIVATOR OF HUMAN ACETYLCHOLINESTERASE INHIBITED BY ORGANOPHOSPHOROUS AGENTS 104

Chemical Mechanism and Significance 104

Objectives of the Study 106

Materials and Methods 108

Results and Discussion 110

Conclusion 128

FUTURE WORKS 129

APPENDIX A 131

APPENDIX B 160

APPENDIX C 175

REFERENCES 180

LIST OF TABLES

Table 1.1: Kinetic data for major nerve agents and the pesticide paraxon.....18

Table 1.2: Kinetic data for oxime reactivators 29

Table 2.1: Half inhibitory concentrations at 0 hour and after 2 hour incubation with AChE 66

Table 2.2: IC_{50} values for inhibitors 2 and 3 over 7 hour period.....67

Table 3.1: Hydrolytic stability data for all β-lactam inhibitors 84

Table 3.2: IC_{50} values obtained over several hours for β-lactam inhibitors 86

Table 4.1: Dimethylsulfonium inhibitors of human Acetylcholinesterase.....99

Table 4.2: Docking results for Inhibitors 7 and 8.....101

Table 5.1 : Half- maximal inhibitory concentration 112

LIST OF FIGURES

Figure 1.1: Chemical structures of some toxic OP pesticides and warfare nerve agents 3

Figure 1.2: 3-D structure of native *Torpedo Californica* Acetylcholinsterase 5

Figure 1.3: Schematic representation of the active site gorge of AChE 6

Figure 1.4: AChE catalytic mechanism 9

Figure 1.5: Some reversible AChE inhibitors use in medicinal chemistry..... 13

Figure 1.6: AChE phosphylation by a nerve agent R, R'-alkyl groups, and X^- leaving group… 15

Figure 1.7: Nucleophilic reactivation of phosphylated AChE by oxime e.g. 2-PAM 16

Figure 1.8: Aging process of soman inhibited AChE 17

Figure 1.9: Some oxime reactivators that are in clinical use for OP intoxication worldwide 21

Figure 1.10: Chemical structures of the ligands that formed complexes with soman-aged BChE. ……..35

Figure 1.11: Crystalographic structures showing the active site of soman-aged human butyrylcholinesterase in complex with 2-PAM..... 36

Figure 1.12: Putative sulfonium reactivators of aged AChE 37

Figure 1.13: Methoxylamine analogs of 2-PAM as aged AChE reactivating agents 38

Figure 1.14: Pyridinium β-Lactams as aged AChE reactivating agents..... 40

Figure 1.15: Epoxide substituted N-Methylpyridiniums as aged AChE reactivating agents 41

Figure 1.16: Methoxypyridinium compounds as aged AChE reactivating agents studied in our research group 43

Figure 2.1: Crystallographic structure of *Torpedo Californica* AChE that has been by soman phosphylated nerve agent (non-aged AChE adduct). 45

Figure 2.2: Crystallographic structure of the aged conjugate of *Torpedo Californica* AChE and the soman nerve agent 46

Figure 2.3: Crystallographic structure of the complex of 2-PAM with the aged conjugate of *Torpedo Californica* AChE and the soman nerve agent 48

Figure 2.4: Sample graph showing time courses of the enzymatic substrate hydrolysis..... 54

Figure 2.5: Example for IC_{50} curve obtained for inhibitor 4 at zero hour time point after incubation with hAChE 65

Figure 2.6: Plot of stop time assay for inhibitor 2 (1µM) for determination of pseudo first-order rate constant 68

Figure 2.7: Chemical structure of monoisonitrosoacetone (MINA)..... 70

Figure 2.8: Chemical structures of the inhibitors used for reactivation of aged AChE for the MINA experiment 71

Figure 3.1: Initial rates of substrate hydrolysis by hAChE in the presence of different concentrations of inhibitor 1 as a function of time..... 87

Figure 3.2: Full time course for substrate hydrolysis by hAChE in the presence of Inhibitor 4. . 88

Figure 3.3: Rate (constructed from figure 3.2) as a function of time for substrate hydrolysis reaction by hAChE in the presence of inhibitor 4 88

Figure 3.4: Plot of continuous assays in the presence of inhibitor 4 at different concentrations and in the absence of inhibitor 4 (control). 89

Figure 3.5: Rates of the substrate hydrolysis reaction by hAChE in the presence of inhibitor 4. 90

Figure 4.1: Dose response curve for Inhibitor 1 97

Figure 4.2: Highest affinity poses for the R/ S enantiomers of inhibitor 7 docked in crystal structure of AChE. 102

Figure 4.3: Highest affinity poses for the R/ S enantiomers of inhibitor 8 docked in crystal structure of AChE 102

Figure 5.1: Chemical structures of some selected aging delaying agents used in this study..... 107

Figure 5.2: Stop-time assay plot for determination of pseudo first-order rate constant for soman analog…….110

Figure 5.3: Oxime-induced (2-PAM) reactivated enzyme activity as a function of time to determine extent of aging for soman analog. 111

Figure 5.4: Plots of the percentage of oxime-induced reactivated sarin inhibited hAChE against incubation time with inhibitors A,B, and C……...…..…113

Figure 5.5: Plots of the percentage of oxime-induced reactivated sarin-inhibited hAChE against incubation time with inhibitors D,E, and F……...……..…..114

Figure 5.6: Plots of the percentage of oxime-induced reactivated soman-inhibited hAChE against incubation time with inhibitors D, E, and F……...……..114

Figure 5.7: Plots of the percentage of non-oxime-induced reactivated sarin-inhibited hAChE against incubation time with the Inhibitors D, E, and F……..115

Figure 5.8: Plots of the percentage of non-oxime reactivated soman-inhibited hAChE against incubation time with inhibitors D, E and F..... 115

Figure 5.9: Oxime-induced reactivation kinetics of sarin-inhibited (Top) and soman-inhibited (Bottom) hAChE by fresh solutions of inhibitors E and F…….117

Figure 5.10: Non-oxime- induced reactivation kinetics of sarin (Top) and soman (Bottom) inhibited hAChE by fresh solutions of inhibitors E and F. 118

Figure 5.11: UV spectra for fresh and old solutions of inhibitors E and F..... 119

Figure 5.12: Oxime-induced (Left) and non-oxime-induced (Right) reactivation of soman-inhibited hAChE by degraded sample of inhibitor E. 119

Figure 5.13: Chemical structures of pyridone products of Inhibitors D, E, and F..... 120

Figure 5.14: Efects of pyridone products of inhibitor D (D'), E (E'), and F (F') on hAChE inhibited by the sarin analog. 121

Figure 5.15: Oxime-induced (Top) and non-oxime-induced (Bottom) reactivations of soman-inhibited hAChE by pyridone products of inhibitor D (D'), E (E'), and F(F')..... 122

Figure 5.16: Oxime induced (Left) and non oxime induced (Right) reactivation of soman-inhibited hAChE by different concentrations of pyridone product of inhibitor D.. 123

Figure 5.17: Chemical structure of starting material of inhibitor D (G)..... 123

Figure 5.18: Oxime-induced (Left) and non-oxime-induced (Right) reactivations of soman-inhibited hAChE by starting material of inhibitor E..... 124

Figure 5.19: Chemical structure of inhibitor H..... 124

Figure 5.20: Chemical structures that can be found in the solution of inhibitor H..... 125

Figure 5.21: Oxime-induced reactivation of sarin-inhibited hAChE by solution of inhibitor H 125

Figure 5.22: Chemical structures of fluorine-substituted methoxy group containing inhibitors.126

Figure 5.23: Oxime-induced (Top) and non-oxime-induced (Bottom) reactivations of sarin-inhibited hAChE by old-frozen samples of inhibitors J and K. 126

Figure 5.24: Oxime-induced (Left) and non-oxime-induced (Right) reactivations of sarin-inhibited hAChE by one year old degraded sample of inhibitor E. 127

Figure A.1: 500 MHz ^{1}H NMR spectrum in $CDCl_3$ 131

Figure A.2: 100 MHz ^{13}C NMR spectrum in $CDCl_3$ 132

Figure A.3: 500 MHz ^{1}H NMR spectrum in Acetone 133

Figure A.4: 500 MHz ^{1}H NMR spectrum in $CDCl_3$ 134

Figure A.5: 100 MHz ^{13}C NMR spectrum in $CDCl_3$ 135

Figure A.6: 477 MHz ^{19}F NMR spectrum in $CDCl_3$ 136

Figure A.7: 500 MHz ^{1}H NMR spectrum in Acetone 137

Figure A.8: 500 MHz ^{1}H NMR spectrum in Acetone 138

Figure A.9: 477 MHz ^{19}F NMR spectrum in Acetone 139

Figure A.10: 500 MHz ^{1}H NMR spectrum in $CDCl_3$ 140

Figure A.11: 100 MHz ^{13}C NMR spectrum in $CDCl_3$ 141

Figure A.12: 477 MHz ^{19}F NMR spectrum in $CDCl_3$ 142

Figure A.13: 500 MHz ^{1}H NMR spectrum in Acetone 143

Figure A.14: 100 MHz ^{13}C NMR spectrum in Acetone 144

Figure A.15: 477 MHz ^{19}F NMR spectrum in Acetone 145

Figure A.16: 500 MHz ^{1}H NMR spectrum in $CDCl_3$ 146

Figure A.17: 100 MHz ^{13}C NMR spectrum in Acetone 147

Figure A.18: 477 MHz ^{19}F NMR spectrum in $CDCl_3$ 148

Figure A.19: 500 MHz ^{1}H NMR spectrum in Acetone 149

Figure A.20: 100 MHz ^{13}C NMR spectrum in Acetone 150

Figure A.21: 477 MHz ^{19}F NMR spectrum in Acetone 151

Figure A.22: 500 MHz ^{1}H NMR spectrum in Acetone 152

Figure A.23: 100 MHz ^{13}C NMR spectrum in Acetone 153

Figure A.24: 500 MHz ^{1}H NMR spectrum in Acetone 154

Figure A.25: 125 MHz ^{13}C NMR spectrum in Acetone 155

Figure A.26: 500 MHz ^{1}H NMR spectrum in DMSO 156

Figure A.27: 500 MHz ^{1}H NMR spectrum in DMSO 157

Figure A.28: 500 MHz ^{1}H NMR spectrum in DMSO 158

Figure A.29: 500 MHz ^{1}H NMR spectrum in DMSO 159

Figure B.1: 500 MHz ^{1}H NMR spectrum in Acetone 160

Figure B.2: 125 MHz ^{13}C NMR spectrum in Acetone 161

Figure B.3: 500 MHz ^{1}H NMR spectrum in Acetone 162

Figure B.4: 125 MHz ^{13}C NMR spectrum in Acetone 163

Figure B.5: 500 MHz ^{1}H NMR spectrum in Acetone 164

Figure B.6: 125 MHz ^{13}C NMR spectrum in Acetone 165

Figure B.7: 500 MHz ^{1}H NMR spectrum in Acetone 166

Figure B.8: 125 MHz ^{13}C NMR spectrum in Acetone 167

Figure B.9: 500 MHz ^{1}H NMR spectrum in Acetone 168

Figure B.10: 125 MHz ^{13}C NMR spectrum in Acetone 169

Figure B.11: 500 MHz ^{1}H NMR spectrum in Acetone 170

Figure B.12: 125 MHz ^{13}C NMR spectrum in Acetone 171

Figure B.13: 500 MHz ^{1}H NMR spectrum in DMSO 172

Figure B.14: 500 MHz ^{1}H NMR spectrum in DMSO 173

Figure B.15: Dose response curve 174

Figure B.16: Dose response curve 174

Figure C.1: Dose response curves at t=0h and t=2hrs 175

Figure C.2: Dose response curves at t=0h and t=2hrs 176

Figure C.3: Dose response curves at t=0h and t=2hrs 177

Figure C.4: Dose response curves at t=0h and t=2 hrs 178

Figure C.5: Dose responses curves at t=0h and t=2hrs 179

LIST OF SCHEMES

Scheme 1.1: Representation of classical enzyme catalytic mechanism of AChE for ACh catalytic reaction……..10

Scheme 1.2: Representation of extended enzyme catalytic mechanism for AChE hydrolysis at higher substrate concentrations…….11

Scheme 2.1: General reaction scheme for preparation of methyl oxime analogs.....49

Scheme 2.2: Enzymatic hydrolysis of the substrate analog acetylthiocholine 53

Scheme 2.3: Breakdown of the disulphide bond of chromogen DTNB by thiocholine to form thionitrobenzoate anion..... 53

Scheme 2.4: Proposed mechanism for the formation of sarin analog for 'F' containing 2-PAM analogs…….64

Scheme 3.1: Reaction method for synthesis of pyridinium β-Lactam..... 76

Scheme 3.2: Reaction method for synthesis of N-methylpyridinium β- lactams 77

Scheme 3.3: Proposed mechanism for suicide inhibition by inhibitor 4 where AChE activity is partially recovered…….....91

Scheme 4.1: Synthesis of Umbelliferyl- containing Dimethylsulfonium inhibitors..... 95

Scheme 4.2: Synthesis of Dimethoxyindanone-containing Dimethylsulfonium inhibitors..... 95

LIST OF EQUATIONS

Equation 1.1: Michalis Menten equation for AChE at lower substrate concentration 11

Equation 2.1: Initial rates equation for the hydrolysis of substrate ATCh by inhibited AChE 55

Equation 2.2: Equation for finding residual activity of inhibited enzyme..... 57

Equation 2.3: Amount of unreactivated hAChE by 2-PAM treatment (% of aged enzyme)..... 57

Equation 2.4: Determination of the recovered activity of aged hAChE. 58

Equation 2.5: Determination of resurrected hAChE activity of aged enzyme 58

Equation 2.6: Pseudo first-order rate equation for OP inhibition of hAChE..... 67

Equation 3.1: Equation used for determining change in molar absorptivity 79

Equation 3.2: Equation used for calculating the rate constant of hydrolysis 79

Equation 4.1: Equation used for determination of half-maximal inhibition constant IC_{50}..... 97

CHAPTER 1: REACTIVATION OF ORGANOPHOSPHORUS NERVE AGENT INHIBITED ACETYLCHOLINESTERASE

Introduction

Organophosphorus compounds (OPs) are used as pesticides, e.g. parathion, which is converted in the body to paraoxon, and chemical warfare nerve agents, such as sarin, soman, cyclosarin, VX, and tabun (Figure 1.1).[1] Even small amounts of OP exposure can be fatal, depending on the toxicity of the compound.[2] Numerous efforts have been taken to minimize or ban the use of these toxic chemicals;[3] however, their continued extensive use results in 300,000 annual cases of acute intoxication, of which more than 200,000 lead to human fatalities worldwide.[4-6]

Furthermore, great stocks of highly toxic chemical warfare nerve agents exist around the world and are considered a serious threat to national security and international stability. Sad examples of their abuse include nerve agent attack against Iraq civilians in 1988, use of sarin gas in the Tokyo subway in Japan in 1995 which caused 12 deaths and thousands of casualities,[7,8] and use of sarin by the Assad regime in Syria in 2013 which killed over 1400 people. OPs exert their toxicity by covalent irreversible inhibition of acetylcholinesterase (AChE),[9] which prevents the enzyme from hydrolyzing acetylcholine (ACh), a neurotransmitter in the central and peripheral nervous systems (CNS and PNS). Therefore, ACh accumulates in the cholinergic synapses throughout the body, which results in overstimulation of the ACh recepters.[3] Death is usually caused by cardiopulmonary failure resulting from the paralysis of neuromuscular function due to overstimulation.[10]

Over the decades of research on OP poisoning treatments, removal of the phosphyl moiety from the OP-bound AChE active site has been a promising method to restore AChE's catalytic activity. This has been achieved by use of strong nucleophiles such as oximes to remove the

phosphyl group from the OP-AChE complex. However, a secondary process called aging also occurs in the OP-AChE complex. Once aging occurs, currently available oximes are ineffective in removing the phosphyl moiety from the enzyme's active site, and hence are ineffective as antidotes against the aged enzyme. Also, currently use oximes have several disadvantages in OP therapy and there is no broad spectrum oxime for a wide range of nerve agents. The objective of this thesis is to discuss the current status of oxime reactivation on nerve agent inhibited AChE and strategies towards the reactivation of the aged-AChE adduct. Furthermore, kinetic evaluation of several inhibitor families on reactivation of initial complex of the OP-inhibited AChE and aged-AChE adduct is presented.

Importance of Acetylcholinesterase

Acetylcholinesterase (EC 3.1.1.7) is a catalytically powerful enzyme that has long been of interest to enzymologists, toxicologists and pharmacologists.[11-13]AChE functions in the central and peripheral nervous systems to terminate the relay of the action potential across nerve-nerve and neuromuscular junctions.[1,11]The physiological function of the enzyme is rapid hydrolysis of its substrate, ACh.[11,14] AChE anchored to the post synaptic membrane starts its action when ACh is liberated from the presynaptic nerve into the synaptic cleft as a result of the arrival of an action potential.[11,15] ACh diffuses to and binds the ACh receptor located in the post synaptic membrane.

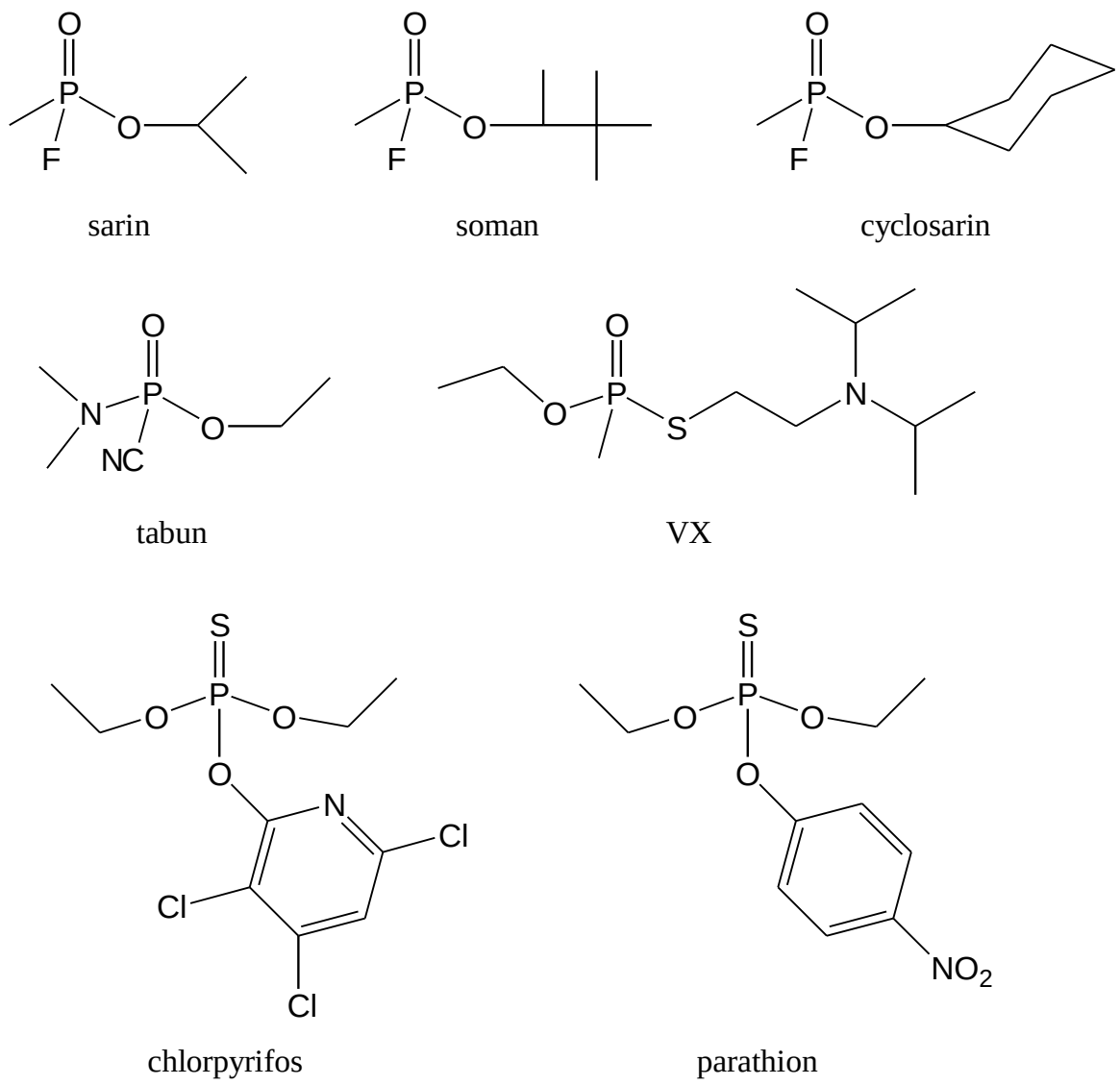

Figure 1.1: Chemical structures of some toxic OP pesticides and chemical warfare nerve agents

The ACh receptor then changes conformation, which allows entry of K^+ into the postsynaptic nerve process or muscles. This process causes postsynaptic membrane depolarization that ultimately results in triggering of the action potential in the postsynaptic cell.[11] AChE rapidly hydrolyzes ACh and terminates the nerve impulse transmission within a few milliseconds. Furthermore, AChE possesses a high specificity for its natural substrate ACh such that the rate of the reaction under bimolecular conditions approximates the diffusion controlled limit.[11,15,16] That

is, the second order rate constant of AChE catalyzed hydrolysis of ACh is higher than 10^8 $M^{-1}s^{-1}$.[11] This is a hallmark of evolutionary enzyme perfection.[15]

In addition to ACh, acetylcholinesterase has a remarkable ability to bind with structurally diverse ligands including carbamates, organophosphorus compounds, and oximes.[17] The pivotal role that AChE plays in the nervous system and the ability of the enzyme to bind with structurally diverse ligands make it an attractive target for designing mechanism-based inhibitors that range from useful pesticides and therapeutic agents to toxic chemical warfare agents.[11,18] AChE inhibitors can be either reversible or irreversible.

Among the AChE inhibitors, organophosphorus inhibitors are widely used in different fields.[6,11] AChE is phosphylated at the active site by a wide variety of organophosphorus compounds. Acute toxicity of the OP arises from the irreversible inhibition of AChE. In order to develop effective nucleophilic oximes for OP intoxication, the understanding of AChE structure and catalytic mechanism is important.

AChE Structure

AChE is a glycoprotein with 45Å × 60Å × 65Å dimensions (Figure 1.2).[19] It is made of 14 α-helices and 12 stranded mixed β-sheets. Central β-sheets are surrounded by α-helices.[19] The enzyme shows molecular polymorphism with soluble, membrane bound and basal lamina-anchored forms.[11,20] AChE is a widely distributed enzyme that is found in nerves, muscles, and red blood cell membranes of humans. AChE can be also found in other animals such as snake and eel in addition to vertebrates. [21]

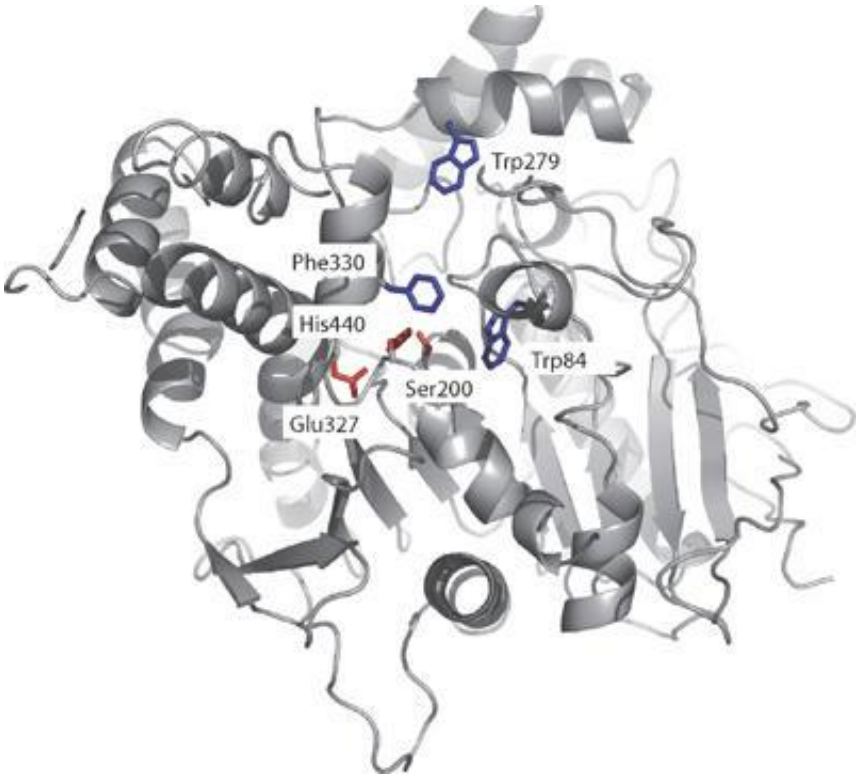

Figure 1.2: 3-D structure of native *Torpedo Californica* Acetylcholinsterase

Highlighting the catalytic triad in red, and the bottleneck residue Phe330 in blue.

This figure has been used with the permission from John Willey & Sons
Source: Colletier, J. P.; Fournier, D.; Greenblatt, H. M.; Stojan, J.; Sussman, J. L.; Zaccai, G.; Silman, I.; Weik, M. *The EMBO Journal* **2006**, *25*, 2746. [22]

AChE Active Site Gorge

The most remarkable feature of the AChE structure is a 20 Å long, narrow active site gorge with a remarkably high electrostatic dipole aligned along the axis of the gorge (Figure 1.3). This gorge penetrates halfway through the enzyme and widens out near the bottom. The AChE active site is located on the bottom of the narrow gorge and consists of three domains: esteratic locus, anionic locus, and a hydrophobic region.[11] The AChE active site contains a catalytic triad, Ser200, His440, and Glu327, that is similar to the catalytic triad of chymotrypsin and other serine proteases, but is of opposite handedness to that of chymotrypsin.[19] Though one might expect the narrow gorge would result in a low catalytic efficiency, AChE has a remarkably higher catalytic efficiency than serine proteases.

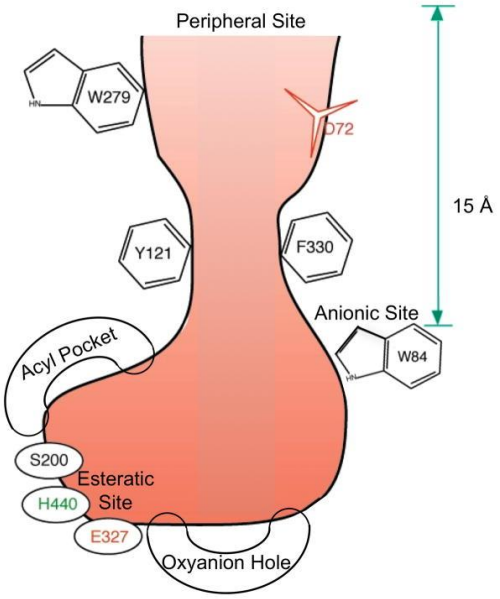

Figure 1.3: Schematic representation of the active site gorge of AChE

This figure has been used with the permission from the Elsevier.
Source: Dvir, H.; Silman, I.; Harel, M.; Rosenberry, T. L.; Sussman, J. L. *Chemico-Biological Interactions* **2010**, *187*, 10.[23]

The γ-oxygen (γO) atom of the Ser200 (S200) residue of the catalytic triad is located at 4Å above the bottom of the gorge. Furthermore, over 60% of the gorge surface area is covered with 14 aromatic residues such as phenylalanine, tyrosine, and tryptophan. A few carboxylate residues, in particular Glu199 and Asp72, also line the active site gorge.[19,24]

In addition to the class of ligands which bind to the AChE catalytic site, there are other types of ligands that bind with AChE, but they do not bind to the catalytic triad in the active site. In 1975, observations obtained from the indophenyl acetate and acetylcholinesterase binding experiment suggested that in addition to the active site, another subsite is located on the mouth of the enzyme through which ligands must pass on their way to the active site.[25] Since then, extensive information has been gathered to support the existence of another ligand binding subsite called the peripheral anionic site (PAS).[16,25,26] Moreover, AChE has other important subsites, the oxyanion hole and acyl pocket, that are located near the catalytic triad to facilitate substrate specificity and catalysis.

AChE Catalytic Mechanism

AChE catalyzes ACh with a turnover number of over 10^4 s^{-1}.[12] AChE has the capability of hydrolyzing its physiological substrate ACh within a few milliseconds of its release in cholinergic synapses.[27] This remarkable catalytic power is due to its unique structure that has been described earlier in this review. This interplay of AChE structure and activity has been probed by 3D structure analysis, site directed mutagenesis and molecular modeling together with kinetics studies.[11,12,19]

The AChE catalytic mechanism involves acylation and deacylation stages (Figure 1.4) and is initiated by nucleophilic attack of the γO atom of Ser200 on the carbonyl carbon of ACh. The overall catalytic mechanism occurs as a general acid, general base reaction, where the His440 imidazole function acts successively as a general base and general acid in the respective formation and breakdown of tetrahedral intermediates in the acylation and deacylation stages of catalysis.[11]

Site-directed mutagenesis experiments provide an in depth insight into the importance of AChE sub sites to the catalytic efficiency.[28] For examples, Trp84 in the anionic locus binds the positively charged quaternary ammonium group of ACh while the acyl pocket holds the acetyl group to orient the substrate for initial attack by the γO atom of Ser200. Reduction in k_{cat}/K_m by 3000-fold for the Trp84Ala mutant of human AChE indicates the importance of interaction of the anionic locus with ACh during the catalysis process.[28,29] This is explained further from the X-ray data obtained by Sussman et al. that show that Trp84 is located at the right distance from the catalytic triad to facilitate cation-pi interactions between ACh's quaternary nitrogen of the choline moiety with Trp84 during the hydrolysis process.[19] Thus, Trp84 properly orients the choline moiety prior to and during the hydrolysis reaction.

The function of the PAS which is located at the mouth of the active site gorge is also clearly described in the literature. It was reported that the PAS plays a critical role in initiating and terminating the catalytic processes[30], and ligand molecules which bind to the PAS allosterically regulate other ligands' binding to the catalytic site during the hydrolysis process.

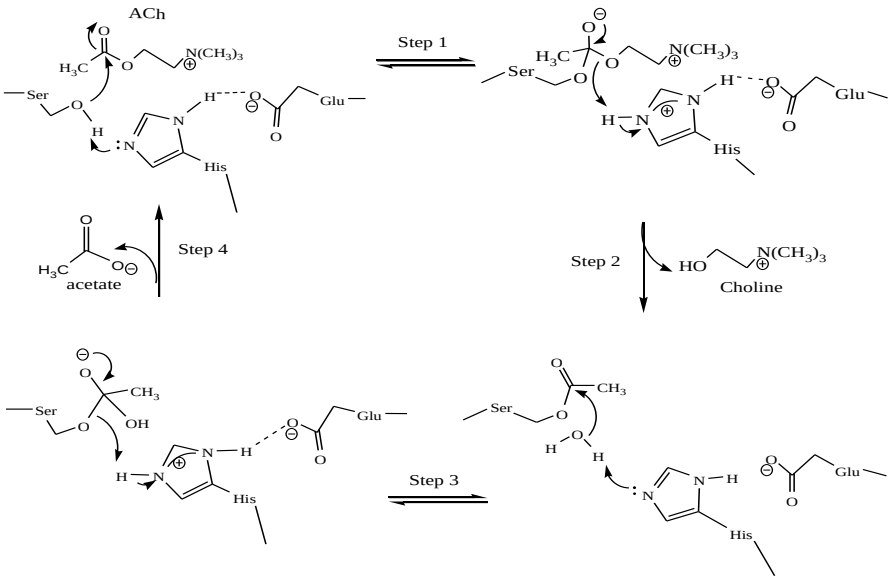

Figure 1.4: AChE catalytic mechanism

Step1- formation of first tetrahedral intermediate; Step 2- formation of acyl enzyme intermediate through first irreversible step; Step 3- formation of second tetrahedral intermediate; Step 4- liberation of free enzyme and second product from second irreversible step.

In the AChE hydrolysis process as illustrated in Figure 1.4, substrate reversibly binds to the enzyme and nucleophilic attack by Ser200 produces the first tetrahedral intermediate which collapses to the acyl enzyme intermediate with release of the choline product. The second tetrahedral intermediate is then formed by nucleophilic attack of active site water on the acylenzyme intermediate, which releases the acetate product to regenerate the free enzyme.

Comparison of the rates of ligand association with and dissociation from the ternary complex with the corresponding binary complex has shown that both the AChE catalytic site (CAS) and PAS interact during the hydrolysis process.[27] It has been reported that at lower concentrations of the substrate, the PAS ensures the proceeding of most substrate molecules which collide with the PAS to the active site. Therefore, at lower substrate concentrations AChE catalytic rate is increasing. However, at higher substrate concentration, substrate binding to the PAS sterically blocks the narrow active site gorge, which reduces the entrance of the substrate molecules to the active site and exit of product molecules from the active site. Thus, reduced catalytic rate is observed at higher substrate concentration.

Therefore, the classical Michaelis-Menten (MM) equation for normal enzyme catalyzed reactions is not valid for representing the AChE catalytic process at all substrate concentrations. The simplest form of the MM equation can be used for AChE catalyzed reaction (Scheme 1.1) at lower substrate concentrations since substrate inhibition is only observed at higher substrate concentrations. However, at higher substrate concentration, the classical MM equation for enzyme catalyzed reaction is not valid for AChE catalytic mechanism due to PAS mediated substrate inhibition. Therefore, an extended form of the classical MM equation is reported (Scheme 1.2).[27] At lower concentrations of the substrate, the MM equation can be derived using kinetic variables from Scheme 1.1 as shown in Equation 1.1.

$$E + A \underset{k_2}{\overset{k_1}{\rightleftharpoons}} EA \xrightarrow{k_3} F + P \xrightarrow{k_5} E + Q$$

Scheme 1.1*:* Representation of classical enzyme catalytic mechanism of AChE for ACh catalytic reaction.

Where, E ≡ free enzyme, A ≡ substrate, EA ≡ Michalis complex, F ≡ acyl-enzyme intermediate, P ≡ choline product and Q ≡ acetate product

$$v_i = \frac{v_{max}[A]}{K_m + [A]}$$

Equation 1.1: Michalis-Menten equation for AChE at lower substrate concentration

where $v_i \equiv$ initial velocity, $v_{max} \equiv$ maximum velocity = $[E]_T k_3 k_5/(k_3+k_5)$, $K_m \equiv$ Michaelis constant = $(k_2+k_3)k_5/\{k_1(k_3+k_5)$, $[A] \equiv$ substrate concentration.

At higher concentration of the substrate molecules, PAS binds to the substrate molecules resulting in enzyme inhibition. Thus, classical MM equation does not work.

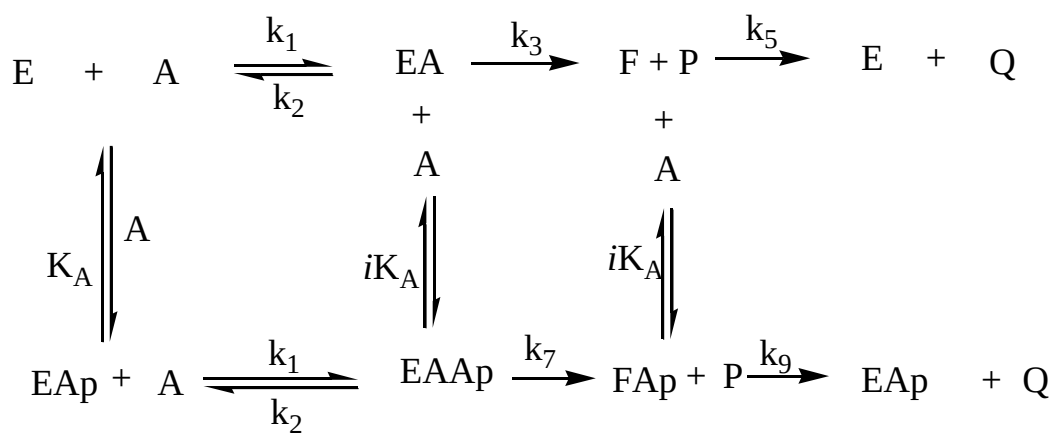

Scheme 1.2: Representation of extended enzyme catalytic mechanism for AChE hydrolysis at higher substrate concentrations

Where, E ≡ free enzyme, A ≡ substrate, EA ≡ Michalis complex, F ≡ acyl-enzyme intermediate, P ≡ choline product and Q ≡ acetate product, EAp ≡ PAS bound enzyme substrate complex, EAAp ≡ ternary Michaelis complex with PAS bound substrate, FAp ≡ acyl enzyme complex with PAS bound substrate.

AChE Inhibitors

Inhibition of AChE is a particular area of interest for various reasons. AChE inhibition is important to development of therapeutic drugs, effective insecticides and toxic nerve agents. Reversible AChE inhibitors play a major role in therapeutic applications while irreversible inhibitors are mostly associated with toxic effects (Figure 1.5).[31] Some examples of the use of reversible inhibitors for therapeutic applications include treatment for Alzheimer's disease (AD), glaucoma, myasthenia, and OP intoxication. Donepezil, rivastigmine, and galantimine are used to treat AD. Physostigmine is used for treating glaucoma while neostigmine is used for treating myasthenia. Many oximes such as 2-PAM and obidoxime are also reversible AChE inhibitors, but they are found to be effectively bound to the phosphylated enzyme, and therefore are useful antidotes for OP intoxication therapy.

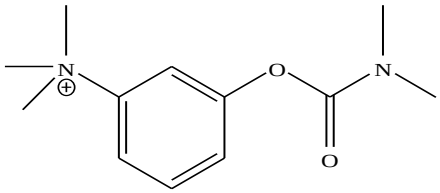

Neostigmine

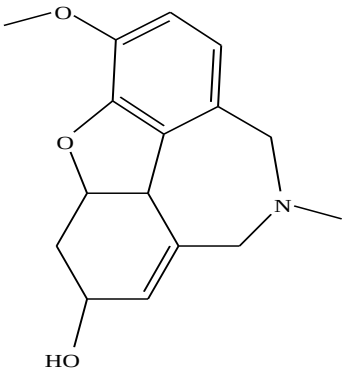

Galantamine

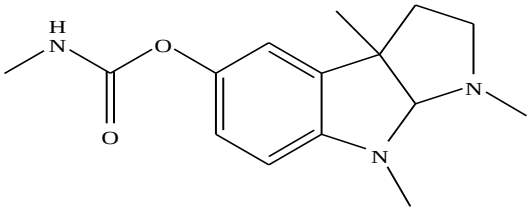

Physostigmine

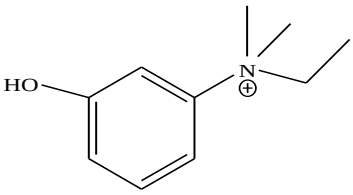

Edrophonium

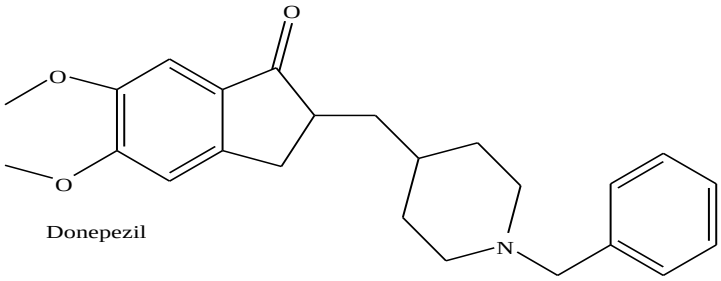

Donepezil

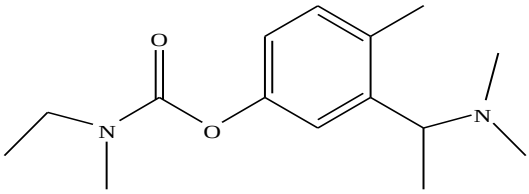

Rivastigmine

Figure 1.5: Some reversible AChE inhibitors use in medicinal chemistry

On the other hand, OP inhibitors are mostly covalent irreversible AChE inhibitors which are known to inactivate AChE upon binding to the enzyme active site. Thus, many are associated with toxic effects and used as pesticides and chemical warfare agents.

AChE inhibitors exert their effects by interacting with different sites of the enzyme. For example, the indanone core of the donepezil interacts with the peripheral site while rivastigmine carbamylates the active site serine of AChE to exert its function. On the other hand, galantamine interacts with the anionic locus and aromatic residues in the gorge. Most interestingly, many OP compounds are known to bind with the active site covalently and inactivate AChE upon binding.

Chemical Warfare Nerve Agents

Among OPs, chemical warfare agents (CWAs) are among the most toxic chemical substances (Figure 1.1) synthesized by mankind, and can cause death within few minutes to hours depending on the nature of the chemical and exposure concentration. The most important feature of the toxic nerve agents is their ability to exert toxic effects at very low concentration. They can be spread in the environment as a solid, gas or liquid.[11,32] Thus, society can be exposed to them via different ways such as wind, drinking water, or contaminated food. AChE is the key enzyme that is targeted by nerve agents and effects of the nerve agents arise from the accumulation of the neurotransmitter acetylcholine at cholinergic synapses due to irreversible inhibition of the enzyme.[6] This accumulation of ACh in peripheral and central cholinergic receptors can lead to a wide variety of health conditions including death.[33]

The first nerve agent, tabun, was developed in the 1930s by German chemist Gerhard Schrader as an attempt to make new insecticides in his research lab.[32] Following that, a series of nerve agents were synthesized that included sarin, soman, cyclosarin, and VX. The use of CWAs for mass destruction extended back to 20th century, and first use was recorded in 1919 during World War 1. Ever since, many incidents have been recorded and use of CWAs for mass destruction is evidenced by recent use of sarin gas in Syria that caused 1400 civilian deaths.[32] Due to the simple chemistry involved in the synthesis and similarity between the pesticides and CWAs,

efforts to minimize the production and usage of these extremely toxic nerve agents have obtained a limited success.[6] Therefore, further evaluation of the inhibitory mechanism and development of antidotes are highly desirable.

Interaction of Nerve Agents with AChE

OP inhibitors react with AChE in manner that is similar to the catalytic mechanism of Figure 1.4, wherein phospylation (Figure 1.6) is analogous to acylation[1,5] and the phosphylation occurs very rapidly for many nerve agents, as evidence by high bimolecular rate constants of inhibition (Table 1.1).[34] The electrophilic phosphorus atom of the OP inhibitor is attacked by the γO atom of Ser200 in a step that is facilitated by the of the general base imidazole moiety of His440 in the same manner as in the acylation process of Figure 1.4. The resultant phosphylated enzyme intermediate (Figure 1.6) resembles the acetylated enzyme intermediate but has a markedly greater stability.

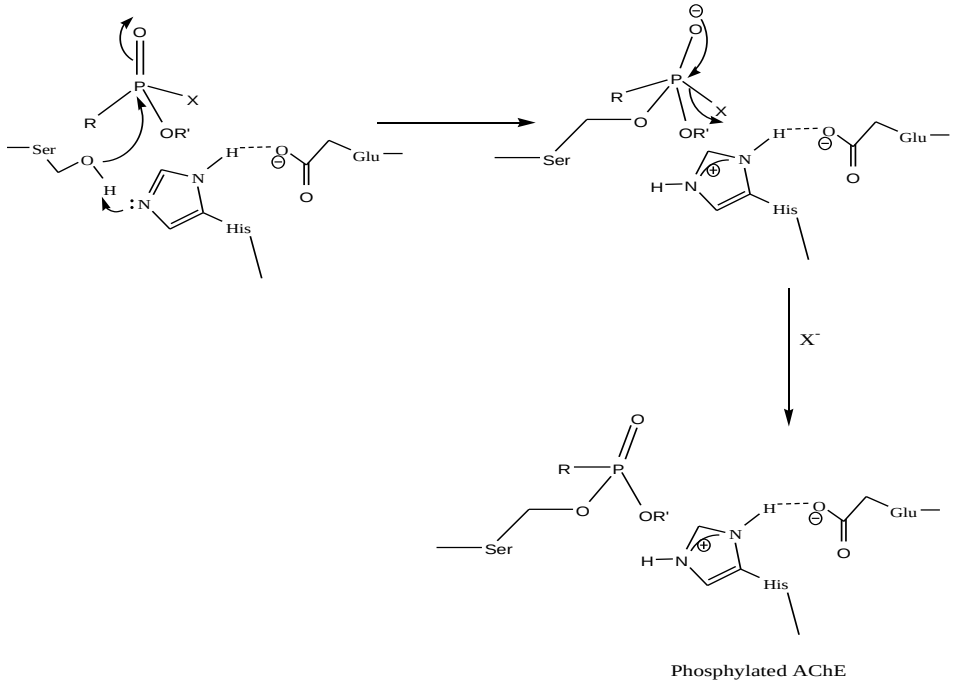

Figure 1.6: AChE phosphylation by a nerve agent. R, R'-alkyl groups, and X^- leaving group

During the deacylation process, the acetyl moiety is released from the acylated enzyme within 50 microseconds to restore AChE's catalytic function. This occurs by nucleophilic attack of an active site water on the acylated enzyme, but in dephosphylation, the rate of the nucleophilic attack by active site water molecules to remove the phosphyl group from the inhibited enzyme (spontaneous reactivation) is very slow and it takes hours to days depending on the nature of the inhibitor (Table 1.1).[5,35] The reactivation can be accelerated using a strong nucleophile which can efficiently bind with the phosphylated AChE adduct (Figure 1.7). The compounds used in this induced reactivation process are called reactivators and oximes are the most efficient reactivators so far for OP intoxication.[36]

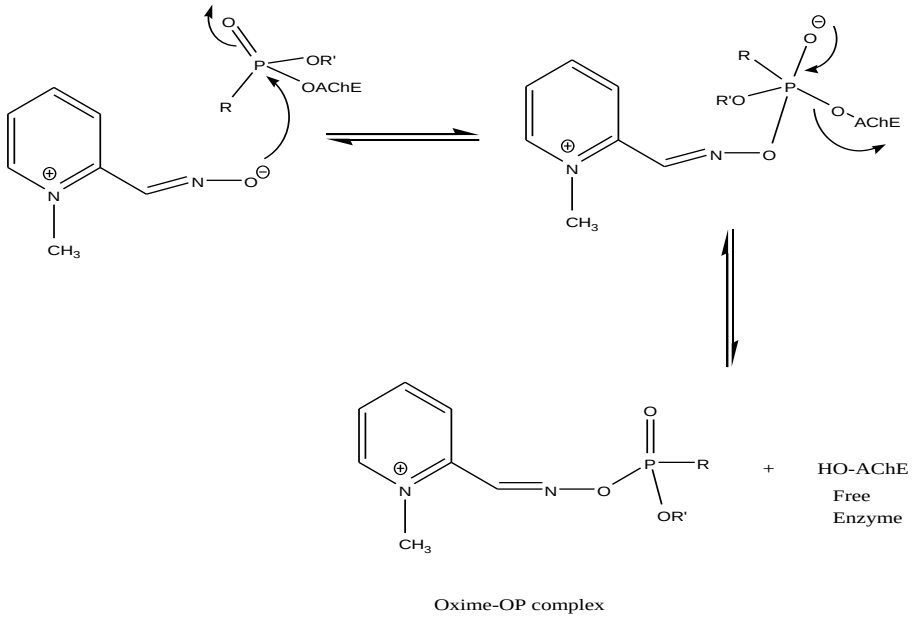

Figure 1.7: Nucleophilic reactivation of phosphylated AChE by oxime e.g. 2-PAM

However, inhibited AChE may also undergo a spontaneous de-alkylation process termed aging (Figure 1.8).[35] Aging converts inhibited enzyme into a phosphyl monoanion complex with AChE that cannot be reactivated by current oxime reactivators.[37]

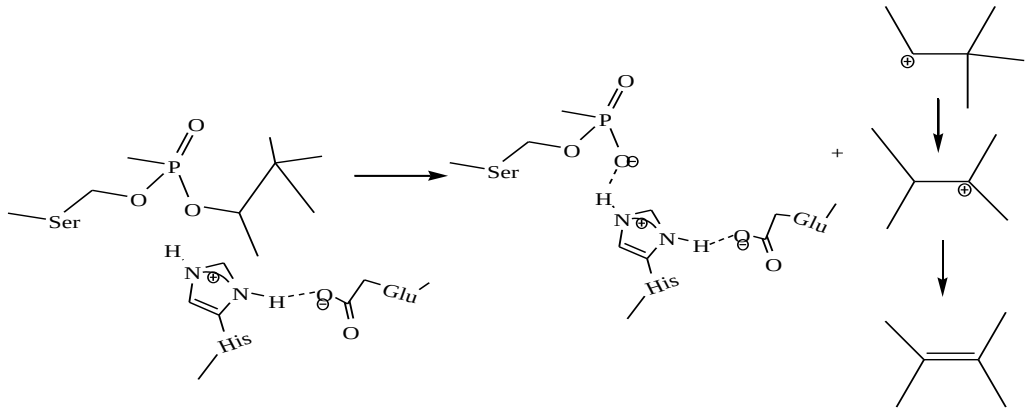

Figure 1.8: Aging process of soman inhibited AChE

Aging rates depend on various factors, such as the nature of the OP leaving group and R groups, the source of the enzyme, and the physicochemical conditions such as pH and temperature of the reaction medium.[35,38-40] For example, butylcholinesterase (BChE) has a greater tendency of aging compared to AChE,[35] aging occurs very rapidly in soman inhibited enzyme wherein the phosphylenzyme complex bears a branched alkyl group,[41] and aging occurs comparatively slowly in tabun and sarin inhibited AChE which have small alkyl groups. For example, the half-life of aging by soman is reported to range from seconds to a few minutes, [42-45] but for tabun it is about 13 hours.[37,46] A number of studies have shown that spontaneous reactivation and aging rates depend markedly on the nature of the nerve agents (see Table 1.1) Thus, it may prove difficult to perceive a structure-activity relationship that will help to generalize the OP poisoning treatments, especially for nerve agent poisoning.

Table 1.1: Kinetic data for major nerve agents and the pesticide paraxon

$k_i \equiv$ second-order rate constant of inhibition, $k_a \equiv$ first order rate constant for aging,

$k_s \equiv$ first order rate constant for spontaneous reactivation.

Nerve agent	AChE source	Species	k_i (M^{-1} min^{-1})	k_a (h^{-1})	k_s (h^{-1})	Ref.
Sarin	Erythrocyte	Human	2.7×10^7	0.228	0	10
		Eel	2.9×10^7			47
	Brain	Rabbit	1.5×10^7			47
	Erythrocyte	Guinea Pig		0.053 ± 0.006		48
	Recombinant	Human		0.064 ± 0.007		48
Cyclosarin	Erythrocyte	Human	4.9×10^8	0.099	0	10
		Eel	2.2×10^8			47
	Brain	Rabbit	1.4×10^8			47
Soman	Erythrocyte	Human	9.2×10^7	6.6	0	10
	Erythrocyte	Guinea Pig		1.7 ± 0.4		48
	Recombinant	Human		7 ± 1		48
		Eel	1.4×10^8			47
	Brain	Rabbit	9×10^7			47
Tabun	Erythrocyte	Human	7.4×10^6	0.036	0	10
	Erythrocyte	Guinea Pig		0.0094 ± 0.0007		48
	Recombinant	Human		0.0070 ± 0.0008		48
		Eel	1.9×10^6			47
	Brain	Rabbit	4.1×10^6			47
VX	Erythrocyte	Human	1.2×10^8	0.019	0.021	10
	Erythrocyte	Guinea Pig		0.0018 ± 0.0004		48
	Recombinant	Human		0.0019 ± 0.0005		48
		Eel	3.2×10^7			47
	Brain	Rabbit	3.4×10^7			47
Paraoxon	Human	Erythrocyte	2.2×10^6	0.022	0.022	10

Source references of the data in the table:[10,47,48]

Treatment for Nerve Agent Poisoning

The current treatments of nerve agents poisoning include administration of atropine and diazepam to reduce the symptoms resulting from ACh accumulation in nerve synapses and neuromuscular junctions while reactivating phosphylated enzyme by using strong nucleophiles, known to induce reactivation to liberate the native enzyme to do its natural function.[1,49] However, once the aging process occurs, the inhibited enzyme is no longer susceptible to nucleophilic reactivaiton.[50] Data obtained from spectroscopic experiments[37] and crystallographic studies have shown that during the aging process a negative charge is formed in the AChE-OP adduct due to de-alkylation, and the negative charge on the oxygen atom is stabilized by hydrogen bonding with the protonated imidazole nitrogen of His440 in the active site (Figure 1.8).[51] The charge and stabilization of the phosphyl monoanion of the aged adduct prevent approach of an incoming negatively charged reactivator to the phosphorus atom of the phosphylated-AChE.[46] However, model studies by Topczewski et.al. and George et.al. with negatively charged phosphonate monoesters suggest that it may be possible to alkylate aged-AChE adducts.[9,52] However, it is experimentally shown from many studies done on kinetic, equilibrium and spectroscopic evaluation of ligand binding on aged and non-aged enzyme that conformational changes occur during the aging process.[40] These conformational changes prevent aged enzyme from obtaining the proper orientation of the phosphorous atom for nucleophilic attack by reactivator.[34,43]

Although several oximes reactivate the non-aged forms of AChE inhibited by nerve agents, there is to date no reactivator that restores aged AChE function.[50] Moreover, there is no single compound that is effective in reactivation of the non-aged forms of AChE inhibited by the whole range of nerve agents.[53] Furthermore, the adduct of the reactivator that results from reactivation of the phosphylated-AChE complex can re-inhibit the free enzyme, and toxicity of the adduct depends

on the nature of the oxime and nerve agent.[33,54,55] Thus, reactivator oximes can interact with both nerve agents and phosphyl-AChE adducts. Therefore, many factors need to be considered during the rational drug design for nerve agent poisoning.

During past decades research has been focused on developing effective reactivators for non-aged and aged AChE adducts. However, there is no effective reactivator so far developed for aged enzyme. Therefore, some research groups including ours are focusing on reversing the aging process by alkylating or acylating the aged complex.[52] Indeed, if aged enzyme is alkylated or acylated, current oxime therapy may be useful to restore enzyme function.

Reactivation of Nerve Agent Inhibited AChE

The effectiveness of reactivators depends on the binding capacity of the reactivator to the inhibited enzyme and the proper orientation of the reactivator nucleophile to attack the phosphorus atom to displace the phosphyl moiety from the enzyme active site.[46] The efficiency of reactivator oxime can be accounted by several experimental constants, where affinity of the oxime to bind with phosphyl-AChE is expressed by dissociation constant K_D, and reactivation rate of the oxime is measured by the unimolecular rate constant k_r and the overall power of the oxime reactivator is expressed by the bimolecular rate constant k_{r2} (k_r/K_D). Of all reactivators developed so far, oximes have shown the greatest potential as therapeutic agents.[56] Though numerous oximes have been synthesized and evaluated on phosphyl-AChE adducts to find effective reactivators for chemical warfare nerve agent poisoning, few are in clinical use (Figure 1.9).[50]

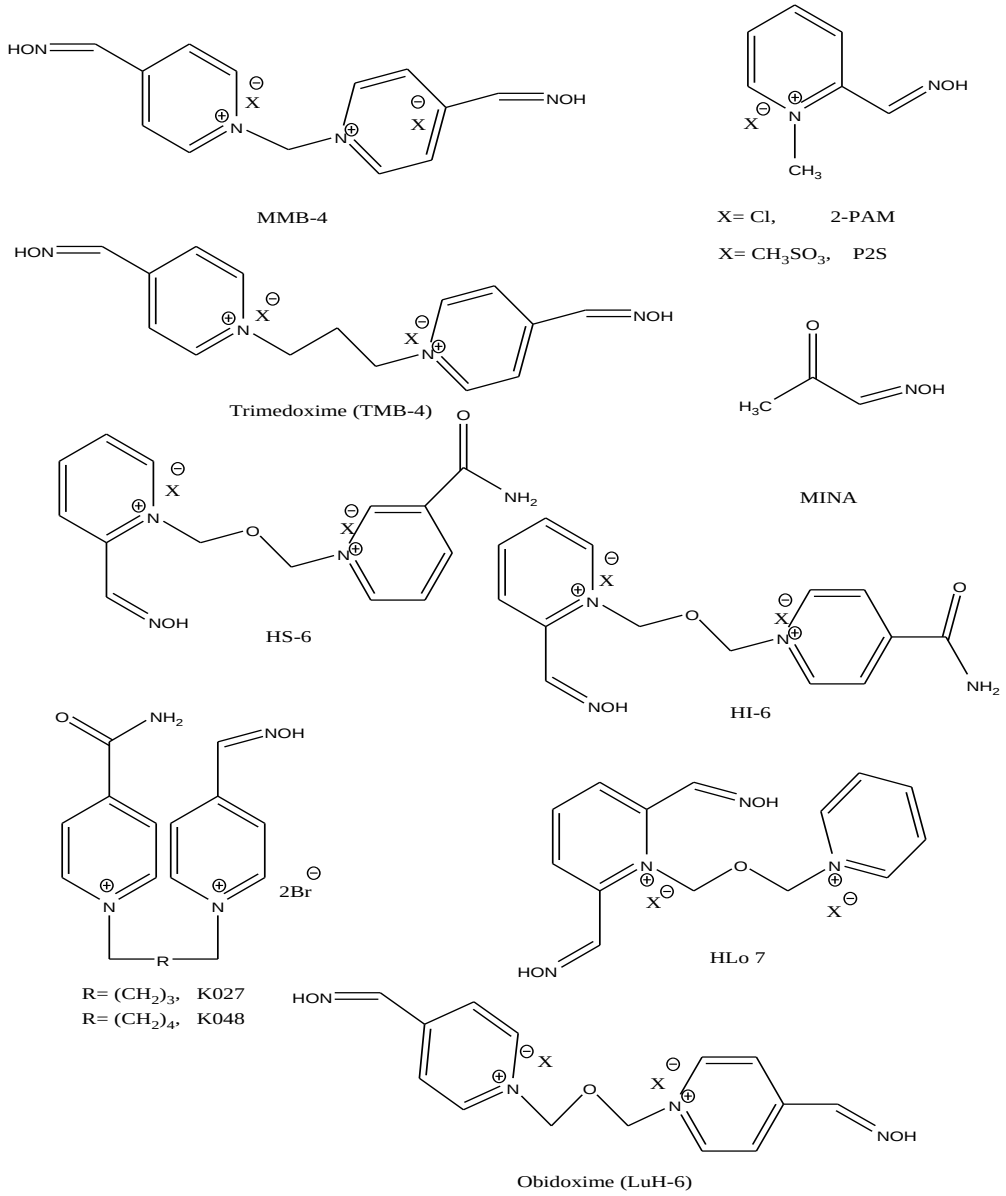

Figure 1.9: Some oxime reactivators that are in clinical use for OP intoxication worldwide

The currently used oxime reactivators are not ideal for the treatment of nerve agent poisoning for several reasons. Some do not penetrate the blood brain barrier due to the presence of a permanent charge and are ineffective in CNS reactivation; e.g., the mono-pyridinium oxime 2-PAM. Some have manufacturing difficulties in large quantities due to low stability in aqueous

media; e.g. HLo7.[50] Some need to be given as a large dose which cannot be administrated using an auto injector as a single dose; e.g. HI-6. Moreover, there is no broad spectrum oxime antidote for the full range of nerve agents.[57,58] Therefore, current reactivators of chemical warfare nerve agents, their drawbacks, and strategies towards the reactivation of aged AChE are topics that are worthy of further discussion and novel research approaches..

In 1952, Wilson found that hydroxyl amine, the simplest compound that bears the N-OH group, was a more effective reactivator than water against the pesticide tetraethylpyrophosphate (TEPP) inhibited AChE.[59] This discovery initiated time-honored efforts for the development of an extensive number of reactivators that incorporate the oxime C=NOH functional group.[56] Many oxime reactivators bind reversibly to AChE at the active site, peripheral site or at both sites of the enzyme. All oxime antidotes bear one or several NOH groups which nucleophilically attack the phosphorus atom of the AChE-OP adduct. Formation of the reactive AChE-OP-oxime complex is followed by nucleophilic attack to liberate the free enzyme and form the oxime-OP complex.

The first oximes that are effective against sarin-inhibited AChE, diisonitrosoacetone (DINA) and monoisonitrosoacetone (MINA), were reported in 1955.[56,60] These two oximes were able to reactivate about 90% of the sarin inhibited human erythrocyte acetylcholinesterase within 15 minutes. Data obtained in these experiments further indicated that these two oximes are capable of reactivating almost all the sarin inhibited human erythrocyte AChE and over 50% of sarin inhibited rat brain AChE at or above 10 mM concentration within less than one hour of the exposure.[56,60]

Furthermore, analysis of the pK_a values of the oximes indicated the importance of the acidity of the oxime group in the reactivation process. Importance of the formation of oximate ion to cleave the P-O bond is discussed in several studies.[56,60,61] When the pK_a of the oxime is much

higher than the physiological pH the fraction of the oximate ion is too low for an effective reactivation process. However, although even if the oxime is in its oximate form at physiological pH, reactivation is not effective if the resultant oximate ion nucleophile is not strong enough to be an efficient reactivator. Furthermore, the steric factors of the oxime may affect the reactivation process since different reactivation rate is observed when changing steric factors of the oxime. For example, Childs et al, indicated that reactivation of sarin-inhibited AChE by *iso*Nitrosoacetophenone (INAP) is significantly lower compared to the reactivation by MINA and *iso*Nitrosoacetylaceton (INAA).[56]

Charge of the pyridine ring[60,62] and the position of the oxime group on the pyridine ring are important determinants of antidotal effectiveness. Structure-activity studies indicated that an oxime group in position 2 is more effective in reactivation of AChE inhibited with soman, whereas an oxime in position 4 is more efficient in reactivation of tabun-inhibited AChE.[63,64] Moreover, in 1955, Wilson and Ginsburg provided the first evidence for the importance of a quaternary ammonium group in the structure of the reactivator.[65] They observed a thousand fold higher reactivation potency for 2-pyridine aldoxime methiodide (2-PAM) compared to 2-pyridine aldoxime (non- quaternary form of 2-PAM) on TEPP inhibited AChE. 2-PAM was the first practically available oxime for OP intoxication. However, the therapy cannot be only focused on the reactivation of inhibited AChE in peripheral tissues because OP inhibited AChE in both pheripheral and central nervous systems causes adverse and sometimes fatal effects. Since charged oximes are not penetrating the blood brain barrier at therapeutically relevant levels, a new class of uncharged pyridinium and non pyridinium oxime reactivators has been reported.[66-68] In one study, the imidazolium aldoxime group has been connected to different PAS binding ligands, e.g. phenyl-tetrahydroisoquinoline, via alkyl spacers. *In vitro* studies of these reactivators have shown similar

or superior reactivation potency to currently used reactivators against sarin, VX and tabun intoxication, but they are not in clinical use.[67] In another study, differently substituted tarcine hydroxypyridine oximes and amidoximes have been evaluated against nerve agent intoxication and found to be more effective in VX and tabun inhibited AChE reactivation than currently use oximes.[66] Furthermore, Radic et.al. in 2013, have studied thirty uncharged oximes that contained tertiary amine or imidazole protonable functional groups to reactivate tabun-inhibited hAChE. Results have shown that one of the imidazole containing compounds was superior in reactivation of tabun-inhibited hAChE However, numerous studies stress the importance of the quaternary ammonium moiety of reactivators for efficient binding with AChE in the reactivation process.[69]

In 1957, Askew used various concentrations of 2-PAM, MINA, and diacetylmonoxime (DAM) to compare the effectiveness of these three oximes along with atropine in the treatment of sarin poisoning.[70] Reactivation potency of these oximes suggested that inherent toxicity, solubility, and stability must also be considered when developing new antidotes. MINA was more toxic to monkeys than rats and mice. MINA was lethal to mice and rats at a dose of 150 mg/kg and to monkeys at 25 mg/kg, but no effect was observed on guinia pigs even at a dose of 150 mg/kg. DAM at dose of 150 mg/kg was not harmful to any of the tested animals.[62] These findings revealed that when developing a new antidote against nerve agent poisoning, oxime poisoning must also be considered. Furthermore, it was observed that 2-PAM was the fastest reactivator *in vitro* but it showed low reactivation potency compared to MINA and DAM *in vivo*.[70] This was interpreted in terms of the inability of 2-PAM, as salt, to penetrate the blood brain barrier to reactivate AChE in the CNS.[70] Therefore, 2-PAM is not a good reactivator alone. However, along with atropine therapy, 2-PAM is effective because atropine reduces the symptoms arising from CNS exposure to sarin, while 2-PAM reactivates AChE in the peripheral nervous system.[70]

Different salt forms (chloride, iodide, methylsulfate and mesylate) of 2-PAM were later available to improve efficiency, and pralidoxime mesylate (P2S) was found to be more effective than 2-PAM in blood brain barrier penetration although it has a permanent charge.[71] P2S has been tested against some nerve agent poisoning, and shown to be effective in VX, and more effective than 2-PAM in sarin and tabun poisioning.[72,73] However, none of the oximes discussed above is effective in soman intoxication[72,74] and they were weak or inefficient reactivators as well for cyclosarin inhibited AChE.[75,76] All these drawbacks motivate efforts to find more effective oximes to reactivate nerve agent inhibited AChE. As a result, 2-PAM analogues, and other oximes which are more effective than 2-PAM, were investigated.

In 1957, a series of PAM analogues was evaluated by Poziomek et al., who observed that 4-PAM (4-pyridine aldoxime methyl iodide) is also effective against sarin inhibited acetylcholinesterase, but to a lesser extent than 2-PAM. However, they hypothesized that reactivation ability of the reactivator could be increased if two structures known to be effective are combined together. Thus, a series of compounds that bear bisquaternary dioxime functions were synthesized and evaluated.[77] The most effective reactivator of this series was trimedoxime bromide bromide (TMB-4, and it showed a second order reactivation rate constant of 1×10^4 M^{-1} min^{-1} when administered with atropine where effectiveness of the 2-PAM was 2×10^3 M^{-1} min^{-1}.[77] Although 2-PAM and its analogues were effective reactivators against sarin and VX, as mentioned above, TMB-4 was the first effective oxime against tabun.[71,78]

Shortly thereafter, MMB-4, which is structurally similar to TMB-4 but with a methylene linker instead of the propyl linker of TMB-4, was introduced and was more potent than TMB-4 against a range of nerve agents.[57] This reveals the importance of the length of the linker between the two pyridinium rings on the reactivation potency.[74] The bispyridinium obidoxime (LuH-6),

structurally similar to TMB-4 but with an ether spacer, was also reported to be effective against tabun, sarin and VX and came to medical practice in 1964.[76] Although all of these previously mentioned bispyridinium compounds are effective in sarin, VX and tabun poisoning, none of them was effective against cyclosarin[76] or soman poisoning [73,78] even with pyridostigmine pre-treatment and atropine and diazepam therapy.[79] Moreover, TMB-4 is found to be toxic to the body.[78] Even though these oximes show antidotal effect against some nerve agent poisoning, it is also reported that phosphylated oximes that result from nerve agent inhibition can also be highly reactive[80] and could be even more potent inhibitors than parent nerve agent. Hackly et al. in 1959 reported that phosphylated oximes of 2-PAM, 4-PAM and TMB-4 from the reactivation process of sarin inhibited eel AChE are more potent than sarin itself. However, phosphyated 2-PAM was unstable (half-life is less than 30 minutes) at physiological pH and temperature, but phosphylated 4-PAM was more stable with a half-life of 200 minutes, which underscores the re-inhibition possibility under physiological conditions.[81] Therefore, future oximes must be designed to have higher reactivation efficiency at low concentration and low stability of the phosphyloxime product in order to minimize the re-inhibition of the reactivated enzyme in the phosphyloxime complex.

The bispyridinium monooxime HI-6 is the best available reactivator, with low toxicity in humans, and a broad spectrum of reactivator potency,[67] It has been evaluated against sarin[79], soman[74,79,82], tabun [79], VX[79] and cyclosarin[75] poisoning, and found to be effective for all the nerve agents including soman before aging, and when animals are pretreated with pyridostigmine, a parasympathomimetic drug (supporting drug treatment that itself gives considerable protection against OP-poisioning).[79,83-85] However, HI-6 itself was ineffective against tabun poisioning, which also indicates the importance of the oxime group at position 4 in reactivation of tabun inhibited AChE.[75,79,85] The importance of the oxime group in position 2 and a second oxime in

position 4 of the pyridinium rings for efficient reactivation of cyclosarin inhibited AChE has also been discussed recently by Worek et al.[75] When both oxime groups are in position 2 or position 4 of the two pyridinium rings, cyclosarin inhibited enzyme was resistant to oxime reactivation. However, considerable reactivation (second order rate constant of 22.4 mM^{-1} min^{-1}) was observed when one pyridine ring bears an oxime group in position 2 and the other pyridinium ring has second non-oxime function, e.g. carbamoyl, on position 4. This indicates the impact of position of the oxime groups and other functionalities in the reactivation potency and necessitates detailed kinetic studies for the reactivators in order to evaluate the effectiveness against nerve agent poisoning.

Although a more soluble analog of HI-6, e.g. HS-6, is available, HI-6 is still found to be superior as a therapeutic agent for soman intoxication with pretreatments.[72,86] HI-6 is more potent than 2-PAM against high lethal levels (e.g.,10 times LD_{50}) of sarin,[85] and HS-6 (at 10^{-4} M) is more effective than P2S (at 10^{-4} M) in both sarin and VX poisoning at higher initial concentration of the inhibited enzyme,10 µM units ml^{-1}.[72] Although HI-6 is an effective reactivator, its hydrolytic stability depends on pH, storage temperature[85] and the storage concentration,[87] which complicates manufacture and storage. However, Eyer et al. reported that the shelf life of HI-6 can be increased up to 20 years if it is stored at 0.1 M in aqueous solution, at pH 2.5, and at lower temperature such as 8 °C. Due to low stability of HI-6 in aqueous solution, it is usually provided in powder form. Moreover, HI-6 is effective when given at higher doses, which is problematic when administered with an auto injector.[88] However, an advantage of the HI 6 compared to other oximes discussed above is that people can tolerate high dosages, even up to 400 mg, without any side effects.[83] Although some reactivators, such as K027 and K048, which are structurally similar to HI-6 and trimedoxime or obidoxime, are shown to be similar or superior in activity in tabun-inhibited AChE reactivation *in vitro*, they are not in clinical use.[89] Further investigations are essential in order to

use them as antidotes for nerve agent poisoning.Oxime HLÖ 7 diiodide, synthesized in Hagedorn's lab by LÖffler in 1986, was shown to be a broad spectrum antidote against major nerve agents sarin, tabun, VX, and soman.[57] In addition, HLÖ 7 is effective against cyclosarin.[88] An experiment was done by Pēteris Albert where rat diaphragm strips were electrically evoked and contractions were blocked with sarin. He observed that HLÖ 7 was able to completely restore contraction at a concentration of 1 mM.[90] HLÖ 7 showed similar effectiveness as obidoxime and HI-6, but was more effective than 2-PAM. Furthermore, Eyer et al. showed that HLÖ 7 was 10 times more potent than HI-6 in atropine-protected sarin poisoned mice. Moreover, it reactivated soman and sarin inhibited AChE rapidly at 30 μM, and is easily soluble in water.[88] HLÖ 7 is available as various salts, and HLÖ 7 dimethanesulfonate is reported to be superior to HI-6 against soman and sarin inhibited AChE in mice. However, HLÖ 7 is found to be slightly less effective than HI-6 in guinia pigs against soman and sarin poisoning but far more effective against tabun poisioning.[64,88,91] Since HLÖ 7 has a lower LD_{50} than HI-6, it is likely to be more toxic to the patient.

As mentioned above, oxime induced reactivation depends on various factors such as structure of the oxime, source of the enzyme, and other factors such as aging. Accordingly, reactivation kinetics of current oximes that are in clinical use are compared in Table 1.2 for better understanding of their reactivation potency against nerve agent poisoning. Many analogues of reactive oximes have been synthesized and tested during past decades that vary positions of the oxime groups, linker lengths of bispyridinium oximes, and substitutions with oxygen, fluorine, or sugar moieties. However, they are not in clinical use due to lack of toxicity data. Therefore, further evaluation of the oximes is important in order to have an optimal reactivator with broad spectrum for nerve agent poisoning.

Table 1.2: Kinetic data for oxime reactivators

$k_r \equiv$ reactivation rate constant, $K_D \equiv$ dissociation constant for inhibitor-AChE-Oxime complex, $k_{r2} \equiv$ bimolecular rate constant

Nerve agent	Reactivator oxime	Species	AChE source	k_r(min)	K_D (μM)	k_{r2}($mM^{-1}min^{-1}$)	ref
Sarin	MINA	Human	erythrocyte	>0.15	> 5000	0.029	92
	2-PAM	Guinea pig	erythrocyte	0.070±0.022	342±126	0.206	48
			Brain	0.230	4074	0.056	93
		Human	recombinent	0.123±0.032	266±150	0.462	48
	Obidoxime	Rat	brain	0.140± 0.013	354±38	0.403	94
		Human	erythrocyte	0.937	31.3	29.98	76
	Trimedoxime	Rat	brain	0.380±0.034	781±57	0.486	94
	MMB-4	Guinea pig	erythrocyte	0.076±0.0005	294±31	0.257	48
	HI-6	Guinea pig	erythrocyte	0.020±0.007	67±12	0.297	48
		Human	recombinant	0.128±0.011	22±10	5.953	48
		Rat	brain	0.210±0.021	9±2	22	94
	HLO 7	Guinea pig	erythrocyte	0.070± 0.009	100±29	0.696	48
		Human	recombinant	0.320±0.046	28±10	11.430	48
Cyclosarin	MINA	Human	Erythrocyte	0.17±0.02	8.6±1.7	0.02±0.0003	92
	2-PAM	Guinea pig	Erythrocyte	0.016±0.004	2234±380	0.007	48
		Human	Recombinant	0.035±0.012	1247±650	0.028	48
			Brain	0.04	1259	0.032	95
	Obidoxime	Human	Brain	0.04	631	0.063	95
	Trimedoxime						
	MMB-4	Guinea pig	Erythrovyte	0.277±0.062	1981±434	0.140	48
	HI-6	Guinea pig	Erythrocyte	0.067±0.054	506±323	0.133	48
		Human	Recombinant	1.040±0.240	35±16	29.70	48
			Brain	0.07	2	35	95
	HLO 7	Guinea pig	Erythrocyte	0.076±0.029	383±288	0.139	48
		Human	Recombinant	1.620±0,453	19±6	85.06	48
			Brain	0.15	1	150	95
Soman	MINA						

	2-PAM	Guinea pig	Erythrocyte	0.029±0,009	1730±240	0.017	48
		Human	Recombinant	0.262±0.113	5090±1590	0.052	48
	Obidoxime						
	Trimedoxime						
	MMB-4	Guinea pig	Erythrocyte	0.064±0.020	2310±520	0.038	48
	HI-6	Guinea pig	Erythrocyte	0.026±0.013	910±310	0.051	48
		Human	Recombinent	0.183±0.043	9±4	21.51	48
	HLO 7	Guinea pig	Erythrocyte	0.067±0.026	490±170	0.140	48
		Human	recombinant	0.307±0.080	12±6	26.180	48
Tabun	MINA	Human	Erythrocyte	>0.0006	>5	0.0001	92
	2-PAM	Guinea pig	erythrocyte	0.002±0.001	1210±340	0.002	48
		Human	recombinant	0.008±0.006	1320±770	0.006	48
	Obidoxime	Human	Recombinant	0.04±0.006	250±110	0.16	66
		Human	brain	0.06	1412	0.042	89
	Trimedoxime	Human	Recombinant	0.085±0.005	145±25	0.7	66
		human	brain	0.08	1585	0.05	89
	MMB-4	Guinea pig	Erythrocyte	0.006±0.001	10580±2450	0.001	48
		Huma	recombinant	0.013±0.008	2990±1230	0.004	48
	HI-6	Human	recombinant	0.020±0.0007	106 ± 15	0.2	66
	HLO 7	Guinea pig	erythrocyte	0.003±0.002	720 ± 410	0.004	48
		Human	recombinent	0.005±0.001	80 ± 4	0.062	48
VX	MINA	Human	Erythrocyte	0.49±0.07	6000±1200	0.08	92
	2-PAM	Human	Recombinant	0.06±0.01	215 ± 75	0.28	66
		Guinea pig	Erythrocyte	0.012±0.001	74 ± 5	0.160	48
		Human	recombinent	0.031±0.013	272±121	0.117	48
	Obidoxime	human	Recombinant	0.60±0.05	54±12	11	66
	Trimedoxime						
	MMB-4	Guinea pig	Erythrocyte	0.184±0.072	2238±1475	0.082	48
		human	recombinant	0.024±0.008	137±60	0.177	48
	HI-6	human	Recombinant	0.44±0.15	50±26	9	66
	HLO 7	human	recombinant	0.49	7.8	63	66
Paraxon	2-PAM	Human	erythrocyte	0.17±0.007	187.3±19	0.91	10
	Obidoxime	Human	BChE	0.07±0.0004	317±2	0.25	96

		Human	erythrocyte	0.81 ± 0.08	32.2 ± 6.9	25.2	10
	Trimedoxime	Human	BChE	0.09 ± 0.0005	578 ± 12	0.15	96
	MMB-4	Human	BChE	0.05 ± 0.001	544 ± 42	0.08	96
	Hi-6	Human	Erythrocyte	0.2 ± 0.009	548.4 ± 46	0.36	10
	HLo 7	Human	erythrocyte	0.34 ± 0.02	47.8 ± 6.9	7.1	96

Source of references for the data in the table: [10,48,66,76,89,92-96]

Status of the Reactivation of Aged Acetylcholinesterase

The inability of any current oximes to reactivate aged AChE indicates the necessity of synthesis and kinetic studies on potential reactivators for the aged enzyme. The chemical basis of the aging process was first explained by Berends et al. in 1959 as the process where an alkyl group is removed from the OP-AChE complex, which converts the complex into an unreactive form which is resistant to any oxime reactivation.[97] Ever since, researchers have tried to reactivate the aged enzyme in different ways but there currently is no compound that can reactivate the aged enzyme adduct.

In 1969, Blumbergs et al. hypothesized that the de-alkylated form of the enzyme could be re-alkylated with an ester of a stronger acid.[98] They synthesized a series of alkylating agents including many esters where the alkyl moiety was in a sulfonate group to increase the rate of the alkyl transfer to phosphonate anion, which is known to be a poor nucleophile.[98] Moreover, a quaternary nitrogen group was included in the structure in order to improve binding efficiency to the enzyme and also to improve the water solubility in neutral media.[98] In 1970, Steinberg et al. did a model study for the reactivation of aged enzyme with different alkylating agents. 4-Nitrophenyl methylphosphonate was reacted with 36 various alkylating agents, and both alkylation and hydrolysis rates of the resultant mixed esters were determined. It was found that alkylating agents that were highly reactive in the model study yet failed to alkylate the aged-AChE adduct.[9] They rationalized their data by suggesting that the phosphonate group may be embedded inside the enzyme due to conformational changes of the enzyme, and that prevents the alkylation of the OP-AChE adduct. Moreover, they hypothesized that the negative charge of the aged-AChE adduct may be stabilized by a positive charge group of the enzyme or the alkylating agent may have reacted with another group of the enzyme instead of reacting with the active site.[9] Later, some of

these assumptions were experimentally supported by mutant study, and by molecular modeling and molecular mechanics calculations using X-ray coordinates of the AChE-aged adduct. It is indicated that the developing charges during the de-alkylation process are stabilized by different amino acids residues in the AChE active site.[35,39,99] Moreover, studies of the crystal structures of AChE inhibited with different nerve agents showed that conformation changes of the enzyme occur during the aging process which prevent efficient binding of the oxime reactivators to the phosphylated AChE.[43]

The catalytic mechanism involves proton transfer from the protonated active site histidine of AChE to the choline moiety during the acylation stage of the reaction. However, protonated histidine cannot transfer a proton to the leaving group of the phosphylated enzyme. Therefore, the positive charge that remains on the catalytic histidine stabilizes the phosphonate anion resulting from the dealkylation process via a salt bridge.[35,99] The importance of the protonated histidine during the aging process of soman inhibited AChE has been explained in detail by Saxena et al. in 1998 with the pH dependent study in the aging process.[39] Also it was found that AChE accelerates the aging process versus non-enzymatic aging by lowering the activation energy.[42,44] Therefore, reactivation of aged AChE is not easily achievable.

In 2009, Sanson et al. presented crystallographic structures of the ternary complex of 2-PAM with soman aged-AChE adduct.[43] It was reported that 2-PAM binds to the catalytic site of the enzyme with the oxime moiety pointed away from the phosphorous atom that needs to be nucleophilically attacked. Furthermore, 2-PAM did not bind to the non-aged AChE adduct effectively due to the presence of the pinacolyl group in the choline binding pocket[2] where 2-PAM usually interacts. Therefore, 2-PAM is not able to reactivate aged enzyme and reactivation of non-aged AChEs that result from soman inhibition is also very slow.[43] Radic et al. in 2010 also observed

nonproductive orientations of oximate ions of 2-PAM and HI-6 with respect to the P atom of the aged AChEs that resulted from VX and cyclosarin analogs.[100] These findings indicate that when new reactivators are designed, they should be able to bind to the enzyme in an orientation where the oximate anion is properly oriented for nucleophilic attack on the phosphorus atom. Moreover, alkylating agents must be designed to bind with the aged enzyme and that are capable of alky transfer to the phosphonate anion of the aged enzyme.

Another important approach for reactivation was to retard the aging process by different compounds, because if these ligands decrease the aging rate, oximes can be used to reactivate phosphylated AChE before aging. This approach is of great interest for nerve agents such as soman that possess fast aging rates. Some bispyridinium salts have been found to decrease the aging rate by several orders of magnitude in AChE inhibited with soman [41,101] while other ligands such as tarcine, gallamine[102] and ketamine were also found to slow the aging rate in sarin-inhibited AChE.[103,104] Furthermore, compounds that can bind to the both PAS and esteratic sites are of interest. It has been shown that PAS binding ligands accelerate oxime induced reactivation.[33,69,105] In 2003, *in vitro* and molecular modeling studies indicated that some cyclic compounds that specifically bind to the PAS with high affinity may prevent entrance of compounds such as some nerve agents with bulky alkyl groups but allow the entrance of small molecules such as acetylcholine to the active site.[106] These types of ligands may be therapeutically useful because they can reduce the entrance of nerve agents such as soman.

In 2013, Wandhammer et al. reported crystal structures of alkylating agents complexed with the aged-BChE adduct produced by soman inhibition.[2] The structures indicated that the alkylating agents methyl 2-(pentafluorobenzyl-oxyimino) pyridinium iodide and benzyl pyridinium-4-methyltrichloroacetimidate bromide (Figure 1.10), were bound near the phosphonyl

serine but the distances between the electrophilic carbons of the alkylating agents and the phosphonyl oxyanion of the aged enzyme were not close enough to allow the alkylation reaction (Figure 1.11). Data further revealed that the distance might be changed by changing the counter ion of the salt. It was also observed that although the choline binding pocket is occupied by inhibitor, the benzyl pyridinium moiety of the alkylating agent is still interacting with the tryptophan of the anionic binding site. This observation provides important information for future design of alkylating agents for aged AChE.

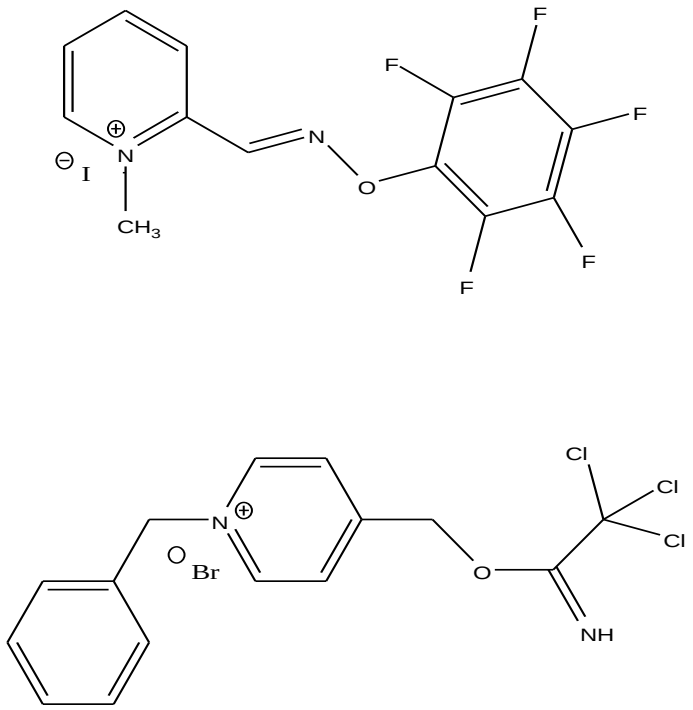

Figure 1.10: Chemical structures of the ligands that formed complexes with soman-aged BChE.

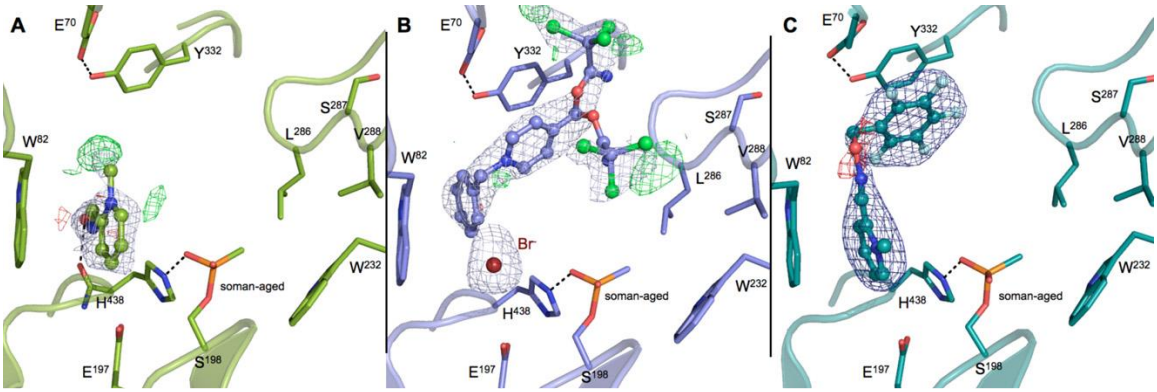

Figure 1.11: Crystalographic structures showing the active site of soman-aged human butyrylcholinesterase in complex with 2-PAM

(A), benzyl pyridinium-4-methyltrichloroacetimidate (B), and methyl 2-(pentafluorobenzyloxyimino)pyridinium (C). Key residues are represented by sticks with oxygen atoms in red, nitrogen atoms in blue, and phosphorus atoms in orange.

This figure was used with the permission from Elsevier.

Source: Wandhammer, M.; de Koning, M.; van Grol, M.; Loiodice, M.; Saurel, L.; Noort, D.; Goeldner, M.; Nachon, F. Chemico-Biological Interactions **2013**, 203, 19

In our research group we synthesized and evaluated more than 75 alkylating and acylating agents including several classes of agents that combine alkylating moieties with known active site or PAS AChE binding motifs.[52,107] Compounds in various structural classes were investigated. The general aim of the research was that successful alkylation or acylation of the phosphonate monoanion of aged AChE would produce neutral phosphyl complexes that would either spontaneously reactivate or would be reactivatable in the presence of oxime antidotes. These compounds are presented in turn below, and the rationale behind their design is discussed.

1. Sulfonium Compounds

Methyl transfers are common in Nature, and the natural transfer agent is S-adenosylmethionine, a sulfonium methyl donor. Consequently, the array of sulfonium compounds shown in Figure 1.12 was synthesized on the expectation that they would bind to the AChE active site and transfer a methyl group to the phosphonate monoanion of the aged enzyme. Though high-affinity binding was noted for these compounds, none of these resurrected the activity of the aged AChE complex.

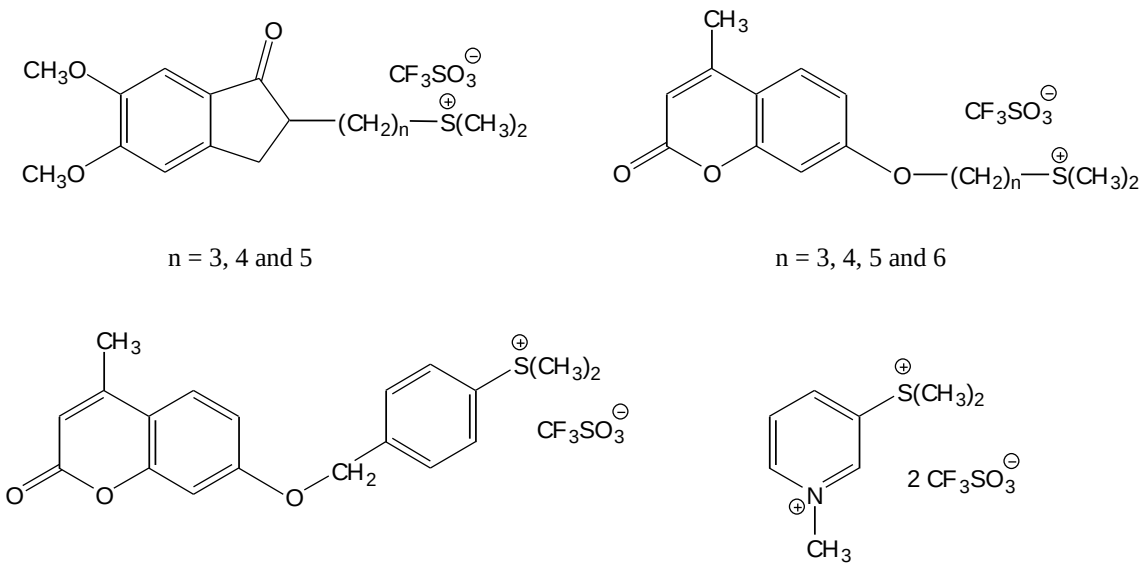

Figure 1.12: Putative sulfonium reactivators of aged AChE

2. 2-PAM Analogs

Methoxylamine analogs of the oxime antidote 2-PAM were synthesized with the aim that methyl transfer to the aged AChE adduct would produce a neutral phosphyl AChE adduct simultaneously with 2-PAM *in situ*, and subsequent 2-PAM nucleophilic attack would reactivate the newly formed neutral phosphyl-AChE adduct. This is an example of a bait (methyl transfer) and switch (*in situ* generated 2-PAM reactivation) strategy, which is outlined in Figure 1.13. However, none of these 2-PAM analogs resurrected the activity of aged AChE.

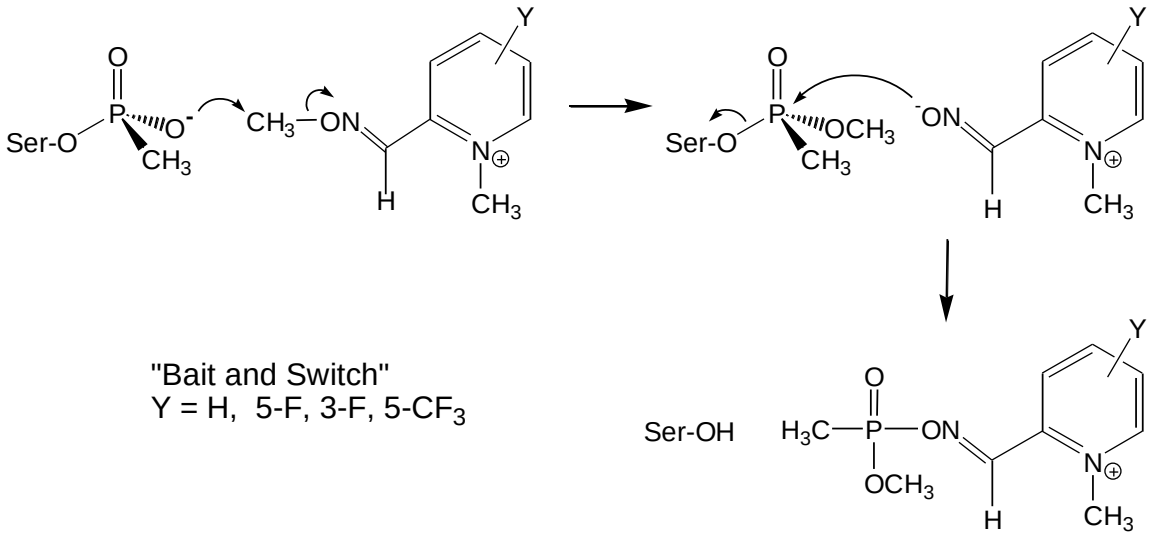

Figure 1.13: Methoxylamine analogs of 2-PAM as aged AChE reactivating agents

3. Pyridinium β-Lactams

Another "bait and switch" strategy for resurrecting the activity of aged AChE utilizes N-methylpyridiniums that are substituted at the 2-position with a β-lactam moiety, as outlined in Figure 1.14. For these compounds, opening of the electrophilic β-lactam (the bait) unmasks a nucleophilic amidine function which could putatively attack at phosphorus (the switch) to expel the free enzyme. For this class of agents, only the active site directed compound that possessed the 5-CF_3 substituent showed possible resurrection of the activity of aged AChE, though activities in both the control and treated samples were low.

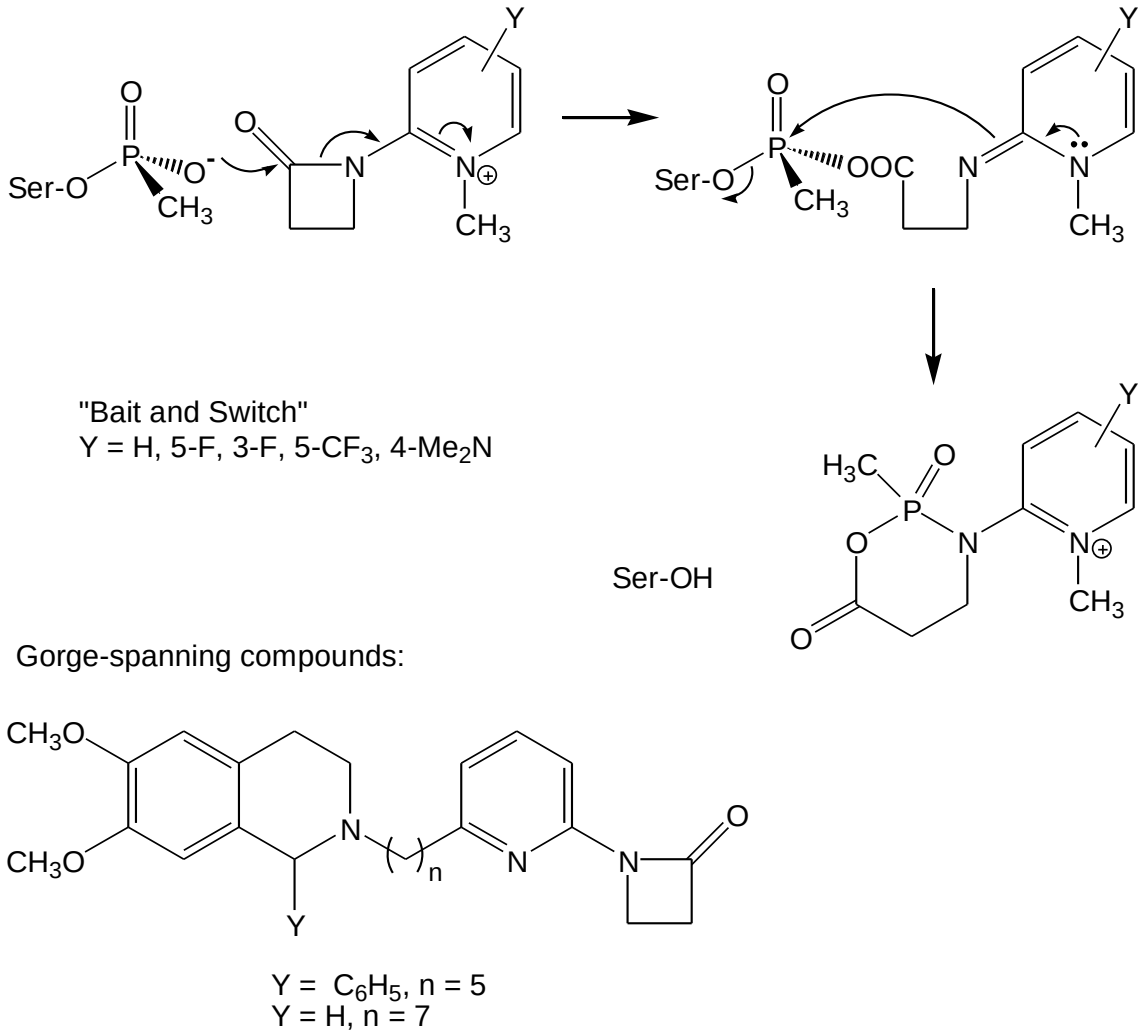

Figure 1.14: Pyridinium β-Lactams as aged AChE reactivating agents

4. Epoxide Substituted N-Methylpyridiniums

A final "bait and switch" strategy is embodied in the compounds shown in Figure 1.15. For epoxide-substituted N-methylpyridiniums, attack of the phosphonate monoanion of aged AChE on the electrophilic epoxide moiety (the bait) would release the alcoholate anion for attack at phosphorus (the switch) and concomitant release of the free enzyme. However, none of the compounds in this class were able to resurrect the activity of aged AChE.

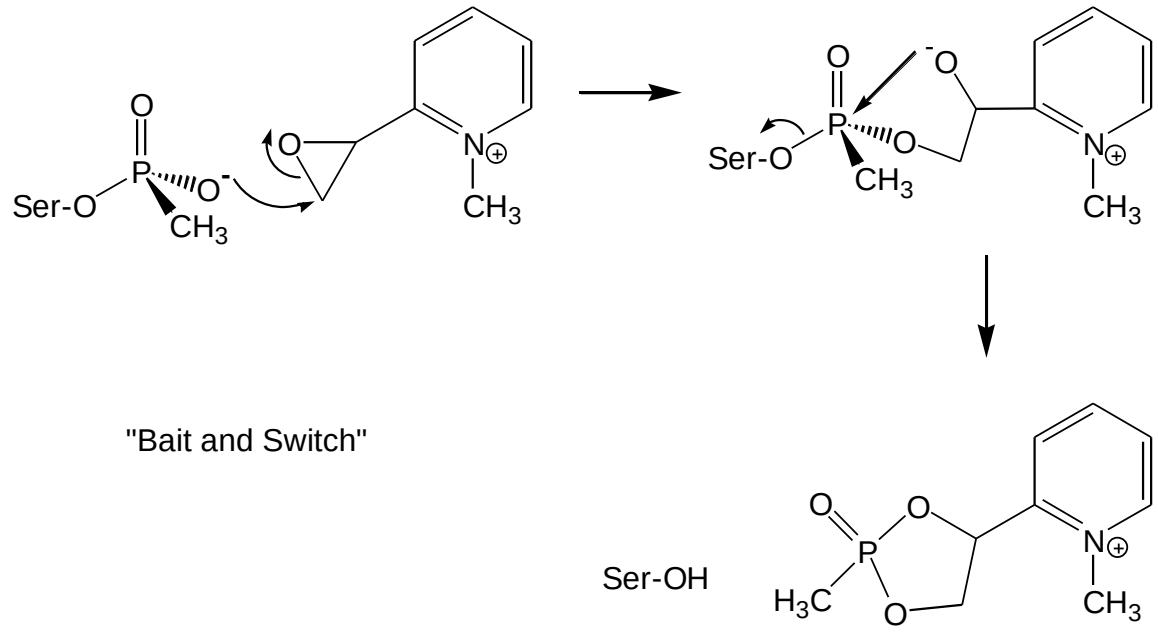

Gorge-spanning compounds (n = 3, 4, 5):

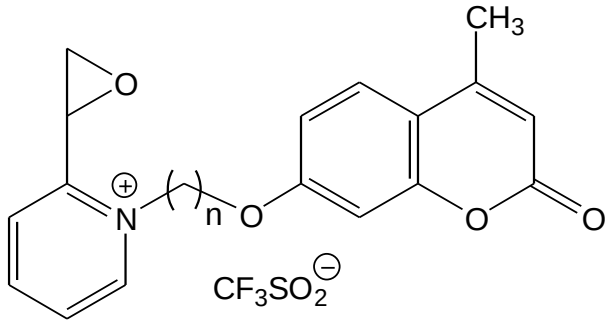

Figure 1.15: Epoxide substituted N-Methylpyridiniums as aged AChE reactivating agents

5. Methoxypyridinium Compounds

A particularly promising class of agents for putative resurrection of the activity of aged AChE, 2-methoxy- and 4-methoxypyridinium compounds, are shown in Figure 1.16. The figure shows two classes of alkylating agents. Compounds of the first set were designed to enter the catalytic site of AChE and subsequently modify the aged enzyme by methyl transfer. These compounds have been shown in a model study to readily alkylate the methoxymethyl phosphonate anion in DMSO as a model of the aged enzyme.[52] However, despite the promising model reaction results, none of these compounds, with the possible exception of the compound bearing the 6-F substituent, was effective in reactivation of the aged phosphyl-AChE complex. The figure also shows a wide array of putative methylating agents that were designed to span the 20 Å active site gorge of AChE. Again, none of these compounds was effective in reactivation of the aged enzyme.

As this introduction details, two major challenges still face researchers in the quest to design effective medicinal agents for counteracting poisoning by AChE-inhibiting nerve agents. The first is that there is no universal oxime antidote. Oximes that are effective against certain nerve agents are ineffective against others. The second is that, despite extensive efforts that span two generations, aged phosphyl-AChE adducts have never been reactivated. However, given the powerful tools of modern structural biology, medicinal chemistry and molecular biology, there is still hope that these considerable challenges can be met.

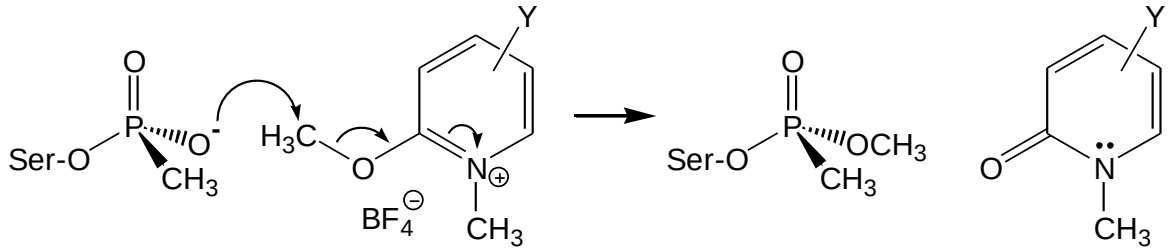

Y = H, 4-CN, 5-CN, 6-CN, 3-F, 5-F, 6-F, 5-NO_2, 5-CF_3, 6-CF_3

Gorge-spanning compounds:

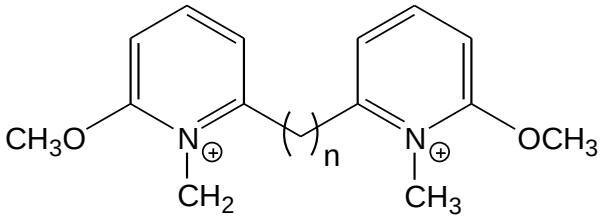

2 $CF_3SO_2^{\ominus}$ n = 2, 5, 6, 7, 8

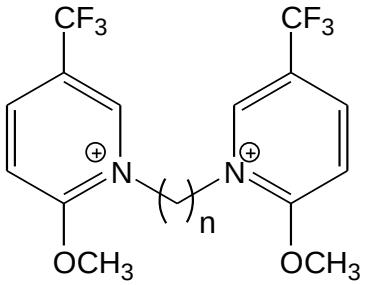

2 $CF_3SO_2^{\ominus}$ n = 3, 5

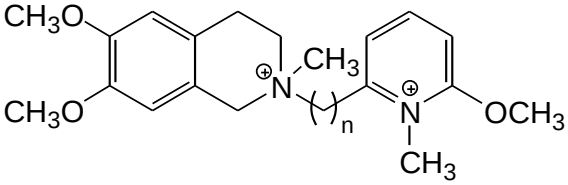

2 $CF_3SO_2^{\ominus}$ n = 4, 5, 6, 7

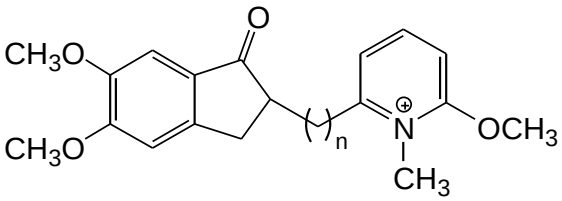

$CF_3SO_2^{\ominus}$ n = 5, 6, 7

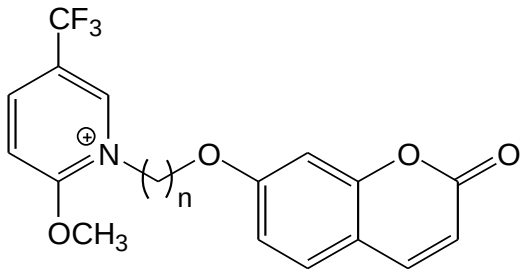

$CF_3SO_2^{\ominus}$ n = 3, 4, 5

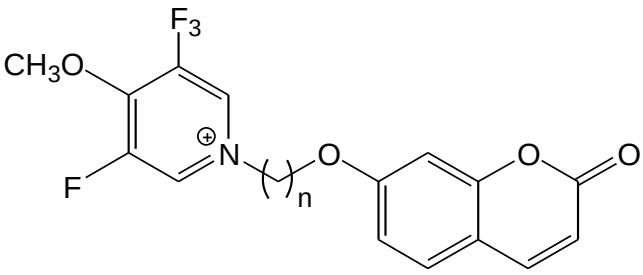

$CF_3SO_2^{\ominus}$ n = 3, 4, 5

Figure 1.16: Methoxypyridinium compounds as aged AChE reactivating agents studied in our research group

CHAPTER 2: SYNTHESIS AND KINETIC EVALUATION OF 2-PYRIDINE ALDOXIME METHYL HALIDE (2-PAM) ANALOGS AS NOVEL ALKYLATING AGENTS OF AGED HUMAN ACETYLCHOLINESTERASE

Chemical Mechanism and Significance

The fundamental role of acetylcholinesterase is to terminate nerve impulse transmission at both cholinergic synapses and neuromuscular junctions by rapid hydrolysis of the neurotransmitter acetylcholine.[11] This principle role of AChE makes it a target of a wide range of toxicants including organophosphorous (OP) nerve agents.[2] Among AChE inhibitors, OP inhibitors are extremely toxic chemicals and OP based insecticides are causing about 200,000 annual deaths throughout the world.[43] OP inhibitors exert their acute toxicity by phosphylating the AChE active site serine hydroxyl group.[3] Thus, inhibited enzyme can not hydrolyze neurotransmitter acetylcholine, resulting in the accumulation of acetylcholine in the cholinergic synapses and neuromuscular junctions of the body, thereby causing overstimulation of cholinergic receptors..

Phosphylation of cholinesterases occurs rapidly and biomolecular rate constants range from 10^7-10^{10} M^{-1} min^{-1}.[34] The resultant phosphylated-enzyme intermediate (Figure 2.1) resembles the acetylated enzyme intermediate that results from the normal substrate catalytic mechanism, but with a greater stability. The half-life of acylated-AChE is reported to be less than 1 ms, whereas phosphylated-AChE half- lives ranged from hours to days.[108] Spontaneous hydrolysis of the phosphylated-enzyme is extremely slow but some AChE-OP conjugates can be readily reactivated by strong nucleophilies such as oximes.[108] However, oxime reactivation of phosphylated enzymes that result from nerve agents such as soman (due to rapid aging) and tabun (because lone electron pair at the amide nitrogen hinders the nucleophilic attack on the phosphorous atom of phosphylated AChE by the oxyanion of the oximes) are also found to be difficult.[109,110]

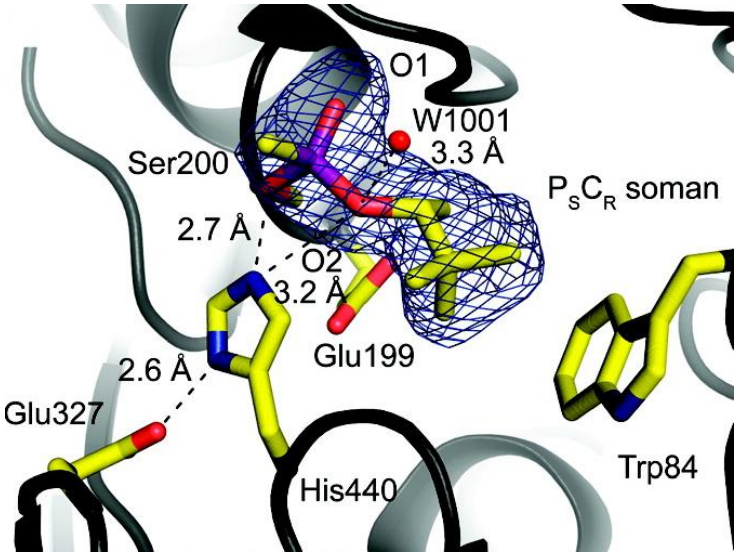

Figure 2.1: Crystallographic structure of *Torpedo Californica* AChE that has been phosphylated by soman nerve agent (non-aged AChE adduct).

Reprinted with permision from Sanson, B.; Nachon, F.; Colletier, J.-P.; Froment, M.-T.; Toker, L.; Greenblatt, H. M.; Sussman, J. L.; Ashani, Y.; Masson, P.; Silman, I.; Weik, M. *Journal of Medicinal Chemistry* **2009**, *52*, 7593. Copyrights (2009) American Chemical Society

The effectiveness of the oxime reactivators as antidotes primarily depends on the nucleophilic displacement rate of the OP moiety from the OP-AChE complex. Moreover, the reactivation of the inhibited enzyme depends on the structure of the OP that caused the inhibition.[34,111] In the oxime reactivation reaction, oximate ions formed in the physiological conditions attack nucleophilically on the phosphorous atom of the phosphylated enzyme and form an oxime-OP product after displacing the enzyme as leaving group, thereby restoring the enzyme function. But, many phosphylated-AChE complexes undergo a spontaneous time-dependent secondary reaction called aging. In the aging process, dealkylation of the phosphylated enzyme occurs through alkyl-oxygen bond scission, which results in an irreversibly inactivated enzyme and so far, none of the reactivators is capable of reactivating aged AChE adducts.[2,42,43,50]

AChE accelerates this de-alkylation by a factor of 10^{10} when compared to a non enzymetic de-alkylation process.[43]

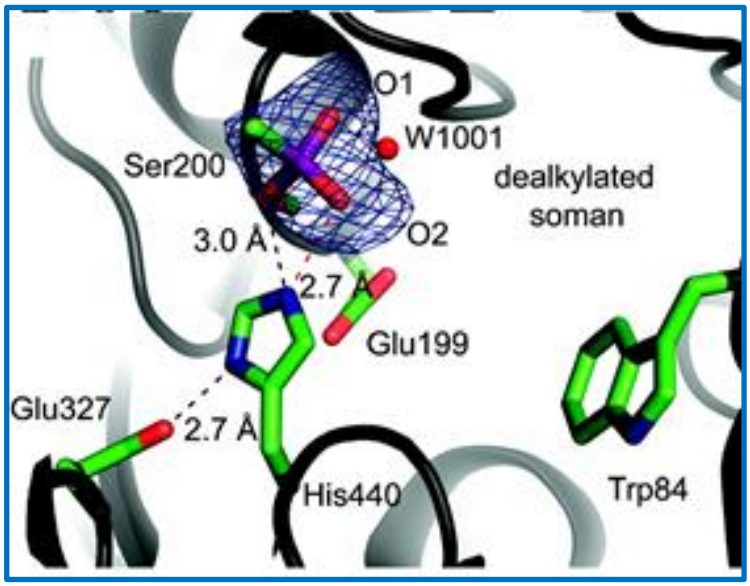

Figure 2.2: Crystallographic structure of the aged conjugate of *Torpedo Californica* AChE and the soman nerve agent

Reprinted with permision from Sanson, B.; Nachon, F.; Colletier, J.-P.; Froment, M.-T.; Toker, L.; Greenblatt, H. M.; Sussman, J. L.; Ashani, Y.; Masson, P.; Silman, I.; Weik, M. *Journal of Medicinal Chemistry* **2009**, *52*, 7593. Copyrights (2009) American Chemical Society

The rate constant of aging (k_a) depends on various factors such as the nature of the OP, nature of the alkyl groups (branched alkyl groups undergo dealkylation much faster than short alkyl chains), nature of the enzyme, the source of the enzyme and the physicochemical conditions such as pH, and temperature of the reaction medium.[76,112,113] A number of studies have also shown that spontaneous reactivation and aging rates depend on the nature of the nerve agents.[10,47,48,113] Aging half-lives are 2-4 min for soman, 5-12 h for sarin, 13-46 h for tabun and 48 h for VX.[3,46] Among many OPs, soman is one of the fastest that produces aged AChE adduct. Dealkylation of

the soman inhibited AChE is accompanied by loss of a pinacolyl group ($CHCH_3C(CH_3)_3$) (Figure 2.2).[42,43] Although the mechanism of enzyme induced aging is not fully understood, it has been found that some amino-acids residues in the active site gorge including Trp84 play significant roles in the aging process.

Since the early 1950s, although numerous nucleophilic oximes including mono pyridinium and bispyridinium compounds have been synthesized and evaluated for reactivation of AChE inhibited by different nerve agents such as soman, tabun and cyclosarin, only a few have been tested for human use [33] Monopyridinium oximes such as 2-PAM and obidoxime are used as current antedotes for OP poisioning. However, some bispyridinium oximes such as HI-6, MMB-4 and HLö 7 are also found to be more effective antedotes for OP inhibition, specially by nerve agents, but are under advanced development.[34,108] For example, aqueous solutions of some of these bispyridinium reactivators such as HI-6, and HLo7 are very unstable at physiological pH, which limits their use as effective reactivators for human use.[50] However, the currently available clinically approved oximes are not potent for all nerve agents' intoxications.[92,114]

2-PAM is one of the longest employed reactivators for OP intoxication and has also been found to bind with aged enzyme that results from some nerve agents, e.g. soman.[43] 2-PAM binds to the catalytic anionic site of the AChE where the pyridinium ring of 2-PAM interacts with indole moiety of Try84 via π-π stacking. However, experiments have shown that 2-PAM is unable to reactivate the aged AChE adduct. For example, the crystal structure of the ternary complex of 2-PAM bound to aged soman-AChE revealed that the oximate ion of the 2-PAM is not properly oriented to make the nucleophilic attack on the electrophilic phosphorous atom of the aged soman-AChE adduct (Figure 2.3).[43]

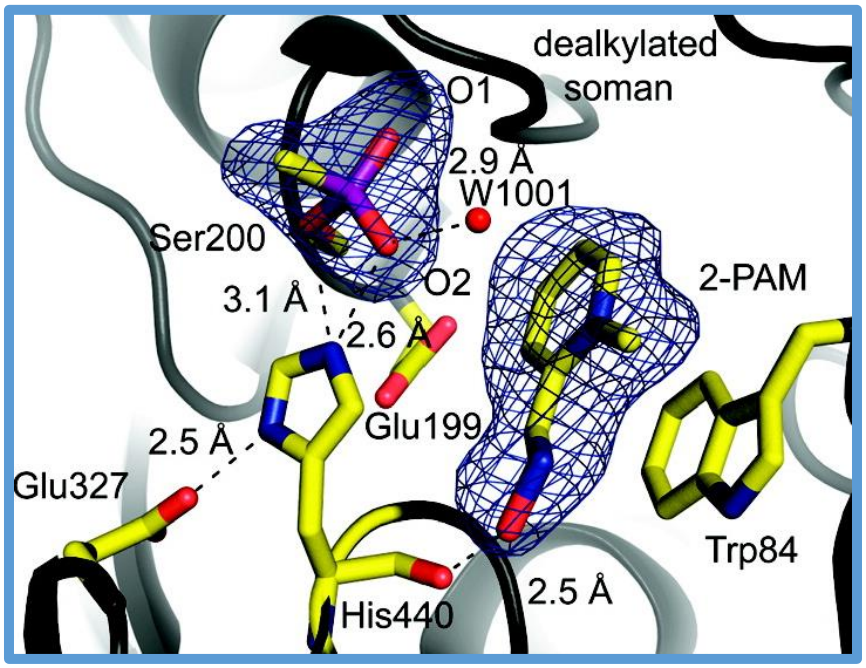

Figure 2.3: Crystallographic structure of the complex of 2-PAM with the aged conjugate of *Torpedo Californica* AChE and the soman nerve agent

Reprinted with permision from Sanson, B.; Nachon, F.; Colletier, J.-P.; Froment, M.-T.; Toker, L.; Greenblatt, H. M.; Sussman, J. L.; Ashani, Y.; Masson, P.; Silman, I.; Weik, M. *Journal of Medicinal Chemistry* **2009**, *52*, 7593. Copyright (2009) American Chemical Society

Objective of the Study

None of the reactivators is capable of reactivating aged enzyme so far.[2] We hypothesize that dealkylation (formation of aged enzyme) could be reversed by novel alkylating agents, so that current oximes would then be used to reactivate the the phosphyl-AChE complex. Since 2-PAM is shown to bind to the active site of aged enzyme, the pyridinium scaffold was used to design our putative alkylating agents. These alkylating agents would bind to the aged enzyme's active site and transfer a methyl group to the aged enzyme, and thereby form both non-aged enzyme and 2-PAM *in situ*. Then, 2-PAM formed *in situ* would reactivate the newly formed non-aged enzyme.

Materials and Methods

This research has the following objectives:

1. Synthesis of relevant alkylating agents

2. Evaluating alkyl transfer abilities in a model reaction

3. Biological evaluation to find the reactivating abilities of alkylating agents for aged-AChE adducts.

1. Synthesis of Relevant Alkylating Agents

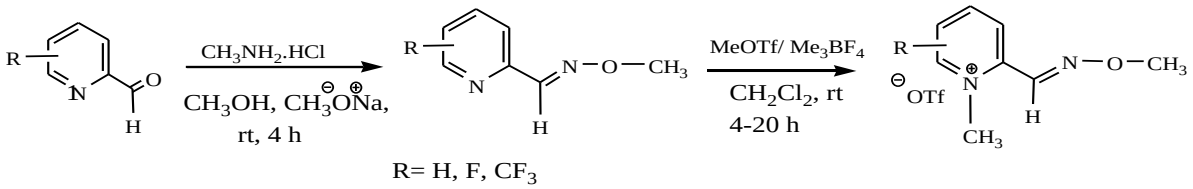

Scheme 2.1: General reaction scheme for preparation of methyl oxime analogous

The N-methyl oximes were synthesized (Scheme 2.1) according to the literature with few modifications.[115] All the chemicals and reagents were obtained from commercial vendors and used without purification. Methoxy amine hydrochloride (Sigma), Sodium methoxide (Aldrich), Methyl triflouromethanesufonate (Sigma-Aldrich), and trimethyloxonium tetraflouroborate (Sigma-Aldrich). Methylene dichloride, Methanol and diethyl ether were obtained from Sigma Aldrich in septum-sealed containers, and were kept under inert gas (e.g. Argon gas). Herein, pyridine-2-carboxaldehydes (Sigma-Aldrich) with various substituents on the pyridine ring were reacted with methoxyamine followed by alkylation with methyl triflate (MeOTf) or trimethyloxonium tetraflouroborate (Me_3OBF_4) at room temperature. Described here is the method in detail for unsubstituted oxime analog. A 108 mg (1.29 mmol) sample of methoxyamine hydrochloride and 81mg of sodium methoxide (1.5 mmol) were added to a round bottom flask equipped with a rubber septum and magnetic stir bar; 5 mL of methanol under argon pressure was then added to the solids via syringe. The reaction was allowed to happen for 15 minutes and the reaction mixture was

filtered through a pipette filter to remove remaining solid materials. To the filtered solution, liquid pyridine-2-carboxaldehyde (100 mg, (0.1 ml), 1.20 mmol) was added. The reaction was allowed to happen under reflux for four hours. The reaction mixture was then filtered through a celite filter with layers of sand and silica. Solvents were evaporated by rotatory evaporator under reduced pressure. The residue was then purified by flash chromatography performed on a Teledyne ISCO CombiFlash RF system utilizing normal phase pre-column cartridges and gold high performance columns eluting with ethyl acetate and hexane (gradient 0%- 100%) with 2% TEA (triethyl amine). Product was obtained by removing solvents by rotatory evaporator under reduced pressure. The final product was characterized by ^{1}H NMR, ^{13}C NMR and ^{31}P NMR.

Methyl oxime (31 mg, 0.23 mmol) was then dissolved in 2.5 mL of dichloromethane. Trimethyloxonium tetraflouroborate (34 mg, 0.23 mmol) was added in one portion at room temperature as well. The reaction flask was kept at room temperature and stirring was maintained at ca. 400-600 rpm. Over the course of the reaction (20 hrs.) white colored precipitate was formed. At the end of the reaction, stirring was stopped and the solvent was removed by pipette. The precipitate was rinsed with DCM (dichloromethane) 3 times (4 mL for each) and solvent was removed by pipette. The residual solvent was removed under vacuum.

All proton (^{1}H) nuclear magnetic resonance spectra were recorded on 400 MHz or 500 MHz Brucker spectrometer. All carbon (^{13}C) nuclear magnetic resonance spectra were recorded on the same spectrometers at 100 or 125 MHz and fluorine (^{19}F) nuclear magnetic resonance spectra were recorded at 477 MHz on above spectrometers with proton decoupling. Chemical shifts are expressed in parts per million (scale) and are referenced to residual ^{1}H in the NMR solvent (acetone: 2.05, DMSO: 2.50), to the central carbon in the NMR solvent (acetone: 204.19, or 30.0, DMSO: 39.5). Data are presented as follows: chemical shift, multiplicity (s = singlet, d = doublet,

t = triplet, q = quartet, m = multiplet, and bs = broad singlet), integration, and coupling constant in Hertz (Hz). Infrared (IR) spectra were collected on a JASCO FT/IR 4100 instrument and are reported in cm^{-1}. High resolution mass spectrometry (Waters GCT-30 meters DB5-MS) utilizing electrospray ionization or electron impact ionization in positive mode was performed to confirm the identity of the compounds.

2. Evaluating Alkyl Transfer Abilities in a Model Reaction

The effectiveness of the above synthesized compounds as methyl transfer agents was first evaluated by using sodium methyl methanephosphonate as an analogue of the aged AChE-OP adduct. Model reactions were conducted in an NMR tube by mixing equimolar concentrations of phosphonate salt (27 mM in d_6-DMSO) with the methyloximes synthesized above. The reaction was monitored by ^{1}H-NMR for a few hours or days depending on the methyl transferring rate.

To a vial (1 mL), 2-PAM analogs synthesized above (3-5 mg) were added, and the vial was sealed and brought into the NMR lab. The NMR was pre-locked and shimmed onto a DMSO-D_6 solution. A relevant volume of 27 mM saturated sodium monomethylmethylphosphonate in DMSO-D_6 was calculated so that the ratio of the 2-PAM analog species and the phosphorous species would be close to unity at time = 0. The calculated amount of DMSO-D_6 solution was added to the 2-PAM analog, the sample was mixed, drawn up by glass pipette, and injected into an NMR tube. The NMR tube was caped, and loaded into the NMR instrument as soon as possible. The time from contact to the time at which a spectrum was first obtained was between 45 and 90 seconds. For simplicity, the first ^{1}H NMR spectrum obtained was set to time = 1 min for all kinetic calculations. The time for subsequent data points was determined to the minute by difference using the FID time stamps. For early time points or for rapid reactions, 16 ^{1}H NMR scans were obtained for every time point. For latter time points, after 10 min, or for slower reactions 32 ^{1}H NMR scans were

obtained for every time point. Between each data acquisition, the tube was maintained at 25 ^{o}C $\pm$ 0.5 ^{o}C either within the NMR instrument (for fast reactions), or in a heated water bath (for slow reactions).

The relative quantity of each species present was obtained from integration of the ^{1}H NMR spectrum at every time point. The P-CH_3 methyl doublet appeared at 1.42 ppm for dimethyl methyl phosphonate and 0.9 ppm–1.1 ppm range was for sodium dimethyl phosphonate (this methyl shifted slowly downfield and broadened as the reaction progressed). The integration of residual ^{1}H-DMSO was used as an internal standard by which the integrations were normalized. Sample ^{1}H NMR spectra, taken at various time points, have been included in the spectra portion of the Appendix for each reaction. Additionally, ^{31}P NMR and ^{19}F NMR analysis of the final mixture confirmed the presence of relevant products for each experiment.

3. Biological Evaluation to Find the Resurrecting Abilities of Alkylating Agents for Aged-AChE adducts

3.1 Half-Inhibitory Concentration (IC_{50}) Determination

IC_{50} of each 2-PAM analog was determined by dose response assay. Each alkylating agent was incubated with human acetylcholinesterase at various concentrations of the alkylating agent and initial rates of the substrate hydrolysis in the presence of alkylating agents were determined using the well-known colorimetric Ellman assay.[116] According to the Ellman assay procedure, acetylthiochiline is used as the substrate analog and allowed to be hydrolyzed by acetylcholinesterase (Scheme 2.2). The thiocholine product resulted from the enzyme hydrolysis reaction then breaks down the disulphide bond of the chromogen 5, 5'-dithiobis (2-nitrobenzoic acid) (DTNB), which forms the thionitrobenzoate anion which absorbs visible light at 412 nm (Scheme 2.3).

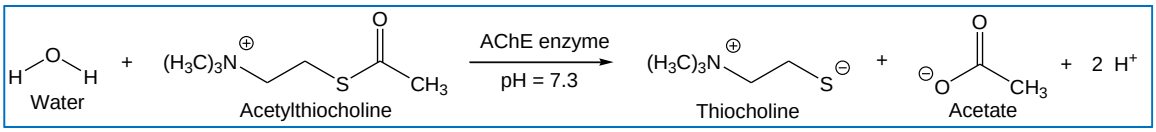

Scheme 2.2: Enzymatic hydrolysis of the substrate analog acetylthiocholine

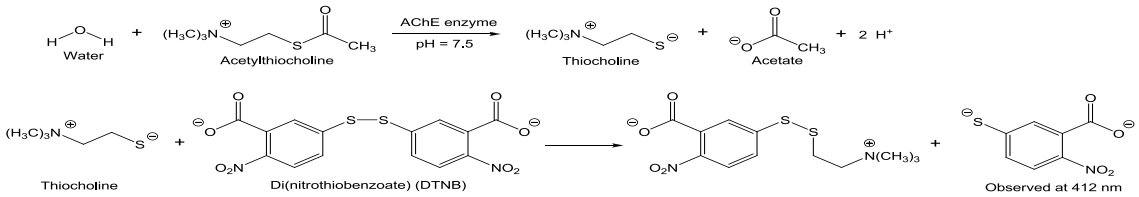

Scheme 2.3: Breakdown of the disulphide bond of chromogen DTNB by thiocholine to form thionitrobenzoate anion

Details of the dose response assay follow. The 50 mM reaction buffer at pH ranging from 7.2-7.4 (phosphate buffer, PB) was prepared using mono basic and dibasic sodium phosphate anhydrous reagents. The relevant masses of the weak acid (NaH_2PO_4) and its conjugate base (Na_2HPO_4) were calculated using the well-known Henderson-Hasselbalch equation and added to a total volume of 1 L of deionized-distilled water (DD water) that was filtered through a Barnstead International hose nipple organic removal ion exchange cartridge into a glass bottle previously washed. The pH of the buffer solution was determined using an ion selective pH electrode that was calibrated with pH 4, 7, and 10 solutions prior to each measurement. Unless otherwise stated, this assay solution was used to conduct the assay in order to measure the initial rates. All stock solutions were prepared from solid or liquid materials and stored in polypropylene containers at 4 ˚C or below. 0.1% w/v bovine serum albumin (BSA, from Sigma-Aldrich) was prepared by dissolving 250 mg of solid BSA in 250 mL of PB. 100 µg/1 mL hAChE (from Sigma-Aldrich) was prepared in 0.1% BSA. A 45 mM solution of the substrate analog acetylthiocholine (ATCh) in DD water, and a 20 mM solution of chromagen 5,5'-dithiobis(2-nitro benzoic acid) (DTNB) in PB were also prepared. Inhibitor (alkylating agents) solutions were prepared in DD water and dilutions were made by micropipette and all solutions were diluted by matching solvents to their parent stock.

Dose response assays were conducted on a Molecular Devices SpectraMaxM2 micro-plate reader using polystyrene 96-well plates (Costar, round bottom from Sigma-Aldrich). Ten different concentrations ranging from mM to µM or µM to nM were used and assays at each concentration were performed in duplicate. Substrate hydrolysis by AChE in the presence of each concentration of alkylating agent was measured spectrometrically at 412 nm (Figure 2.4) and 27 ˚C following the method described by Ellman.[116] Data were collected for ten minutes with minimum possible intervals and initial rates were determined by least square analysis of the time courses at less than 10% turnover of the initial substrate concentration.

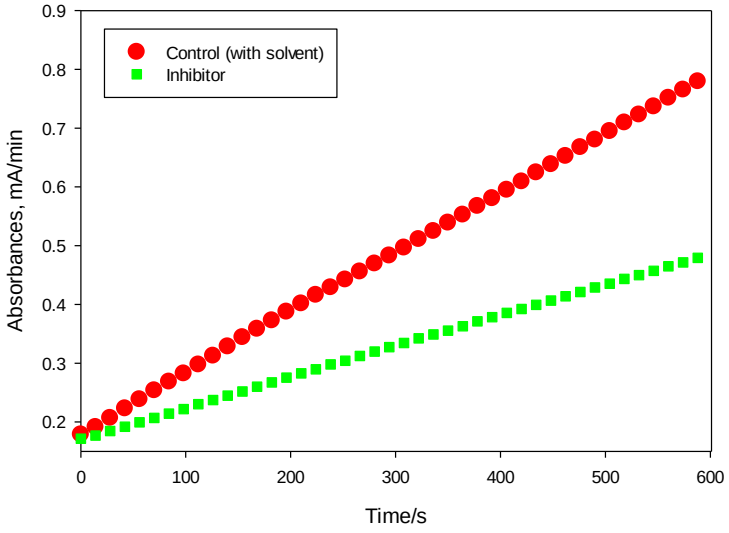

Figure 2.4: Sample graph showing time courses of the enzymatic substrate hydrolysis

At substrate concentration of 1.5 x 10^{-4} M in the presence (at 3.7 x 10^{-5} M) and absence of the inhibitor 4

All rates were corrected for non-enzymatic hydrolysis of the substrate. Non-linear regression analysis was performed using Sigma Plot 12.0 to obtain inhibition parameters. K_i^{app} values were calculated by plotting initial rates as a function of inhibitor concentration and by fitting

to Equation 2.1. Half inhibitory concentrations were determined at initial time points and after 2 hours of incubation with the enzyme to check if time dependent inhibition had occurred.

$$v_i = \frac{v_0}{1 + \frac{10^{\log[I]}}{\mathrm{K_i^{app}}}}$$

Equation 2.1: Initial rates equation for the hydrolysis of substrate ATCh by inhibited AChE

Where, K_i^{app} - apparent inhibitor dissociation constant (M), v_i and v_0 are initial rates in the presence and absence of inhibitor respectively (mA/min), [I] is the inhibitor concentration (M).

3.2 Resurrection Assay

Resurrection assays were performed by treating aged hAChE with alkylating agent and checking activity of the incubation mixture at different time points of the incubation. Details are provided later in this chapter.

3.2.1 Synthesis of Nerve Agent Analog

A nonvolatile analog of nerve agent sarin was synthesized by following the procedure which was initially conducted by Joseph Topczewski. A round bottom flask containing a stir bar was charged with solid 7-hydroxy-4-methylumbelliferone (from Aldrich, 181 mg, 1.07 mmol) and methylphosphonic dichloride (from Sigma-Aldrich, 300 mg, 2.27 mmol). The flask was kept under argon pressure. 5 mL of dry benzene were added to the flask to dissolve the solids. The flask was cooled to 0 °C (5 minutes) on ice and triethyl amine (from Sigma, 410 mg, 4.06 mmol) was added dropwise to the reaction mixture over 5 minutes. The mixture was allowed to warm gradually to room temperature over two hours and dry isopropanol (from Sigma-Aldrich, 119 mg, 1.99 mmol) was then added to the reaction mixture. Reaction was allowed to occur over 18 hours and stopped

by adding ethyl acetate. The mixture was gravity filtered and solvents were evaporated by rotatory evaporator under reduced pressure. The residue was then purified by flash chromatography performed on a Teledyne ISCO CombiFlash RF system utilizing normal phase pre-column cartridges and gold high performance columns eluted with an isopropyl alcohol and hexane (gradient 0%- 100%). The racemic mixture of the product was obtained as a clear oil and was characterized by ^{1}H NMR, ^{13}C NMR and ^{31}P NMR spectroscopies.

3.2.2 Preparation of Aged-hAChE

Phosphylation of hAChE by the sarin analog was achieved by incubating hAChE with excess sarin analog. Herein, 1000 µL of 4.8 nM hAChE in 0.1% BSA and sarin analog in acetonitrile (3×10^{-4} M) were prepared. 483 µL of the hAChE was then mixed with 17 µL of inhibitor solution or acetonitrile separately to prepare the respective experimental and control solutions. After 30 minutes of incubation at 27 °C, completeness of inhibition was determined by checking initial rates of substrate hydrolysis of the uninhibited (control) and inhibited (experimental) enzymes. Once enzyme is fully inhibited by the sarin analog (inhibited enzyme activity < 2% of control enzyme activity), excess inhibitor was separated from the enzyme to avoid the re-inhibition of recovered enzyme if any during the resurrection process. Sephadex G-50 Quick Spin Columns (Roche) were used in the separation and the column was standardized with 1200 µL of 0.1% (w/v) BSA by adding 300 µL each time for 4 times. The column was then packed by centrifugation at 1100 x g for 4 minutes. 500 µL from each uninhibited and inhibited hAChE were loaded to two separate columns by adding 250 µL at a time. Columns were centrifuged at 600 x g for 6 minutes. Separated enzyme was then allowed to age at 27 °C and extent of aging was determined at various time points (1h,10h and 48h) by following 30 minutes incubation of 10 fold

diluted enzyme (from control and experimental) with 100 µM 2-PAM followed by initial rates determination of substrate hydrolysis with uninhibited or oxime reactivated enzyme.

$$\%\ hAChEop\ residual = \frac{v_{i\ of\ hAChEop}}{vi\ of\ hAChEcontrol} x100$$

Equation 2.2: Equation for finding residual activity of inhibited enzyme (%hAChEop reactivated) following treatment with 2-PAM. v_i- hAChEop ≡ initial rates of the substrate hydrolysis by inhibited enzyme (in the presence of 2-PAM) (mA/min), v_i-hAChEcontrol ≡ initial rate of the substrate hydrolysis of uninhibited enzyme in the presence of 2-PAM (mA/min).

% hAChEaged = 100 - % hAChEop residual

Equation 2.3: Amount of unreactivated hAChE by 2-PAM treatment (% of aged enzyme)

Once phosphylated enzyme is almost completely aged (residual activity (calculated from Equation 2.2) of OP inhibited hAChE < 2% of control hAChE)), resurrection assays were performed by incubating aged enzyme (Equation 2.3 was used to calculate the aged AChE percentage) with resurrecting agents (2-PAM analogs). hAChE with only solvent that is used for OP preparation (control) was also incubated with resurrecting agent in parallel for comparison. The experiment was set up by preparing 100 µL of two incubation solutions containing inhibited enzyme and a 10 x IC_{50} concentration of 2-PAM analog and uninhibited enzyme (control) and a 10 x IC_{50} concentration of 2-PAM analog separately. Solutions were incubated at 27 °C for a 24 hour period. Substrate hydrolysis by experimental and control hAChE was then measured at each time point of 1h, 4h and 24h. A 10 µL aliquot was then added to the 300 µL well containing 50 mM PB, and 100 µM in-well concentration of 2-PAM. After 30 minutes incubation with 2-PAM, substrate (0.3 mM in-well ATCh) and chromagen (6.7 mM in-well DTNB) were added and initial rates of the substrate hydrolysis were determined. The percent of reactivated enzyme by 2-PAM

was determined by Equation 2.4. The percentage of resurrected enzyme at each time point was determined by Equation 2.5.

$$\%\ \text{reactivated hAChE} = \frac{vi\ hAChE\ aged}{vi\ hAChE\ control} x\ 100$$

Equation 2.4: Determination of the recovered activity of aged hAChE after incubation with resurrecting agent (alkylating agent) and 2-PAM.

%hAChE resurrected activity = % hAChE react activity- % residual hAChE activity

Equation 2.5: Determination of resurrected hAChE activity of aged enzyme

Where; % hAChE resurrected activity ≡ % of recovered activity of aged enzyme only with the presence of resurrecting agent. % hAChE react activity ≡ % total recovered activity of aged hAChE in the presence of resurrecting agent and 2-PAM. % residual hAChE activity ≡ % activity of aged hAChE without treating with resurrecting agent but only with 2-PAM incubation.

Results and Discussion

All the 2-PAM analogs and 4-PAM analogs were synthesized and characterized using spectroscopic methods mentioned in Materials and Methods. All the spectral data are shown in Appendix A.

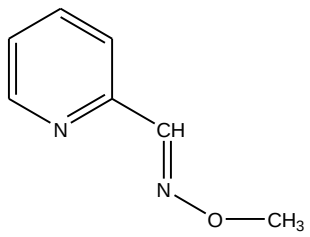

This compound has been previously synthesized and characterized. The data given here are in accordance with the literature report and are provided for convenience.

Reaction time: 4h, colorless oil, isolated yield: 24 %

^{1}H NMR ($CDCl_3$, 500 MHz): δ = 8.60 (dq, *J* = 4.8 Hz, 0.9 Hz, 1H), 8.43 (dt, *J* = 7.9 Hz, 1.1 Hz, 1H), 7.67 (m, 1H), 7.24(m, *J* = 5.6 Hz, 1H), 4.01 (s, 3H).

^{13}C NMR ($CDCl_3$, 125 MHz): δ = 151.6, 149.7, 149.1, 123.9, 121.0, 62.4.

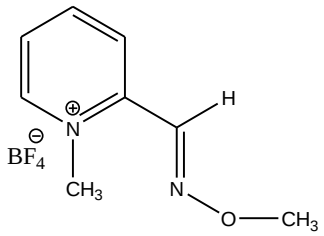

This compound has been previously synthesized and characterized. The data given here are in accordance with that report and are provided for convenience.

Reaction time: 24h, (white crystals) isolated yield: 62 %**^{1}H NMR (acetone, 500 MHz):** δ = 9.06 (d, *J* = 6.2 Hz, 1H), 8.82 (s, 1H), 8.67 (t, *J* = 8.0 Hz, 1H), 8.51 (d, *J* = 8.2 Hz, 3H), 8.17 (m, 1H), 4.63 (s, 3H), 4.16 (s, 3H).

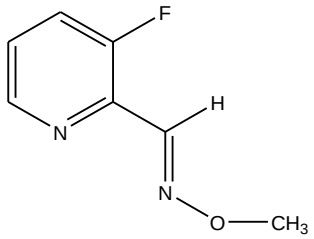

Reaction time: 24h, (light yellow oil) isolated yield: 77 %

^{1}H NMR ($CDCl_3$, 500 MHz): δ = 8.45 (dt, *J* = 4.6 Hz, 1.4 Hz, 1H), 8.32 (d, 0.7 Hz, 1H), 7.41 (m, 1H), 7.27 (m, 1H), 4.04 (s, 3H).

^{13}C NMR (acetone, 125 MHz): δ = 157.9 (d, $J_{C\text{-}F}$ = 265 Hz), 146.0 (d, $J_{C\text{-}F}$ = 5.2 Hz), 143.0 (d, $J_{C\text{-}F}$ = 2.2 Hz), 139.3 (d, $J_{C\text{-}F}$ = 10.3 Hz), 125.3 (d, $J_{C\text{-}F}$ = 3.7 Hz), 62.8.

^{19}F NMR (acetone, 470 MHz): δ = -124.6 (1F)

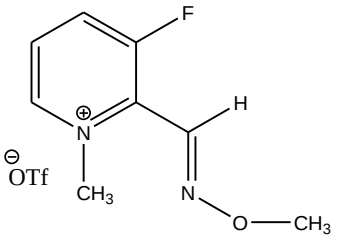

Reaction time: 24h, (white crystals) isolated yield: 95 %

^{1}H NMR (acetone, 500 MHz): δ = 9.09 (d, *J* = 6.1 Hz, 1H), 8.68 (t, *J* = 8.8 Hz 1H), 8.63 (s, 1H), 8.25 (m, 1H), 4.65 (s, 3H), 4.17 (s, 3H).

^{13}C NMR (acetone, 125 MHz): δ = 159.2 (d, $J_{C\text{-}F}$ = 261.1 Hz), 145.1, 138.2 (d, $J_{C\text{-}F}$ = 1.5 Hz), 137.0 (d, $J_{C\text{-}F}$ = 20.2 Hz). 133.5 (d, $J_{C\text{-}F}$ = 20.2 Hz), 129.0 (d, $J_{C\text{-}F}$ = 9.5 Hz), 63.6, 48.5.

^{19}F NMR (acetone, 470 MHz): δ = -79.0.0 (3F), -113.3 (1F)

IR (film, cm^{-1}): ν = 3102, 1632, 1508, 1473, 1157, 1045, 1030, 930.

HRMS (TOF EI+): calc. for $C_8H_{10}OFN_2$ $(M)^+$: 169.0779; found: 169.0777.

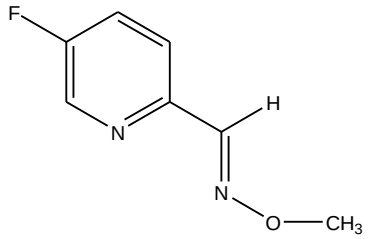

Reaction time: 24h, (colorless oil) isolated yield: 27 %

^{1}H NMR ($CDCl_3$, 500 MHz): δ = 8.42 (d, *J* = 2.9 Hz, 1H), 8.09 (s, 1H), 7.78 (m, 1H), 7.38 (m, 1H), 3.97 (s, 3H).

^{13}C NMR (acetone, 125 MHz): δ = 159.5 (d, $J_{C\text{-}F}$ = 258.5 Hz), 148.0 (s), 147.96 (s), 137.9 (d, $J_{C\text{-}F}$ = 24.2 Hz), 123.5 (d, $J_{C\text{-}F}$ = 19.1 Hz), 122.0 (d, $J_{C\text{-}F}$ = 5.1 Hz) 62.5.

^{19}F NMR (acetone, 470 MHz): δ = -125.3 (1F)

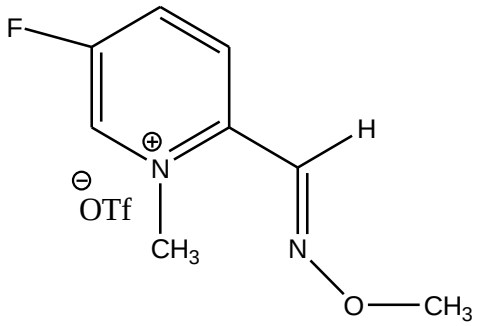

Reaction time: 24h, (white crystals) isolated yield: 98 %

^{1}H NMR (acetone, 500 MHz): δ = 9.29 (m, 1H), 8.77 (s, 1H), 8.59 (m, 2H), 4.64 (s, 3H), 4.14 (s, 3H).

^{13}C NMR (acetone, 125 MHz): δ = 160.1 (d, $J_{C\text{-}F}$ = 255.1 Hz), 144.7, 140.6 (d, $J_{C\text{-}F}$ = 1.5 Hz), 136.9 (d, $J_{C\text{-}F}$ = 36.2 Hz), 133.0 (d, $J_{C\text{-}F}$ = 19.2 Hz), 127.7 (d, $J_{C\text{-}F}$ = 8.1 Hz), 63.6, 47.2.

^{19}F NMR (acetone, 470 MHz): δ = -79.0 (3F), -118.3 (1F)

IR (film, cm^{-1}): ν = 3102, 1632, 1508, 1473, 1157, 1045, 1030, 930.

HRMS (TOF EI+): calc. for $C_8H_{10}OFN_2$ $(M)^+$: 169.0771; found: 169.0777.

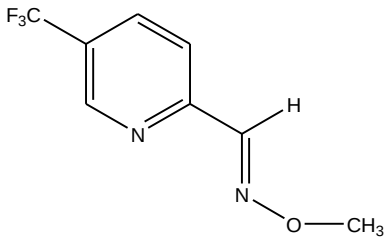

Reaction time: 24h, (greenish yellow oil) isolated yield: 54 %

^{1}H NMR ($CDCl_3$, 500 MHz): δ = 8.86 (m, 1H), 9.04 (dd, 1H), 7.92 (m, 2H), 4.05 (s, 3H).

^{13}C NMR (acetone, 125 MHz): δ = 155.40 (m), 148.15 (s), 146.38 (q, $J_{C\text{-}F}$ = 4.3 Hz), 133.92 (q, $J_{C\text{-}F}$ = 3.4 Hz), 125.14 (s), 122.44 (s), 120.09 (s), 62.16 (s).

^{19}F NMR (acetone, 470 MHz): δ = -63.09 (3F)

HRMS (TOF EI+): calc. for $C_8H_8N_2OF_3$ $(M+H)^+$: 205.0574; found: 205.0589.

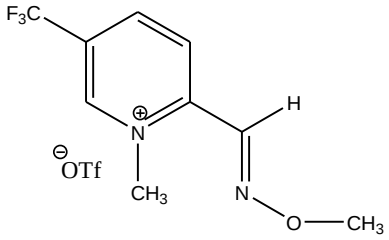

Reaction time: 24h, (brown solid) isolated yield: 50 %

^{1}H NMR (acetone, 500 MHz): δ = 9.68 (s,1H), 9.04 (dd, J = 8.8 Hz,1.8 Hz,1H), 8.94(s,1H), 8.80 (d, J = 8.6 Hz,1H), 4.80 (s, 3H), 4.23 (s, 3H).

^{13}C NMR (acetone, 125 MHz): δ = 150.9, 145.5, 142.0 (q, $J_{C\text{-}F}$ = 3.5 Hz), 140.9, 121.3 (2 q) 64.2, 47.2.

^{19}F NMR (acetone, 470 MHz): δ = -63.0 (3F), -78.9 (3F)

IR (film, cm^{-1}): ν = 3102, 1632, 1508, 1473, 1157, 1045, 1030, 930.

HRMS (TOF EI+): calc. for C_7H_9OFN $(M)^+$: 169.0777; found: 169.0779.

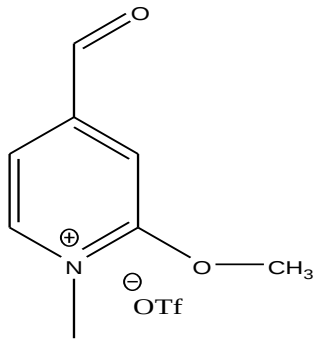

Reaction time: 24h, (colorless oil) isolated yield: 24 %

^{1}H NMR (acetone, 500 MHz): δ = 10.30 (s,1H), 8,90 (d, *J* = 6.5 Hz,1.8 Hz,1H), 8.29 (d, *J* = 1.2 Hz,1H), 7.90 (dd, *J* = 6.5 Hz,1.5 Hz,1H) 4.50 (s, 3H), 4.24 (s, 3H).

^{13}C NMR (acetone, 125 MHz): δ = 189.8, 162.8, 149.6, 145.6, 116.4, 108.1, 59.8, 42.9.

HRMS (TOF EI+): calc. for $C_8H_{10}NO_2$ $(M)^+$: 152.0695; found: 152.0712.

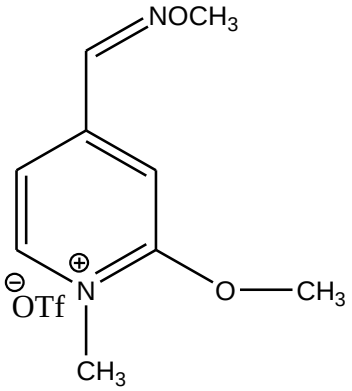

Reaction time: 24h, (brown liquid) isolated yield: 90 %

^{1}H NMR (acetone, 500 MHz): δ = 8.66 (d, *J* = 6.7 Hz, 1H), 8.29 (s, 1H), 7.95 (d *J* = 1.5 Hz, 1H) (dd,*J* = 6.7 Hz, 1.7 Hz, 1H) 4.43 (s, 3H), 4.08 (s, 3H), 3.83 (s,3H).

^{13}C NMR (acetone, 125 MHz): δ = 161.5, 150.6, 145.0, 143.8, 114.5, 108.7, 63.0, 59.3, 41.1.

Five PAM analogs (four 2-PAM analogs and one 4-PAM analog) were synthesized and characterized using spectroscopic methods explained in the experimental procedure. All the

spectra are recorded in Appendix A. All compounds were novel AChE inhibitors and all four inhibitors but not 2-PAM analog were newly synthesized and were not reported in the literature.

In the model study, the progress of the reaction was monitored by formation of the product dimethoxymethyl phosphonate and a sarin analog. Model study showed that the aged enzyme analog was methylated by unsubstituted and CF_3 (a strong electron withdrawing group) containing 2-PAM analogs up to some extend (3% after 28 hours and 8% after 24 hours respectively) while 2-PAM analogs containing F substituents on the pyridinium ring showed formation of a sarin analog (33% after 24 hours). The 4-PAM analog showed no reaction with aged analog (some sample spectra for the model reaction with each inhibitor are shown in the Appendix A. A proposed mechanism of the formation of the sarin analog is shown in the scheme 2.4

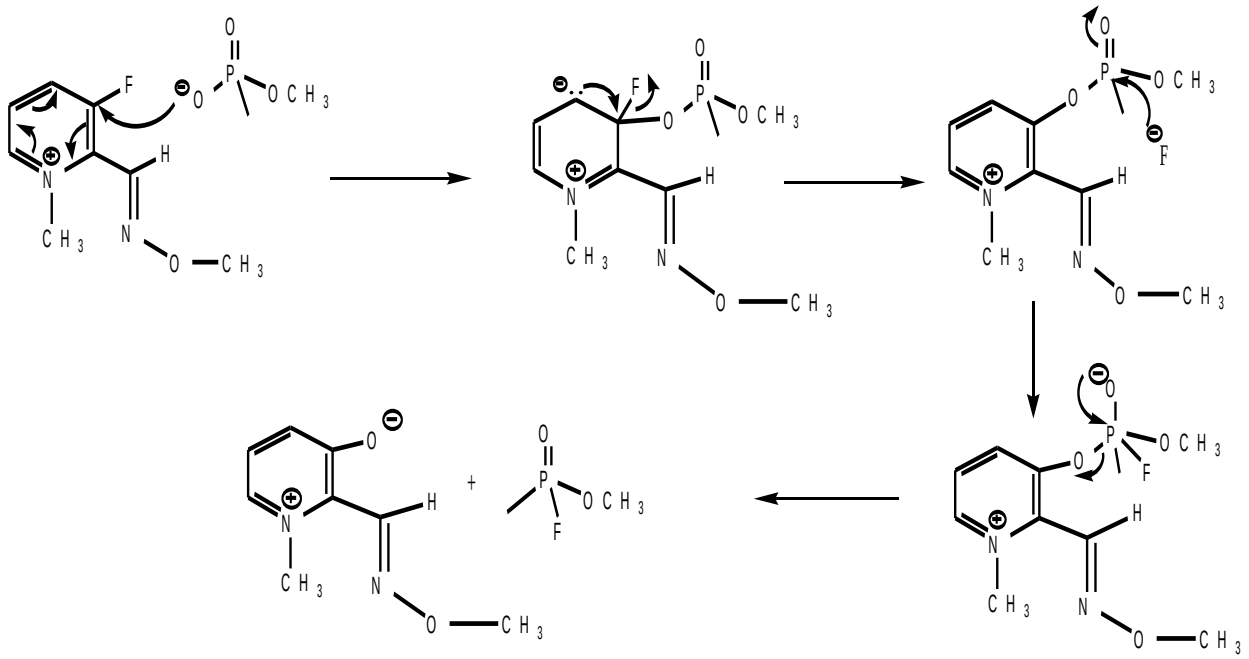

Scheme 2.4: Proposed mechanism for the formation of sarin analog for 'F' containing 2-PAM analogs

In the case of sarin analog formation, the electron withdrawing ability of the flourine substituent makes the aromatic carbon attached to it more susceptible for nucleophilic attack from the oxyanion of the aged enzyme analog than is in the methyl group on the oxime moiety. Thus, inhibitors in which pyridine rings are substituted with fluorine showed formation of methylsarin instead of methylating the aged enzyme analog. All the biological assay data were collected by me and Alexander Lodge. For convenience, all the data are shown in this thesis.

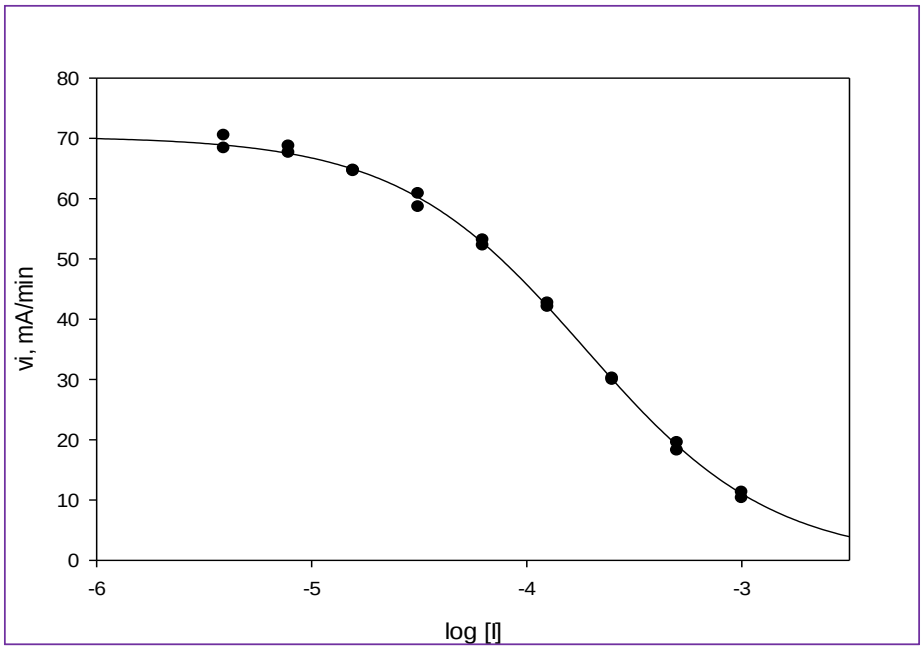

Figure 2.5: Example for IC_{50} curve obtained for inhibitor 4 at zero hour time point after incubation with hAChE

Table 2.1: Half inhibitory concentrations at 0 hour and after 2 hour incubation with AChE

Entry	R	IC_{50}/ µM	
		t=0 h	t=2h
1	H	70 ± 20	80 ± 40
2	3-F	110 ± 20	33 ± 4
3	5-F	70 ± 10	9 ± 2
4	5-CF_3	90 ± 2	160 ± 20
5	2-OCH_3, 4-$CNOCH_3$	340 ± 40	340 ± 60

IC_{50} values for all the inhibitors in this family ranged from 70- 340 µM. Regioisomer 3 was more potent inhibitor than its counterpart 2. All the 2-PAM analogs were more potent inhibitors of hAChE than the 4-PAM analog. Inhibitors containing F substitution on the aromatic ring showed time-dependent inhibition from the preliminary assay. Therefore, discontinuous stop time assay was conducted for inhibitors 2 and 3. IC_{50} values were collected for several hours. Data from the stoptime assay are shown in Figures 2.6 and Table 2.2. The pseudo-first order rate constants (k_{obs}) were obtained by finding the percent of control activity remaining at each time point using Equation 2.6.

$$\%\text{hAChE activity}_{(\text{inhibitor})} = \%\text{hAChE activity}_{(\text{control})}\, e^{-k_{obs}t}$$

Equation 2.6: Pseudo first-order rate equation for OP inhibition of hAChE

k_{obs} ≡ observed pseudo first-order rate constant; t≡ time; %hAChE activity $_{(inhibitor)}$ ≡ activity of the hAChE in the prescence of inhibitor, % hAChE activity (control)≡ activity of the uninhibited hAChE.

Table 2.2: IC_{50} values for inhibitors 2 and 3 over 7 hour period

Inhibitors	**IC_{50} /µM**						
	0 min	30 min	60 mim	2 h	3 h	4 h	7 h
2	74 ± 10	45 ± 4	31 ± 3	22 ± 2	21 ± 2	19 ± 3	22 ± 2
3	100 ± 6	-	104 ± 6	90 ± 8	79 ± 5	58 ± 8	34 ± 3

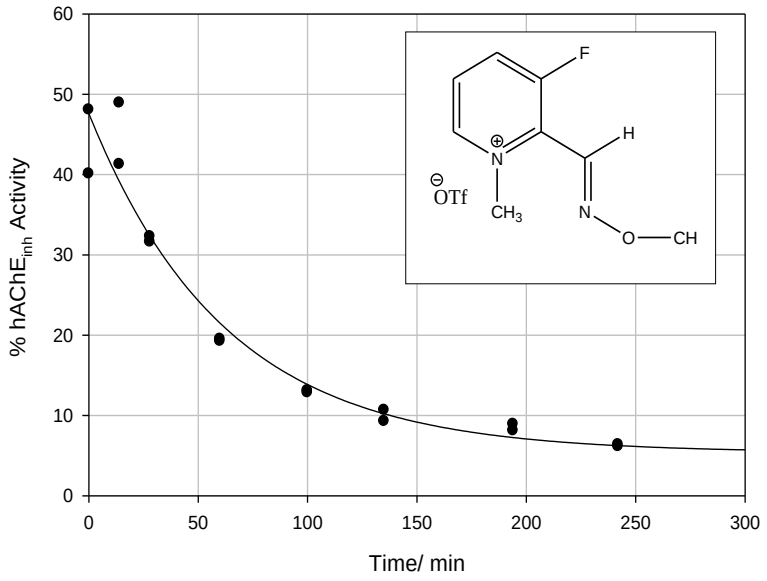

Figure 2.6: Plot of stop time assay for inhibitor 2 (1µM) for determination of pseudo first-order rate constant

Apparent reduction of half maximal inhibitory concentration over time and plots for pseudo first order rate determination confirmed the irreversible inhibition of hAChE from 2-PAM analogs that have flourine substituents on the aromatc ring (inhibitors 2 and 3).

Conclusion 1

Novel 2-PAM and 4-PAM analogs were successfully synthesized and their inhibition kinetics on hAChE were determined. The reactivation kinetics on aged hAChE that resulted from organophosphorous nerve agent sarin analog inhibition were also obtained. All the inhibitors of this family were more potent inhibitors of hAChE at the initial time point than commercially available 2-PAM. Unsubstituted and triflouromethyl (a strong electron withdrawing group) containing inhibitors were reversible inhibitors of hAChE while fluorine substituted inhibitors showed time dependent inhibition. From the model study, it was observed that flourine substituted inhibitors formed the sarin analog methylsarin (nerve agent analog) with the aged AChE analog, which suggested a nucleophilic aromatic substitution mechanism. This nucleophilic aromatic substitution suggests the formation of an arylated phosphyl-AChE complex during the reactions of aged AChE and the fluorine-containing compounds. However, from the preliminary data, although some 2-PAM analogs showed methyl transfer ability, none of the 2-PAM analogs or 4-PAM analog were able to resurrect (via methylation or arylation of aged AChE) the aged enzyme. Since 2-PAM is a comparatively big molecule, steric hindrance might prevent relevant nucleophilic attack on the putative arylated phosphyl-AChE complex. Thus, no activity of the aged enzyme was observed for the resurrection assay when 2-PAM is used as the oxime reactivator for the experiment. However, smaller oximes than 2-PAM might be able to resurrect the arylated enzyme due to less steric hindrance. Several research studies have found that MINA (monoisonitrosoacetone) is effective on reactivation of sarin inhibited acetylcholinesterase before aging occurs.[117] Since MINA is a small oxime, it would be able to reach to the hAChE active site easily and reactivate the arylated enzyme that would result from the incubation of aged hAChE with fluorine substituted oxime analogs.

3.3 Resurrection Assay with MINA

Chemical Significance

Treatments of OP poisoning mainly include the use of the muscarinic antagonist atropine and salts of monopyridinium or bispyridinium oximes such as 2-PAM and obidoxime. These salts do not readily penetrate the blood brain barrier so that they show limited efficacy on reactivation of brain AChE. Before introducing quarternized pyridinium oximes, lipid soluble tertiary oximes that penetrate the blood brain barrier were introduced and one of the widely studied tertiary oximes was MINA (Figure 2.7). MINA was tested as an OP reactivator against different OPs and found to be effective at relatively higher concentration against nerve agent sarin poisoning in various cases.[56,60,62,92,118]

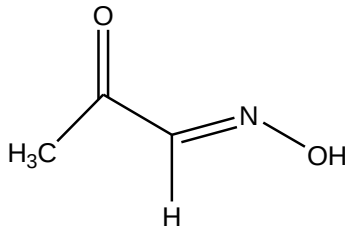

Figure 2.7: Chemical structure of monoisonitrosoacetone (MINA)

Objective of the study

According to the proposed mechanism explained above for the formation of methylsarin in the model study, it was suggested that arylated phosphyl-AChE complex may result from the incubation of aged hAChE with inhibitors 2 and 3. Formation of methylsarin was also observed for another set of inhibitors that have fluorine on the aromatic ring, 2-Methoxy N-methyl pyridinium inhibitors (structures are shown in right after Figure 2.8 and reaction with Inhibitor 6 was very fast under the experimental conditions (Joseph Topczewski, personal communication of unpublished results). Although none of the compounds resurrected the activity of the aged enzyme when 2-PAM is used as the oxime reactivator from the previous study, a small oxime such as MINA may be able to reach to the hAChE active site easily and reactivate the arylated enzyme.

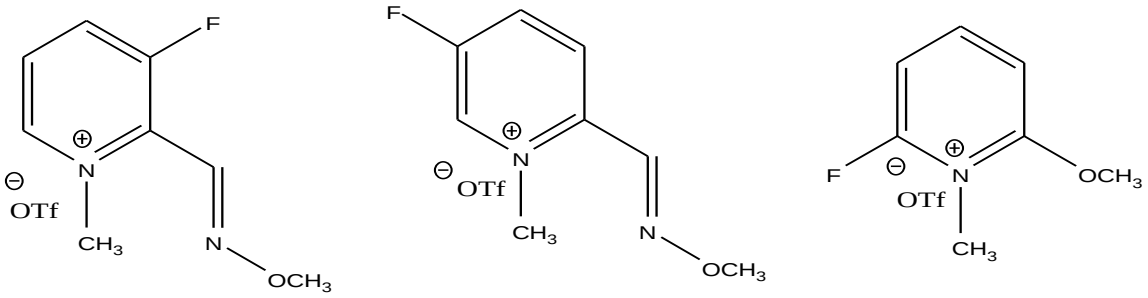

Inhibitor 2 Inhibitor 3 Inhibitor 6

Figure 2.8: Chemical structures of the inhibitors used for reactivation of aged AChE for the MINA experiment

Materials and Methods

Phosphylated hAChE was achieved by incubating hAChE with excess sarin analog as explained earlier in the resurrection procedure. After 30 minutes of incubation at 27 °C, completeness of inhibition was determined by checking initial rates of substrate hydrolysis of the uninhibited and inhibited enzymes. Once enzyme is fully inhibited by sarin analog (< 2% of control), excess inhibitor was separated from the enzyme using Sephadex G-50 Quick Spin Columns to avoid the re-inhibition of recovered enzyme. Separated enzyme was then allowed to age at 27 °C and extent of aging was determined as explained earlier. Aged enzyme was then incubated at 27 °C for 24 hour period with different concentration of inhibitors (eg., 10 K_i, 5 K_i, 2.5 K_i, 1 K_i. etc). A 10 µL aliquot was then added to the 300 µL well containing 50 mM PB, and 10 mM MINA. After 30 minutes incubation with MINA, substrate (0.3 mM ATCh) and chromagen (0.45 mM DTNB) were added and initial rates of the substrate hydrolysis were determined. The percent of reactivated enzyme by MINA from the resurrected enzyme was determined by Equations 2.4.and 2.5. Incubation with 2-PAM was also performed in parallel for comparison.

Since these inhibitors showed time dependence inhibition, another experiment was performed by only incubating aged enzyme with a 5 K_i concentration of 6-flouro-N-methyl 2-methoxypyridinium triflate (Inhibitor 6) for 45 minutes and excess inhibitor was removed by Sephadex G-50 Quick Spin Collumn. Here, excess inhibitor was removed to prevent the reinhibition of resurrected hAChE if any. Both oximes 2-PAM and MINA were then used for the reactivation of resurrected enzyme as above at 100 µM and 10 mM in-well concentrations, respectively.

Results and Discussion

According to the literature, MINA is able to reactivate sarin-inhibited AChE at higher concentration. However, in this experiment, MINA was not able to resurrect aged hAChE even at comparatively higher concentration (100 mM).

Conclusion 2

Even though arylated hAChE resulted from the incubation with the above three inhibitors, MINA might not be able to reach to the active site with correct orientation in order to effect nucleophilic attack on the arylated enzyme inhibitor complex due to bulkiness of the complex.

CHAPTER 3: EVALUATION OF N-METHYL PYRIDINIUM β-LACTAM COMPOUNDS AS SUICIDE INHIBITORS OF HUMAN ACETYLCHOLINESTERASE

Chemical Mechanism and Significance

Introduction of β-Lactam antibiotics dates back to 1940s and ever since β-Lactam substrates have obtained significant interest due to a wide range of biological activities such as antibiotic, antioxidant, antiviral and anticancer properties.[119,120] Also, β-lactams are studied as inhibitors of serine-dependent enzymes, metalloproteases and cysteine proteases.[120] The β-lactam ring is a four-membered ring with high ring strain. This highly reactive β-lactam ring is part of the core structure of several antibiotic families including penicillins, cephalosporins, and carbapenemes. The amide bond of the β-lactam ring is ruptured to form a covalent bond with the active site serine residue of the enzymes essential to the formation of bacterial cell wall. Inhibition of these essential enzymes of bacteria leads to irregularities in cell wall structure that ultimately leads to cell death.

Although β-lactams are broad-spectrum antibiotics over a majority of bacterial groups, growing numbers of bacteria produce β-Lactamase, which provides resistance to the effects of β-lactam antibiotics.[120,121] There are two families of β-lactamases: serine-β-lactamases which hydrolyze β-lactam rings by use of an active site serine and metallo- β-lactamases which hydrolyze β-lactam rings by use of a neucleophilic hydroxyl group activated by a metal.[120]

Organophosphorous inhibitors are used as pesticides and chemical warfare agents. Even small amounts of OP exposure can be fatal due to large scale inactivation of the AChE enzyme which is essential in acetylcholine mediated neurotransmission in both central and peripheral nervous systems. Phosphylated enzyme is a mimic of the transition state of the acylated enzyme that results from the normal catalytic process on the neurotransmitter acetylcholine. Thus, phosphylated enzyme is very stable under physiological conditions. For many OP nerve agents, a

spontaneous dealkylation process may occurs that is termed aging.[35] The aged enzyme is no longer reactivated by current reactivators.[37] However, aged enzyme would be reactivated only if aging process is reversed by some processes such as alkylation, acylation, or arylation.

Objectives of the Study

The phosphyl oxyanion formed during the aging process may be susceptible to reaction with strong electrophiles. Thus, aged AChE may attack a highly reactive β-lactam ring, which thereby would get attached to the aged AChE OP complex. The resultant acylated OP AChE complex (AChE-OP β-lactam complex) may then be reactivated by currently available reactivators such as oximes. The present study describes the synthesis of N-methylpyridinium β-lactams, and evaluation of their inhibitory action on human acetylcholinesterase.

Materials and Methods

This research has the following objectives.

1. Synthesis of relevant acylating agents (β-lactam inhibitors)

2. Evaluating acyl transfer abilities in a model reaction

3. Evaluation of hydrolytic stability of β-lactam inhibitors in phosphate buffer

4. Biological evaluation to find the resurrection abilities of β-lactam compounds on aged-AChE adducts.

1. Synthesis of β-Lactam Inhibitors

General Procedure for the Cross Coupling:

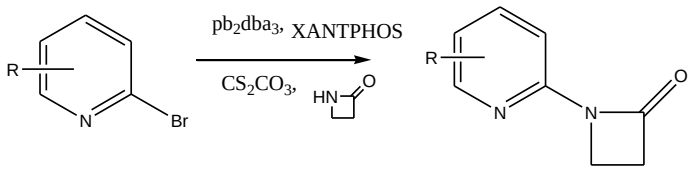

Scheme 3.1: Reaction method for synthesis of pyridinium β-Lactam

This project was initiated by Dr. Alexander M. Lodge and Dr. Joseph Topczewski and continued by me. The synthesis procedure (Scheme 3.1) is in accordance with the procedure used by Dr. Joseph Topczewski i. The example given here if for R = H and the β-Lactam ring is at the 2 position of the pyridinium ring. All β-lactam inhibitors were synthesized by me and Dr. Joseph Topczewski. The β-lactams inhibitors synthesized or resynthesized by me are recorded in this thesis.

The synthesis procedure is described briefly here. A round bottom flask was brought into a glove box and charged with solid pd_2dba_3 (30 mg, 0.033 mmol), XANTPHOS (Sigma-Aldrich, 35 mg, 0.064 mmol) and Cs_2CO_3 (Sigma-Aldrich, 1.2 g, 3.7 mmol). The flask was sealed and removed from the glove box. In a separate flask, 2-bromopyridine, 3-bromopyridine or 4-

bromopyridine (Sigma, 0.40 mL, 1.5 mmol) and azetidin-2-one (Sigma-Aldrich) 120 mg, 1.69 mmol) were dissolved in toluene (Aldrich, 2 mL) upon mild heating. This solution was then transferred to the previously measured solid catalyst via syringe. The mixture was stirred and heated to 100 ^{o}C. After 4 h at this temperature, the reaction was cooled, diluted with diethyl ether, filtered through celite, and concentrated *in vacuo*. The residue was purified by column chromatography (0%-100% ethyl acetate in hexanes) to afford the desired non methylated β-lactams.

General Procedure for the Methylation:

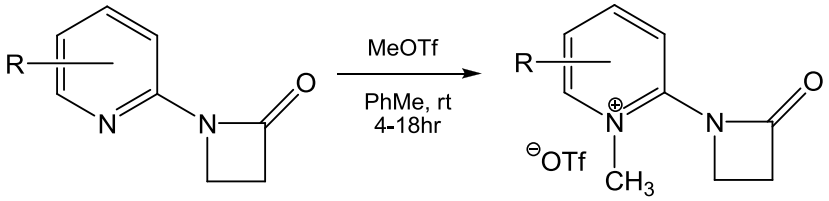

Scheme 3.2: Reaction method for synthesis of N-methylpyridinium β- lactams

The following procedure (Scheme 3.2) is for the unsubstituted compound (R = H). A 3 mL glass vial was equipped with a rubber septum and magnetic stir bar. The vial was brought into a glove box and charged with methyl trifluoromethylsulfonate (Sigma-Aldrich, MeOTf, 36 µL, 0.33 mmol) by micropipette with polypropylene tip. The vial was sealed and removed from the glove box. To a separate 3 mL vial was added unmethylated pyridinium β-lactam (49 mg, 0.33 mmol) which was dissolved in toluene (0.2 mL). The solution of pyridine was then added via syringe into the sealed vial of MeOTf at room temperature. The vial which contained the pyridine was rinsed with another portion of toluene (0.2 mL) and the rinse solution was injected into the reaction vial. The reaction vial was kept at room temperature and stirring was maintained at ca. 400-600 rpm. Over the course of the reaction (4-20 hr), a precipitate (solid or oil) was gradually formed. At the end of the reaction, toluene (2 mL) was added after which stirring was stopped. Any solid or oil

was allowed to settle and the solvent was removed by glass pipette. The solid or oil was then rinsed with several portions of hexanes or CH_2Cl_2 to remove any unreacted starting materials, again removing the solvent by pipette. Residual solvent was then removed *in vacuo* to provide the desired final product.

2. Evaluating Acyl Transfer Abilities in a Model Reaction

The effectiveness of the above synthesized compounds as acyl transfer agents was evaluated by using sodium methyl methanephosphonate as an analogue of the aged AChE -OP adduct. The detailed procedure is explained in chapter 2. Simply, model reactions were conducted in an NMR tube by mixing equimolar concentrations of phosphonate salt (27 mM in d_6-DMSO) with the β-lactam inhibitors synthesized above. The reaction was monitored by ^{1}H-NMR for a few hours or days depending on the acylation reaction rate.

3. Hydrolytic Stability of Inhibitors in Phosphate Buffer

The four membered β-lactam ring is easily susceptible to nucleophilic attack. Thus, the rate of hydrolysis of the inhibitors was determined in 50 mM phosphate buffer by UV analysis. Each set of inhibitor solutions was prepared fresh from solid prior to use. Absorbance maxima for the β-lactam inhibitors were obtained at a concentration of 100 μM in DD-H_2O. Inhibitors were allowed to incubate at 27 ºC for 30 minutes in 1 mM NaOH to produce hydrolysis products. Data were obtained using a black walled 1 mL, 10 mm quartz cuvette on a Molecular Devices SpectraMaxM2 micro plate reader's single cuvette holder. Data were collected from 250 nm to 450 nm at 1 nm increments. Table 3.1 lists the absorbance maxima for both reactant and hydrolysis product for each inhibitor. Because the $\Delta\lambda_{max}$ value were small, $\lambda_{\Delta A}$ values were determined between the two absorbance curves. The corresponding wavelengths for the maximum ΔA ($\lambda_{\Delta Amax}$) values were used to monitor hydrolysis of each inhibitor. The change in molar absorptivity (Δε)

was calculated from Equation 3.1 for each inhibitor. Data were collected over several hours. Rates of hydrolysis (k_{hyd}, s^{-1}) were estimated at 50 µM in 50 mM phosphate buffer at pH 7.3 using equation 3.2 Hydrolysis experiment was monitored via UV at relevant wavelengths in polystyrene 96 well-plate.

$$\Delta\varepsilon = \frac{\Delta A}{[I]}$$

Equation 3.1: Equation used for determining change in molar absorptivity (Δε, Abs/M), ΔA≡ change in absorbance, [I]≡ inhibitor concentration, M)

$$k_{hyd} = \frac{v_i/\Delta\varepsilon}{[I]}$$

Equation 3.2: Equation used for calculating the rate constant of hydrolysis (k_{hyd}, s^{-1}),v_i ≡ initial rate of the hydrolysis reaction (A/s)

Biological Evaluation

3.1. Half-Inhibitory Concentration (IC_{50}) Determination

IC_{50} of each β-lactam inhibitor was determined by dose response assay. Each β-lactam was incubated with human acetylcholinesterase at various concentration of the β-lactam and initial rates of the substrate hydrolysis were determined using the Ellman assay explained in Chapter 2.[116] IC_{50} values were determined at initial time points and 2 hour of incubation with the enzyme to check time dependent inhibition or hydrolysis occurred.

4. Resurrection Assay

The resurrection assay was performed by the same procedure as in Chapter 2. Simply, aged hAChE was prepared by mixing enzyme with excess sarin analog. After removing excess sarin on a G-50 Sephadex column, the resultant mixture was allowed to stay at 27 °C temperature for aging. Aged enzyme was then treated with each β-lactam compound. Rates of the substrate hydrolysis by

incubated solutions were measured at several time points after treating with oxime reactivators 2-PAM or MINA for 30 minutes. Detailed methods are explained in chapter 2.

Continuous assay and stop time assay

Continuous assays were performed at various concentrations of selected β-lactam inhibitors where activity of AChE was monitored continuously over several hours. Each well was prepared as follows: 270 µL of 50 mM PB at pH 7.3, 10 µL of different concentrations of β-lactam inhibitor in DD-H_2O, 10 µL of 4.5 mM ATCh, 10 µL of 0.02 M DTNB and 10 µL of 4.2 nM hAChE. Control experiments were performed in parallel with all additions but injection of DD-H_2O instead of inhibitor. Assays were performed in duplicate at each concentration and time courses were followed for 4 hours or more and first order rate constants were determined.

Stop time assays were conducted the same way as continuous assays but the activity of the inhibited enzyme was checked at different time points during the incubation period.

Results and Discussion

All the β-lactam inhibitors synthesized were characterized using the following spectroscopic methods: ^{1}H NMR, ^{13}CNMR, IR, HR-MS and elemental analysis. Spectra of all the β- lactam inhibitors synthesized by me are recorded in this thesis in Appendix B.

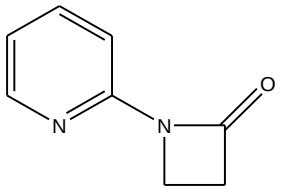

1-(pyridine-2-yl)azetidin-2-one

13% yield. **^{1}H NMR (acetone, 500 MHz):** δ = 8.29 (dq, *J* = 5.0 Hz, *J* = 0.8 Hz 1H), 7.75 (m, IH), 7.66 (dt, *J* = 8.37 Hz, *J* = 1.11Hz, 1H), 7.06 (m, 1H), 3.74 (t, *J* = 4.7 Hz, 2H), 3.08 (t, *J* = 4.8 Hz, 2H).

^{13}C NMR (acetone, 125 MHz): δ = 164.8, 150.3, 148.3, 137.7, 119.1, 11236, 37.7, 35.6.

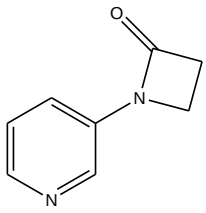

1-(pyridine-3-yl)azetidin-2-one

8.3% Yield. **^{1}H NMR (acetone, 500 MHz):** δ = 8.63 (d, *J* = 2.5 Hz, 1H), 8.28 (dd, *J* = 4.8, 1.4 Hz, 1H), 7.77 (m, 1H), 7.33 (m, 1H), 3.74 (t, *J* = 3.76 Hz, 2H), 3.15 (t, *J* = 4.6 Hz, 2H).

^{13}C NMR (Acetone, 125 MHz): δ = 164.8, 144.4, 137.8, 135.6, 123.7, 122.6, 37.7, 36.5.

IR (film, cm^{-1}): ν = 2963, 1748, 1588, 1573, 1488, 1379, 1152, 814.

HRMS (TOF EI+): calc. for $C_8H_8N_2O$ (M-OTF)$^+$: 148.0642; found: 148.0637.

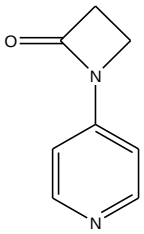

1-(pyridine-4-yl)azetidin-2-one

27.3% Yield. **^{1}H NMR (acetone, 500 MHz):** δ = 8.45 (dd, *J* = 4.4 Hz, 1.6 Hz, 2H), 7.26 (dd, *J* = 4.5, 1.6 Hz, 2H), 3.73 (t, *J* = 4.9 Hz, 2H), 3.16 (t, *J* = 4.7 2H).

^{13}C NMR (Acetone, 125 MHz): δ = 165.5, 150.6, 144.6, 110.4, 37.9, 36.4.

IR (film, cm^{-1}): ν = 2964, 1737, 1600, 1424, 1378, 1202, 1066, 820.

HRMS (TOF ES+): calc. for $C_8H_8N_2O$ (M-OTF)$^+$: 149.0715; found: 149.0718.

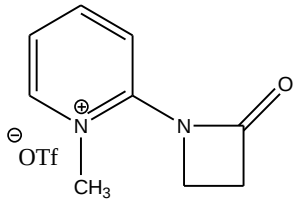

1-methyl-2-(2-oxoazetidin-1-yl)82yridine-1-ium trifluoromethanesulfonate

58.5% Yield.

^{1}H NMR (acetone, 500 MHz): δ = 8.76 (m, 1H), 8.53 (m, 1H), 8.26 (dd, *J* = 8.7 Hz, *J* = 1.0 Hz, 1H), 7.77 (m, 1H), 4.50 (s, 3H), 4.40 (t, *J* = 5.4 Hz, 2H), 3.47 (t, *J* = 5.3 Hz, 2H).

^{13}C NMR (acetone, 125 MHz): δ = 166.3, 147.3, 145.9, 145.0, 122.0, 129.9, 45.5, 44.3, 38.1.

(This compound has been already characterized)

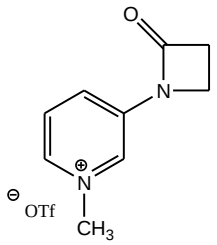

72.3% Yield.

1-methyl-3-(2-oxoazetidin-1-yl)pyridin-1-ium trifluoromethanesulfonate

^{1}H NMR (acetone, 500 MHz): δ = 9.00 (s, 1H), 8.75 (d, *J* = 6.2, 1.4 Hz, 1H), 8.56 (d, *J* = 9.1 Hz, 1H), 8.15 (t, *J* = 7.4 Hz, 1H), 4.59 (s, 3H), 3.96 (t, *J* = 4.9 Hz, 2H), 3.32 (t, *J* = 4.9 Hz, 2H).

^{13}C NMR (acetone, 125 MHz): δ = 165.9, 139.8, 138.7, 133.2, 130.8, 128.5, 48.6, 39.2, 37.4.

IR (film, cm^{-1}): ν = 3068, 1758, 1646, 1532, 1258, 1151, 1029.

HRMS (TOF ES+): calc. for $C_9H_{11}N_2O$ $(M\text{-}OTF)^+$: 163.0873; found: 163.0871.

Anal. Calcd. for $C_{10}H_{11}F_3N_2O_4S$: C, 38.46; H, 3.55 Found: C, 38.45; H, 3.74.

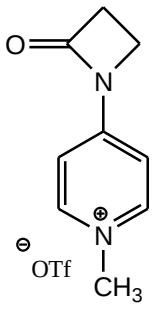

1-methyl-4-(2-oxoazetidin-1-yl)pyridin-1-ium trifluoromethanesulfonate

34.4% Yield· **^{1}H NMR (acetone, 500 MHz):** δ = 8.82 (d, *J* = 7.5 Hz, 2H), 7.86 (d, *J* = 5.8 Hz, 2H), 4.38 (s, 3H), 4.03 (t, *J* = 5.3 Hz, 2H), 3.39 (d, *J* = 5.3 Hz, 2H).

^{13}C NMR (acetone, 125 MHz): δ = 166.8, 149.6, 146.4, 112.7, 46.6, 39.7, 37.8.

IR (film, cm^{-1}): ν = 3068, 1777, 1646, 1532, 1249, 1164, 1029.

HRMS (TOF ES+): calc. for $C_{10}H_{11}F_3N_2O_4S$ (M-OTF)$^+$: 163.0873; found: 163.0871.

Anal. Calcd. for $C_{10}H_{11}F_3N_2O_4S$: C, 36.37; H, 3.97 Found: C, 36.72; H, 3.83.

The model study was conducted using methylmethane phosphonate monoanion as an aged enzyme analog. No acyl transfer was observed with the aged enzyme analog for all of the unsubstituted inhibitors synthesized by me in this study. Spectral data are recorded in Appendix B. Hydrolytic stability of all the β-lactam inhibitors in 50 mM phosphate buffer at pH 7.3 are shown in Table 3.1 for convenience. Rates of the spontaneous hydrolysis, maximum absorbances of reactants and their hydrolysis products, differences in molar absorptivity, and half-lives of the reactions are also shown.

Table 3.1: Hydrolytic stability data for all β-lactam inhibitors

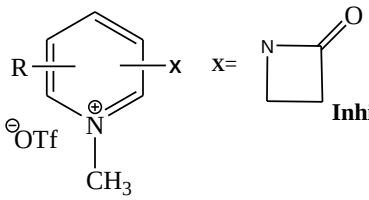

entry	R =	X-position	λ_{max} (nm) Inhibitors	λ_{max} (nm) Hydrolysis Products	Δε (ΔA/M x 10^3)	k_{hyd} (s^{-1})	Assay λ (nm)	$t_{½ (hyd)}$/ h
1	H	2	296	311	5.8	1.5 x 10^{-5}	297	13
2	5-F	2	306	325	6.1	2.0 x 10^{-5}	302	10
3	3-F	2	298	294	4.0	1.5 x 10^{-5}	302	13
4	5-CF_3	2	301	303	6.4	5.4 x 10^{-4}	297	0.33
5	4-$N(Me)_2$	2	290	287	1.7	ND	297	-
6	H	3	300	311	1.9	5.3 x 10^{-7}	297	363
7	H	4	284	282	2.3	9.6 x 10^{-6}	280	20

All the β-lactam inhibitors except that which contains the strong electron withdrawing group triflouromethyl (inhibitor 4) were relatively stable in phosphate buffer. However, the hydrolytic stability of inhibitor 4 was relatively low. The half-life of inhibitor 4 indicates that almost all the reactants would hydrolyze within 2 hours. This is because the strong electron withdrawing ability of the triflouromethyl substituent makes the carbonyl carbon of inhibitor 4 susceptible to nucleophilic attack. These hydrolytic stabilities also provides insight into the observed hAChE inhibition behaviors.

The inhibitor concentration that produces 50% inhibition (IC_{50} value) for each inhibitor of this family is tabulated in Table 3.2. IC_{50} values of inhibitors were determined immediately on addition of each inhibitor to the enzyme (i.e. at t = 0 hr) and after two hours of incubation prior to initial rate assay (t = 2 hr). If IC_{50} values changed significantly in these two time points, stop time

assays were conducted to see time dependent inhibition. IC_{50} values do not change to a significant extent as a function of time for inhibitors 5, 6 and 7. It is concluded that the compounds 5, 6 and 7 are reversible inhibitors of hAChE, rather than time-dependent inhibitors (1-4) that covalently modify the enzyme. All the β- Lactam inhibitors described herein are micromolar potency inhibitors of hAChE (at initial time point IC_{50} values ranged from 15- 140 μM), however, some of them were reversible inhibitors while others inhibit enzyme by covalent modification.

From the IC_{50} values obtained over a 24 h period, it was previously observed by Alex M. Lodge that IC_{50} decreased for 2 hours, followed by gradual increase afterwards for inhibitor 4, which contain the triflouromethyl substituent on the pyridine ring. This can be explained by considering the hydrolysis rate that was reported earlier in this chapter. According to the half-life of the inhibitor 4 hydrolysis reaction, it is expected that almost all the inhibitor 4 molecules are hydrolyzed by 2 hours. Thus, no inhibitor is available for reinhibition of the recovered hAChE if any. Thus, increases of the IC_{50} values would result from formation of free enzyme from the turnover of the AChE-β-lactamyl complex. Since it is expected that the inhibitor is fully hydrolyzed by 2 hours no further inhibition results. Thus, IC_{50} values are increased with time after some time point due to increasing free enzyme.

Table 3.2: IC_{50} values obtained over several hours for β-lactam inhibitors

Inhibitor			**IC_{50} (μM)**					
entry	R =	**X-position**	**0 hr**	**2 hr**	**4 hr**	**6 hr**	**10 hr**	**24 hr**
1	H	2	43 ± 3	31 ± 6	15 ±5	8 ± 3	ND	ND
2	5-F	2	47 ± 8	30 ± 2	30 ± 9	16 ± 4	13 ± 6	ND
3	3-F	2	140 ± 30	50 ± 10	50 ± 10	50 ± 10	40 ± 10	24 ± 6
4	5-CF_3	2	33 ± 6	6 ± 2	7 ± 3	13 ± 4	15 ± 5	14 ± 4
5	4-$N(Me)_2$	2	25 ± 2	34 ± 3	30 ± 3	34 ± 3	21 ± 4	20 ± 6
6	H	3	15 ± 1	15 ± 0.5	ND	ND	ND	ND
7	H	4	56 ±2	56 ± 3	ND	ND	ND	ND

In an effort to further understand the recovery of AChE following inhibition, stopped time assay and continuous assay experiments were conducted for inhibitors 1 and 4 after analyzing their hydrolysis rates. hAChE activity in the presence of inhibitor 1 was determined for a long period of time and in the presence of inhibitor 4 was determined continuously for 5 hours. For inhibitor 1 at higher concentrations, such as 3.5 mM, it was observed that activity of the enzyme goes down (Figure 3.1) and almost complete inhibition occurs. But, at lower concentrations, e.g. 0.3 mM, enzyme activity goes down to a finite level followed by recovery of activity, but which never reaches the initial activity (Figure 3.1). For inhibitor 4, at higher concentration, e.g. 0.7 mM or higher, almost complete inhibition occurred and little AChE recovery was observed (Figures 3.2 and 3.3). At lower concentrations, significant recovery was observed (Figures 3.4 and 3.5).

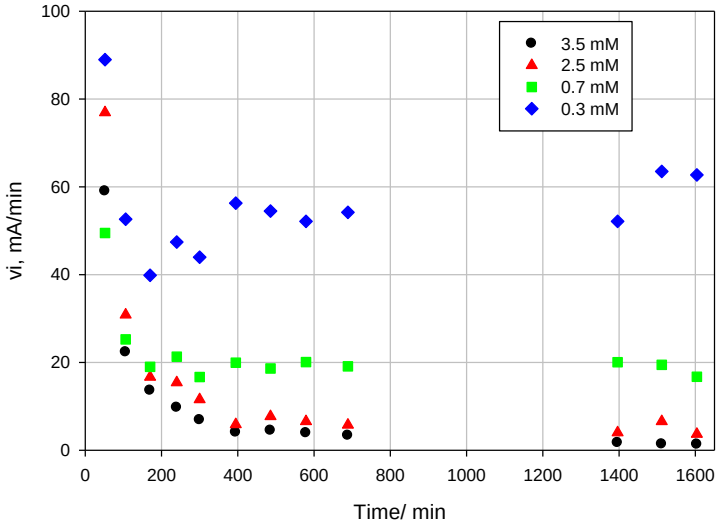

Figure 3.1: Initial rates of substrate hydrolysis by hAChE in the presence of different concentrations of inhibitor 1 as a function of time

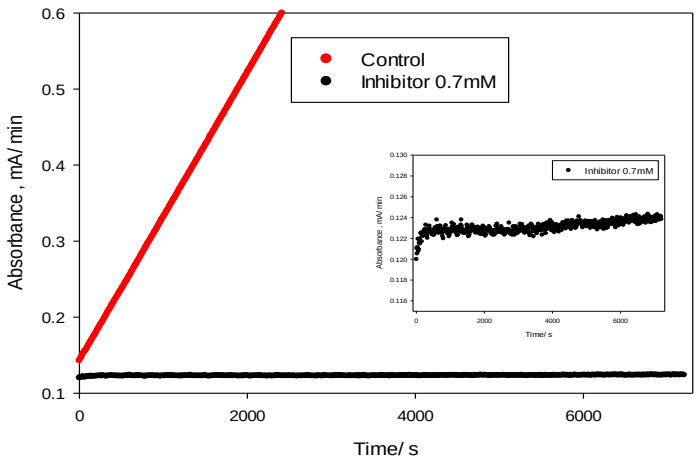

Figure 3.2: Full time course for substrate hydrolysis by hAChE in the presence of Inhibitor 4. Control ≡ in the absence of inhibitor, inhibitor 0.7 mM ≡ in the presence of inhibitor at 3.5 mM in-well concentration.

This is well explained by the reduction of the rate (constructed from the Figure 3.2) of the enzyme substrate hydrolysis reaction with time (Figure 3.3).

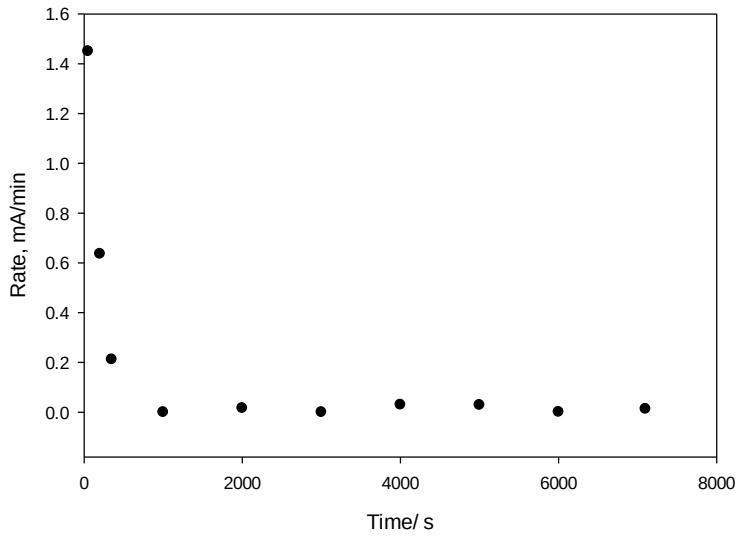

Figure 3.3: Rate (constructed from Figure 3.2) as a function of time for substrate hydrolysis reaction by hAChE in the presence of inhibitor 4, in-well concentration-3.5 mM

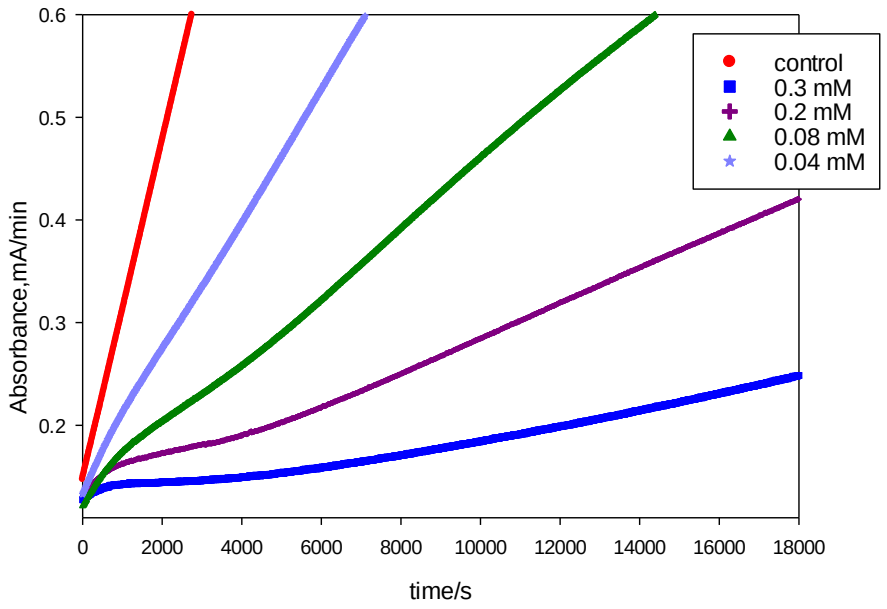

Figure 3.4: Plot of continuous assays in the presence of inhibitor 4 at different concentrations and in the absence of inhibitor 4 (control).

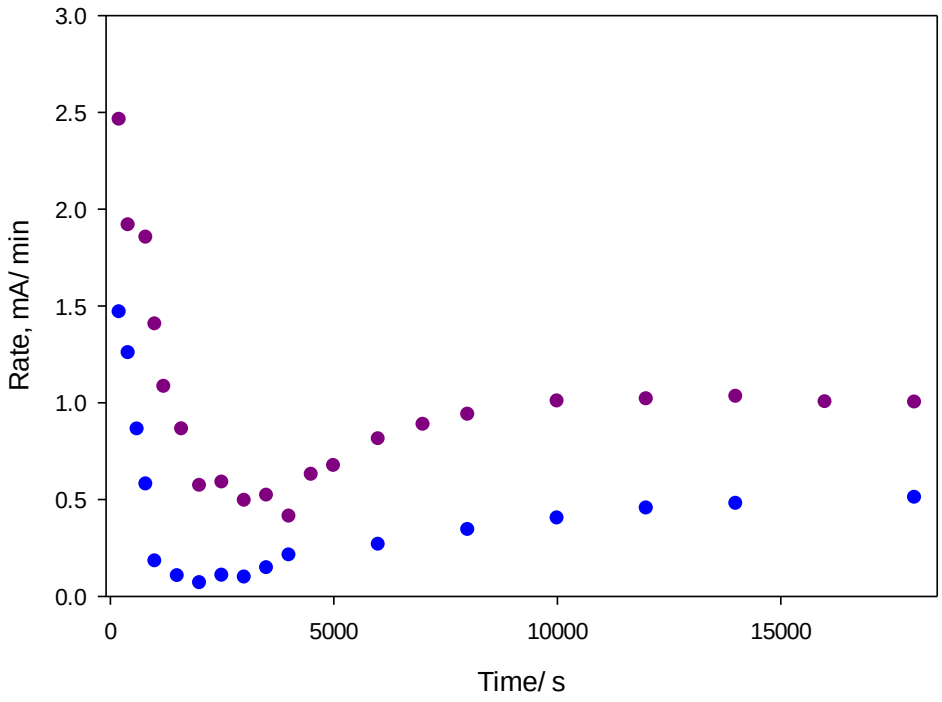

Figure 3.5: Rates of the substrate hydrolysis reaction by hAChE in the presence of inhibitor 4. Blue - at 0.3 mM concentration; Purple- 0.2 mM concentration

Thus, the AChE inhibition by inhibitor 4 is consistent with a suicide inhibition mechanism where AChE activity is partially recovered. This behavior of the inhibitor can be explained by following mechanism (Scheme 3.3).

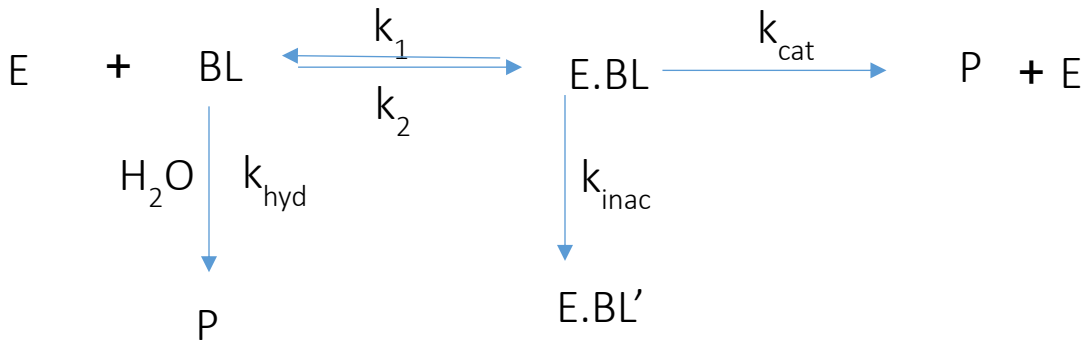

Scheme 3.3: Proposed mechanism for suicide inhibition by inhibitor 4 where AChE activity is partially recovered.

Where; E≡ hAChE, BL≡ β-Lactam inhibitor, E.BL≡ Michalis type AChE-Inhibitor complex, E-BL'≡ Inactive AChE-inhibitor complex, P≡ product, k_1≡ rate constant of the forward reaction, k_2≡ rate constant of the backward reaction, k_{cat}≡ turn over rate constant, k_{hyd} ≡ rate constant of the hydrolysis of inhibitor, k_{inac}≡ rate constant of the inactivation of enzyme

Conclusion

N-Methylpyridinium β-lactams were initially designed with the aim of resurrecting the aged hAChE activity. None of the inhibitors showed considerable resurrection of aged hAChE after 30 minutes incubation with either 2-PAM or MINA reactivators. All inhibitors have micromolar affinity towards hAChE so that they bind to the enzyme efficiently. Hydrolytic stability data and the structure of the inhibitors clearly indicate that the position of the β-lactam group on the pyridinium ring and other substituent of the pyridine ring can affect the stability of the inhibitors in phosphate buffer. Hydrolytic stability data and binding affinities are parallel for some inhibitors. Unsubstituted and strong electron withdrawing triflouromethyl group containing inhibitors, both having β-lactam groups on 2 position of the pyridinium ring, were suicide inhibitors of hAChE where enzyme activity was partially recovered. The rate of the turnover was higher in inhibitor 4 than inhibitor 1. To the best of my knowledge, these would be the first suicide inhibitors of hAChE. It was hoped that if the rate of the recovery of the inhibited enzyme is fast enough the suicide inhibitors described herein would be good candidates in medicinal chemistry where partiall inhibition of AChE is required.

CHAPTER 4: SULFONIUM SPECIES AS REVERSIBLE INHIBITORS OF HUMAN ACETYLCHOLINESTERASE

Chemical Mechanism and Significance

The most remarkable feature of AChE is a 20 Å long, narrow active site gorge that penetrates halfway through the enzyme and widens out near the bottom. The AChE active site is located on the bottom of the narrow gorge and mainly consisted of three domains: esteratic locus, anionic locus, and a hydrophobic region.[11] These remarkable features allow AChE to hydrolyze its substrate with a higher efficiency than other serine esterases.[12,28] The AChE catalytic triad, Ser-His-Glu, is located 4 Å above the bottom of the gorge.[17] In addition to the catalytic triad, AChE possesses remarkable sites that are important for increasing catalytic efficiency and specificity. The quaternary ammonium binding site, which consists of Trp 86 in human AChE, is one of them that particularly makes a decisive contribution to the selectivity of the enzyme by recognizing the cationic quaternary ammonium function of acetylcholine (ACh) and other AChE ligands. Moreover, another subsite called the peripheral anionic site (PAS)[30] is located on the mouth of the narrow gorge, approximately 20 Å away from the active site, through which ligands must pass on their way to the active site. Propidium, gallamine, decamethonium and fasciculin have been identified as PAS binding inhibitors.[122] Furthermore, PAS binds to the substrate ACh and the related analog acetylthiocholine (ATCh).[30,123] The complex architecture of AChE provides provocative opportunities for the design and synthesis of multifunctional ligands that are potent inhibitors of AChE.

Objectives of the Study

Like the quaternary ammonium function of typical AChE ligands and substrates, sulfonium groups should interact effectively with the quaternary ammonium loci in the PAS and catalytic locus. The sulfonium group is a highly polarizable function. Thus, it is expected to interact with the polarizable Trp groups in the catalytic locus or in the PAS. The present study describes the evaluation of multifunctional sulfonium-containing inhibitors of AChE that provide a decisive test of this hypothesis.

Materials and Methods

All the inhibitors described herein were synthesized by Joseph J. Topczewski or Sarah Gross (an undergraduate under my direction). All the biological assays were done by Alexander M. Lodge or me. For easy understanding, synthetic procedures will be provided in addition to the detailed biological methods.

Synthesis of Sulfonium Inhibitors

Synthetic procedures for dimethylsulfonium inhibitors that incorporate the methyumbelliferyl aromatic function are outlined in Scheme 4.1. The phenoxide anion of 4-methyumbelliferone was reacted either with the appropriate benzyl bromide, or with 1, ω-dibromoalkanes followed by reaction with methanethiolate anion, to produce methylthioesters. These were then reacted with methyltriflate to obtain relevant dimethyl sulfonium inhibitors.

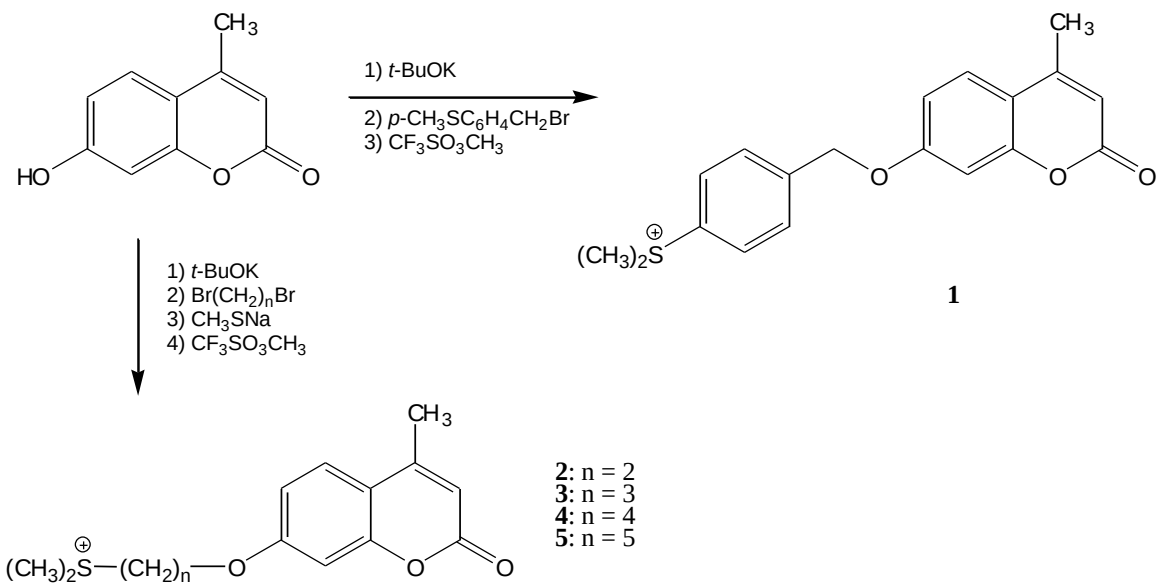

Scheme 4.1: Synthesis of Umbelliferyl- containing Dimethylsulfonium inhibitors

A similar procedure, as shown in Scheme 4.2, was used to synthesize dimethoxy indanone aromatic function-containing dimethylsulfonium inhibitors. Herein, dimethoxyindanone enolate anion was alkylated with the respective bromoalkyl tert-Butyldimethylsilyl (TBS) ethers followed by deprotection. These were converted to terminal bromides via the mesylate esters. Bromides were then subjected to S_N2 displacement with sodium methanethiolate, and the resulting thioethers were reacted with methyltriflate to obtain desired dimethyl sulfonium inhibitors.

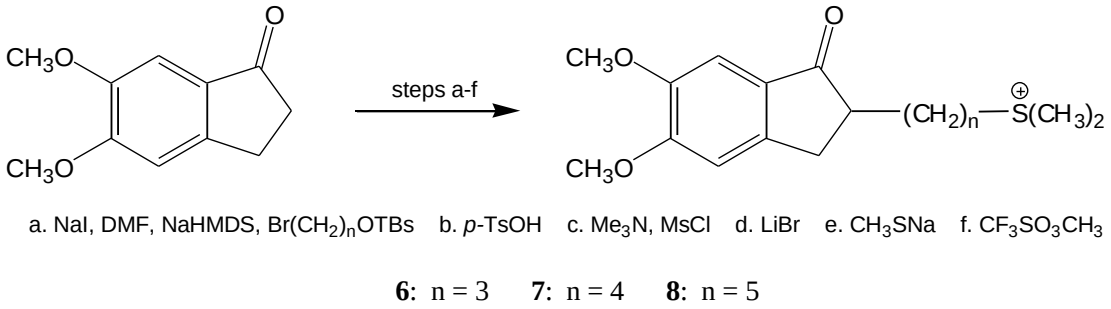

Scheme 4.2: Synthesis of Dimethoxyindanone-containing Dimethylsulfonium inhibitors

Determination of Half Maximal Inhibitory Concentration (IC_{50})

Ten different concentrations of each sulfornium compound were prepared and used to determine the IC_{50} value. Solutions of the compounds studied were prepared in acetonitrile or a mixture of the acetonitrile and distilled and deionized water (DD-H_2O). All stock solutions were prepared from solid and stored in disposable scintillation vials or polypropylene containers at -4 to 4 ^oC. Phosphate buffer (PB, 50 mM) was prepared by using sodium hydrogen phosphate monobasic monohydrate ($NaH_2PO_4.H_2O$) and sodium phosphate dibasic (Na_2HPO_4). pH of the buffer solution was measured by ion selective pH electrode (Fisher accumet basic AB15) which was calibrated prior to the measurement. pH ranged from 7.3-7.5. Stock solutions of 0.1% (w/v) BSA (Bovine Serum Albumin) in PB, 1.4 nM human acetylcholinesterase (hAChE) in 0.1% (w/v) BSA, 0.045 M acetyl thiocholine (ATCh) in deionized and distilled H_2O, 0.02 M 5,5'-dithiobis-2-nitrobenzoic acid (DTNB) in PB, and 0.009 M 2-pyridine aldoxime methyl chloride (2-PAM) (for resurrection assays) in deionized and distilled H_2O were prepared and used for preparations of working solutions. Solvents were matched to the parent stock solutions when working solutions were prepared.

Assay experiments were conducted on a Molecular Devices SpectraMaxM2 microplate reader using sterile polystyrene 96-well plates (Costa, flat bottom). IC_{50} values against hAChE were measured following a well-known colorimetric method developed by Ellman et al. at 27 ^oC.[116] Herein, acetylthiocholine (ATCh) is used as the enzyme substrate. The rate of thiocholine production from acetylthiocholine hydrolysis was measured by UV-visible spectroscopy. This was accomplished by continuous reaction of thiocholine with DTNB and measuring the production of yellow color at 412 nm. Each experimental well was loaded with phosphate buffer containing DTNB, human AChE (hAChE) and the sulfornium inhibitor in each concentration. The control

well was loaded in the same way but with only the solvent which was used for stock preparation of the sulfornium agent. Finally, ATCh was added to all wells and initial rates of the reaction at less than 10% turnover of the initial substrate concentration were measured. Initial rates were corrected for background (non-enzymatic) hydrolysis of ATCh and measured in duplicates. Initial velocity of the reaction was measured over a 10 minutes duration with minimum possible time point reading interval. IC_{50} values were determined by non-linear fit of data to equation 4.1, wherein v_i is the reaction rate in the presence of inhibitor I, v_0 is the least-squares calculated reaction rate in the absence of inhibitor, and IC_{50} is the inhibitor concentration that produces half-maximal inhibition.

$$v_i = \frac{v_0}{1 + \frac{10^{\log[I]}}{IC_{50}}}$$

Equation 4.1: Equation used for determination of half-maximal inhibition constant IC_{50}

Equation 4.1 and Figure 4.1 provide an example of the data and analysis for determination of the IC_{50} value.

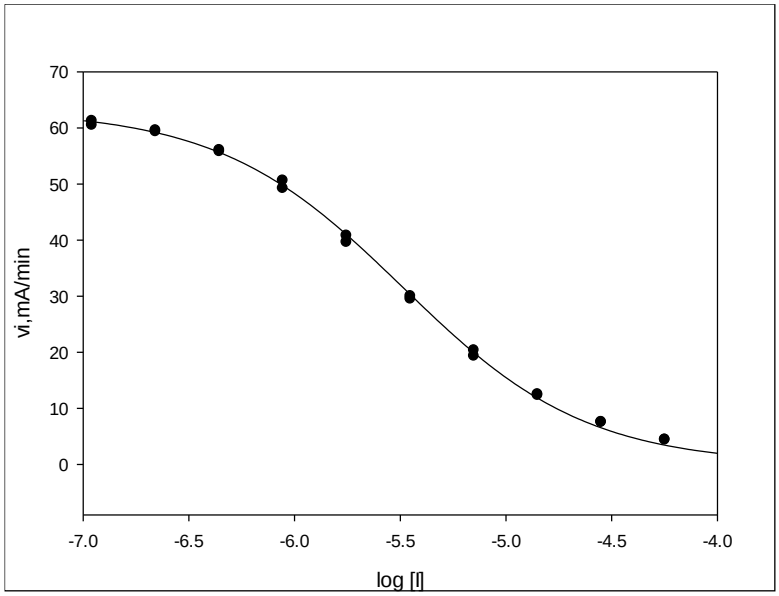

Figure 4.1: Dose response curve for Inhibitor 1

Resurrection Assay

Resurrection assays were performed by following the procedure explained in Chapter 2. Simply, aged hAChE was prepared by mixing enzyme with excess sarin analog. After removing excess sarin analog by G-50 Sephadex column, the resultant mixture was allowed to stay at 27 °C temperature for aging. Aged enzyme was then treated with each sulfornium inhibitor. Rates of substrate hydrolysis in incubated solutions were measured at several time points after treating with the oxime reactivator 2-PAM for 30 minutes. Detailed methods are explained in chapter 2.

Results and Discussion

The eight multifunctional dimethylsulfonium compounds described herein were evaluated as inhibitors of human AChE-catalyzed hydrolysis of acetylthiocholine (ATCh). Results of all other sulfonium inhibitors evaluated in this project and all the graphs of dose response curves are shown in appendix C. Inhibitor characterization involved measuring the effect of varying concentrations of inhibitors on the initial rate of AChE-catalyzed hydrolysis of ATCh. The inhibitor concentrations that produce 50% inhibition (IC_{50} value) were determined as explained above, and are tabulated in Table 4.1. IC_{50} values were determined immediately on addition of inhibitors to the enzyme (i.e. at t = 0 hr) and after two hours of incubation (t= 2 h) prior to initial rate assay as described earlier in the chapter. Since the IC_{50} values do not change to a significant extent as a function of time, it is concluded that the compounds are reversible inhibitors, rather than time-dependent inhibitors that covalently modify the enzyme.

Table 4.1: Dimethylsulfonium Inhibitors of Human Acetylcholinesterase

Inhibitor	**IC_{50} (t = 0 hr, μM)**	**IC_{50} (t = 2 hr, μM)**
1	3.26 ± 0.08	2.6 ± 0.1
2	11 ± 2	14 ± 1
3	35 ± 2	41 ± 3
4	12 ± 1	13 ± 1
5	2.1 ± 0.1	2.4 ± 0.1
6	7.0 ± 0.2	6.2 ± 0.4
7	9.0 ± 0.6	8.2 ± 0.5
8	0.028 ± 0.008	0.036 ± 0.008

All of the compounds described herein are potent inhibitors of human AChE, with IC_{50} values in the nanomolar to micromolar range. Also of note is the influence of the spacer length on inhibitor affinity. In the set of compounds that incorporates the methylumbelliferyl group (**1**-**5** in Table 4.1) the affinity for **5** (n = 5) is about an order of magnitude higher than for **2**-**4**, where spacer length is in the range n = 2-4. Notably, **1** possesses a rigid benzyl spacer that approximates the methylene spacer of **5**, and these two inhibitors have nearly the same AChE affinity. The affinity trend is yet more dramatic for compounds that incorporate the dimethoxyindanone function (**6**-**8** in Table 1); i.e. **8** (n = 5) has an AChE affinity that is 200 to 300-fold greater than the affinities of compounds **6** (n = 3) and **7** (n = 4) that have shorter spacers.

In an effort to further understand the influence of spacer length on AChE affinity, binding poses were determined for inhibitors **7** and **8** by molecular modeling conducted in the laboratory of Dr. Jason Morrill of William Jewell College. Docking analysis was performed using the molecular modelling package Molecular Operating Environment, where the x-ray crystal structure from recombinant human AChE in the apo state (PDBID:4EY4) was used. Docking results are shown in Table 4.2 and Figures 4.2 and 4.3.

Table 4.2: Docking results for Inhibitors 7 and 8

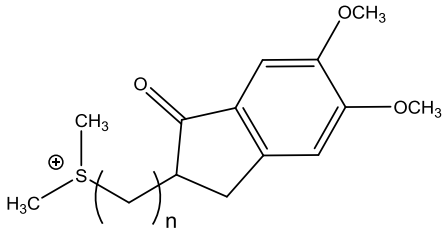

Inhibitor	**n**	**Stereochemical Configuration**	**Computed Binding Affinity (kcal/mol)**
7	4	*R*	-6.97
7	4	*S*	-6.69
8	5	*R*	-7.82
8	5	*S*	-7.37

As shown in Figures 4.2 and 4.3, the *R*/*S* enantiomer pairs of the docked ligands exhibit very similar binding poses in the active site of AChE. In all poses the dimethoxyindanone moiety is interacting with aromatic residues Tyr72, Trp286, and Tyr341 at the mouth of the gorge, with the aliphatic linker spanning the gorge. It appears that in this crystal structure the AChE binding site is large enough to accommodate each enantiomer pair with similar affinity, as indicated by the similar computed binding affinities (Table 4.2) for the *R*/*S* pairs. Further, the lower IC_{50} concentration for entry 8 can be rationalized on the basis of the longer aliphatic linker for this *R*/*S* pair of inhibitors placing the dimethylsulfonium moiety in closer proximity to the AChE active site, providing an opportunity for more favorable nonbonding interactions giving rise to a higher computed binding affinity for 8.

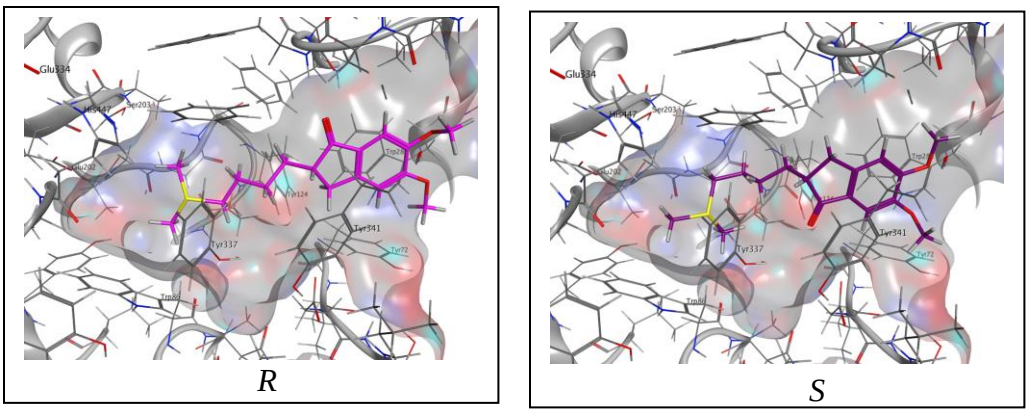

Figure 4.2: Highest affinity poses for the R/ S enantiomers of inhibitor 7 docked in crystal structure of AChE.

The gray area indicates the surface of the binding site accessible to the inhibitor.

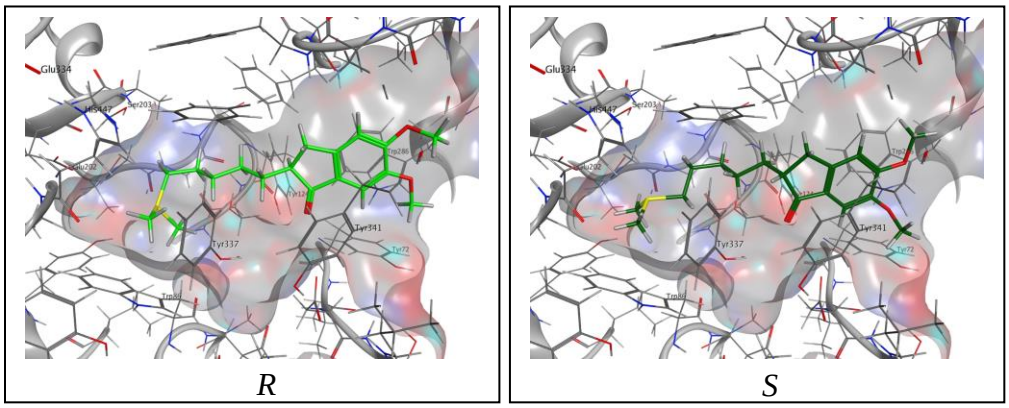

Figure 4.3: Highest affinity poses for the R/ S enantiomers of inhibitor 8 docked in crystal structure of AChE

The gray area indicates the surface of the binding site accessible to the inhibitor

The modeled complex of AChE with **8** shows that the dimethylsulfonium function interacts with Trp86 of the active site. The geometry of this interaction is reminiscent of the cation-π interaction between the active site tryptophan and the ligand's quaternary ammonium function that is manifest in the x-ray structure of the complex of *Torpedo californica* AChE with the transition state analog *m-N,N,N*-trimethylammonio trifluoroacetophenone (TMTFA).[124] Hence, the potency of the compounds described herein, especially that of **8**, suggests that the dimethylsulfonium function can serve as a surrogate for the quaternary ammonium group in modular syntheses of effective AChE inhibitors.

Conclusion

It is worthy of mention that the dimethylsulfonium compounds described herein were designed with the aim of resurrecting the activity of aged AChE. When AChE is inhibited by organophosphorus (OP) covalent inhibitors, which include the onerous chemical warfare agents sarin and soman,[13] the initial complex can be reactivated with nucleophilic antidotes such as pyridine-2-aldoximine methiodide (2-PAM).[65] However, a subsequent dealkylation reaction of the initial OP-AChE covalent complex produces a monoanionic phosphyl complex (i.e. aged AChE)[125] for which there is no known antidote. It was hoped that the dimethylsulfonium ligands described herein would methylate the phosphyl monoanion moiety of the aged AChE complex and hence render the complex susceptible anew to oxime reactivation. Though none of the dimethylsulfonium ligands was found to resurrect the activity of aged AChE it is gratifying nonetheless that these compounds were potent AChE inhibitors and that their potency reveals a novel avenue for inhibition of this pharmacologically and toxicologically prominent enzyme.

CHAPTER 5: UNKNOWN REACTIVATOR OF HUMAN ACETYLCHOLINESTERASE INHIBITED BY ORGANOPHOSPHOROUS AGENTS

Chemical Mechanism and Significance

Acetylcholinesterase (AChE) is an essential enzyme in the human neuronal system.[11] The essential role of AChE makes it a main target for the development of organophosphorus compounds (OP) such as pesticides and extremely toxic chemical warfare agents (CWAs).[3] The phosphylated enzyme undergoes a hydrolysis process by nucleophilic attack of active site water molecules thereby liberating free enzyme; this process is called spontaneous reactivation.[113] Spontaneous reactivation depends on several factors. For example, the nature of the OP inhibitor and enzyme. The spontaneous reactivation occurs very slowly for many OP inhibitors of AChE, especially for toxic nerve agents. However, reactivation can be speeded up using strong nucleophile such as oximes. Use of oximes is the main treatment method currently used in OP intoxication.[50,56]

The phosphylated enzyme may undergo a secondary dealkylation process called aging where the enzyme is irreversibly inhibited.[51] The aged enzyme complex with monophosphonate anion is resistant towards the current treatments by oximes, hence, complete loss of active enzyme results.[51] Therefore, sufficient doses of CWAs lead to death. For example, aging by soman is so fast (half-life < 4 min) that spontaneous reactivation is not clinically significant. Thus, it is important that immediate administration of oxime along with the atropine takes place to reactivate the inhibited enzyme before aging occurs.

It is suggested that if the phosphonate anion of the aged-AChE adduct is alkylated, known oximes could then be used to reactivate the OP-inhibited AChE. Therefore, we synthesized potential alkylating (methylating) agents and studied kinetic parameters to determine the ability of reactivation of the aged-AChE adduct. Our preliminary studies showed that some N-methyl-2-

methoxy-pyridinium species are potential methylating agents for an analog of aged-AChE.[52] However, *in vitro* evaluation indicated that none of the species was able to reactivate the aged-AChE adduct when known oximes such as 2-pyridine aldoxime methyl chloride (2-PAM) and monoisonitrosoacetone (MINA) were used as oxime reactivators for the resurrected (methylated) enzyme, if any.

However, recent mutagenesis studies indicated that replacement of some negatively charged amino acid residues with neutral residues results in significant reduction of the rate of the aging process.[112] Therefore, further kinetic assessment of these potential methylating agents for the alkylation of those amino acids residues is important.

Objectives of the Study

The aging process is a serious threat to the people exposed to OP inhibitors since the classical 2-PAM antidote is incapable of reactivating the aged enzyme complex. Thus, the development of an antidote which is capable of preventing or delaying aging is highly desired. According to the literature findings, we hypothesized that if the negatively charged amino acid glutamate residue (E202, which is proximal to the P-O-C linkage of OP-inhibited enzyme) is alkylated, the aging process could then be prevented or delayed[112], and thereby reactivation of the OP-inhibited AChE by current antidotes such as 2-PAM and MINA would be practical. Presented here is the biological evaluation of some potential methylating agents (Figure 5.1) as potential aging delaying agents.

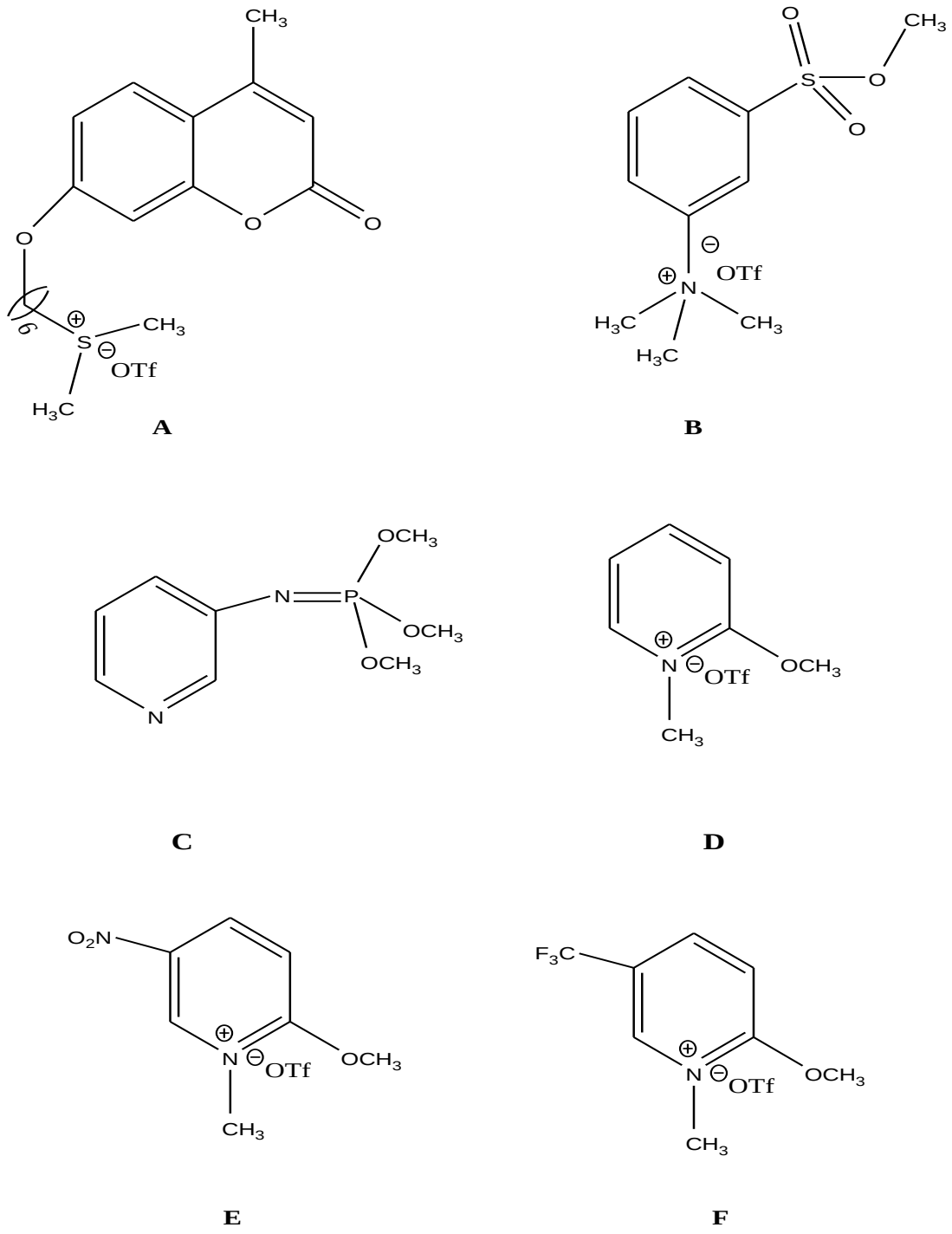

Figure 5.1: Chemical structures of some selected aging delaying agents used in this study

Materials and Methods

All inhibitors used in this study were originally synthesized by Joseph J. Topczewski, Jacob Frueh, or Sarah Gross, or resynthesized by me or commercially bought. All reagents were purchased from commercial venders in the highest purity available and were used without further purification. Human acetylcholinesterase from erythrocytes (hAChE), acetylthiocholine iodide (ATCh), 5, 5'-dithiobis (2-nitro benzoic acid) (DTNB), and 2-PAM were obtained from Sigma Aldrich. ATCh, DTNB, and 2-PAM were prepared according to the methods explained in chapter 2. Human acetylcholinesterase from erythrocytes is not as stable in 0.1% w/v BSA as recombinant human acetylcholinesterase. Therefore, hAChE from erythrocytes was prepared in 1% Triton X-100 in 50 mM phosphate buffer (mono basic and dibasic sodium phosphate reagents were obtained from Alfa Aeser).

Phosphylated hAChE was achieved by incubating the enzyme with excess sarin analog (umbelliferyl sarin). Herein, 1000 µL of 5.71 x 10^{-8} M hAChE in 1% Triton X-100 and sarin analog in acetonitrile (from Sigma Aldrich) (3 x 10^{-4} M) were prepared. A 483 µL aliquot of the hAChE was then mixed with 17 µL of sarin inhibitor solution or acetonitrile, respectively, to prepare experimental and control solutions. After 30 minutes of incubation at 27 ˚C, completeness of the inhibition was determined by checking initial rates of substrate hydrolysis of the uninhibited (control) and inhibited enzymes. Once enzyme is fully inhibited by sarin analog (< 2% of control), excess inhibitor was separated from the enzyme to avoid the re-inhibition of recovered enzyme if any during the reactivation process. A Sephadex G-50 Quick Spin Column (Roche) was used in the separation and the column was standardized with 1200 µL of 1% Triton X-100 buffer by adding 300 µL each time for 4 times. The column was then packed by centrifugation at 1100 x g for 4 minutes. 500 µL from uninhibited and inhibited hAChE samples were loaded to two separate

columns by adding 250 µL at a time. Columns were centrifuged at 600 x g for 6 minutes. Enzymes (control and sarin inhibited) were diluted using 1% Ttriton X-100 buffer until a conveniently measurable enzyme activity for the control was realized in the spectrophotometric assay. After dilution, control and OP inhibited enzyme were incubated with 5 x K_i (previously determined by me and Alex during the other projects) of each aging delaying agents for 24 hours. Then oxime-induced reactivation of the hAChE in incubated solutions was determined at various time points of the incubation period by following 30 minutes incubation of 10 fold diluted enzyme with 100 µM 2-PAM prior to the measurement. Furthermore, non-oxime-induced reactivation was also determined by checking AChE activity of the incubated solutions without 30 minutes 2-PAM incubation.

Initial rates of substrate hydrolysis were determined during the activity measurement. Another control experiment (no aging delaying agent incubation, named residual) was performed in parallel for comparison (to measure the extent of aging). For all the experiment, 5 x K_i of 2-PAM (1 mM, measured by Dr. Alexander Lodge) was also used as a reference aging delay/ preventive agent. Percentages of reactivated hAChE incubated with each aging delaying agent in the presence of oxime or without oxime were determined at each time point during the incubation period. In addition to sarin analog, some selected compounds were also evaluated as aging delaying agent for soman analog (Me-Umbelliferryl-*t*Bu-soman, synthesized by Alexander Lodge) inhibited hAChE.

Results and Discussion

According to the aging kinetics, the incubation time of an aging delaying agent with each OP-inhibited hAChE was determined. Aging kinetics of sarin and soman analogs were initially determined (at pH7.28-7.32, temperature 27 ^{o}C, and 50 mM phosphate buffer) by Dr. Alexander Lodge, and half- lives were 630 and 75 minutes, respectively. Since soman analog-inhibited AChE ages rapidly, in order to increase the number of data points that can be acquired during the aging preventive experiment, inhibition and aging kinetics by soman analogs were repeated with concentration modifications. Aging delaying experiments were then designed according to the half-life of aging of each OP-inhibited hAChE. Inhibition and aging kinetics for soman analog at one of the concentrations are shown in Figures 5.2 and 5.3. These kinetics data were used for the remaining experiments. Herein, incubation of sarin analog-inhibited and soman analog-inhibited AChE with aging delaying agents were approximately 24 hours and 6 hours, respectively. However, data acquisition time was varied according to the experiment.

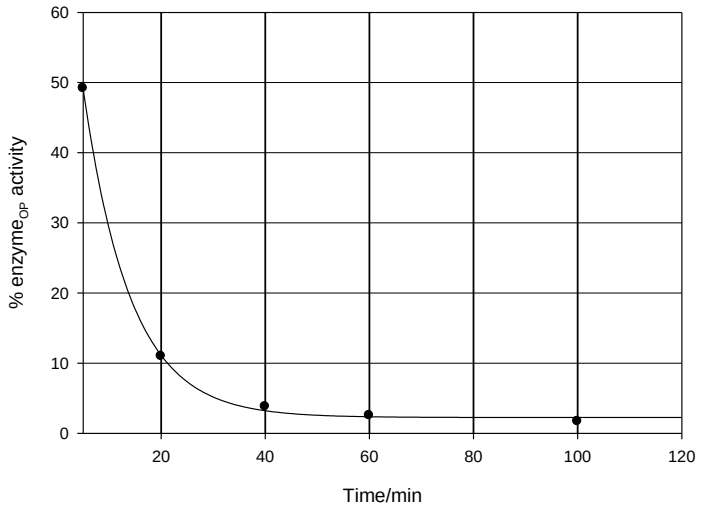

Figure 5.2: Stop-time assay plot for determination of pseudo first-order rate constant for soman analog

Inhibitor concentration-(4.08 x 10^{-5} M), temperature 27 ^{o}C, pH 7.2, 50 mM phosphate buffer, 0.11 min^{-1}

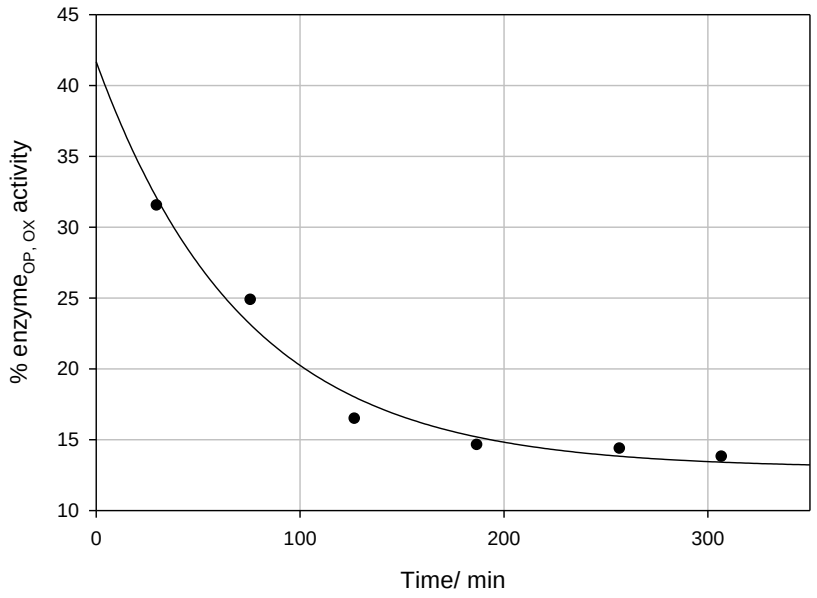

Figure 5.3: Oxime-induced (2-PAM) reactivated enzyme activity as a function of time to determine extent of aging for soman analog. Temperature 27 ^{o}C, pH 7.2, 50 mM phosphate buffer

All the compounds shown in Figure 5.1 were assayed for their *in vitro* aging delaying ability or reactivation potency with or without other oximes (i.e. 2-PAM) at different time point at 5 x K_i concentrations. Herein, percentage enzyme activity (activity of the inhibited enzyme (OP-inhibited) in relation to the control enzyme (no OP-inhibition, but with incubation of aging delaying agent)) of the oxime induced or non-oxime induced reactivations of the sarin or soman-inhibited hAChE in the presence of each aging preventive agent was determined at different time intervals during the incubation period. Affinities of the aging preventive compounds towards hAChE are shown in Table 5.1. The affinities of the inhibitors towards AChE were already determined in earlier projects by me and Alexander Lodge and those values were used for this project. However, dose response assay was repeated for some inhibitors where it is necessary.

Table 5.1: Half- Maximal inhibitory concentration

Compound	IC_{50} (M)
A	2.14×10^{-6}
B	$1.1 (\pm 0.3) \times 10^{-2}$
C	$9.4 (\pm 0.7) \times 10^{-4}$
D	$7.3 (\pm 0.9) \times 10^{-5}$
E	$1.5 (\pm 0.1) \times 10^{-5}$
F	$4.6 (\pm 0.2) \times 10^{-5}$

The six inhibitors shown in Figure 5.1 were examined to check their ability to reactivate non-aged hAChE inhibited with organophosphorous inhibitors sarin and soman analogs. These inhibitors were also evaluated against aged-AChE inhibited by the sarin analog. None of them showed reactivation of the aged-AChE adduct. Inhibitors A, B, and C were evaluated with only the sarin analog and aging delaying experiments were conducted for almost two days. Data are shown in Figure 5.4. First order kinetics data of apparent reduction of the percentage of oxime induced reactivated hAChE for residual (OP-inhibited, but no aging delaying agent) indicates that aging is occurring with the time, where 2-PAM can reactivate only the non-aged form of the OP-AChE complex, but not the aged OP-AChE complex. Thus, AChE activity is reduced with the time in control experiment. Percentages of reactivated enzyme are also getting reduced for the sarin-AChE complexes that are incubated with inhibitors A and B. Therefore, these inhibitors are not capable of reactivating OP-inhibited hAChE in order to prevent or delay the aging process. However, inhibitor C is able to maintain AChE activity approximately 20% higher than control activity. Moreover, as in the literature,[34] it is confirmed again in these experiments that 2-PAM is able to reactivate only non-aged form of the OP-AChE complexes but not the aged-AChE complexes.

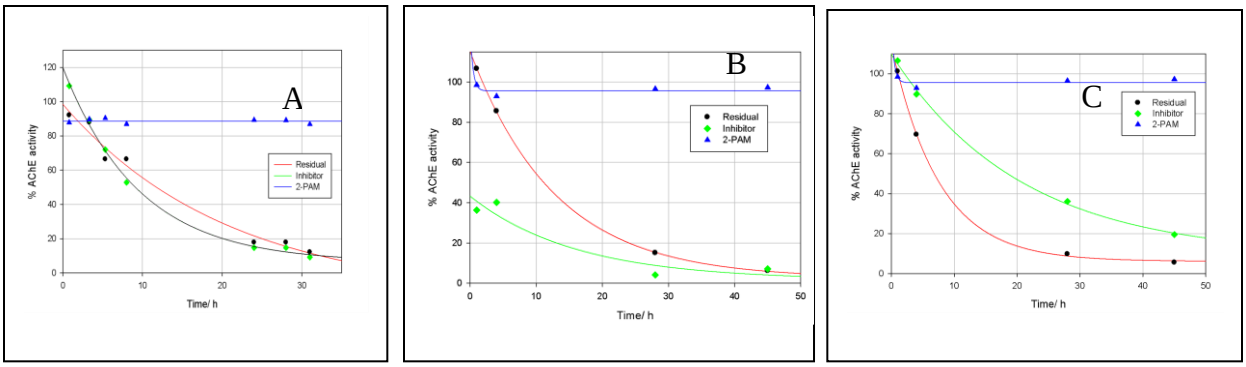

Figure 5.4: Plots of the percentage of oxime-induced reactivated sarin inhibited hAChE against incubation time with inhibitors A, B, and C.

Inhibitors D, E, and F that contained a methoxy group on the pyridine ring 2-position were already tested as methylating agents against aged OP-AChE complexes. From the previous studies done by other group members, it was observed that these methoxy containing inhibitors are good at transferring a methyl group to the aged OP-AChE analog.[52] Therefore, these inhibitors were tested as aging delaying agents against both sarin inhibited and soman inhibited hAChE. As shown in Figures 5.5 and 5.6, all three inhibitors were able to maintain hAChE activity throughout the experimental period to a significant level. At each time point, 30 minutes incubation with 2-PAM was performed prio to the initial rates measurement (oxime-induced reactivation). Reduction of the residual activities with the time indicates the aging of OP-AChE complexes with the time. Thus, 2-PAM is unable to reactivate the aged-AChE. 2-PAM at 5 x K_i was also used as reference aging delaying agent (blue line). It was observed that 2-PAM is maintaining AChE activity at higher level by continuous reactivation of the non-aged-AChE complex, thereby preventing or delaying the aging process. The similar results were observed for the inhibitors D, E and F which contained methoxy groups on the pyridinium ring. The experiment was repeated without oxime-induced (without 30 minutes incubation of 2-PAM as an oxime reactivator) reactivation to see if these three inhibitors are capable of reactivating OP-inhibited hAChE.

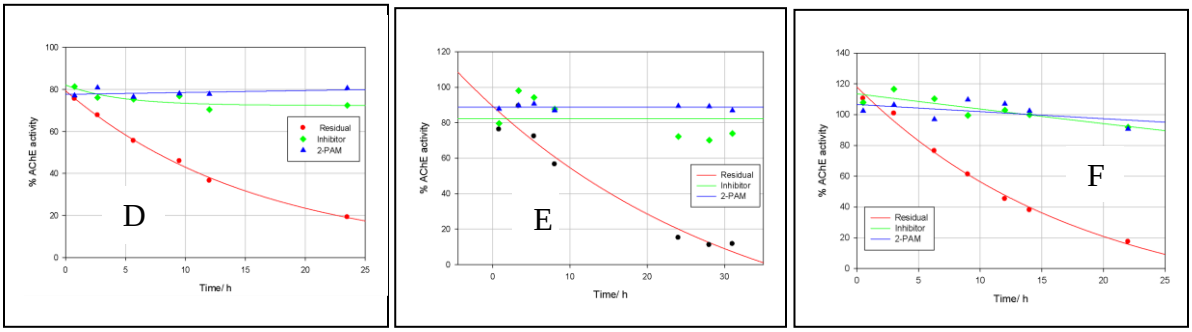

Figure 5.5: Plots of the percentage of oxime-induced reactivated sarin-inhibited hAChE against incubation time with Inhibitors D, E, and F.

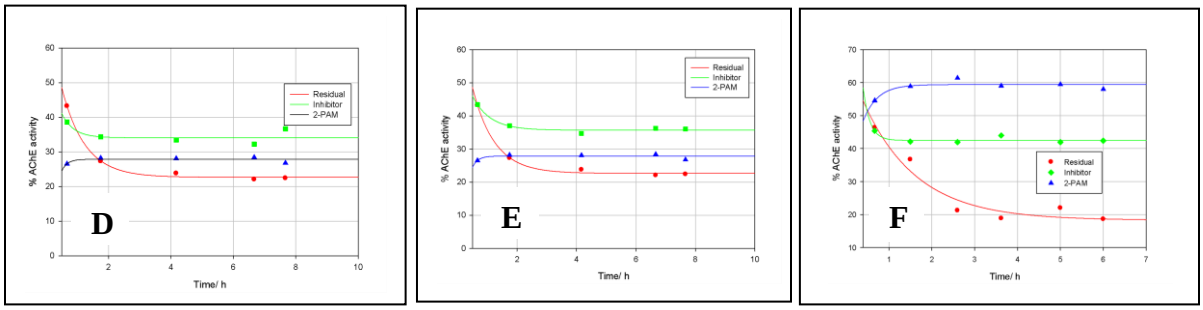

Figure 5.6: Plots of the percentage of oxime-induced reactivated soman-inhibited hAChE against incubation time with inhibitors D, E, and F.

For non-oxime-induced AChE reactivation, sarin or soman-inhibited AChE was incubated with each tested methoxy compound (D, E, or F) and intial rates of substrate hydrolysis were determined at different time points by directly adding substrate to the incubated solution in phosphate buffer. Initial rates of substrate hydrolysis were then measured without 30 minutes of 2-PAM incubation. Data are shown in Figure 5.7 (sarin-inhibited) and Figure 5.8 (soman-inhibited).

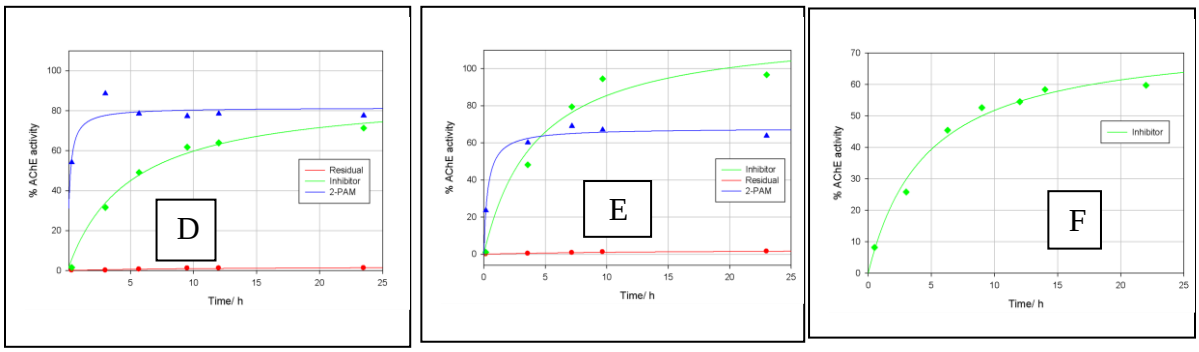

Figure 5.7: Plots of the percentage of non-oxime-induced reactivated sarin-inhibited hAChE against incubation time with the Inhibitors D, E, and F.

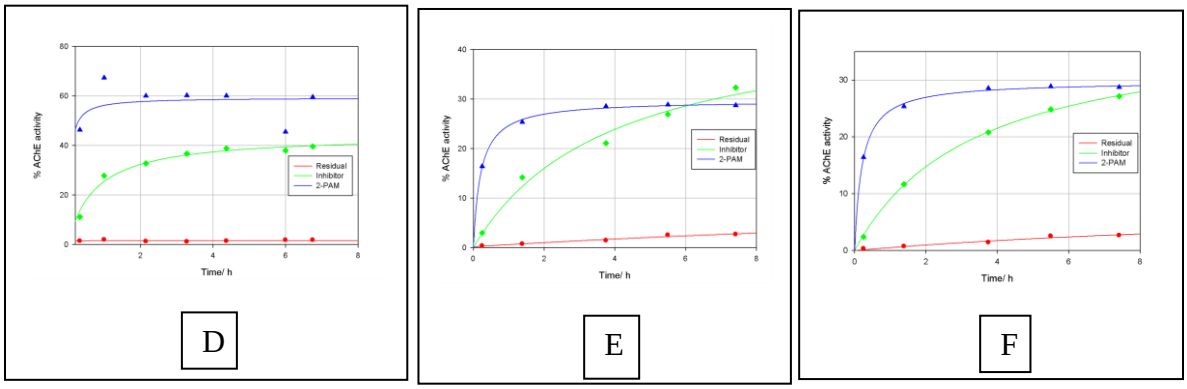

Figure 5.8: Plots of the percentage of non-oxime reactivated soman-inhibited hAChE against incubation time with Inhibitors D, E and F.

It appears in the Figures 5.7 and 5.8 that like 2-PAM, all three inhibitors that included methoxy groups on the pyridine ring are capable of reactivating both sarin and soman-inhibited AChE complexes to significant levels without help of other oxime reactivators, whether the pyridine ring is substituted or not. But, the substitution of pyridine ring with the electron withdrawing groups (i.e. CF_3 and NO_2) changes the rate of the reactivation process. Comparison of the reactivation versus residual (i.e. in the absence of inhibitor D, E or F) revealed that all these three inhibitors are capable of reactivating both sarin and soman-inhibited hAChE to some extent and prevent (or delay) aging of the OP-AChE complexes by continuous reactivation. Unsubstituted

inhibitor reactivates approximately 60 % of sarin-inhibited AChE and 40 % of soman-inhibited AChE while triflouro group containing inhibitor F reactivates nearly 60 % of the sarin-inhibited AChE and 30 % of the soman-inhibited AChE in non-oxime induced reactivation. Furthermore, most pronounced reactivation (approximately 100 %) was observed for the sarin-inhibited AChE that was incubated with nitro group substituted inhibitor E while approximately 35 % of the soman-inhibited AChE was reactivated by the incubation of soman-inhibited AChE with this inhibitor E. In all the experiments, it was clearly observed that residual activities (no aging preventive agents, but with OP) were approximately zero (for sarin-inhibited AChE) or less than 5 % (for soman-inhibited AChE). Thus, reactivation of sarin or soman-inhibited AChE by these three tested inhibitors is obvious.

All three methoxy group containing inhibitors were obtained from the stock solutions that were in the freezer for approximately one year. In order to make sure the chemical constituents of these inhibitor solutions are the same as the structures shown in the Figure 5.1, experiments were repeated with fresh solutions prepared by dissolving solids of each inhibitors (D and F) in the relevant solvents right before the experiment starts. If the chemical constituents are similar in both old and fresh solutions, similar reactivity should be observed. The results of these experiments are shown in Figures 5.9 and 5.10 for sarin and soman-inhibited AChE, respectively. These results showed that OP-inhibited AChE activities were only recovered by oxime-induced reactivation. No reactivation is observed without 2-PAM. This clearly indicates that the reactivation achieved earlier (non-oxime induced reactivation) was not because of the inhibitors D, E, and F shown in the Figure 5.1. Thus, the observed reactivation must be due to something else in the old frozen solution. The marked difference of the results obtained for two solutions of the same inhibitor

(frozen and fresh) necessitated further experiments to investigate the compound that is giving this reactivation of both sarin and soman-inhibited hAChE.

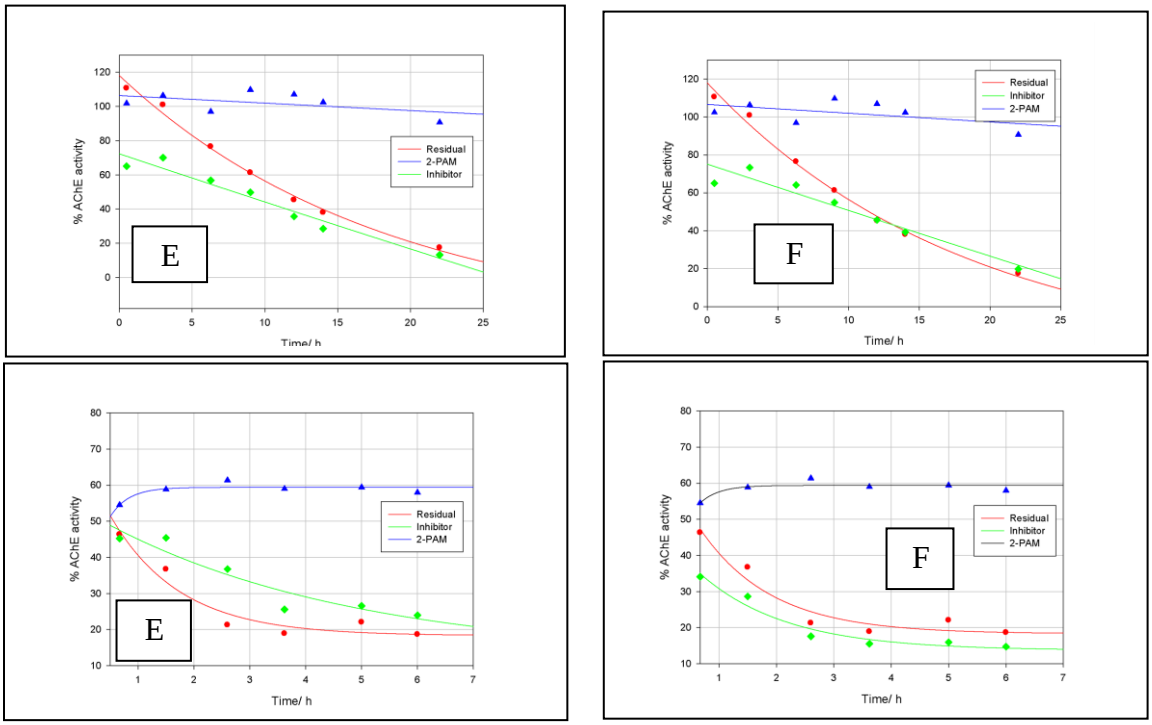

Figure 5.9: Oxime-induced reactivation kinetics of sarin-inhibited (Top) and soman- inhibited (Bottom) hAChE by fresh solutions of inhibitors E and F.

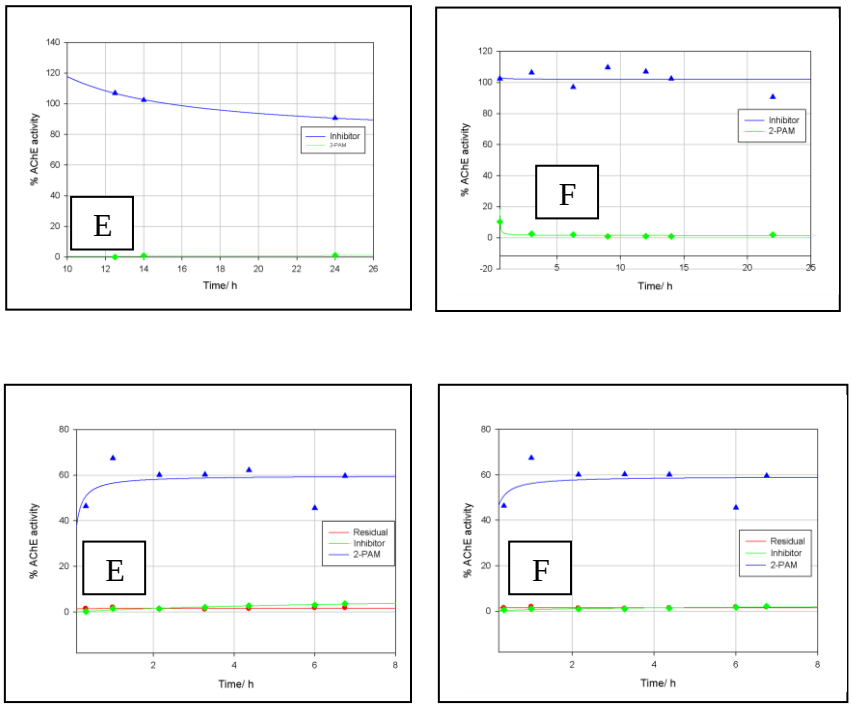

Figure 5.10: Non-oxime- induced reactivation kinetics of sarin (Top) and soman (Bottom) inhibited hAChE by fresh solutions of inhibitors E and F.

For further understanding of this unknown reactivator, absorbance spectra of fresh and old solutions of each inhibitors (E and F) were obtained and shown in Figure 5.11. The difference of the spectral data of each inhibitor for the same concentration of the fresh and old- frozen solutions indicated the difference of the chemical constituents of these old and fresh solutions. Therefore, for further clarifications, inhibitor E, that degraded fast in water, was selected to prepare degraded sample and degradation was monitored by ^{1}H NMR. Once degradation was completed, a reactivation experiment was performed with soman-inhibited hAChE using degraded sample. The results are shown in Figure 5.12. It was observed that degraded sample of inhibitor E reactivates only about 5 % higher than control in the oxime-induced reactivation process which is approximately 25 % less than what was observed with the old solution of the inhibitor E while it

was approximately 8 % in non-oxime-induced reactivation that is approximately 20 % reduced from the reactivation observed for non-oxime induced reactivation with the old frozen sample of E. Since degraded sample showed some reactivation against sarin inhibited AChE, and the major degradation product was the pyridone (Structures are shown in Figure 5.13), pyridone products of inhibitors D, E and F were also evaluated against sarin and soman inhibited hAChE using 5 x K_i concentrations. The results are shown in Figures 5.14 and 5.15.

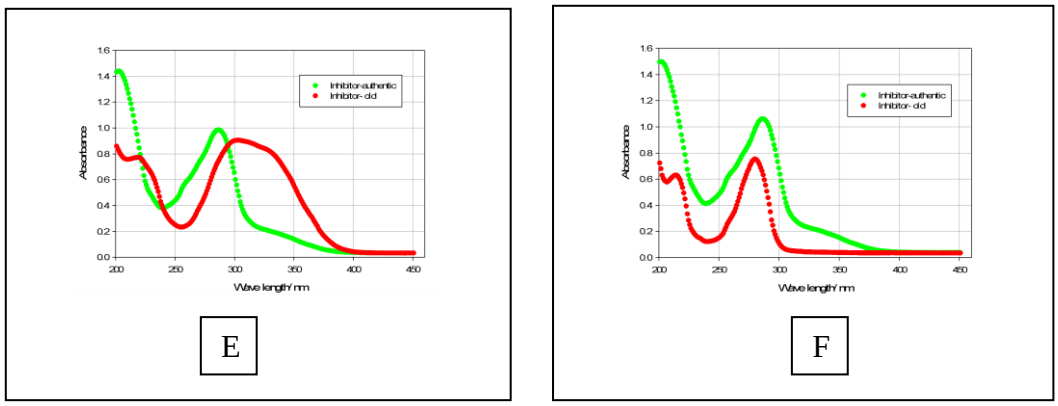

Figure 5.11: UV spectra for fresh and old solutions of inhibitors E and F. Concentration 100 µM

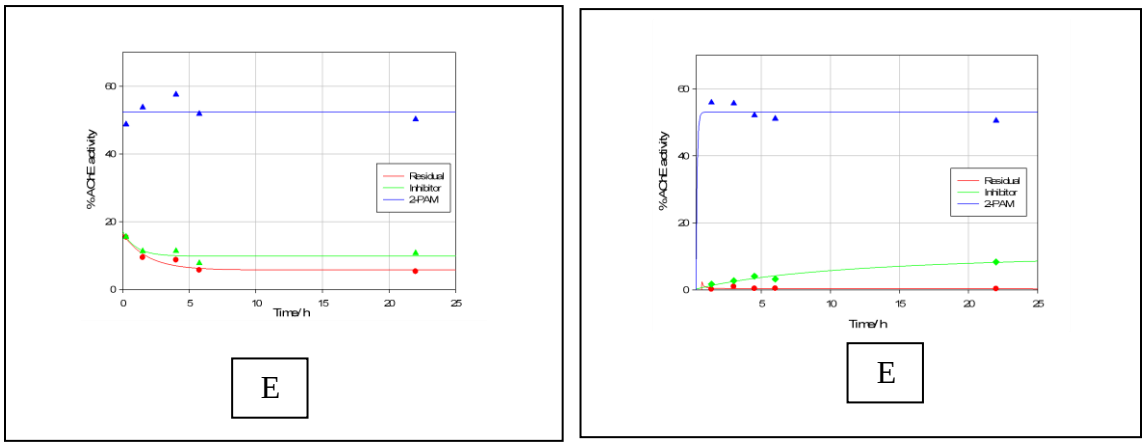

Figure 5.12: Oxime-induced (Left) and non-oxime-induced (Right) reactivation of soman-inhibited hAChE by degraded sample of Inhibitor E.

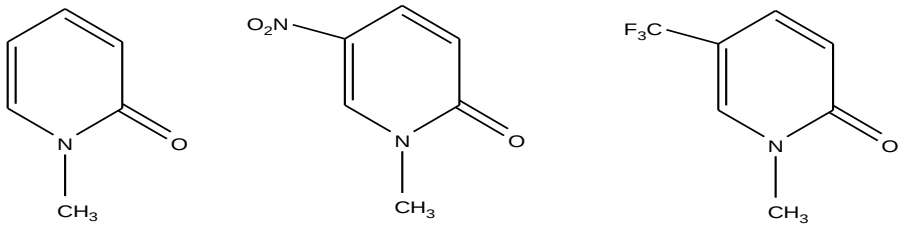

D ' **E '** **F '**

Figure 5.13: Chemical structures of pyridone products of Inhibitors D, E, and F.

As illustrated in Figures 5.14 (sarin-inhibited) and Figure 5.15 (soman-inhibited), none of the pyridones reactivates the sarin or soman inhibited hAChE without using 2-PAM as an oxime reactivator. However, pyridone product of inhibitor F showed maintaining of the hAChE activity only in the oxime-induced reactivation. Therefore, the experiment was repeated with unsubstituted pyridone product (D') with higher concentration (10 K_i, 100 K_i) since pyridones are not strong inhibitors of hAChE (K_i of inhibitor F is 3.7 mM). Because 5 K_i concentrations of pyridones may not be sufficient enough to bind with all the OP-AChE complexes to reactivate them. Results are shown in Figure 5.16. It was observed that higher concentrations of pyridone do not make considerable changes of the reactivation. That is obvious in the non-oxime induced reactivation. Thus, investigation of this unknown reactivator was continued further. In order to understand the chemical content of the old frozen samples, water suppressed H-NMR, and high resolution MS were obtained and evaluated. The major degradation products of these samples were pyridones.

This did lead us to think of starting material of these inhibitors as the unknown reactivators. Because residual amounts of starting materials would have remained in the inhibitor solutions.

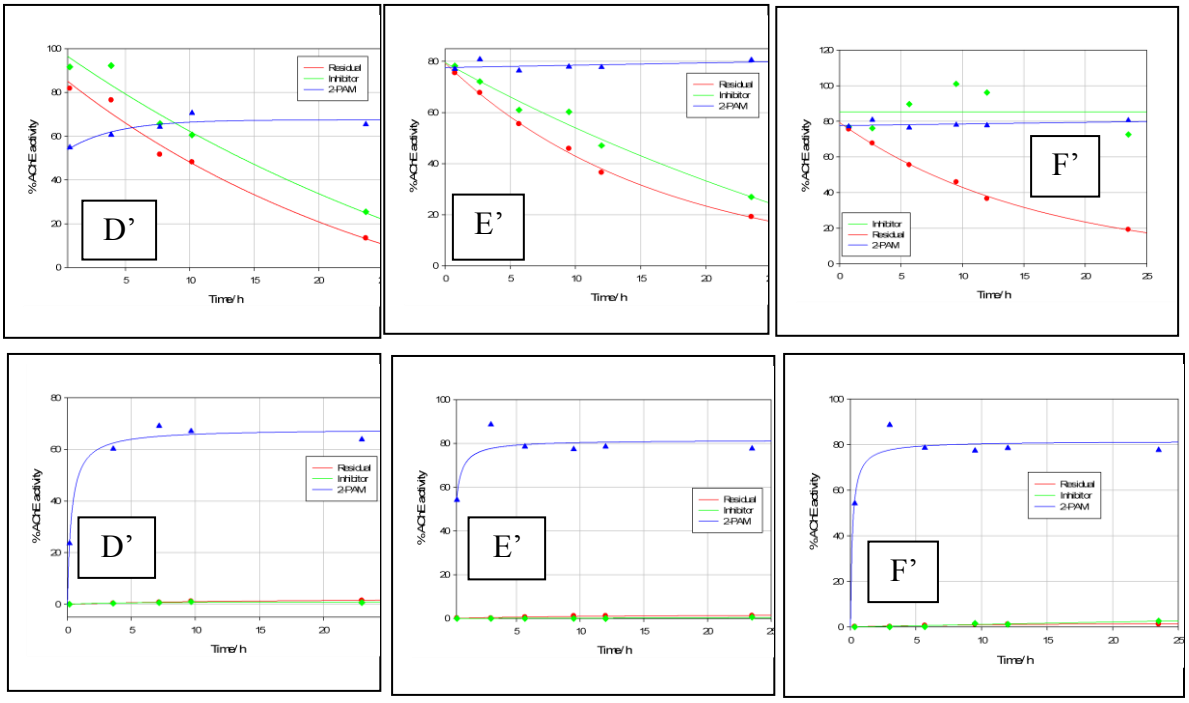

Figure 5.14: Effects of pyridone products of inhibitor D (D'), E (E'), and F (F') on AChE inhibited by the sarin analog

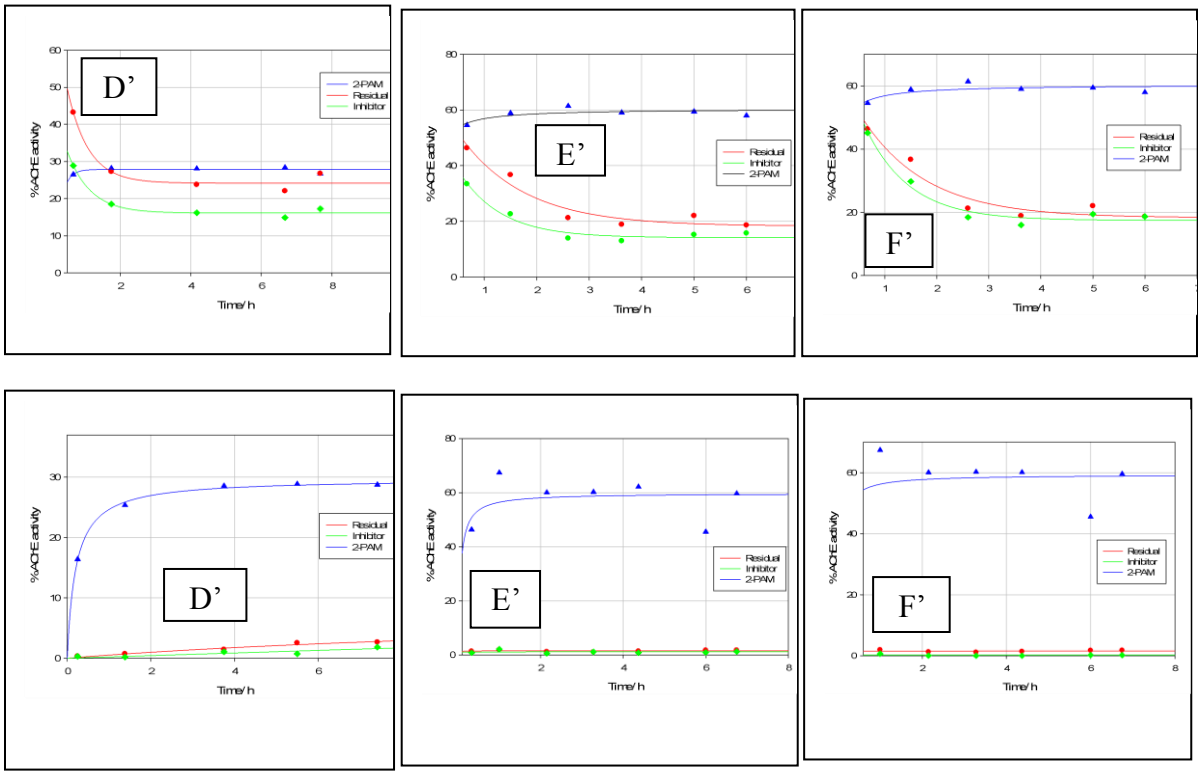

Figure 5.15: Oxime-induced (Top) and non-oxime-induced (Bottom) reactivations of soman-inhibited hAChE by pyridone products of inhibitor D (D'), E (E'), and F (F')

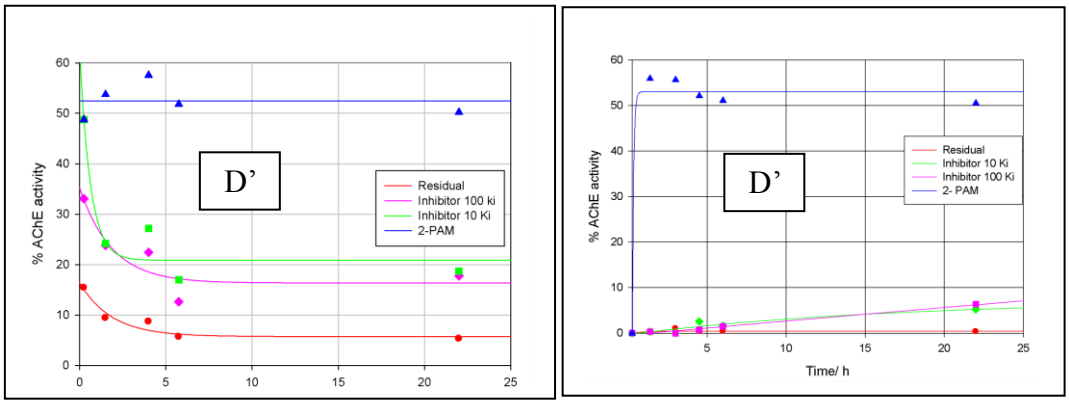

Figure 5.16: Oxime induced (Left) and non oxime induced (Right) reactivation of soman-inhibited hAChE by different concentrations of pyridone product of inhibitor D

Reactivation by the starting material of inhibitor E (Figure 5.17) was then evaluated to see whether this unknown reactivation is due to a residual amount of starting material left with the inhibitor during the synthesis process. Results (Figure 5.18) confirmed that the unknown reactivator is not the starting materials of these inhibitors.

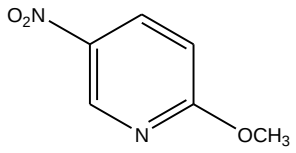

G

Figure 5.17: Chemical structure of starting material of Inhibitor D (G)

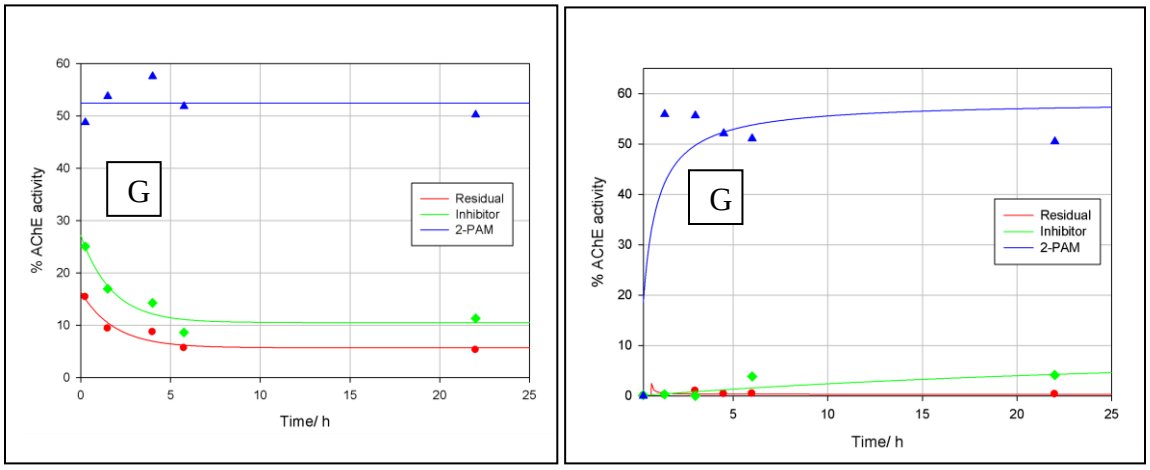

Figure 5.18: Oxime-induced (Left) and non-oxime-induced (Right) reactivations of soman-inhibited hAChE by starting material of inhibitor E

Further thinking about this unknown reactivator made us check the activity of the solutions of the structure shown in Figure 5.19 (pKa~19)[b]. Although the mechanism for the formation of inhibitor I (pKa~ 3.3)[a] from the old-frozen solutions is not known, if there is a possibility to have the equillibrium reaction shown in Figure 5.20 in the presence of enzyme, there is a high possibility to transfer methyl group to the enzyme. Thus, aging delay would be observed as expected. However, data recorded in Figure 5.21 indicate that unknown reactivation is not due to the structures shown in Figure 5.20.

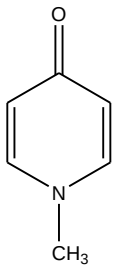

H

Figure 5.19: Chemical structure of Inhibitor H

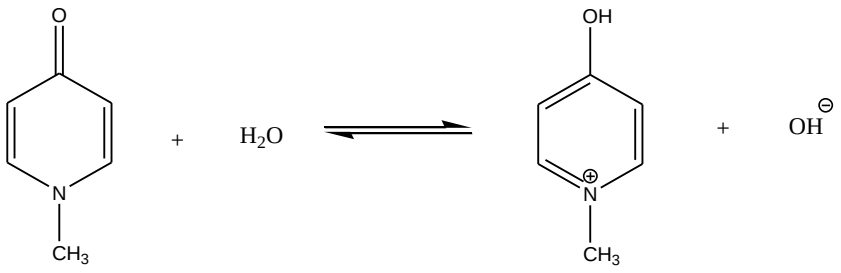

H **I**

Figure 5.20: Chemical structures that can be found in the solution of inhibitor H
(a)Albert, A.; Phillips, J. *Journal of the Chemical Society (Resumed)* **1956**, 1294
(b) Cook, M. J.; Katritzky, A. R.; Linda, P.; Tack, R. D. *Journal of the Chemical Society, Perkin Transactions 2* **1973**, 1080

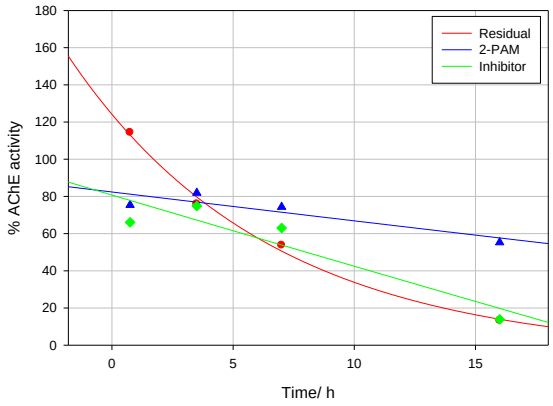

Figure 5.21: Oxime-induced reactivation of sarin-inhibited hAChE by solution of inhibitor H

Finally it was decided to evaluate old frozen samples of flourine-substituted methoxy pyridinium inhibitors since all methoxy group containing salts have the flourine in their counter ion. With the long period of time in the solvent, these inhibitors might have gotten flourine replacement on the pyridinium ring. However, the mechanism is not known. If flourine substitution happens in the old samples of inhibitors D, E, and F, they might have one of the structures as shown in Figure 5.22. If so, they are similar to the structures of flourine substituted inhibitors that were evaluated in early projects as resurrecting agents of aged-hAChE. The results of the reactivation kinetics by old frozon samples of inhibitors J and K are shown in Figure 5.23.

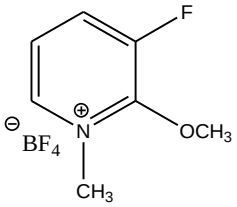

J

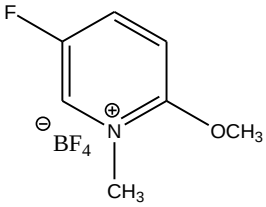

K

Figure 5.22: Chemical structures of fluorine-substituted methoxy group containing inhibitors.

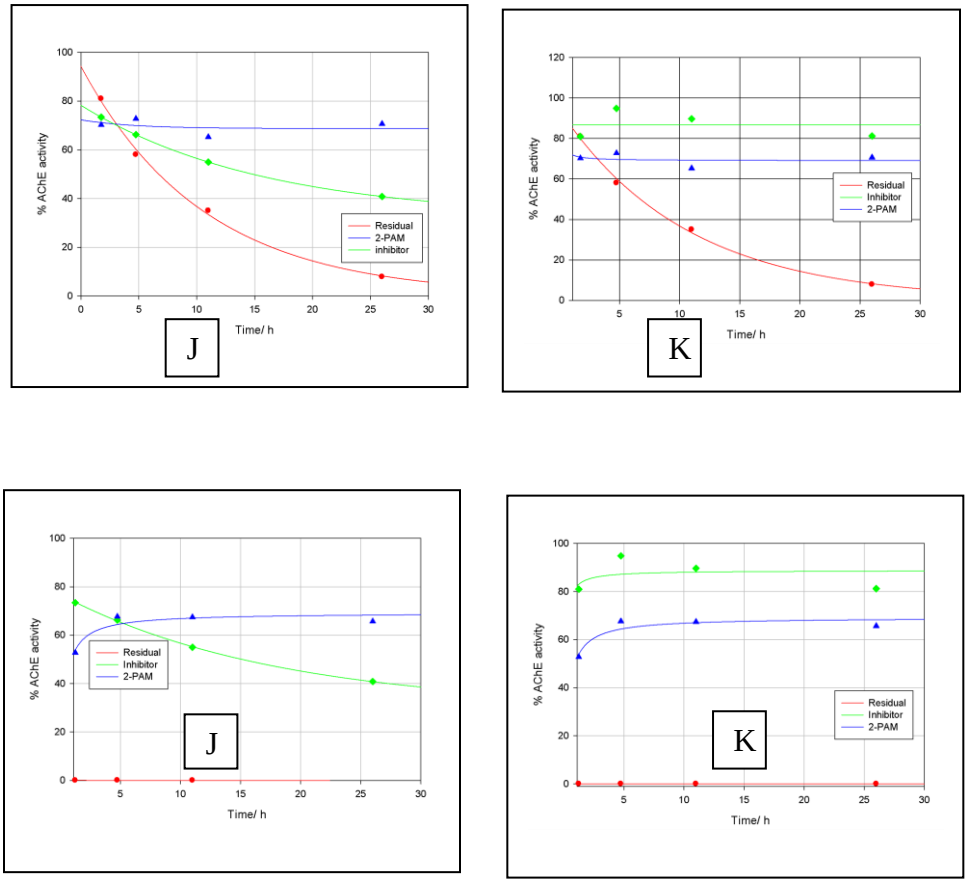

Figure 5.23: Oxime-induced (Top) and non-oxime-induced (Bottom) reactivations of sarin-inhibited hAChE by old-frozen samples of inhibitors J and K.

As illustrated in Figure 5.23, significant reactivation was observed for non-oxime induced reactivation for sarin inhibited hAChE by old samples of inhibitors J and K. 40 % and 60 % reactivations were observed for inhibitor J and K respectively compared to the residual (no aging preventive agents). However, based on these results, it is hard to come to a conclusion that the unknown reactivator would be flourine-substituted inhibitors without doing further experiments.

Moreover, repeated experiments for degradated sample (approximately after one year from the preperation) of inhibitor E (Figure 5.24) confirmed that some chemical in the degradated sample (with low concentration) is reactivating the initial complex of OP-inhibited AChE.

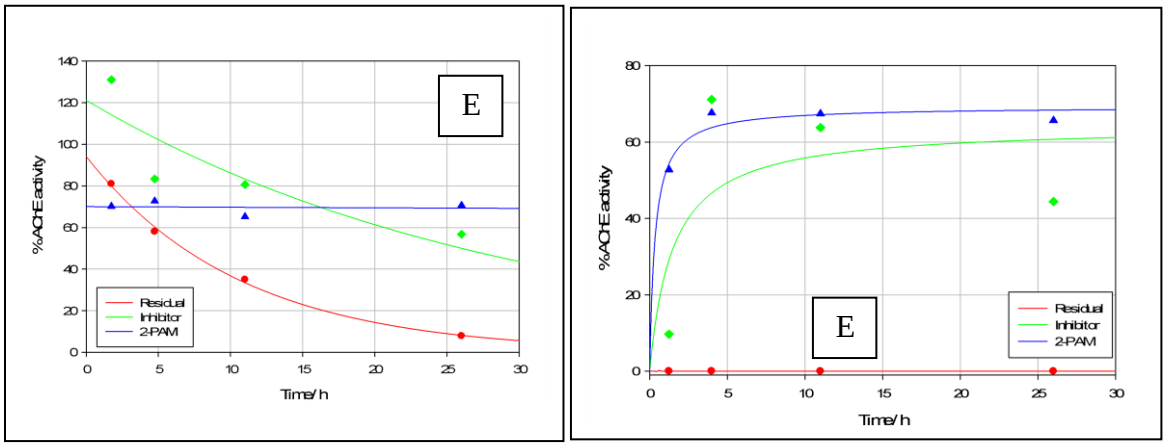

Figure 5.24: Oxime-induced (Left) and non-oxime-induced (Right) reactivations of sarin-inhibited hAChE by approximately one year old degraded sample of Inhibitor E.

Conclusion

It is important to mention here that the all the original compounds were initially designed with the aim of resurrecting the aged AChE. None of them resurrected (via transfer of methyl) the aged-AChE adduct *in vitro*. However, many of the methoxy group containing inhibitor salts were better methyl transfer agents to the aged-AChE analog.[52] As mentioned early in the chapter, when AChE is inhibited by OP inhibitors, including sarin and soman, the initial complex (non-aged) can be reactivated with nucleophilic antedotes such as 2-PAM.[65] However, subsequent de-alkylation of initial OP-AChE complex results in a mono anionic phosphyl complex named aged-AChE, for which there is no known antedote. Furthermore, no broad spectrum antedote exists for reactivating all the initial OP-AChE complexes. Thus, the unknown reactivators described herein would be a new family of inhibitors for the reactivation of initial OP-AChE complexes if the chemical structure is investigated. Therefore, futher experiments on identification of this unknown reactivator would provide a novel avenue for reactivation of the initial OP-AChE complexes that result from exposure of AChE to the nerve agents.

FUTURE WORKS

Reaction of fluorine substituted 2-PAM analogs with the aged-enzyme analog showed formation of methylsarin suggesting nucleophilic aromatic substitution and possible formation of the non-aged form of the enzyme analog. In the *in vitro* studies, 2-PAM and MINA were used as oxime reactivators to reactivate the non-aged OP-AChE complex if any from the nucleophilic aromatic substitution. Preliminary data obtained from those experiments indicated no reactivation. Since 2-PAM is a comparatively big molecule, it may not have a proper orientation to attack to the phosphorous atom of the OP-AChE complex in the active site, resulting in no reactivation. Furthermore, from the preliminary studies, MINA also did not reactivate aged AChE. Since MINA has lower binding affinity to the human AChE, this experiment needs to be continued with a series of different concentrations in order to evaluate the reactivatability of aged enzyme.

Furthermore, our research group studied methyl transfer ability of a family of ligands (inhibitors) that contain methoxy groups on the 2-position of the pyridine ring. Some of the inhibitors transferred a methyl group to the aged enzyme analog at a fast rate and from the *in vitro* studies, some showed about 10% resurrection of the aged enzyme by 24 hours. However, activity of the control enzyme was also low. It could be due to higher inhibitory potency of the studied ligands at the used concentration. Therefore, the resurrection experiment needs to be repeated with different concentrations of the ligand. If the control enzyme activity can be maintained at a higher level and the reactivation of the aged enzyme is observed, even 10% of aged enzyme reactivation is significant, specifically in the soman intoxication since the soman-AChE complex ages fast.

Moreover, some of the methoxy group containing ligands explained in chapter 5 showed apparent reduction (or prevention) of the aging process with oxime–induced reactivation and some (especially the solution of nitro group substituted methoxypyridinium) showed a pronounced

reactivation of the OP-AChE complex that resulted from both sarin and soman analogs in the absence of oxime incubation. Some of the inhibitors were also better reactivators of initial OP-AChE complex than commercially available 2-PAM. However, the actual reactivator of those ligand solutions that showed apparent prevention of the aging and reactivation of the OP-AChE complex is still unknown. From the HR-MS data analysis, it is expected that N-methyldihydroxy pyridine may have formed in the inhibitor solution and this may be the source of the observed reactivation. Therefore, whole experiments need to be repeated with the ligand mentioned above to evaluate aging prevention and reactivation of initial OP-AChE complex. If the reactivator is the suggested molecule, it may provide a lead for a family of reactivators of OP inhibited AChE.

According to the literature findings, replacement of the negatively charged E202 with an uncharged residue reduces the rates of both phosphylation and aging. But, it is not confirmed that the apparent reduction of the aging and reactivation of the OP-AChE complex in our studies is due to alkylation of the E202 residue. Thus, crystallographic studies for those reactivators complex with OP-AChE are highly desired in order to identify the relevant structures and their interactions. Those data will provide key interactions to design new reactivators of OP inhibited AChE.

APPENDIX A

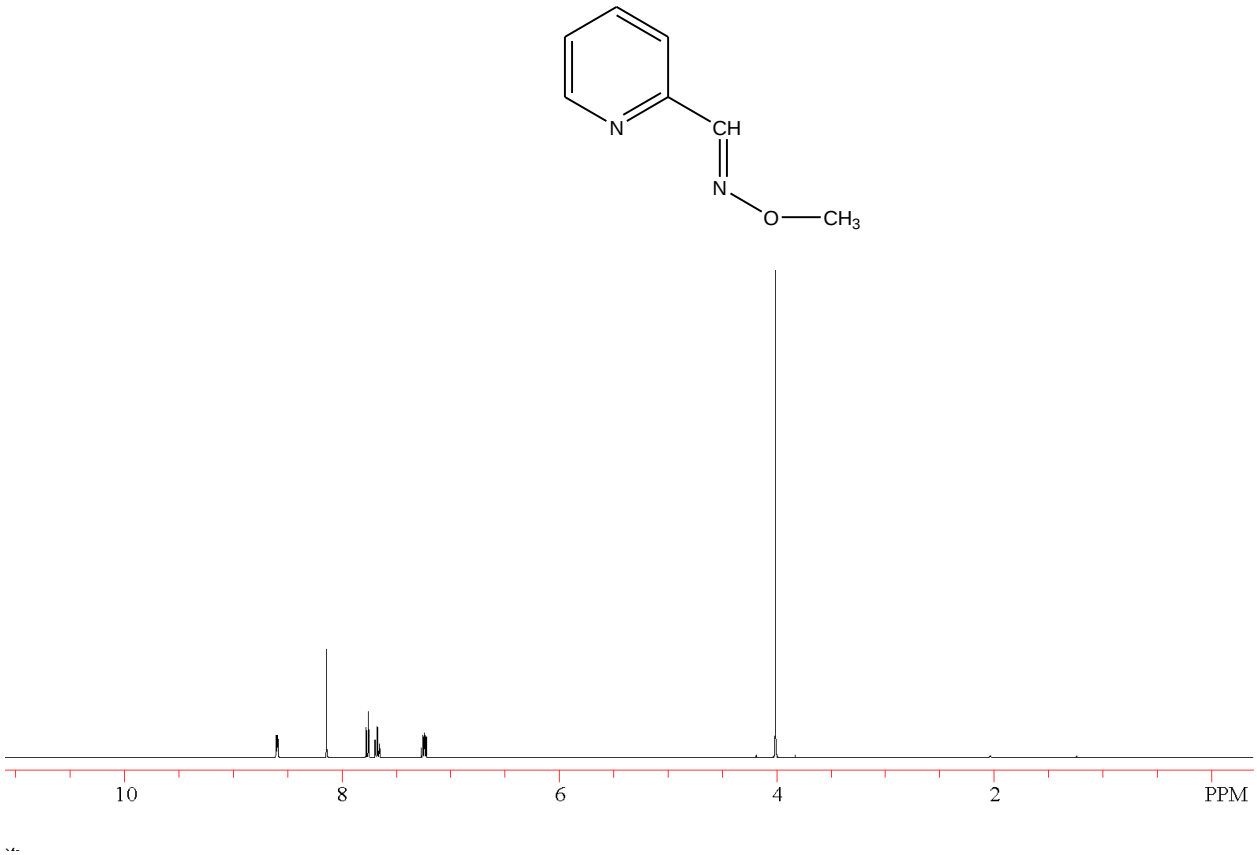

Figure A.17: 500 MHz **^{1}H NMR** spectrum in $CDCl_3$

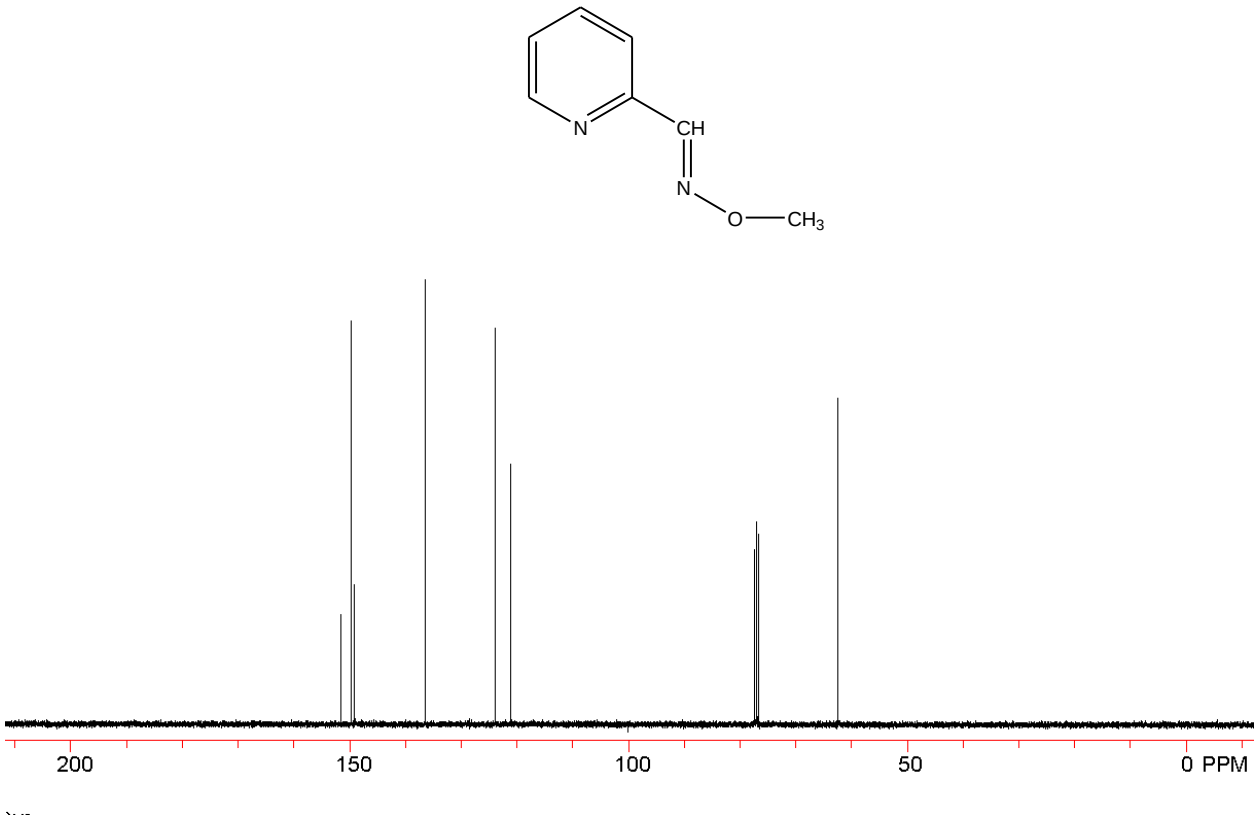

Figure A.2: 100 MHz **^{13}C NMR** spectrum in $CDCl_3$

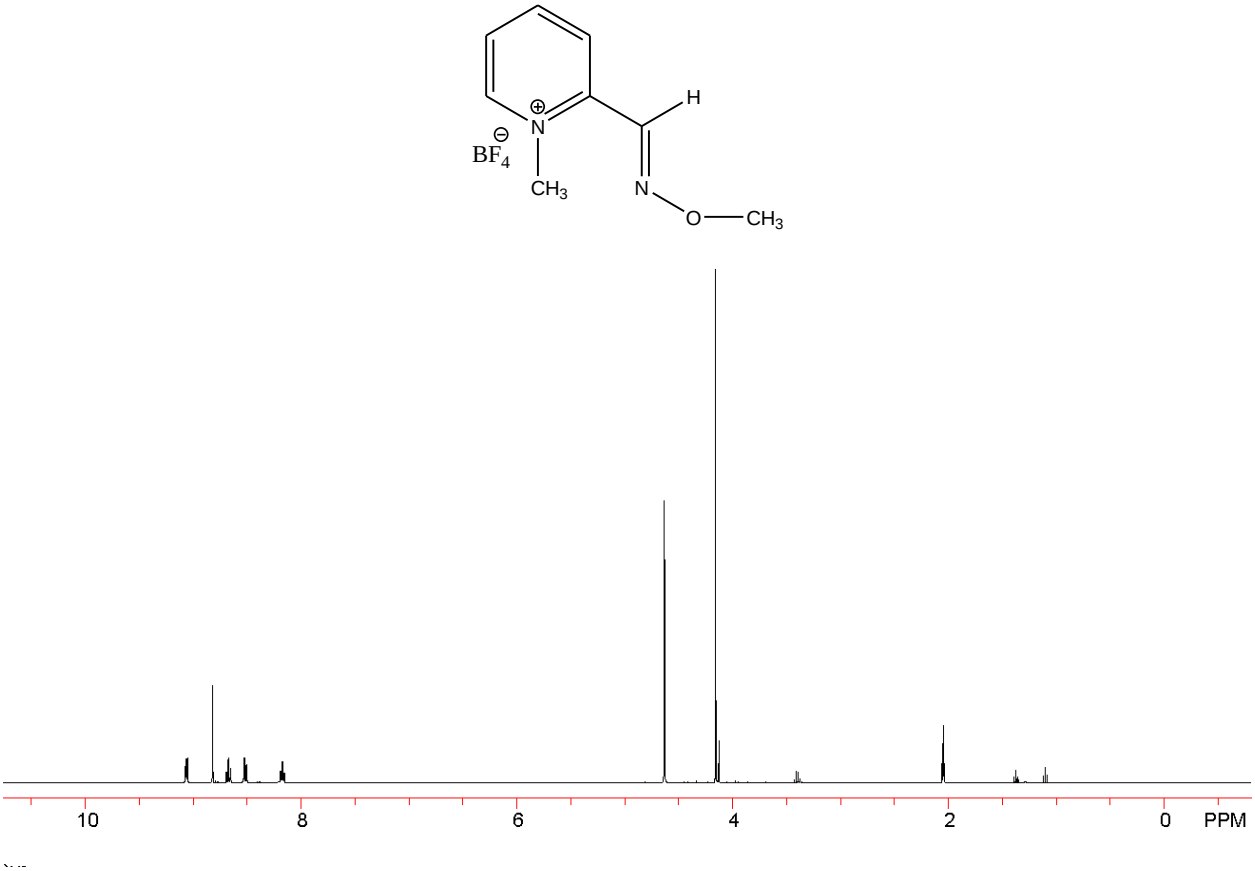

Figure A.3: 500 MHz **^{1}H NMR** spectrum in Acetone

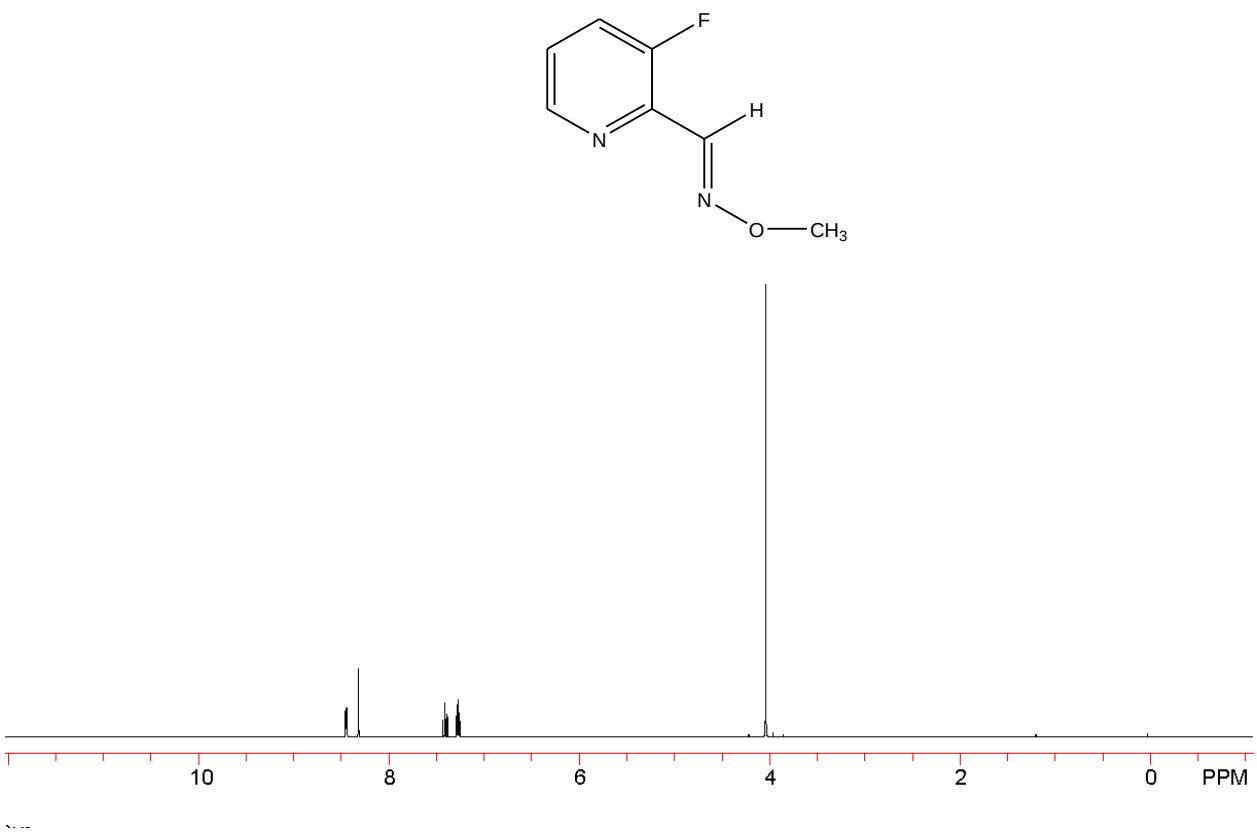

Figure A.4: 500 MHz **^{1}H NMR** spectrum in $CDCl_3$

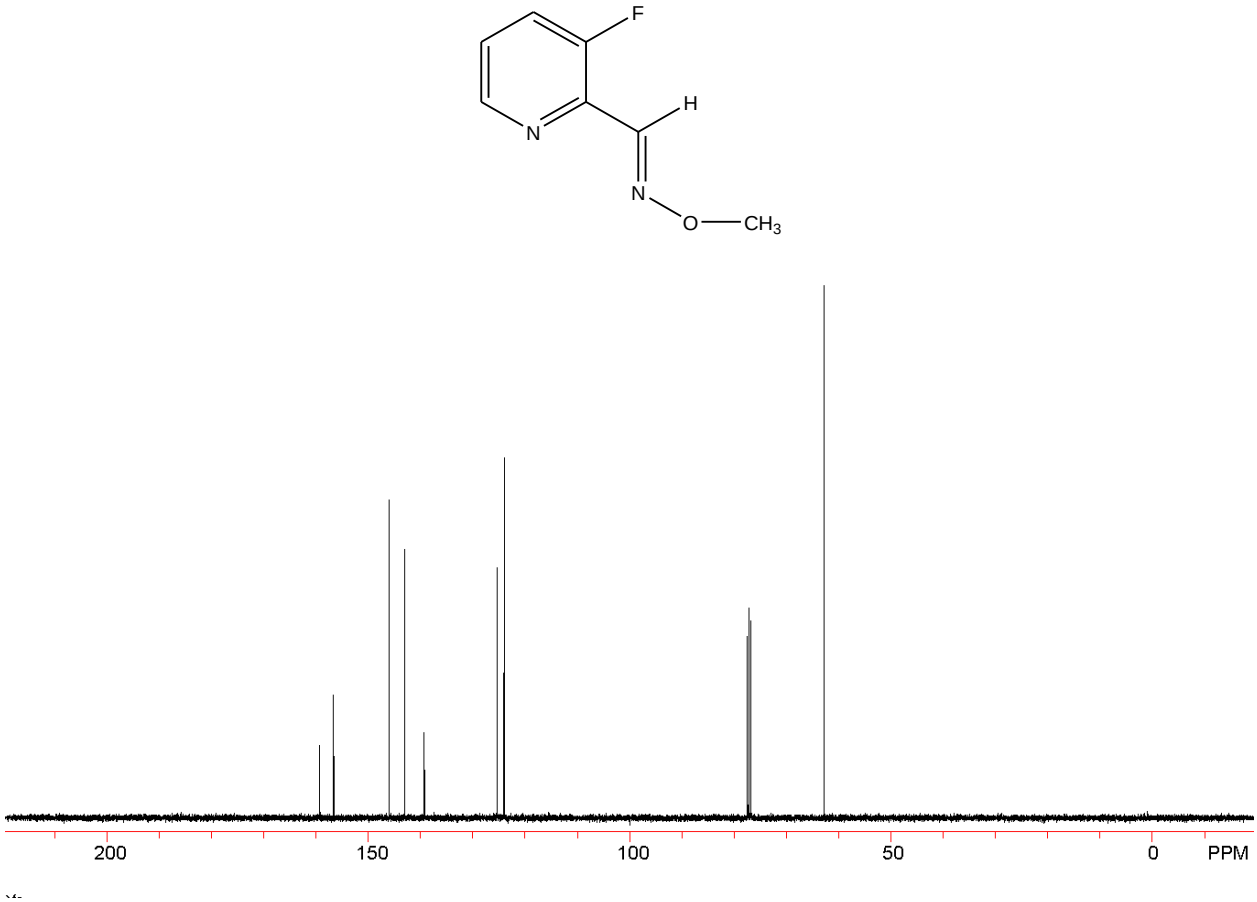

Figure A.18: 100 MHz ^{13}**C NMR** spectrum in $CDCl_3$

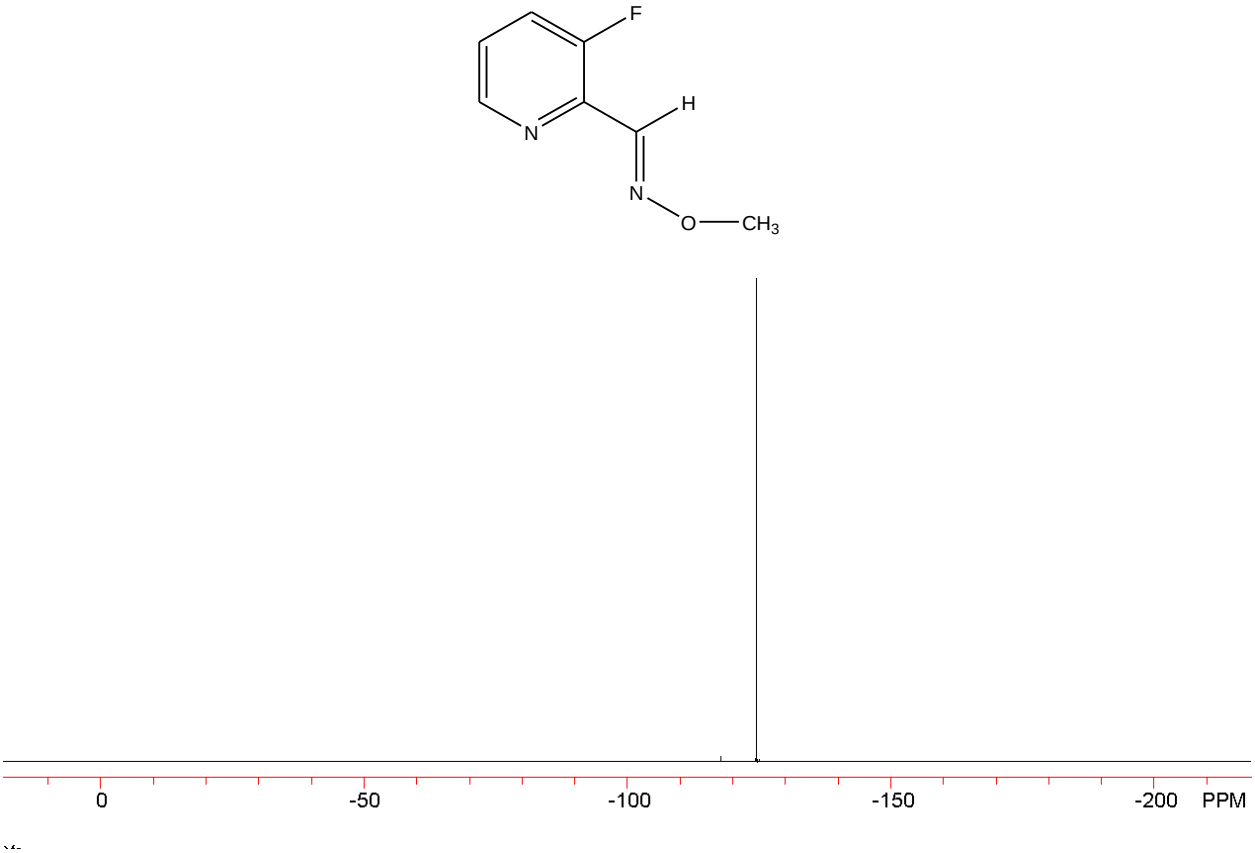

Figure A.6: 477 MHz ^{19}**F NMR** spectrum in $CDCl_3$

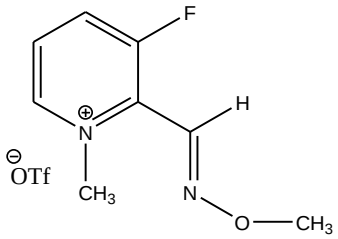

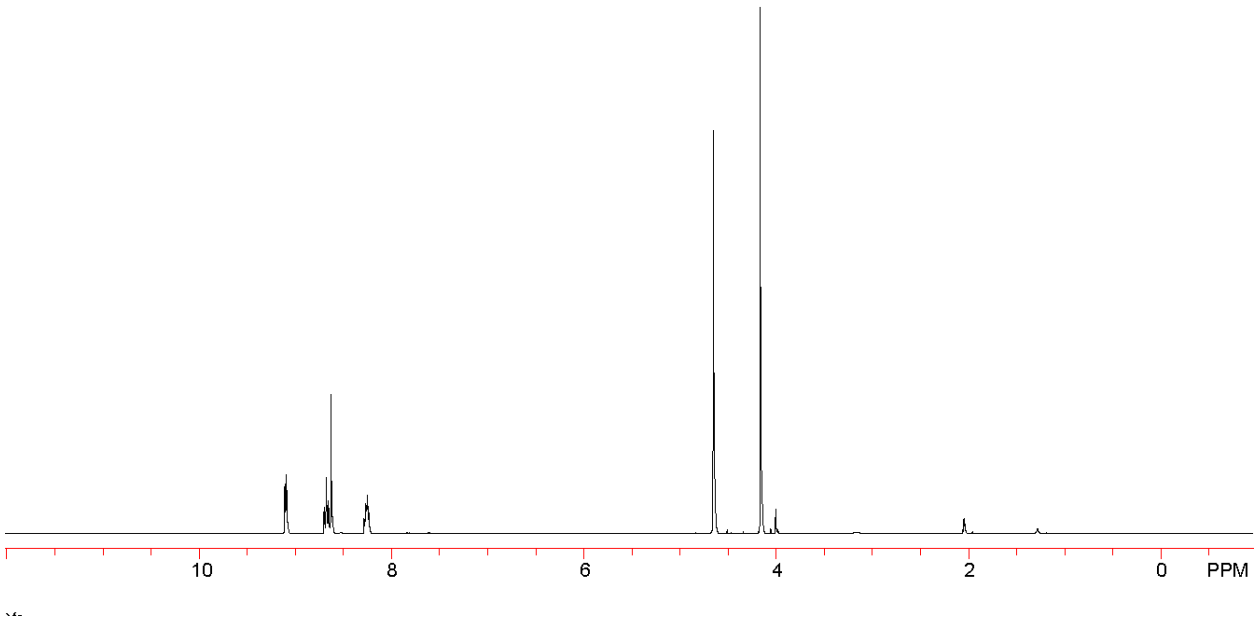

Figure A.7: 500 MHz **^{1}H NMR** spectrum in Acetone

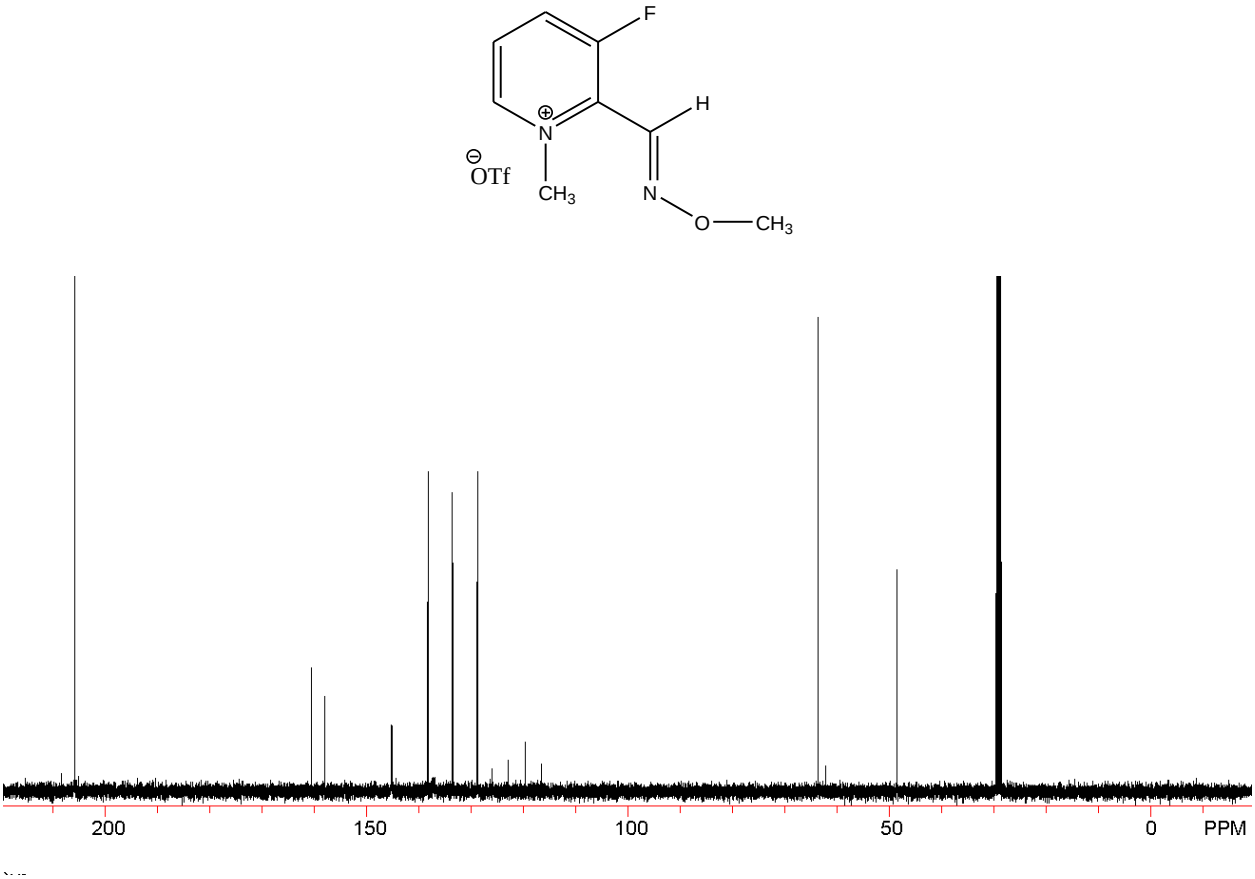

Figure A.8: 500 MHz **^{1}H NMR** spectrum in Acetone

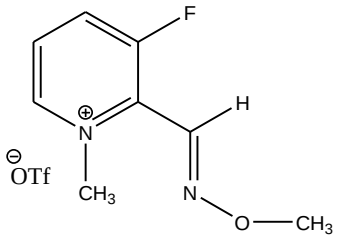

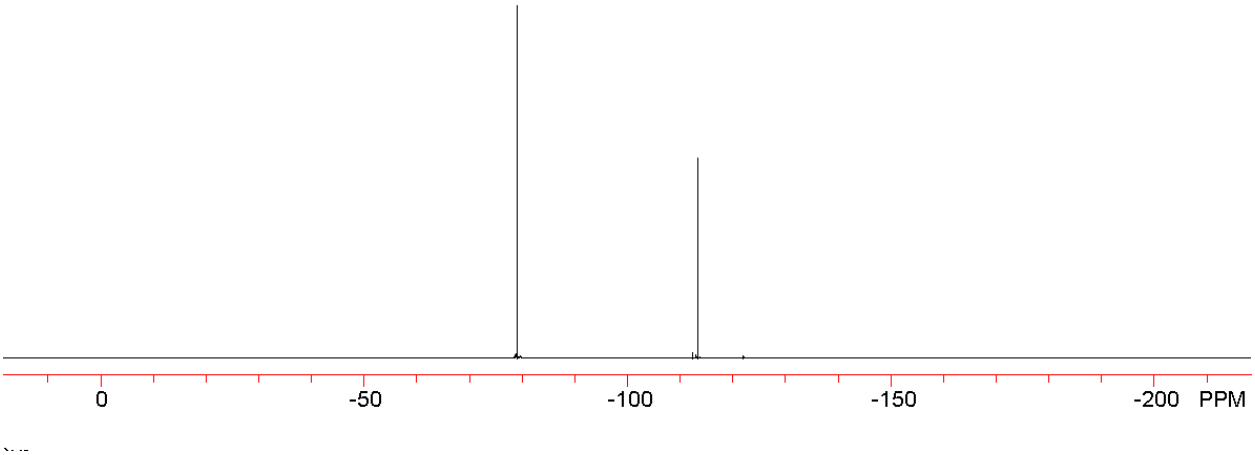

Figure A.9: 477 MHz ^{19}**F NMR** spectrum in Acetone

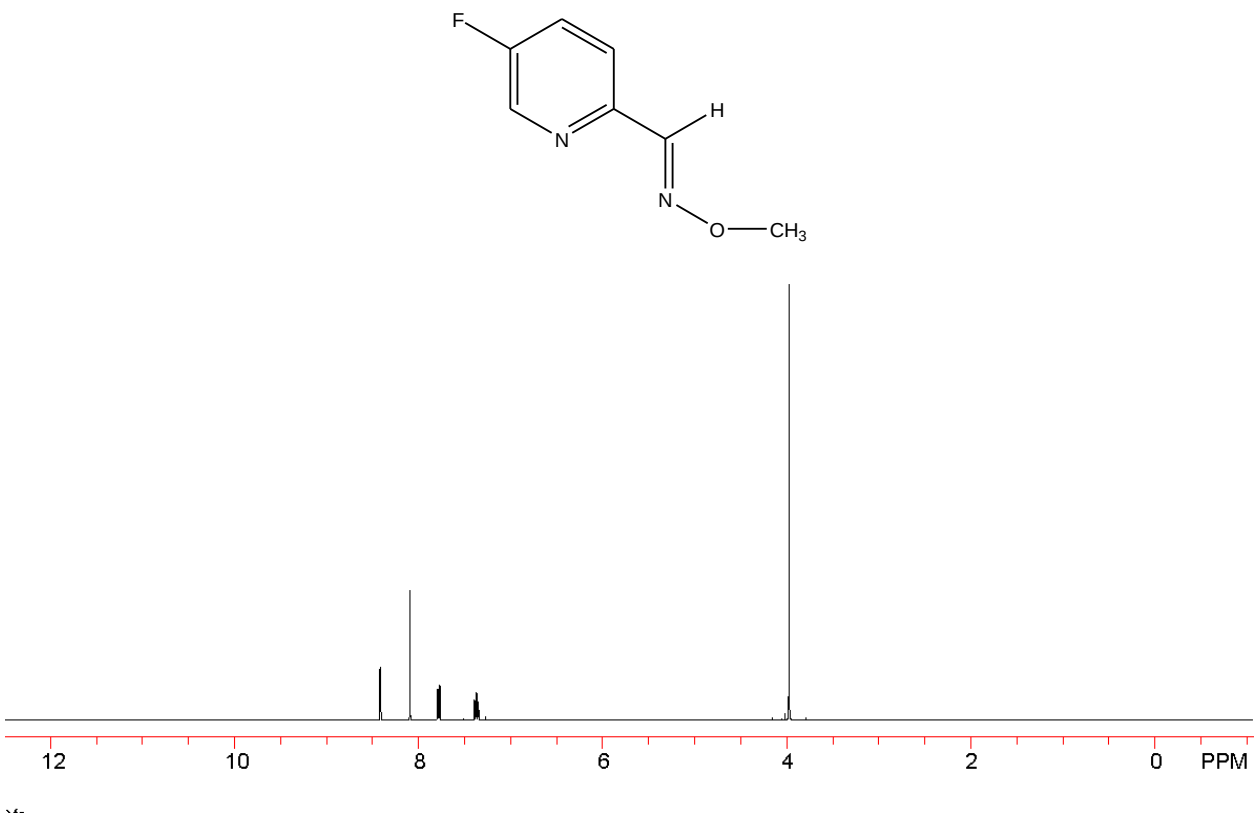

Figure A.10: 500 MHz **^{1}H NMR** spectrum in $CDCl_3$

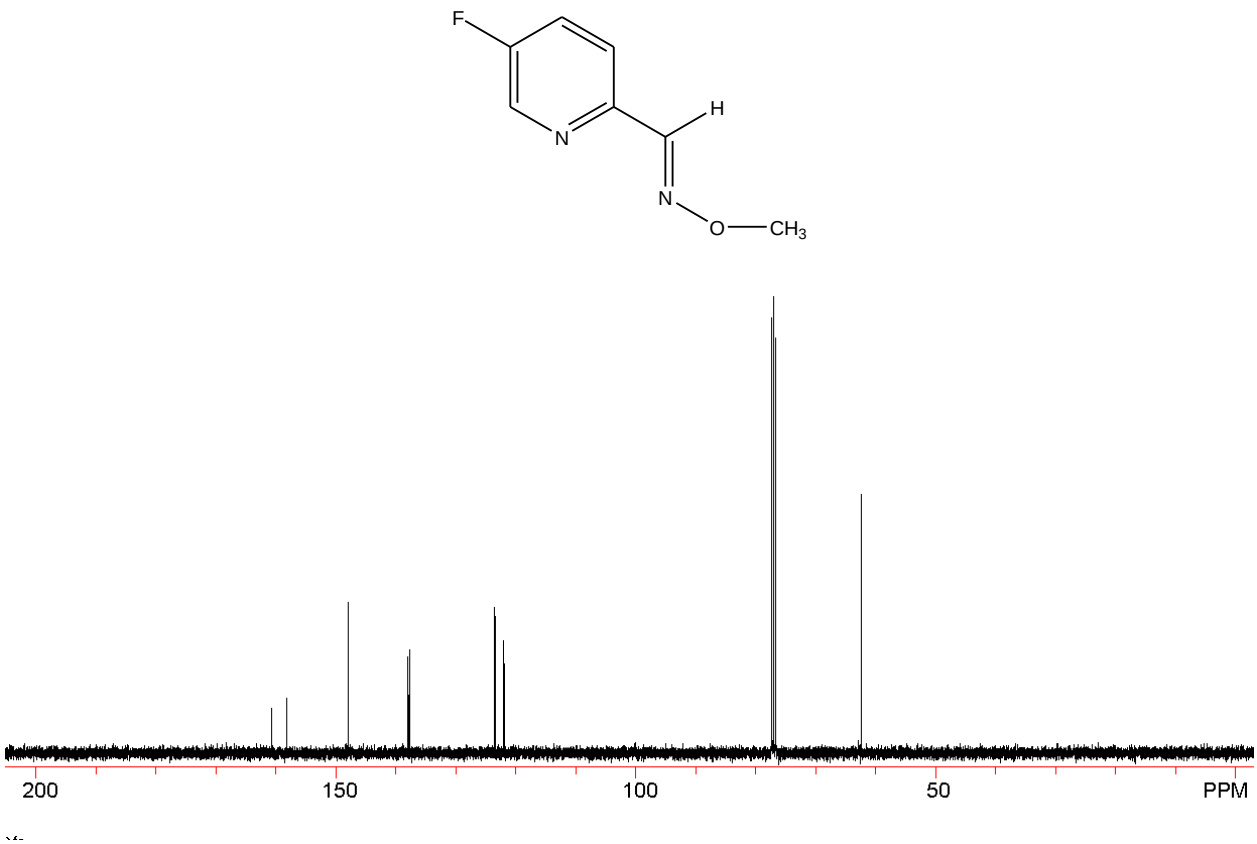

Figure A.11: 100 MHz ^{13}**C NMR** spectrum in $CDCl_3$

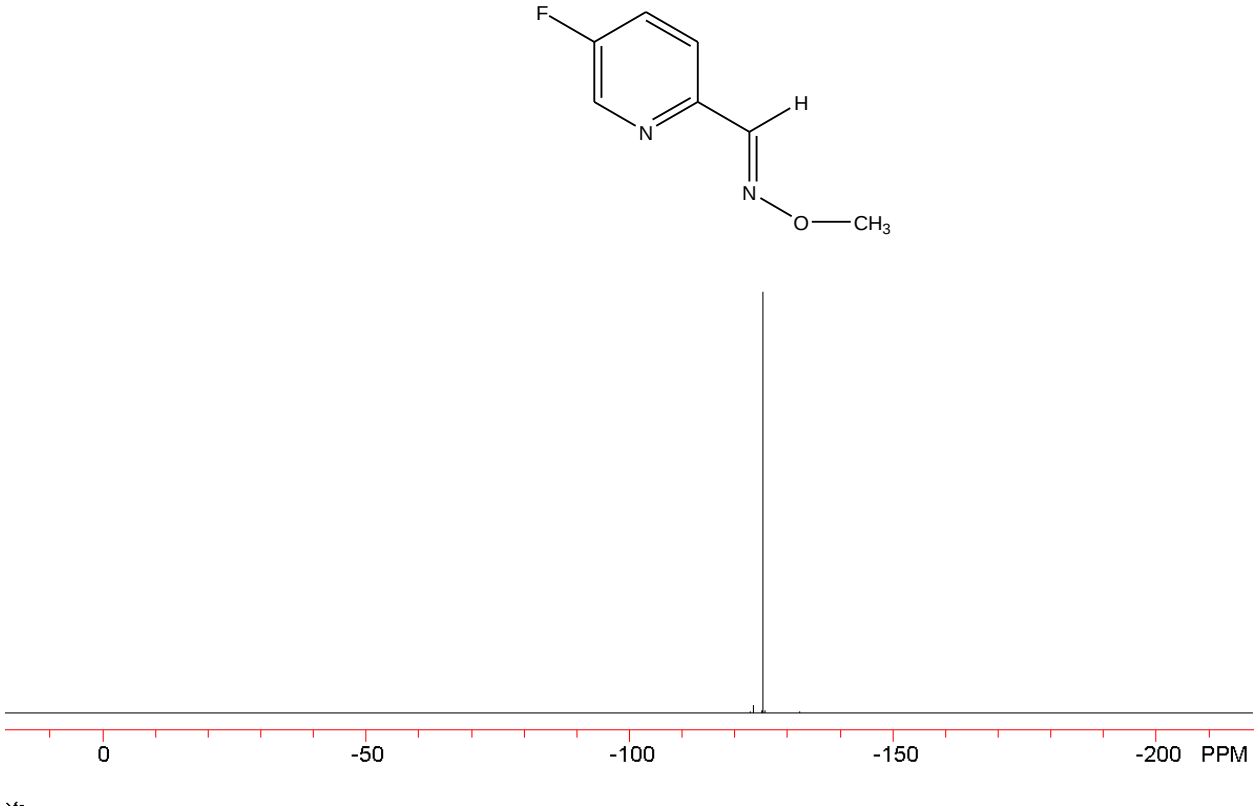

Figure A.12: 477 MHz ^{19}**F NMR** spectrum in $CDCl_3$

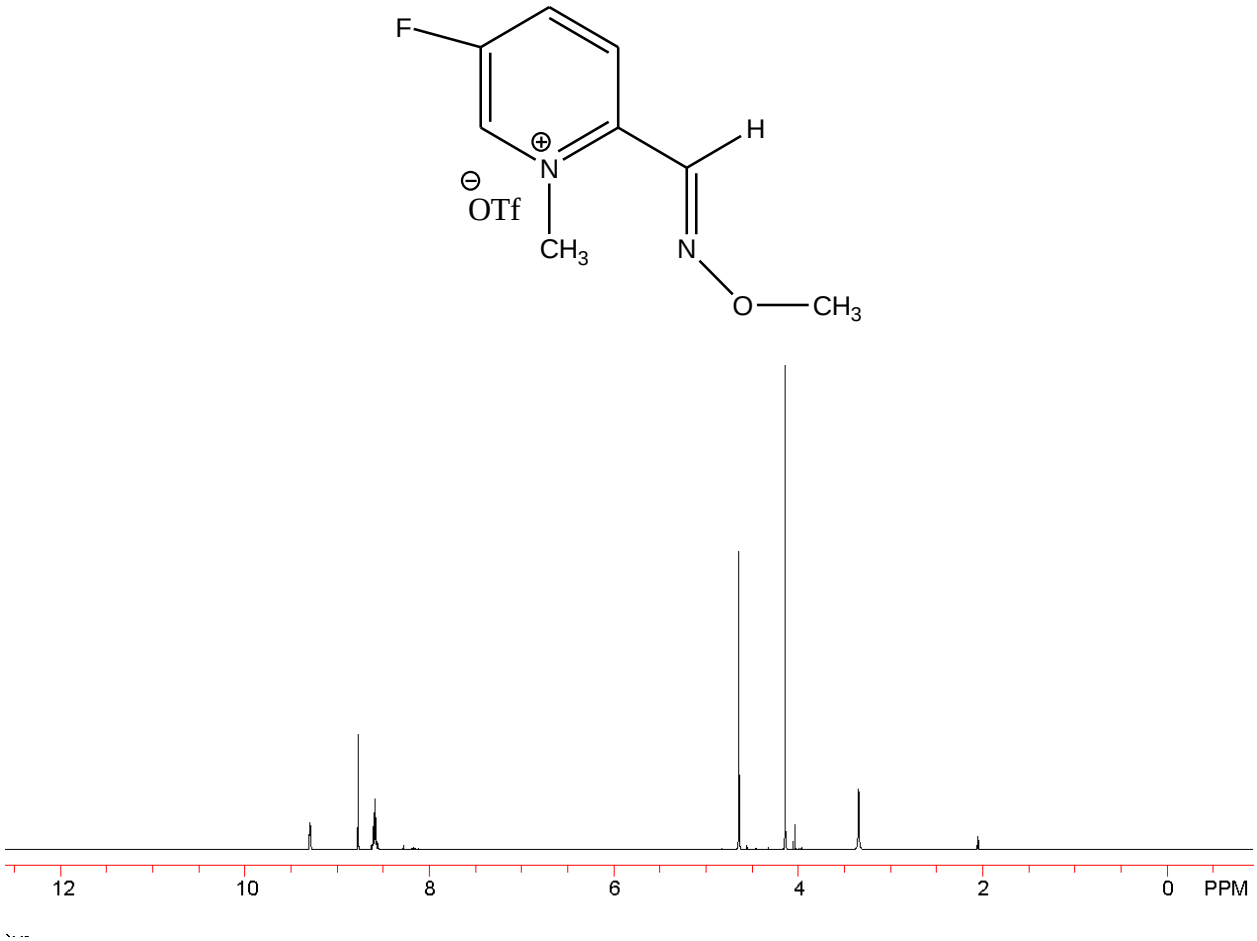

Figure A.13: 500 MHz **^{1}H NMR** spectrum in Acetone

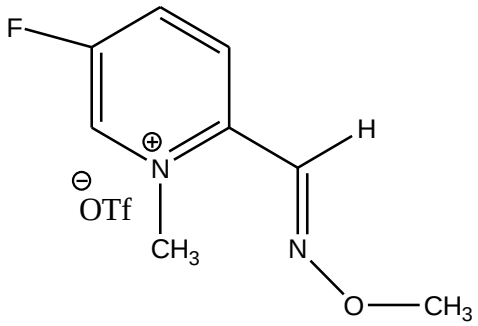

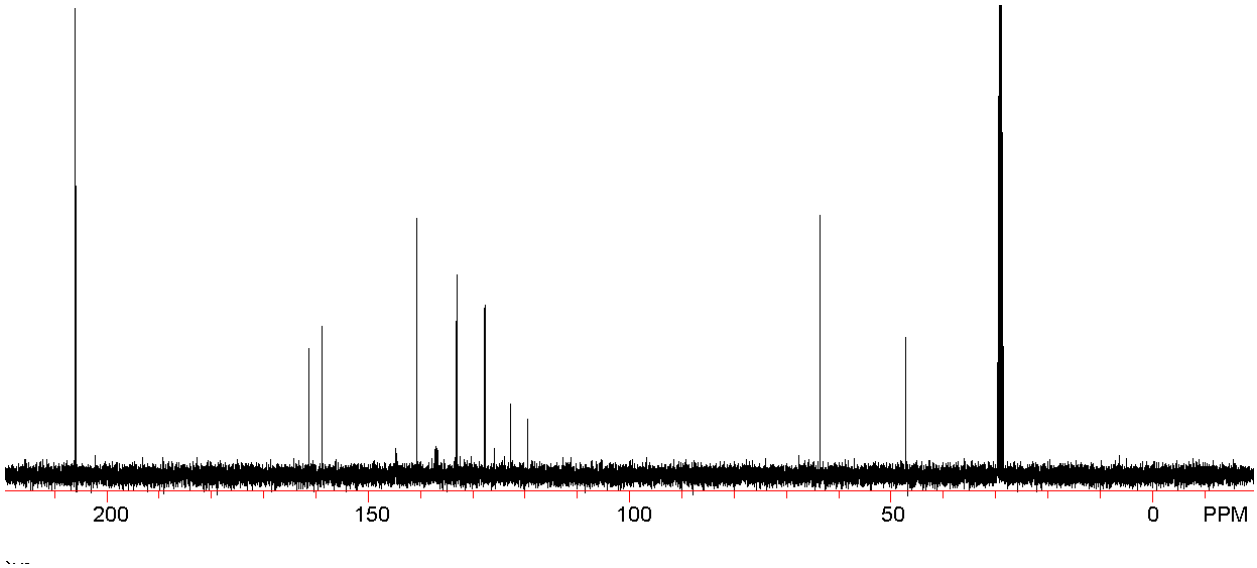

Figure A.14: 100 MHz ^{13}**C NMR** spectrum in Acetone

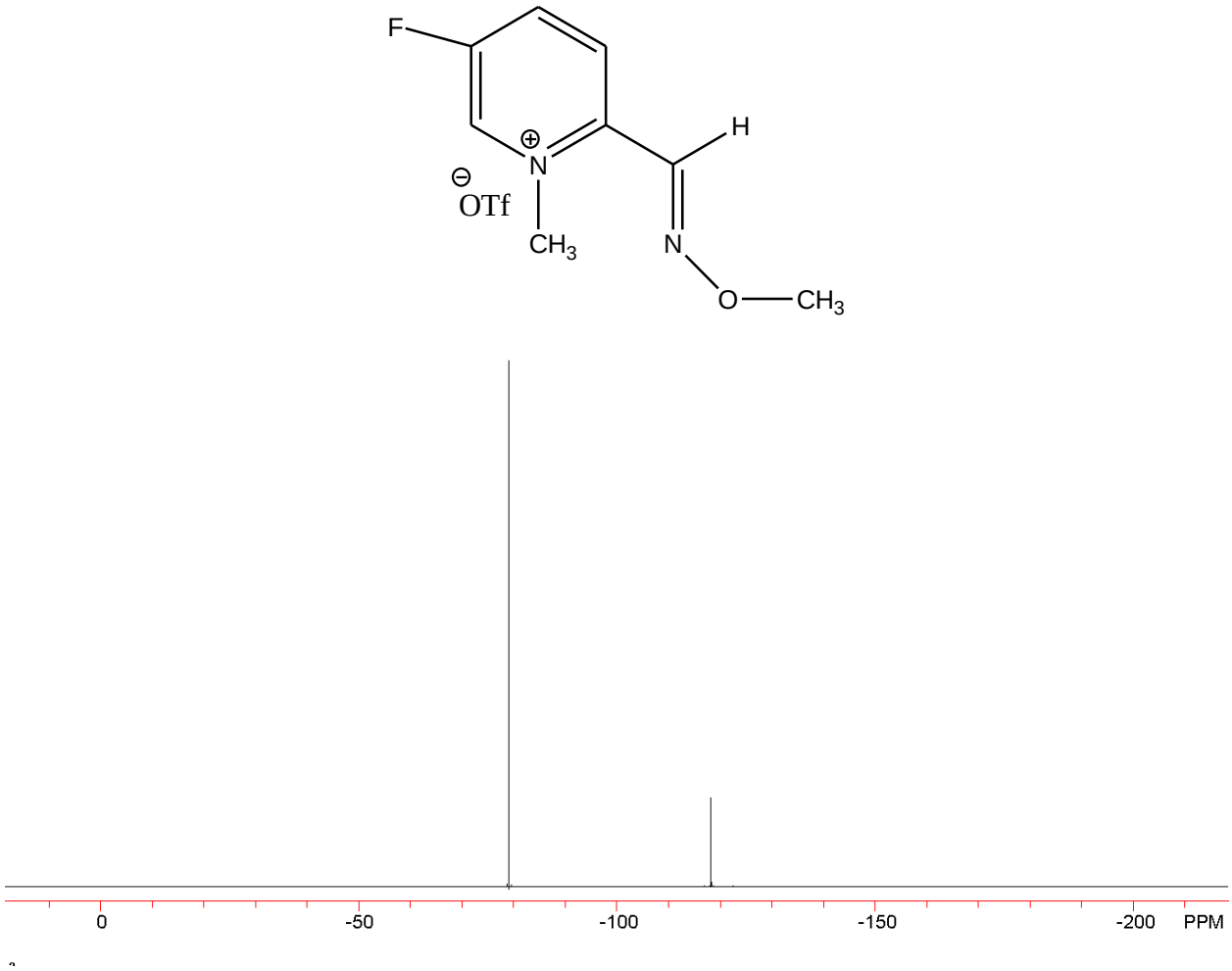

Figure A.15: 477 MHz ^{19}**F NMR** spectrum in Acetone

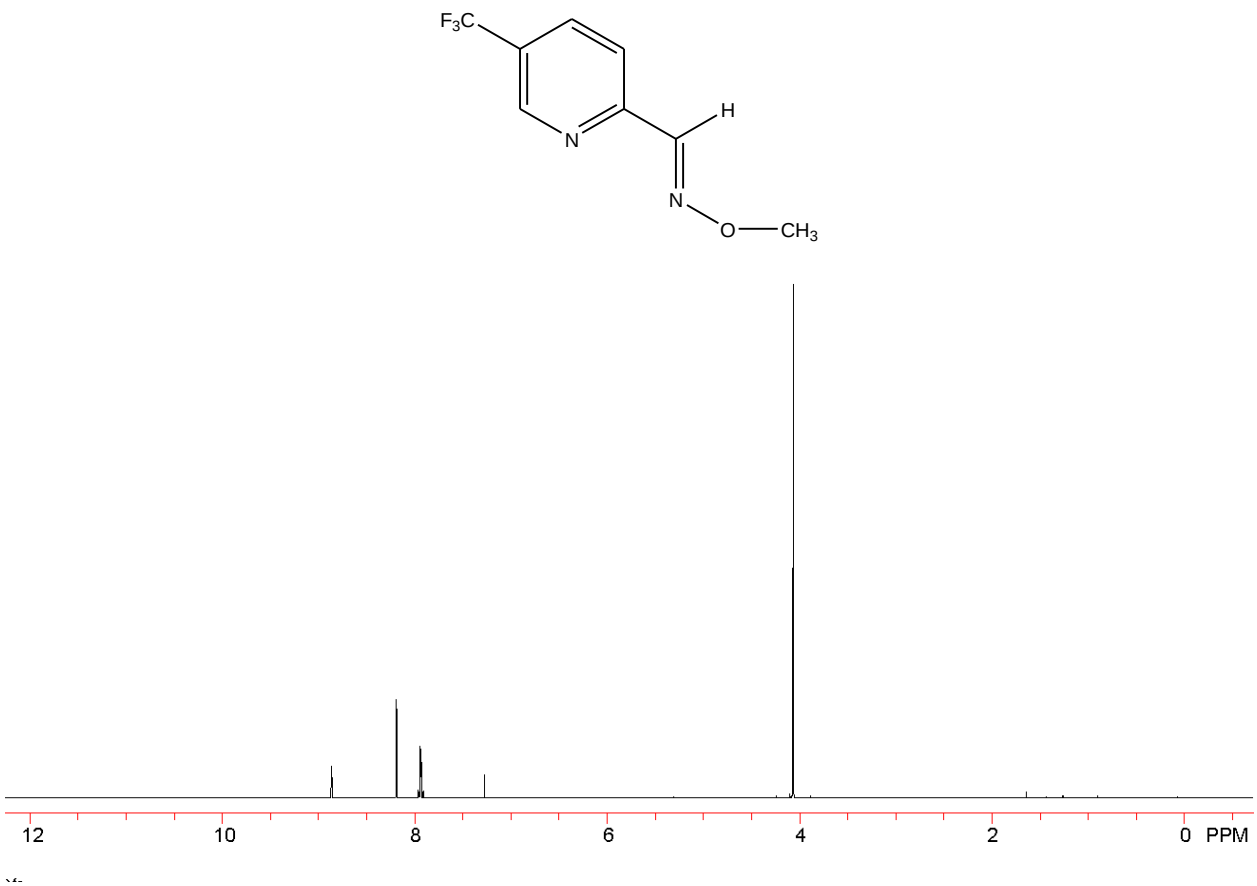

Figure A.16: 500 MHz **^{1}H NMR** spectrum in $CDCl_3$

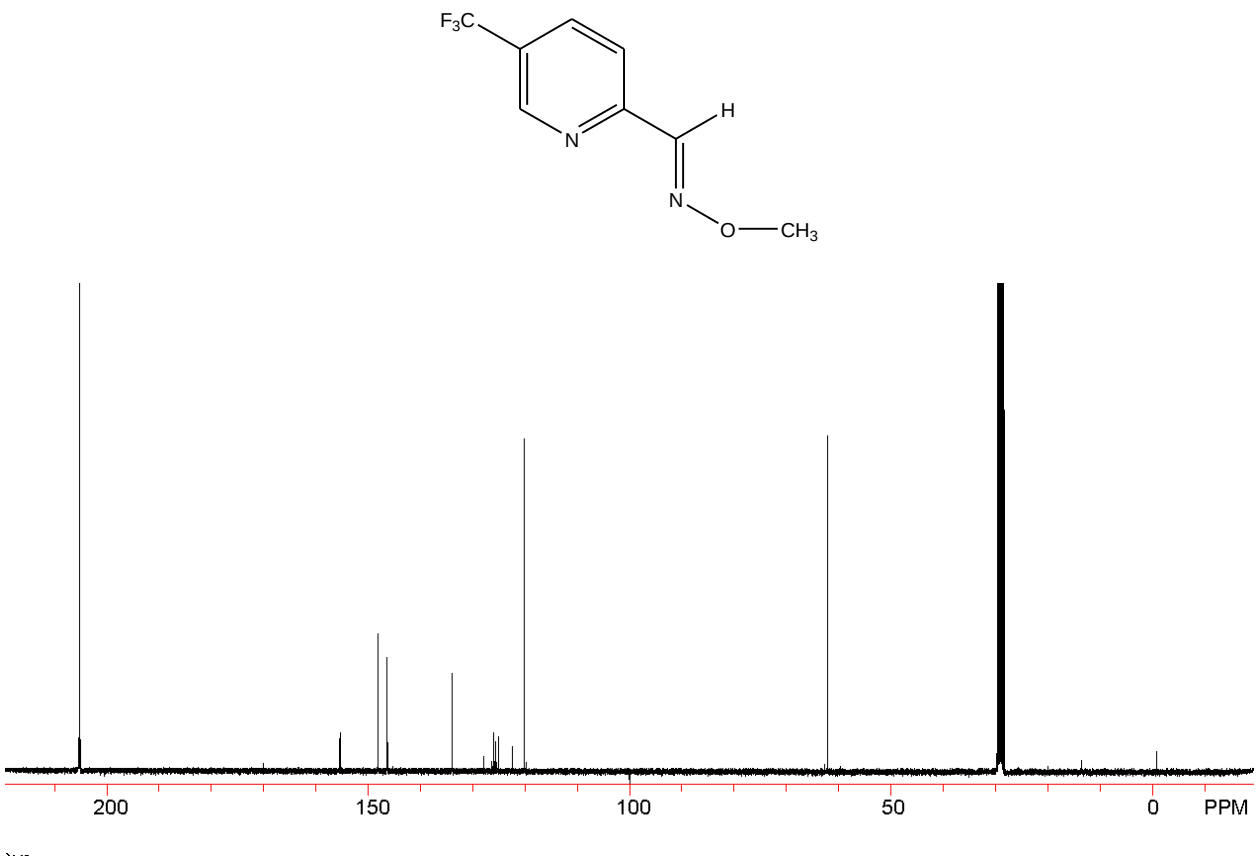

Figure A.17: 100 MHz ^{13} **C NMR** spectrum in Acetone

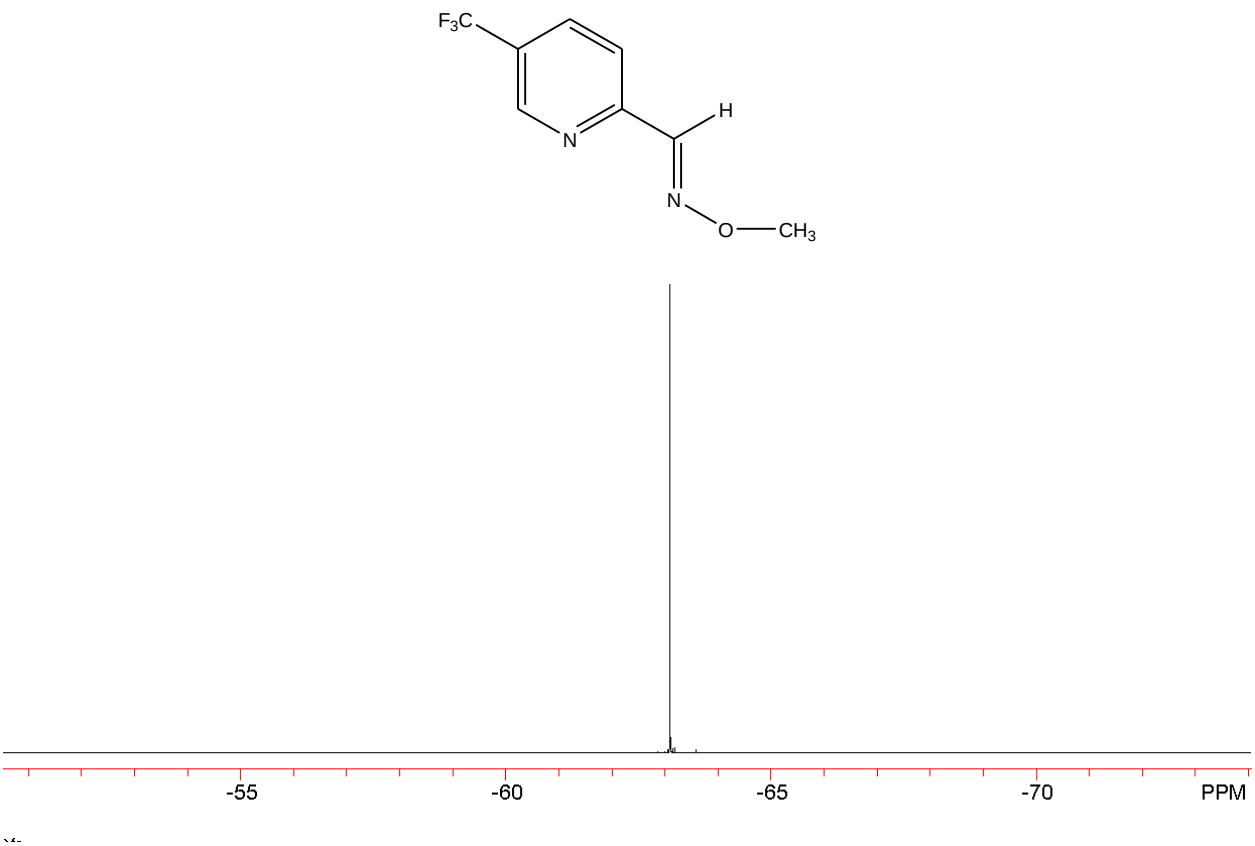

Figure A.18: 477 MHz ^{19}**F NMR** spectrum in $CDCl_3$

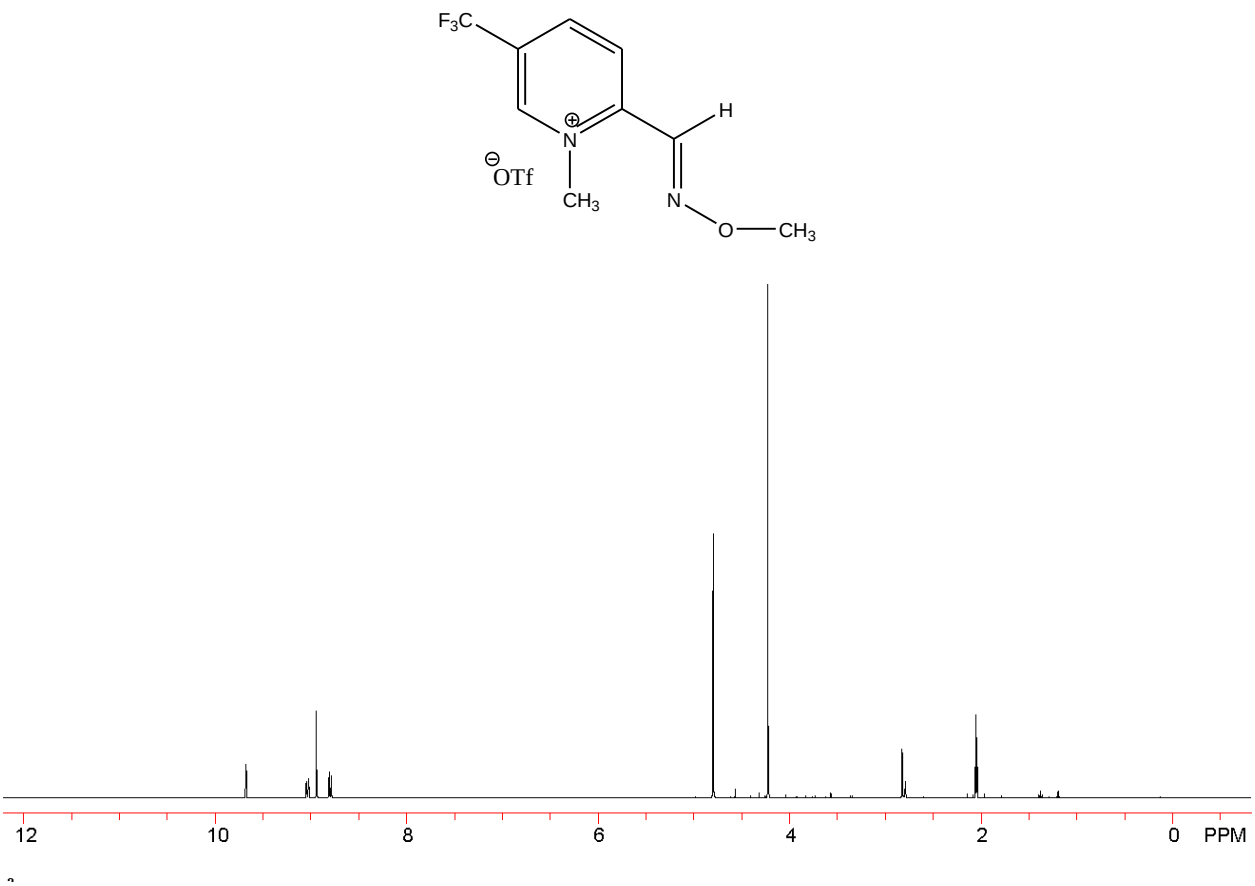

Figure A.19: 500 MHz **^{1}H NMR** spectrum in Acetone

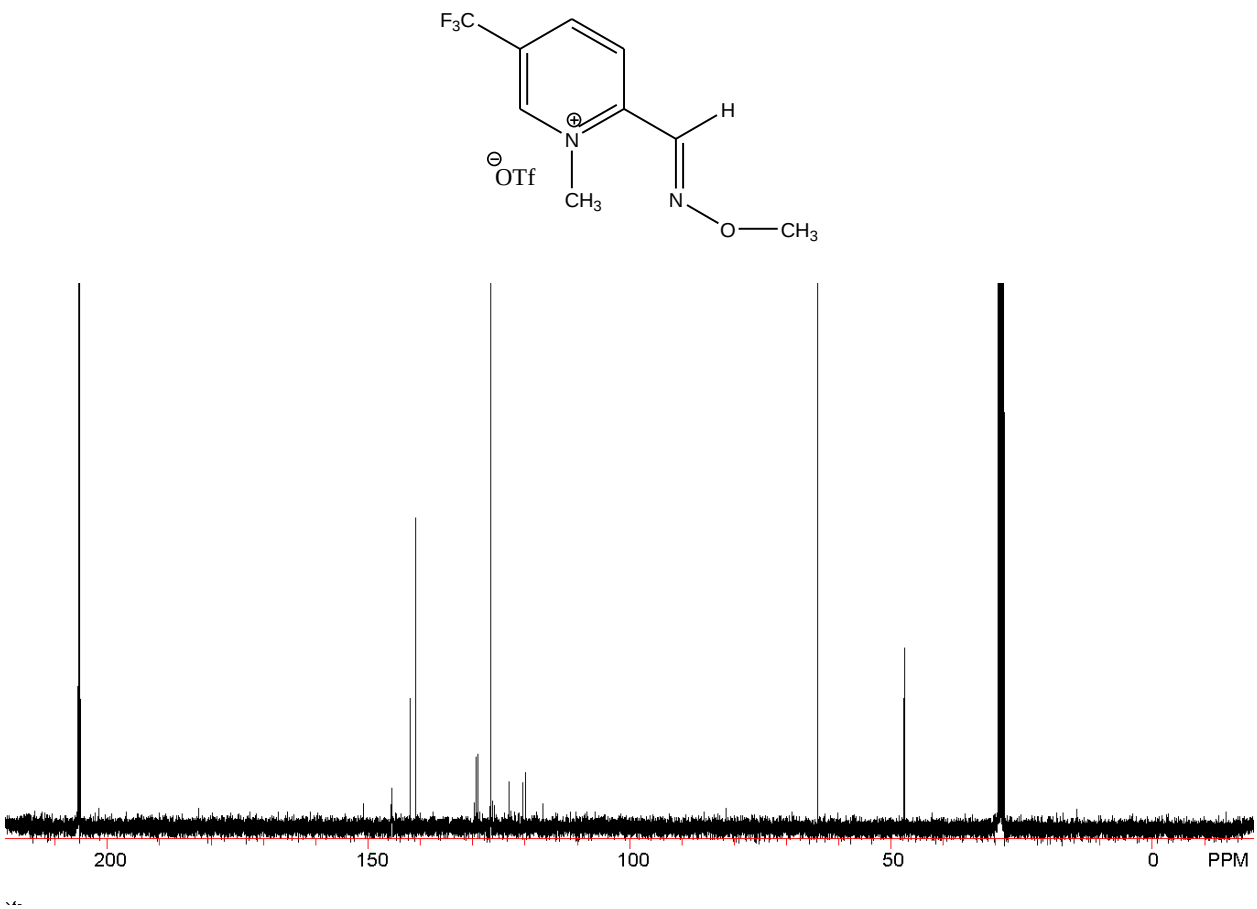

Figure A.20: 100 MHz ^{13}**C NMR** spectrum in Acetone

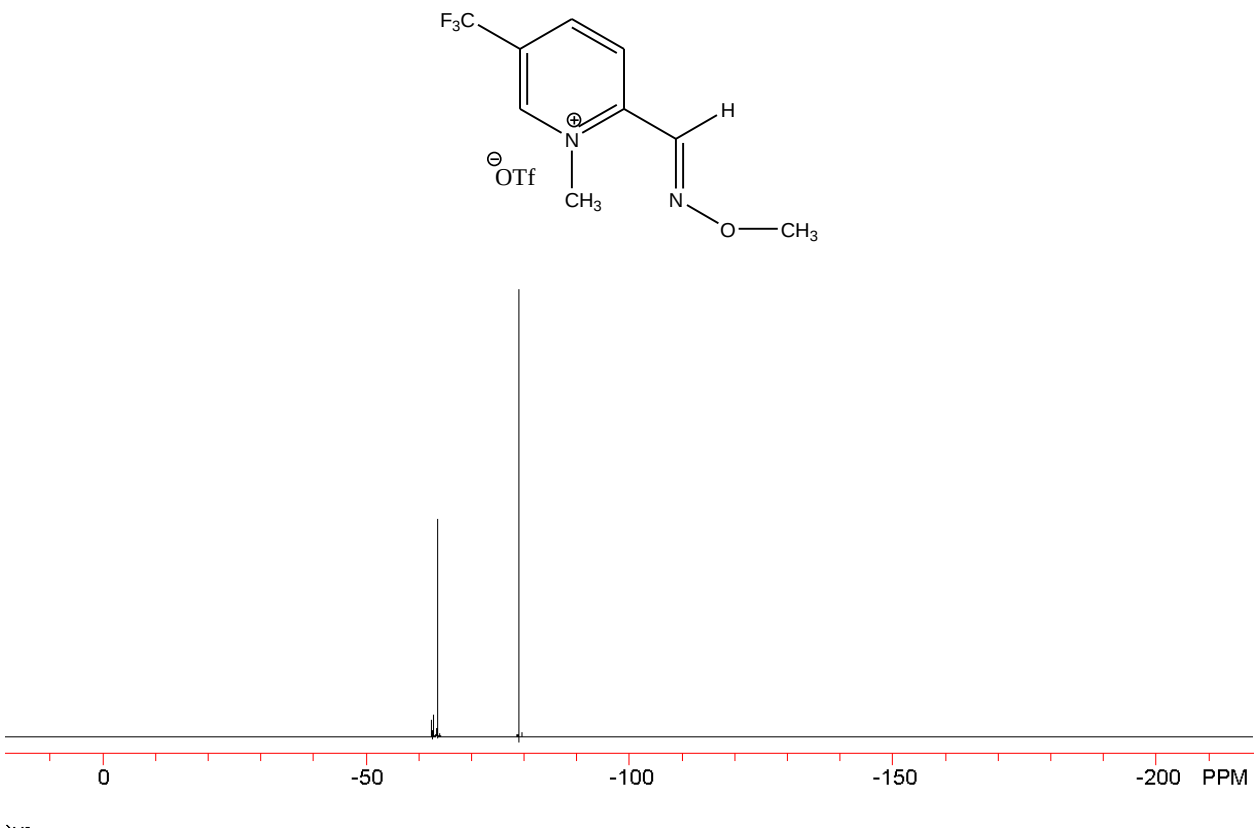

Figure A.21: 477 MHz ^{19}**F NMR** spectrum in Acetone

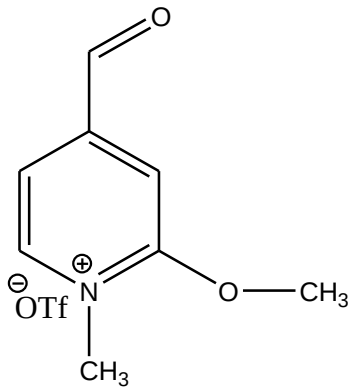

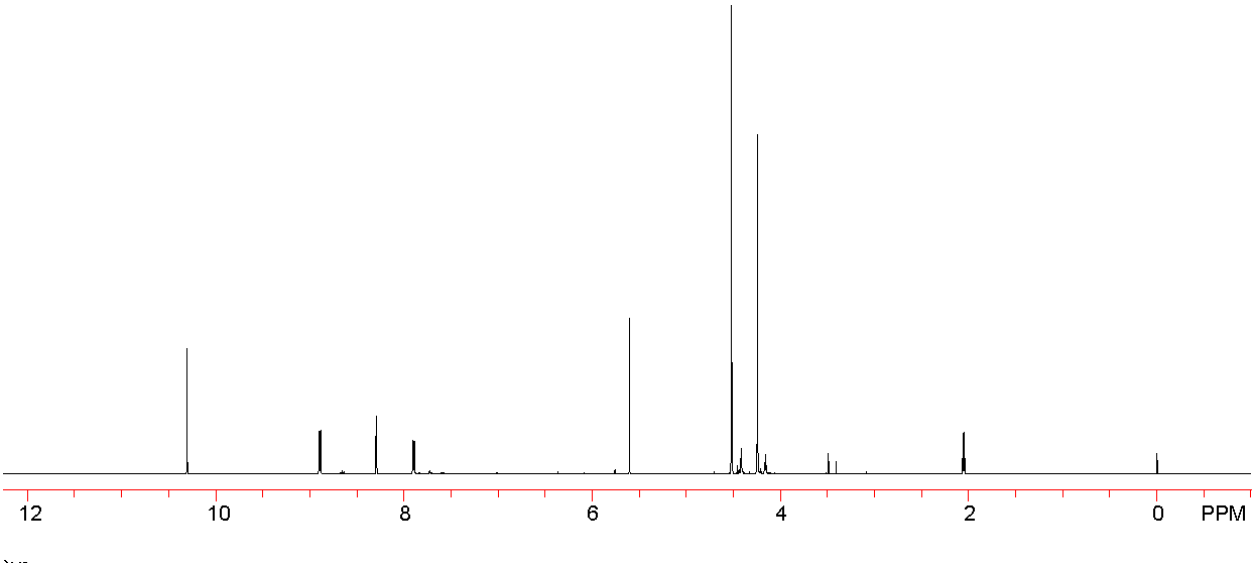

Figure A.22: 500 MHz **^{1}H NMR** spectrum in Acetone

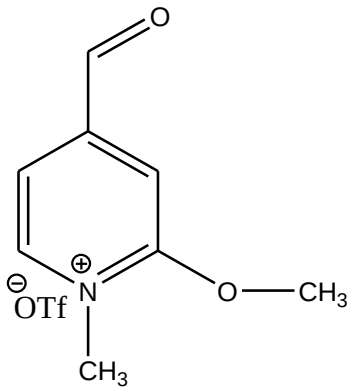

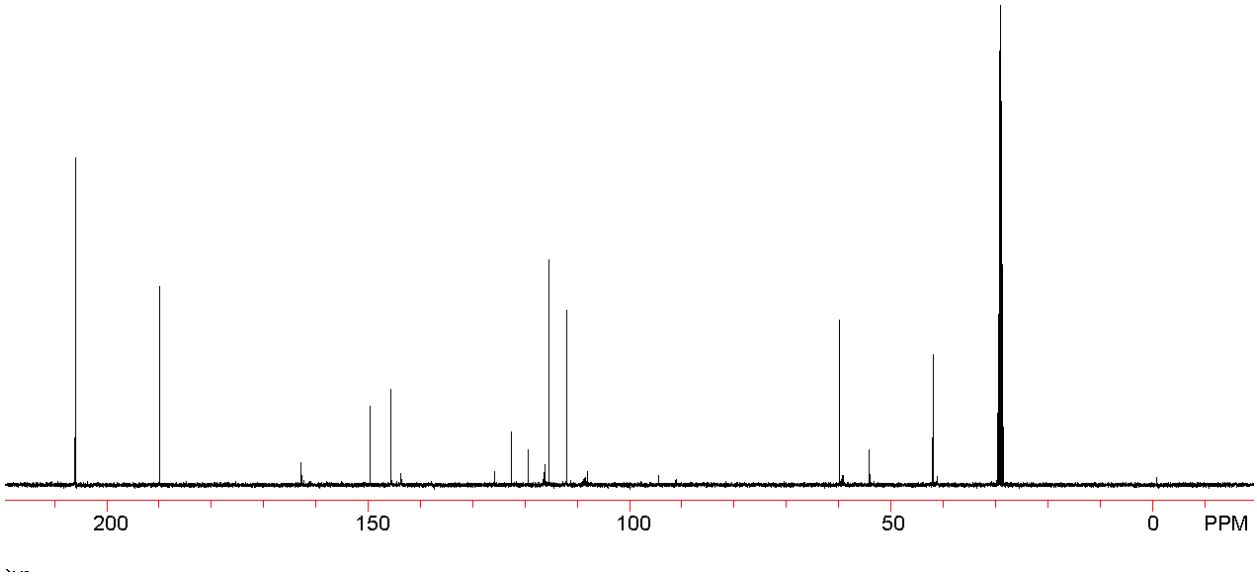

Figure A.23: 100 MHz ^{13}**C NMR** spectrum in Acetone

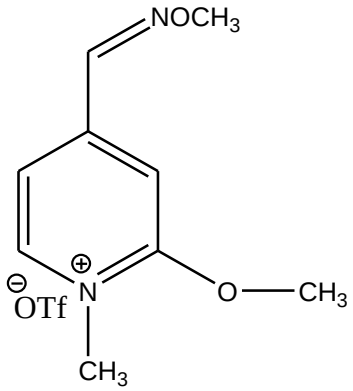

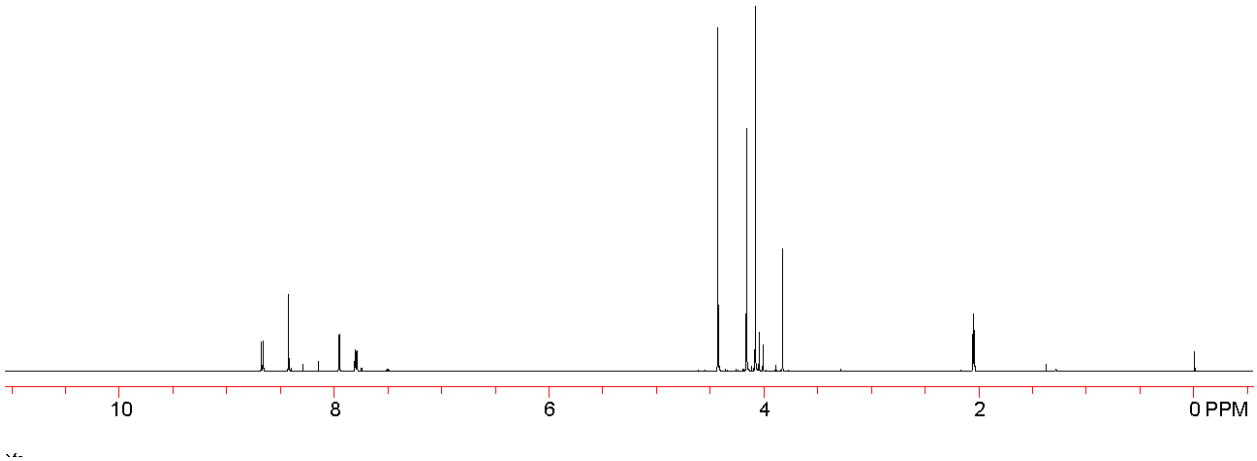

Figure A.24: 500 MHz **^{1}H NMR** spectrum in Acetone

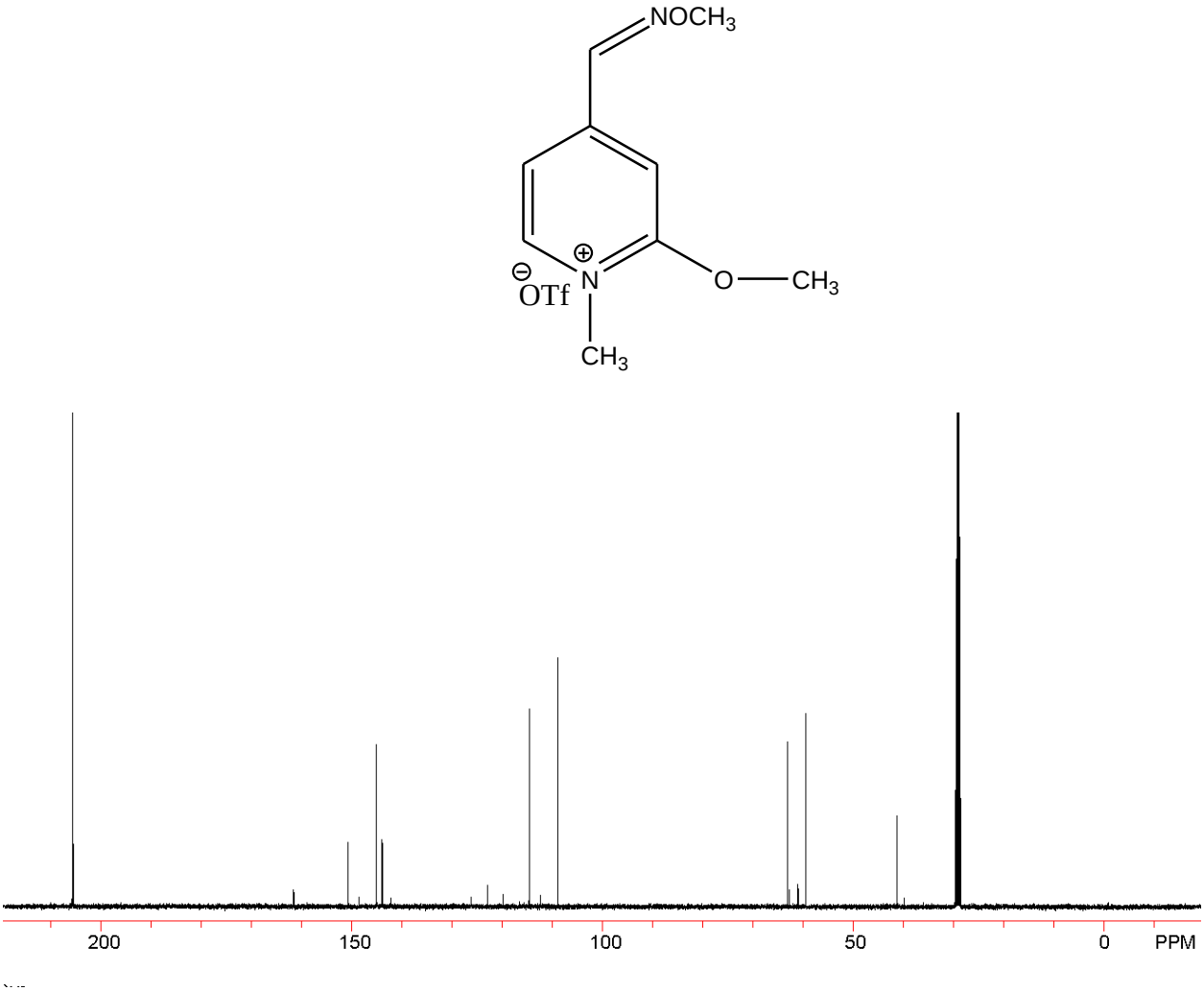

Figure A.25: 125 MHz ^{13}**C NMR** spectrum in Acetone

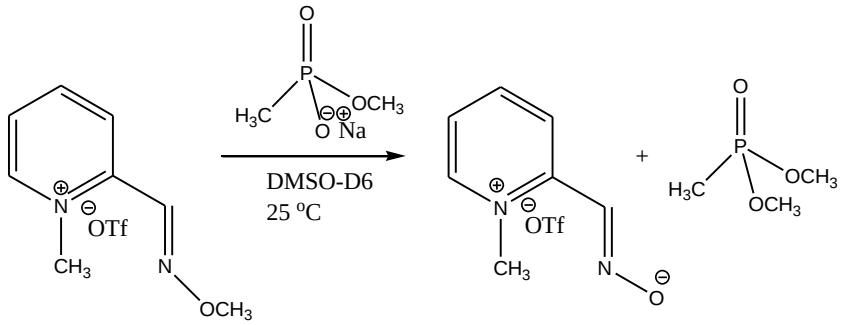

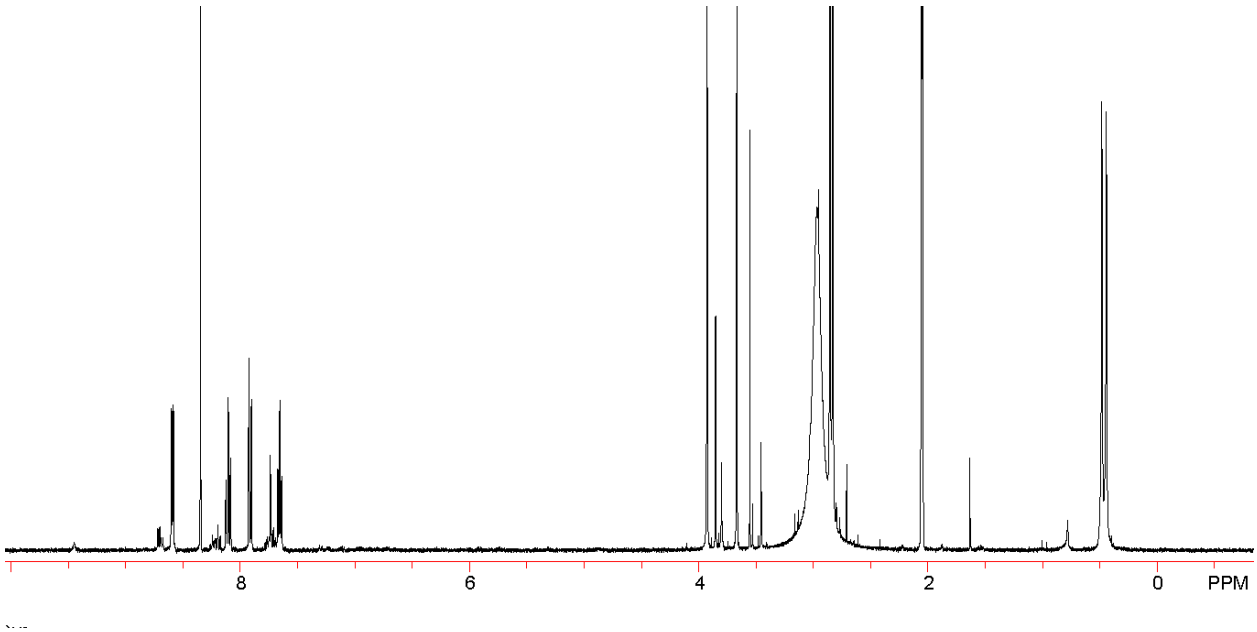

Figure A.26: 500 MHz ^{1}**H NMR** spectrum in DMSO

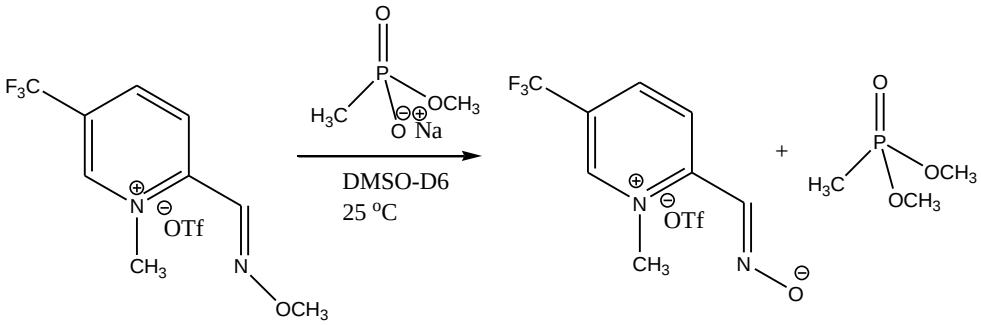

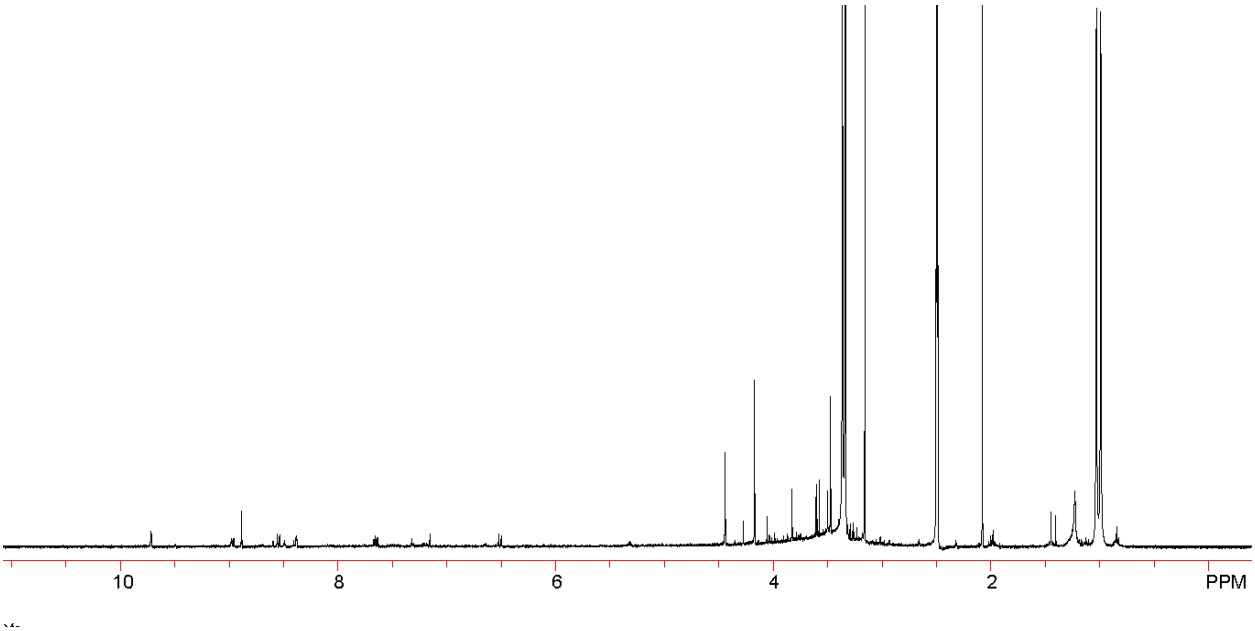

Figure A.27: 500 MHz ^{1}**H NMR** spectrum in DMSO

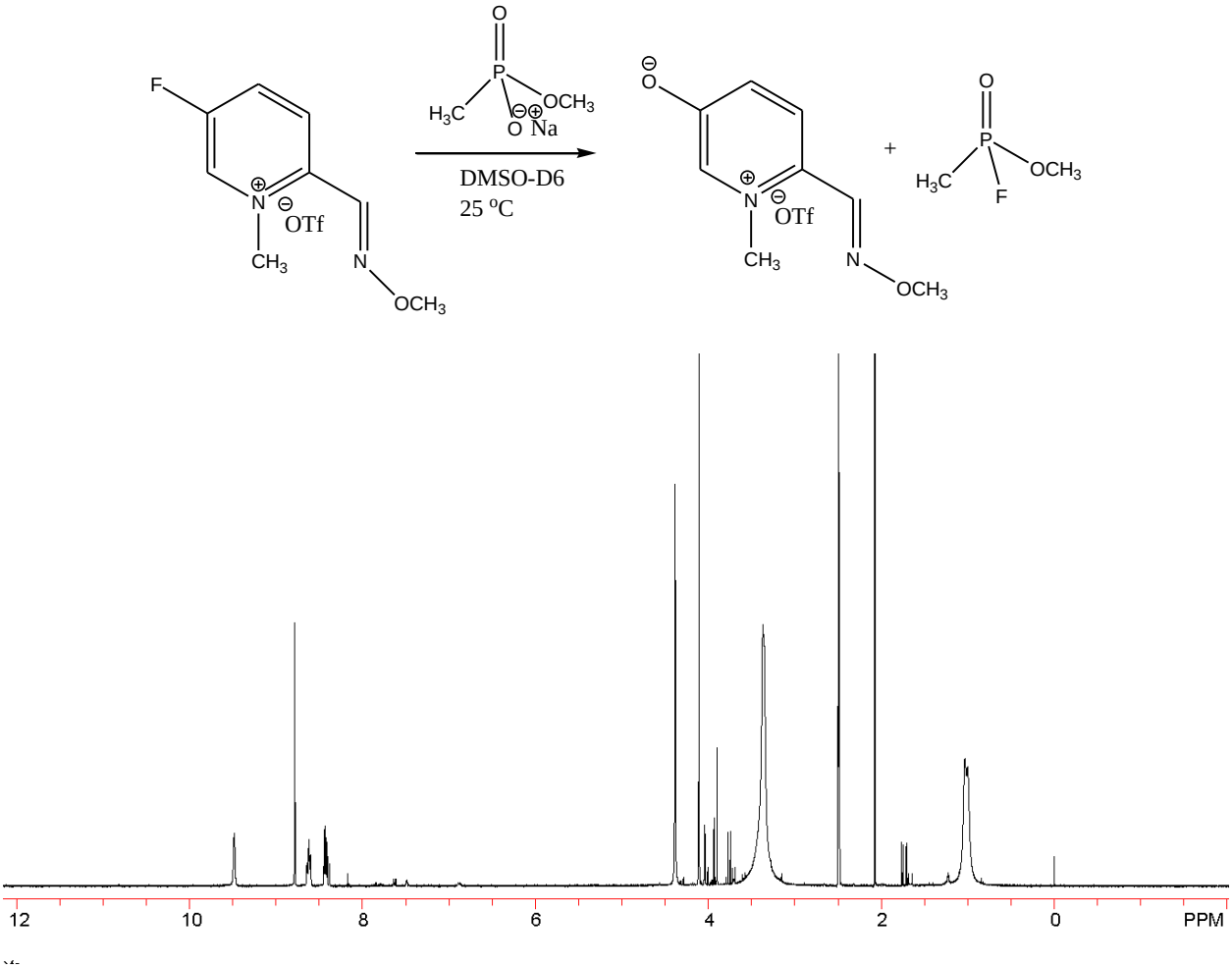

Figure A.28: 500 MHz ^{1}**H NMR** spectrum in DMSO

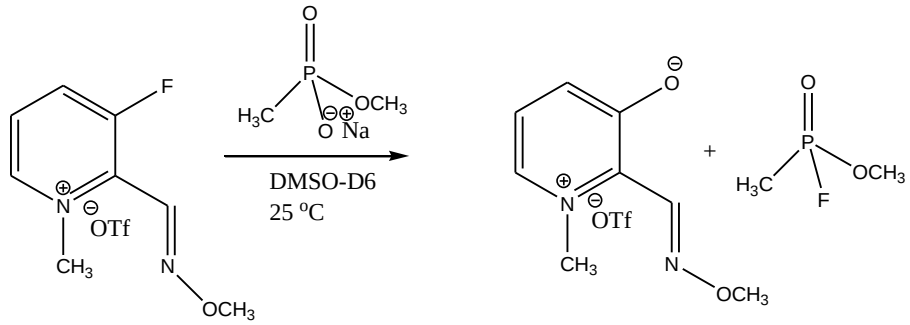

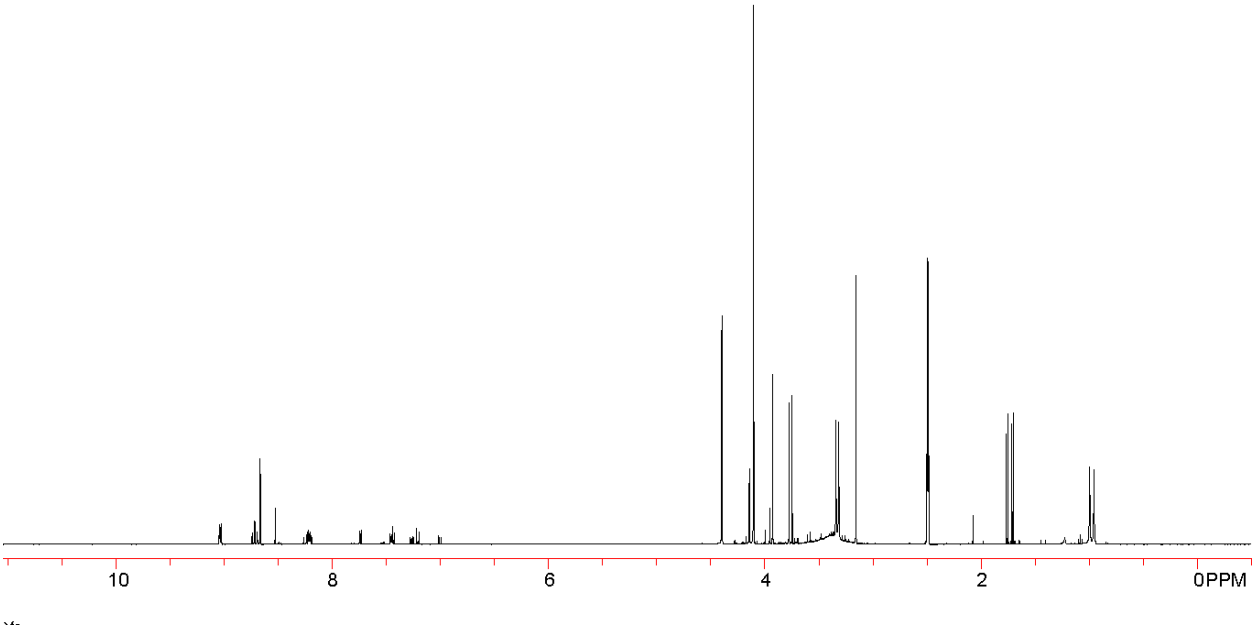

Figure A.29: 500 MHz ^{1}**H NMR** spectrum in DMSO

APPENDIX B

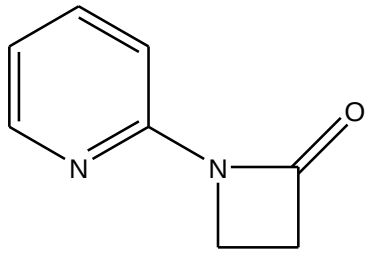

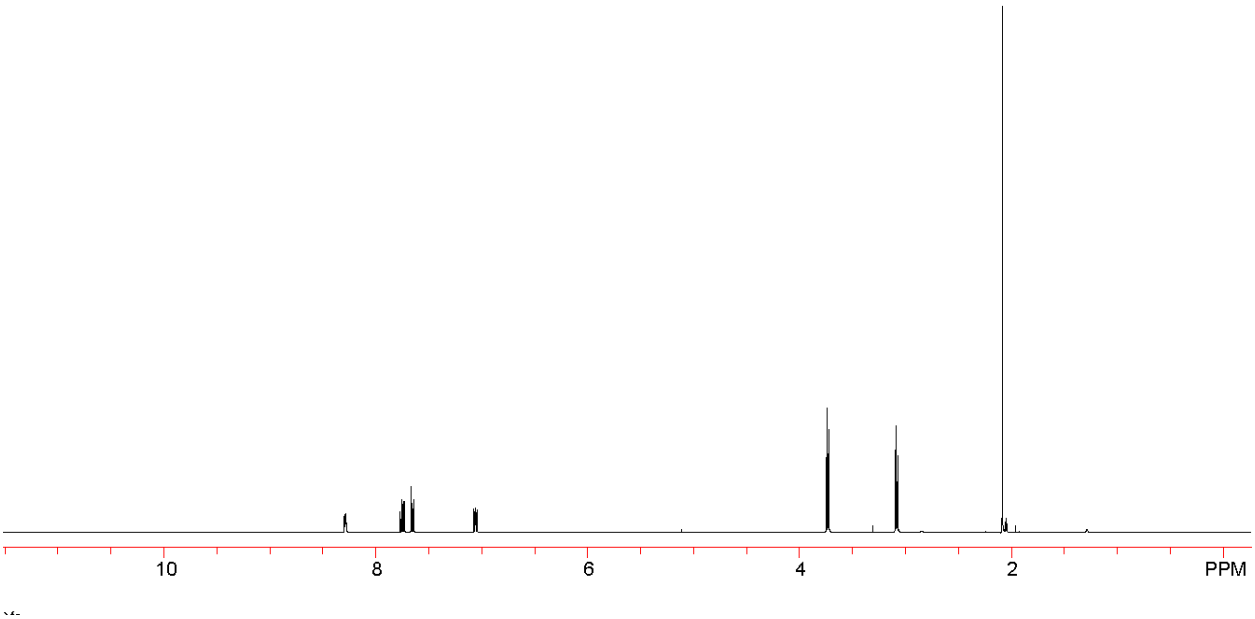

Figure B.1: 500 MHz ^{1}**H NMR** spectrum in Acetone

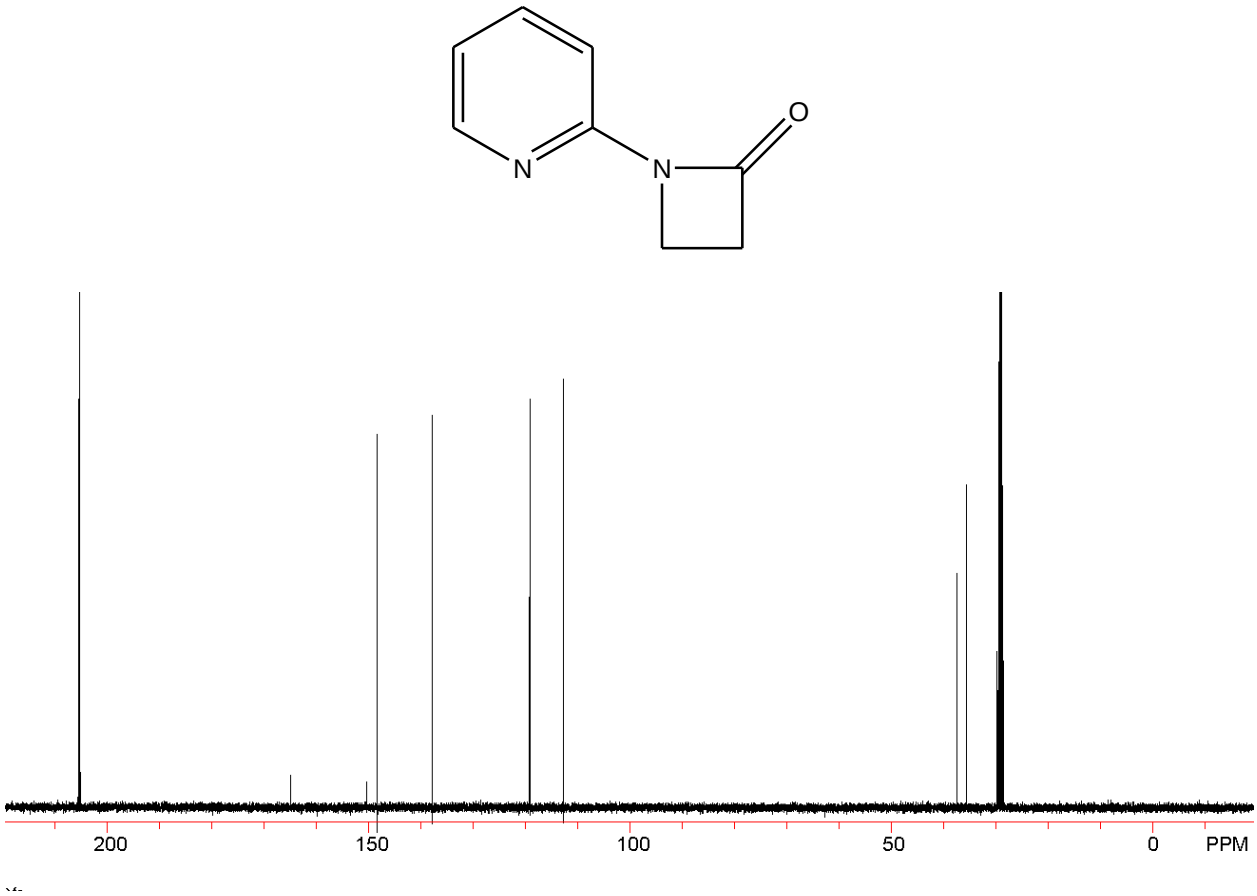

Figure B.2: 125 MHz ^{13}**C NMR** spectrum in Acetone

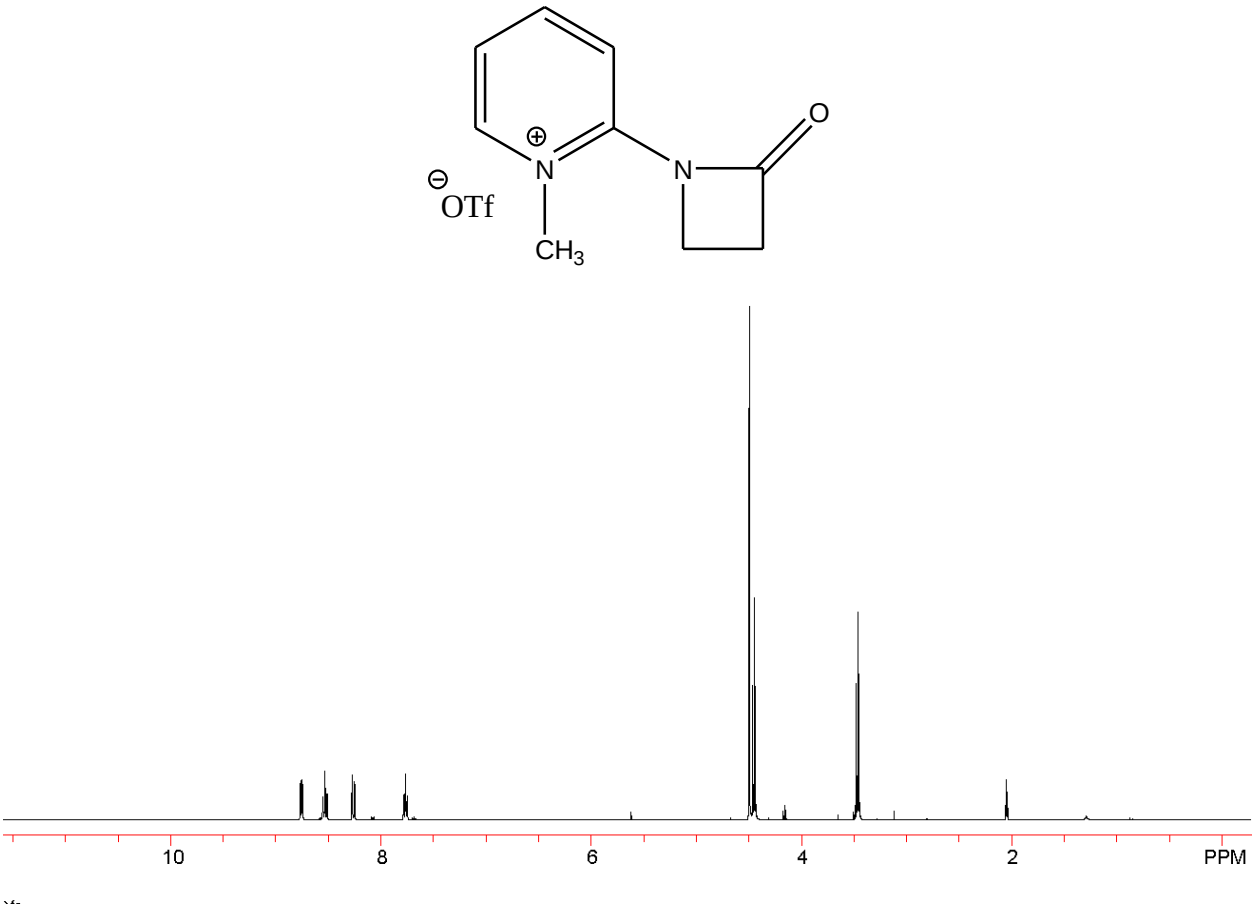

Figure B.3: 500 MHz **^{1}H NMR** spectrum in Acetone

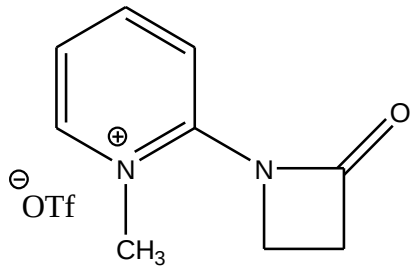

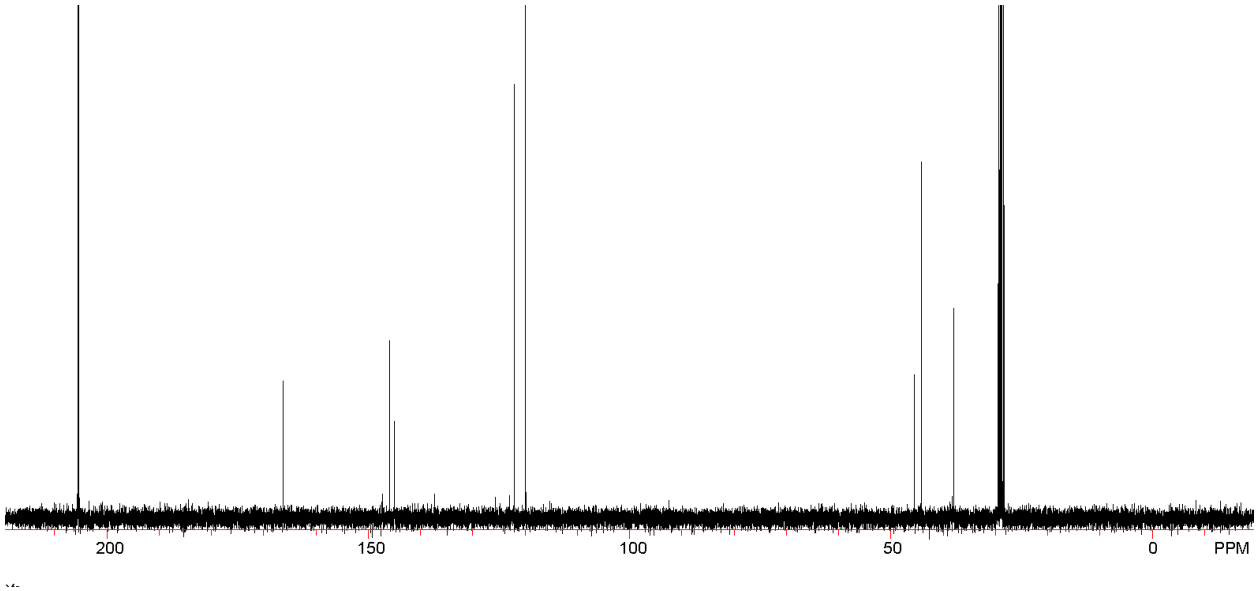

Figure B.4: 125 MHz ^{13}**C NMR** spectrum in Acetone

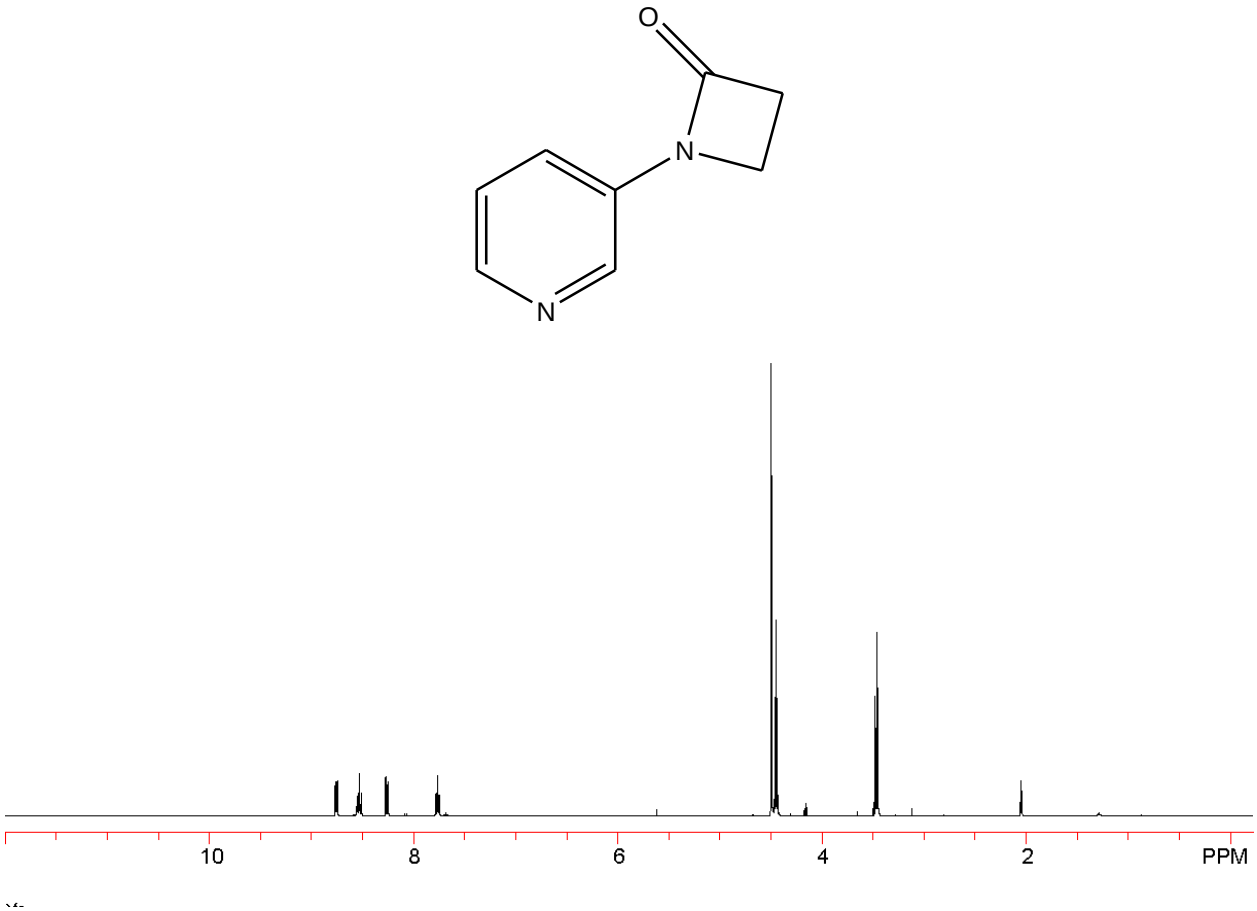

Figure B.5: 500 MHz **^{1}H NMR** spectrum in Acetone

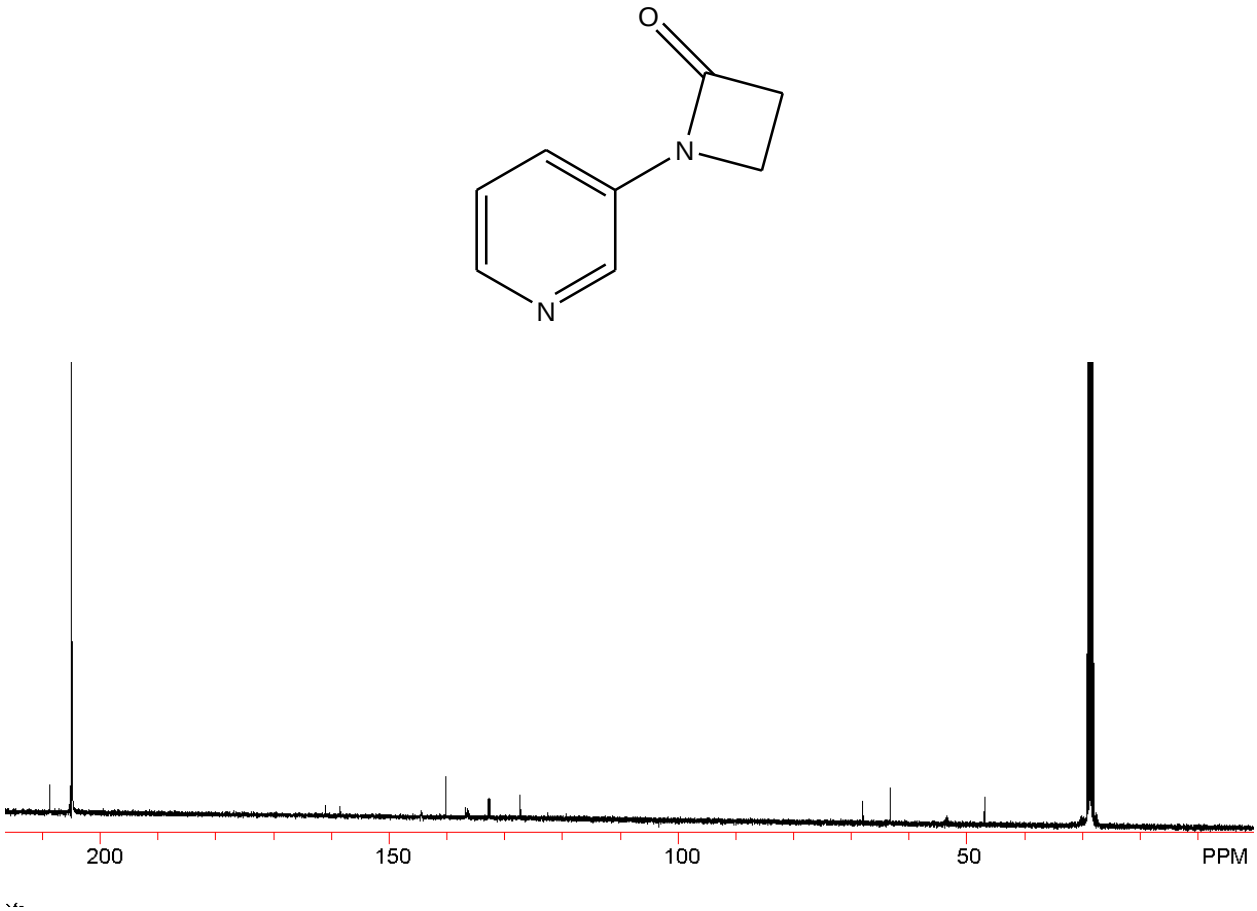

Figure B.6: 125 MHz ^{13}**C NMR** spectrum in Acetone

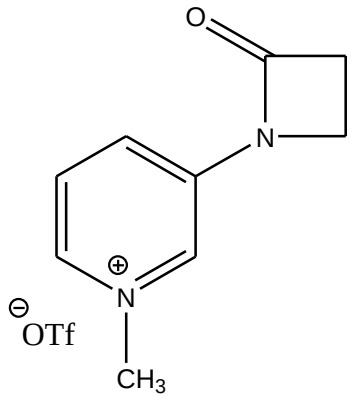

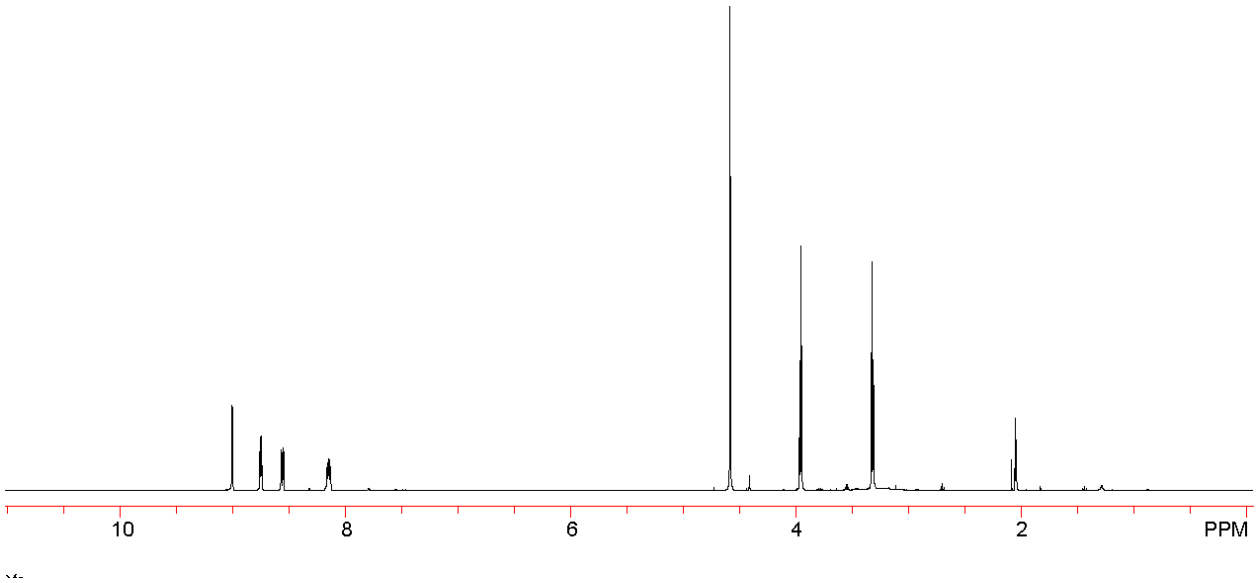

Figure B.7: 500 MHz **^{1}H NMR** spectrum in Acetone

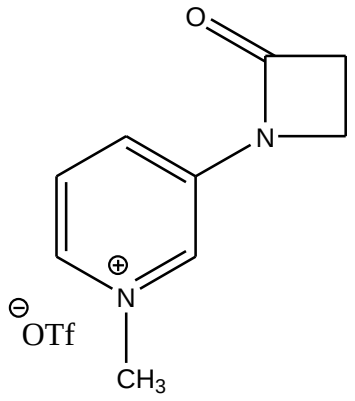

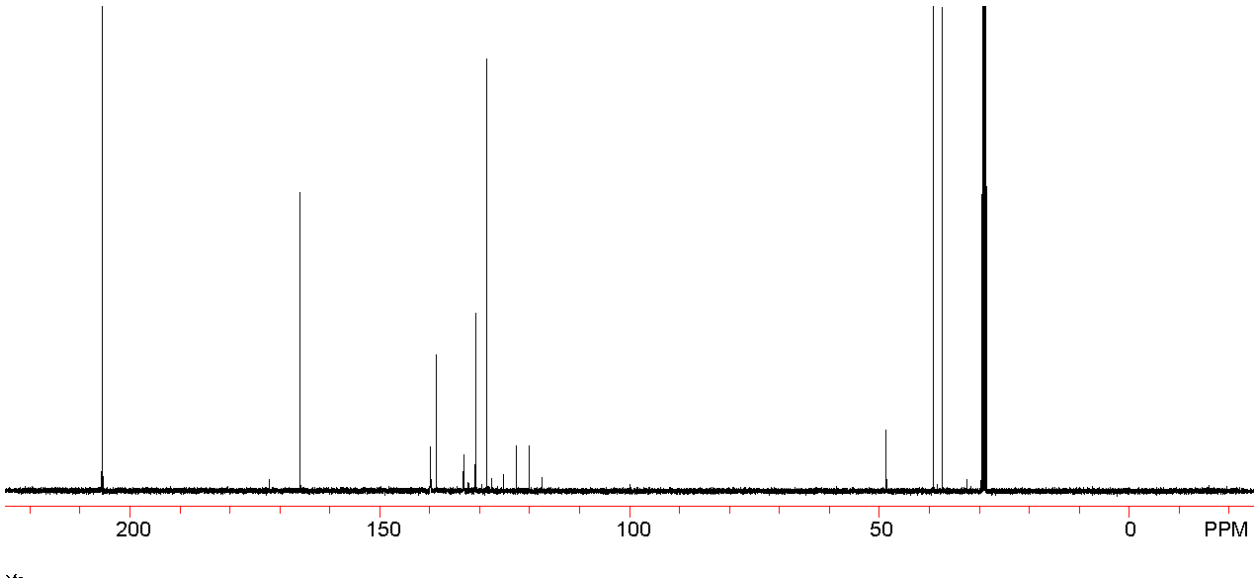

Figure B.8: 125 MHz ^{13}**C NMR** spectrum in Acetone

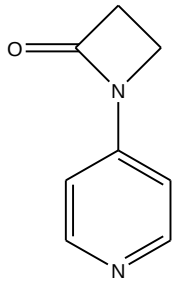

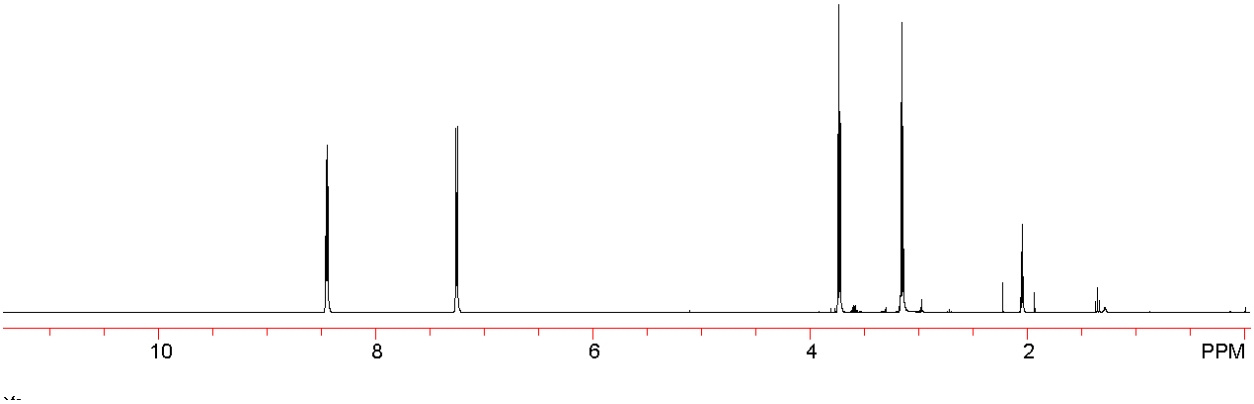

Figure B.9: 500 MHz **^{1}H NMR** spectrum in Acetone

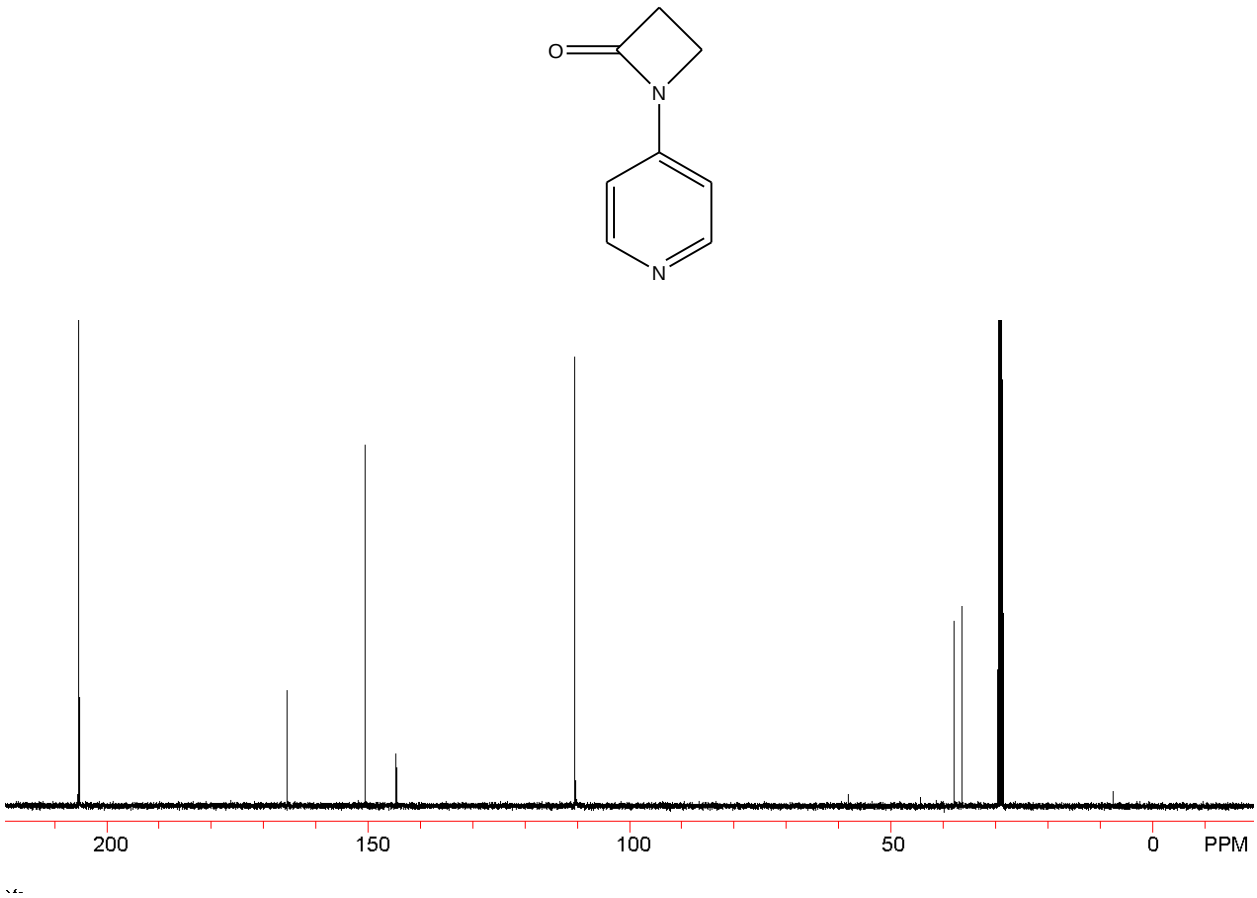

Figure B.10: 125 MHz ^{13}**C NMR** spectrum in Acetone

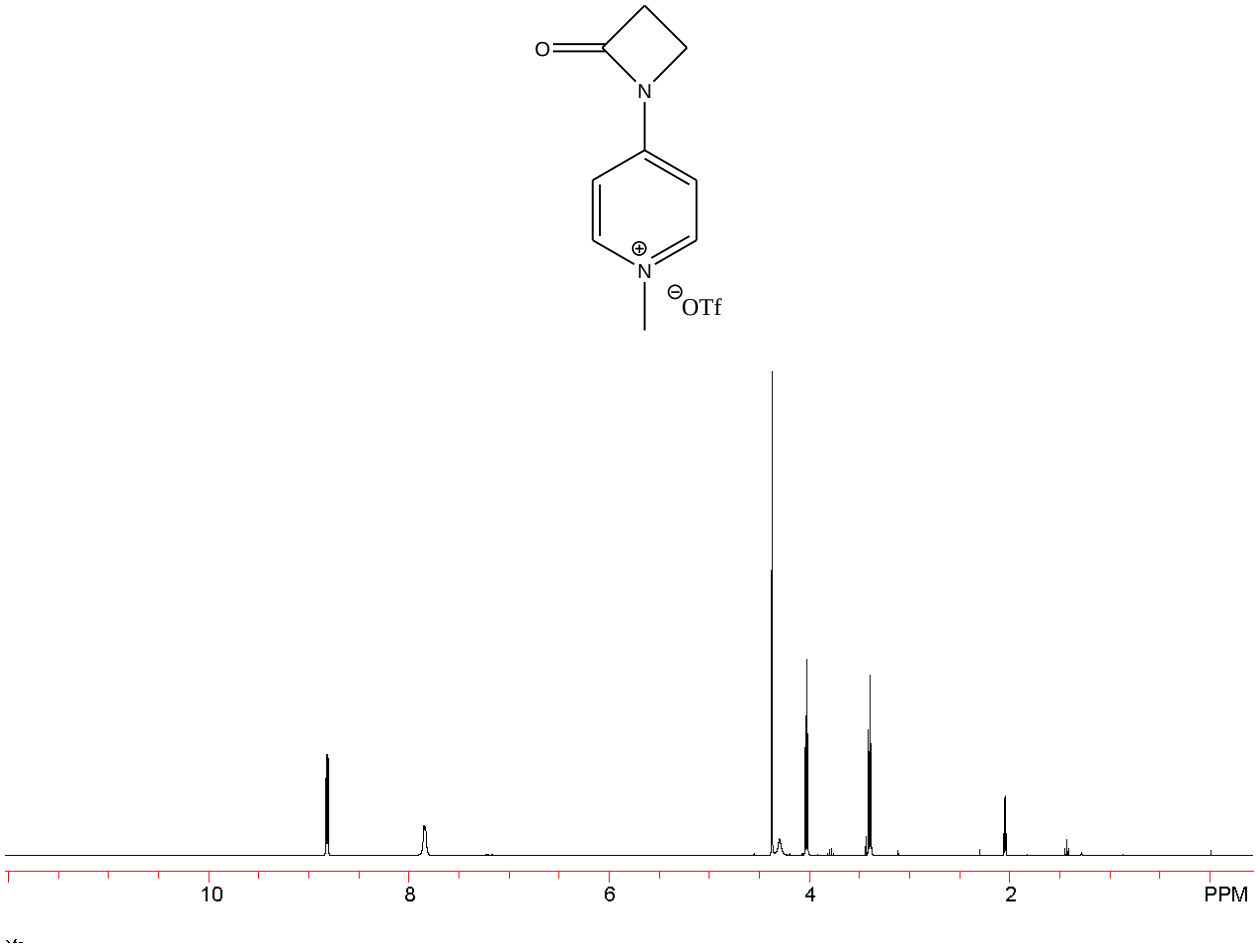

Figure B.11: 500 MHz **^{1}H NMR** spectrum in Acetone

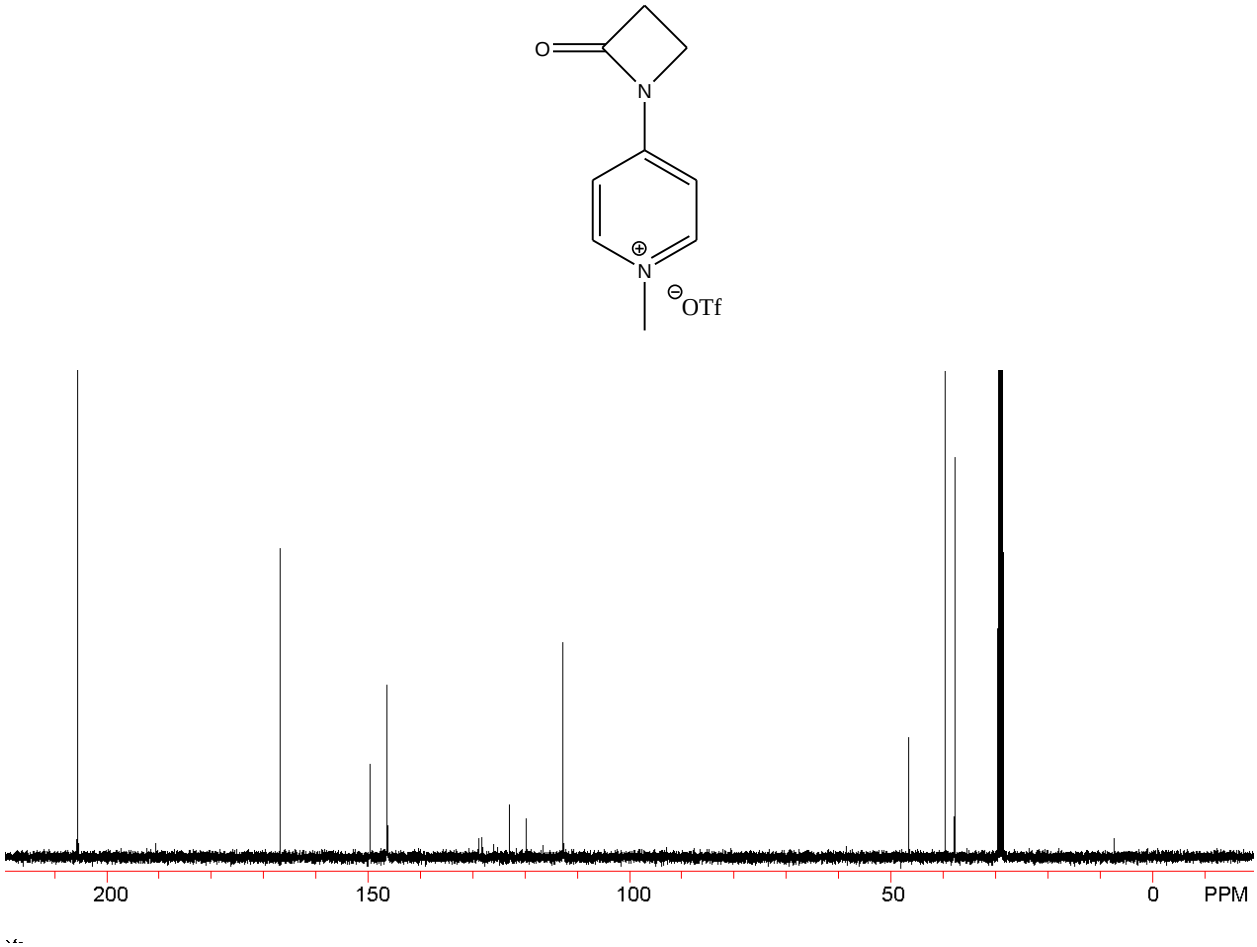

Figure B.12: 125 MHz ^{13}**C NMR** spectrum in Acetone

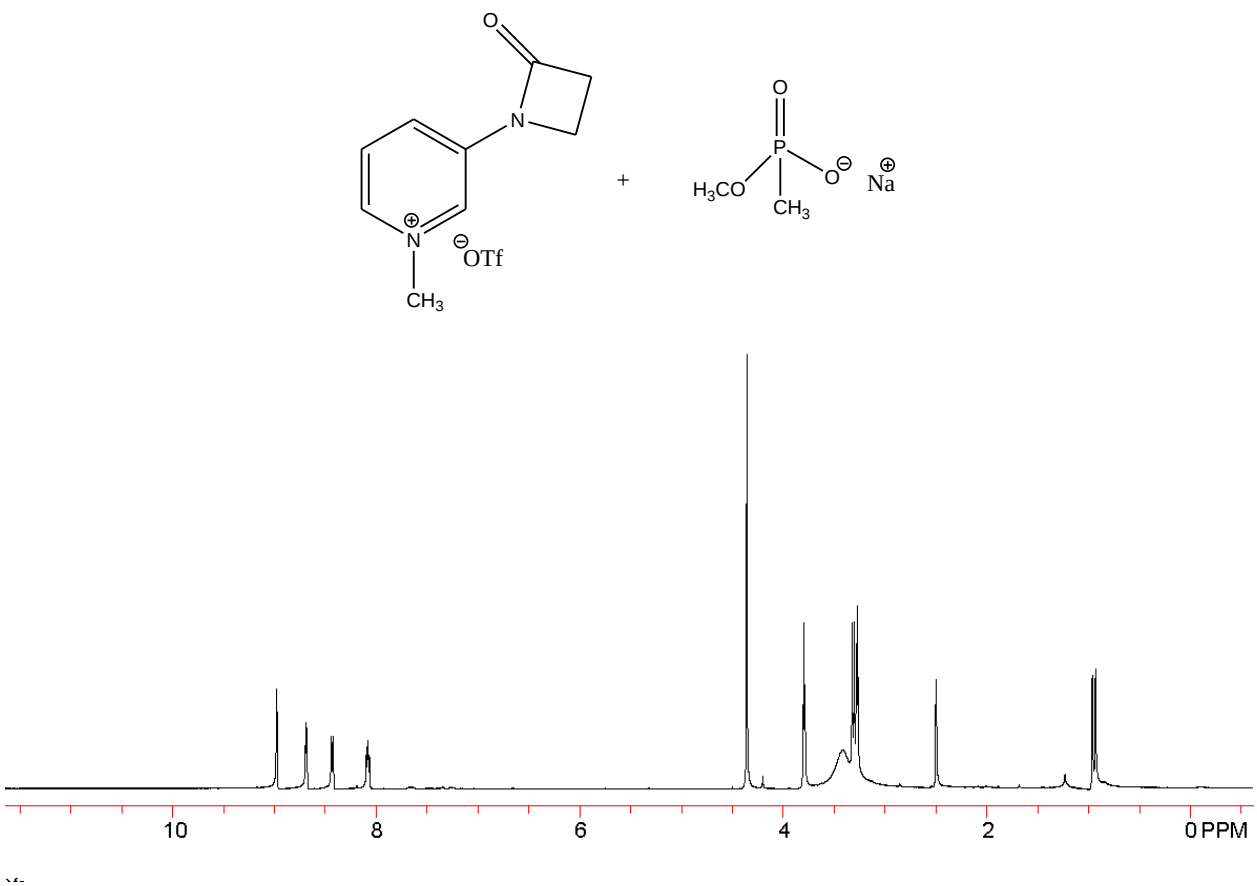

Figure B.13: 500 MHz **^{1}H NMR** spectrum in DMSO

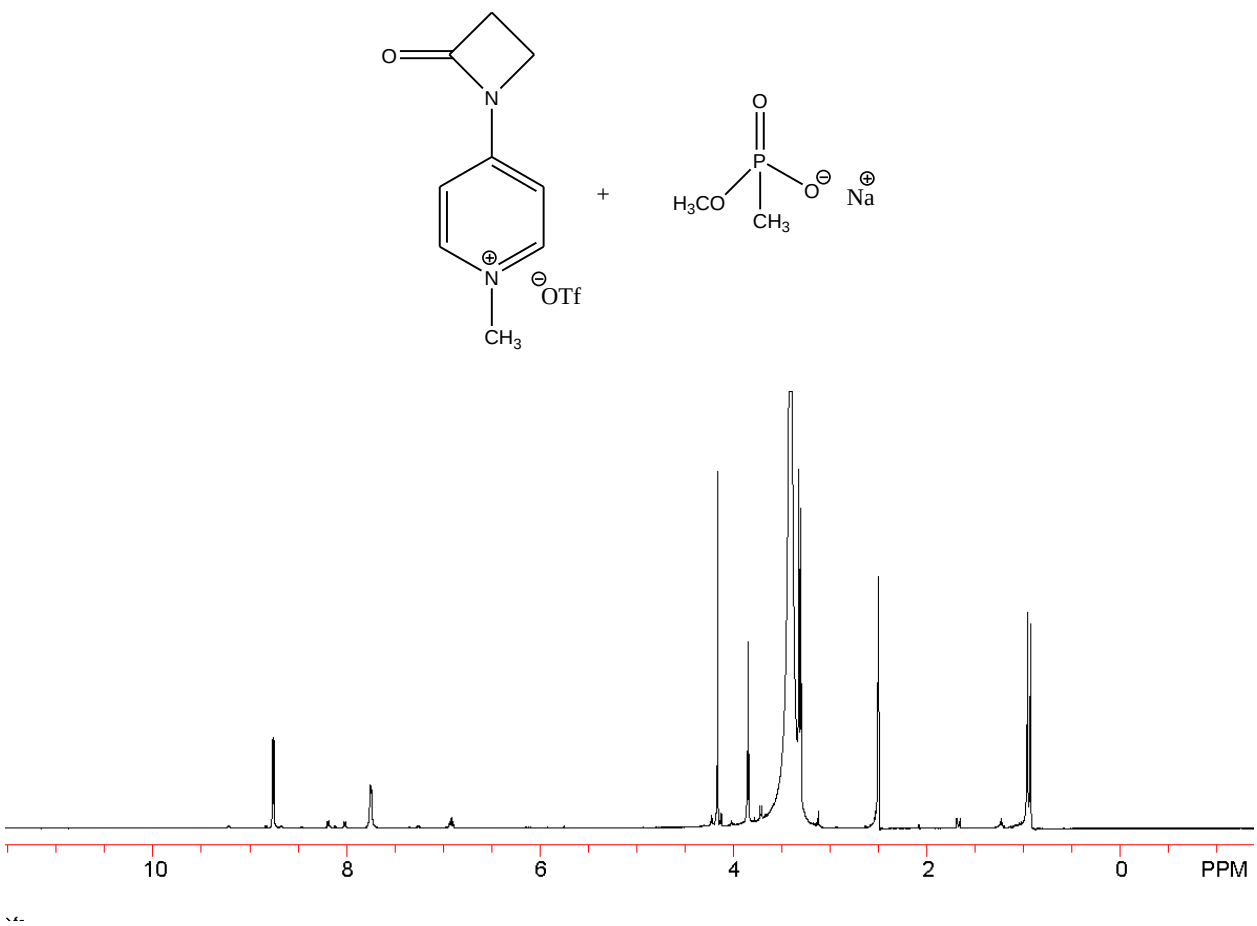

Figure B.14: 500 MHz **^{1}H NMR** spectrum in DMSO

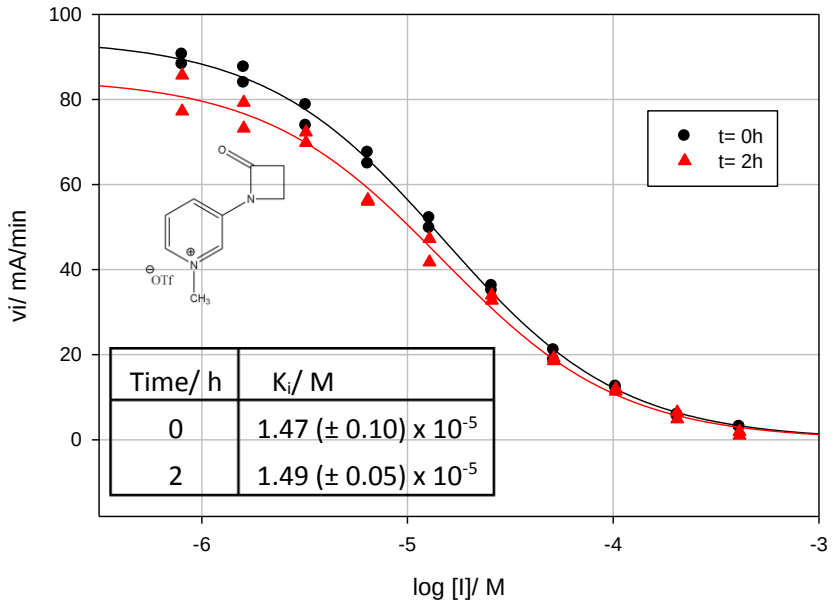

Figure B.15: Dose response curve

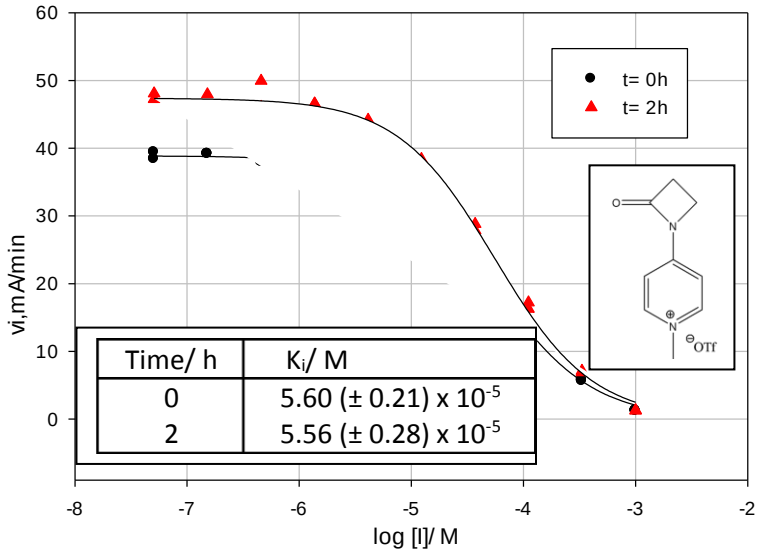

Figure B.16: Dose response curve

APENDIX C

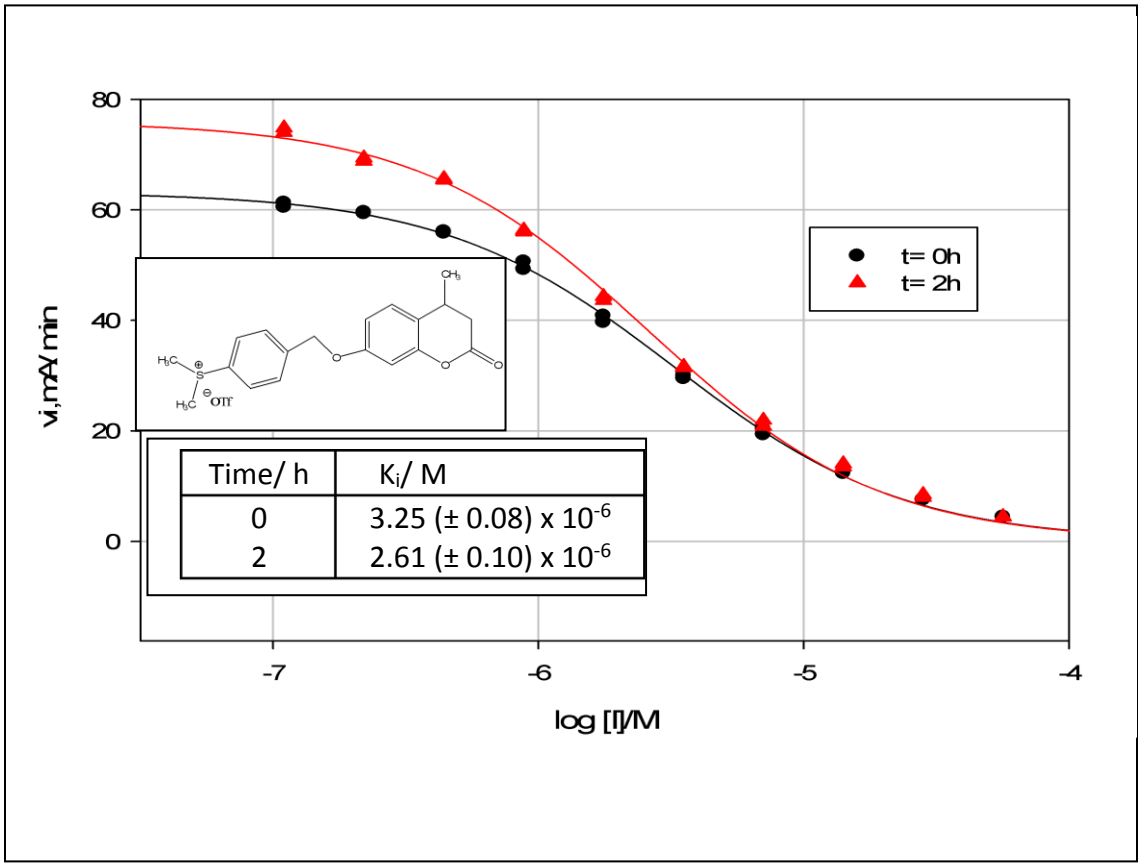

Figure C.1: Dose response curves at t=0h and t=2hrs

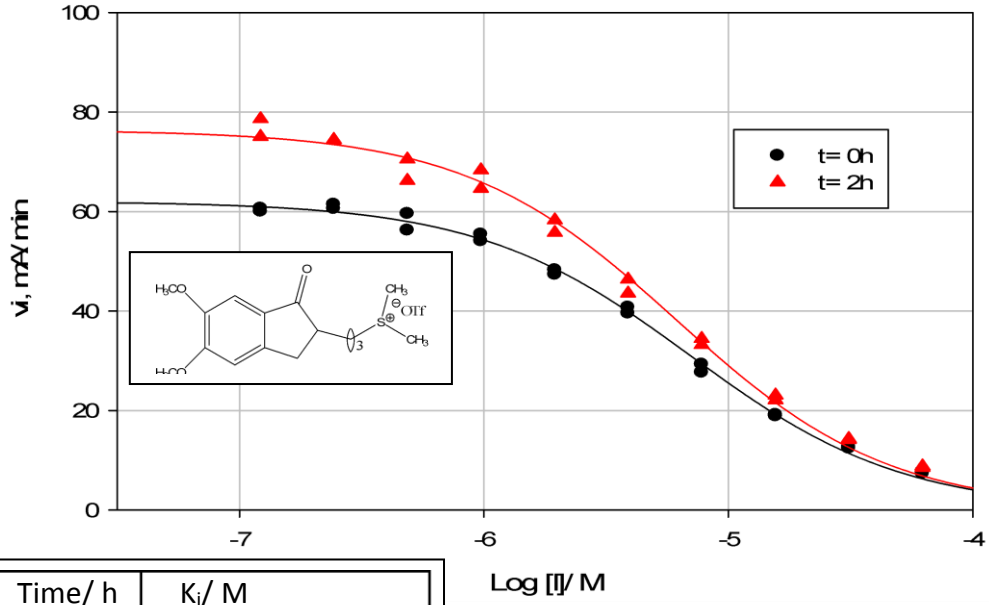

Time/ h	K_i/ M
0	7.00 (± 0.24) x 10^{-6}
2	6.14 (± 0.32) x 10^{-6}

Figure C.2: Dose response curves at t=0h and t=2hrs

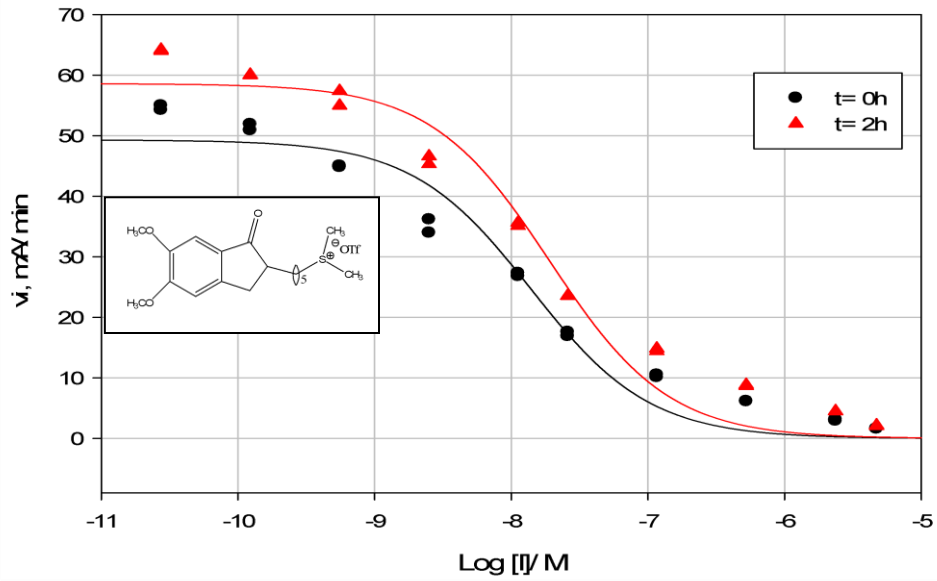

Time/ h	K_i/ M
0	1.40 (± 0.36) x 10^{-8}
2	1.91 (± 0.43) x 10^{-8}

Figure C.3: Dose response curves at t=0h and t=2hrs

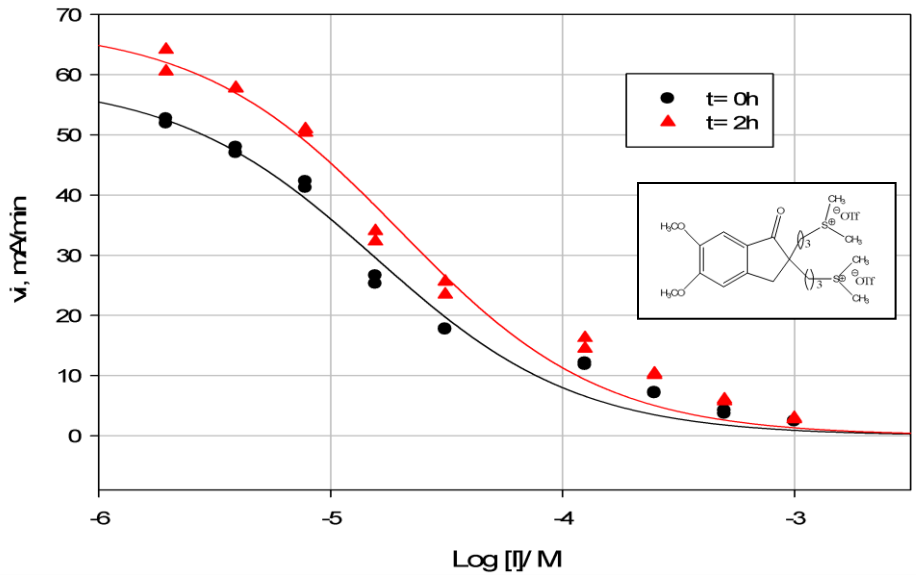

Time/ h	K_i/ M
0	1.57 (± 0.23) x 10^{-5}
2	1.99 (± 0.30) x 10^{-5}

Figure C.4: Dose response curves at t=0h and t=2 hrs

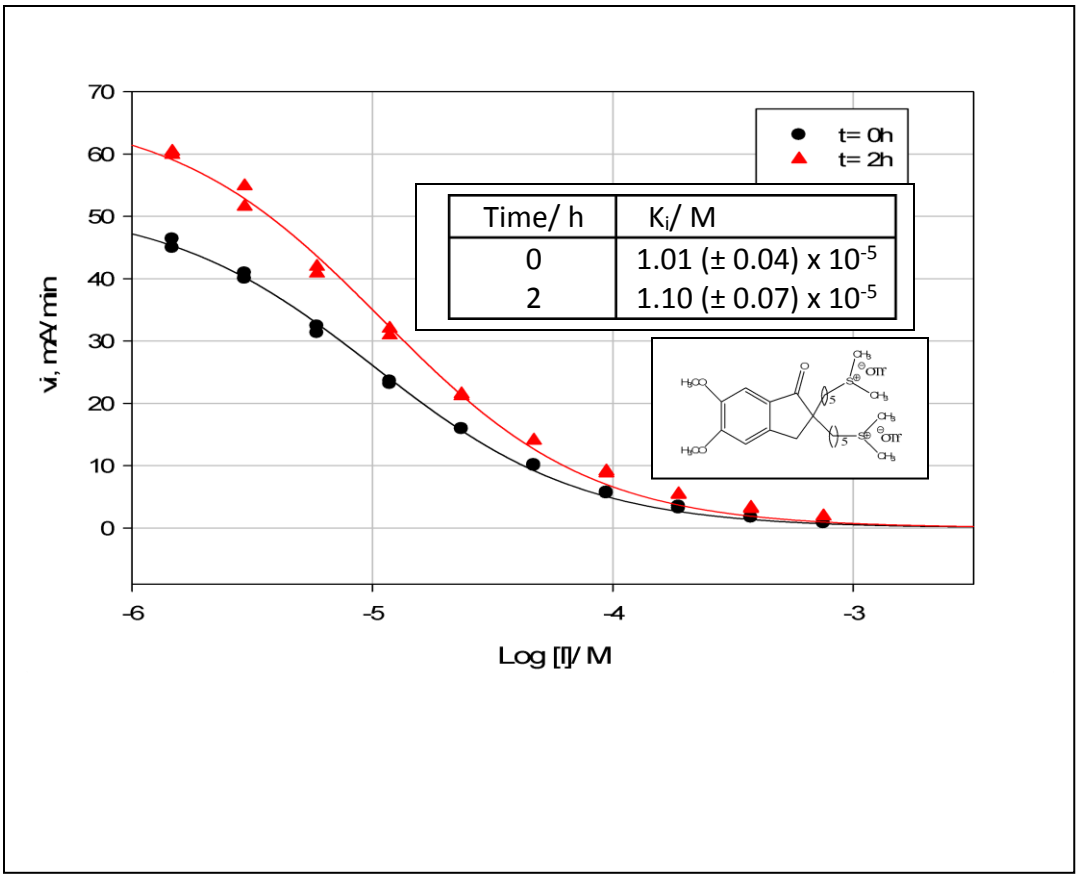

Figure C.5: Dose responses curves at t=0h and t=2hrs

REFERENCES

(1) Jokanović, M. *Toxicology Letters* **2009**, *190*, 107.
(2) Wandhammer, M.; de Koning, M.; van Grol, M.; Loiodice, M.; Saurel, L.; Noort, D.; Goeldner, M.; Nachon, F. *Chemico-Biological Interactions* **2013**, *203*, 19.
(3) Jokanovic, M.; Prostran, M. *Current Medicinal Chemistry* **2009**, *16*, 2177.
(4) Wille, T.; Thiermann, H.; Worek, F. *Arch Toxicol* **2011**, *85*, 193.
(5) Eyer, P. *Toxicol Rev* **2003**, *22*, 165.
(6) Kliachyna, M.; Santoni, G.; Nussbaum, V.; Renou, J.; Sanson, B.; Colletier, J.-P.; Arboléas, M.; Loiodice, M.; Weik, M.; Jean, L.; Renard, P.-Y.; Nachon, F.; Baati, R. *European Journal of Medicinal Chemistry* **2014**, *78*, 455.
(7) Nagao, M.; Takatori, T.; Matsuda, Y.; Nakajima, M.; Iwase, H.; Iwadate, K. *Toxicology and Applied Pharmacology* **1997**, *144*, 198.
(8) Delfino, R. T.; Ribeiro, T. S.; Figueroa-Villar, J. D. *Journal of the Brazilian Chemical Society* **2009**, *20*, 407.
(9) Steinberg, G. M.; Lieske, C. N.; Boldt, R.; Goan, J. C.; Podall, H. E. *Journal of Medicinal Chemistry* **1970**, *13*, 435.
(10) Worek, F.; Thiermann, H.; Szinicz, L.; Eyer, P. *Biochemical Pharmacology* **2004**, *68*, 2237.
(11) Quinn, D. M. *Chemical Reviews* **1987**, *87*, 955.
(12) Velan, B.; Barak, D.; Ariel, N.; Leitner, M.; Bino, T.; Ordentlich, A.; Shafferman, A. *FEBS Letters* **1996**, *395*, 22.
(13) Bourne, Y.; Taylor, P.; Radić, Z.; Marchot, P. *The EMBO Journal* **2003**, *22*, 1.
(14) Aldunate, R.; Casar, J. C.; Brandan, E.; Inestrosa, N. C. *Brain Research Reviews* **2004**, *47*, 96.
(15) Kesharwani, M. K.; Ganguly, B.; Das, A.; Bandyopadhyay, T. *Acta Pharmacologica Sinica* **2010**, *31*, 313.
(16) Berman, H. A.; Becktel, W.; Taylor, P. *Biochemistry* **1981**, *20*, 4803.
(17) Sussman, J. L.; Harel, M.; Silman, I. *Chemico-Biological Interactions* **1993**, *87*, 187.
(18) Harel, M.; Kryger, G.; Rosenberry, T. L.; Mallender, W. D.; Lewis, T.; Fletcher, R. J.; Guss, J. M.; Silman, I.; Sussman, J. L. *Protein Science* **2000**, *9*, 1063.
(19) Sussman, J. L.; Harel, M.; Frolow, F.; Oefner, C.; Goldman, A.; Toker, L.; Silman, I. *Science* **1991**, *253*, 872.
(20) Massoulié, J.; Pezzementi, L.; Bon, S.; Krejci, E.; Vallette, F.-M. *Progress in Neurobiology* **1993**, *41*, 31.
(21) Silman, I. *Trends in Biochemical Sciences* **1976**, *1*, 225.
(22) Ravelli, R. B. G.; Raves, M. L.; Ren, Z.; Bourgeois, D.; Roth, M.; Kroon, J.; Silman, I.; Sussman, J. L. *Acta Crystallographica Section D* **1998**, *54*, 1359.
(23) Dvir, H.; Silman, I.; Harel, M.; Rosenberry, T. L.; Sussman, J. L. *Chemico-Biological Interactions* **2010**, *187*, 10.
(24) GhattyVenkataKrishna, P.; Chavali, N.; Uberbacher, E. *Chem. Pap.* **2013**, *67*, 677.
(25) Krupka, R. M. *Biochimica et Biophysica Acta (BBA) - Enzymology* **1975**, *410*, 120.
(26) Johnson, G.; Moore, S. W. *Current Pharmaceutical Design* **2006**, *12*, 217.
(27) Rosenberry, T. *J Mol Neurosci* **2010**, *40*, 32.
(28) Nair, H. K.; Seravalli, J.; Arbuckle, T.; Quinn, D. M. *Biochemistry* **1994**, *33*, 8566.

(29) Ordentlich, A.; Barak, D.; Kronman, C.; Flashner, Y.; Leitner, M.; Segall, Y.; Ariel, N.; Cohen, S.; Velan, B.; Shafferman, A. *Journal of Biological Chemistry* **1993**, *268*, 17083.
(30) Szegletes, T.; Mallender, W. D.; Thomas, P. J.; Rosenberry, T. L. *Biochemistry* **1999**, *38*, 122.
(31) Čolović, M. B.; Krstić, D. Z.; Lazarević-Pašti, T. D.; Bondžić, A. M.; Vasić, V. M. *Current Neuropharmacology* **2013**, *11*, 315.
(32) Ganesan, K.; Raza, S. K.; Vijayaraghavan, R. *Journal of Pharmacy and Bioallied Sciences* **2010**, *2*, 166.
(33) Scheffel, C.; Thiermann, H.; Worek, F. *Toxicology Letters* **2015**, *232*, 557.
(34) Masson, P.; Nachon, F.; Lockridge, O. *Chemico-Biological Interactions* **2010**, *187*, 157.
(35) MASSON, P.; FORTIER, P.-L.; ALBARET, C.; FROMENT, M.-T.; BARTELS, F. C.; LOCKRIDGE, O. *Aging of di-isopropyl-phosphorylated human butyrylcholinesterase*, 1997; Vol. 327.
(36) Kozer, E.; Mordel, A.; Haim, S. B.; Bulkowstein, M.; Berkovitch, M.; Bentur, Y. *The Journal of Pediatrics* **2005**, *146*, 41.
(37) Segall, Y.; Waysbort, D.; Barak, D.; Ariel, N.; Doctor, B. P.; Grunwald, J.; Ashani, Y. *Biochemistry* **1993**, *32*, 13441.
(38) Carletti, E.; Li, H.; Li, B.; Ekström, F.; Nicolet, Y.; Loiodice, M.; Gillon, E.; Froment, M. T.; Lockridge, O.; Schopfer, L. M.; Masson, P.; Nachon, F. *Journal of the American Chemical Society* **2008**, *130*, 16011.
(39) Saxena, A.; Viragh, C.; Frazier, D. S.; Kovach, I. M.; Maxwell, D. M.; Lockridge, O.; Doctor, B. P. *Biochemistry* **1998**, *37*, 15086.
(40) Berman, H. A.; Decker, M. M. *Journal of Biological Chemistry* **1986**, *261*, 10646.
(41) Schoene, K. *Biochimica et Biophysica Acta (BBA) - Enzymology* **1978**, *525*, 468.
(42) Viragh, C.; Akhmetshin, R.; Kovach, I. M.; Broomfield, C. *Biochemistry* **1997**, *36*, 8243.
(43) Sanson, B.; Nachon, F.; Colletier, J.-P.; Froment, M.-T.; Toker, L.; Greenblatt, H. M.; Sussman, J. L.; Ashani, Y.; Masson, P.; Silman, I.; Weik, M. *Journal of Medicinal Chemistry* **2009**, *52*, 7593.
(44) Saxena, A.; Doctor, B. P.; Maxwell, D. M.; Lenz, D. E.; Radic, Z.; Taylor, P. *Biochemical and Biophysical Research Communications* **1993**, *197*, 343.
(45) Shafferman, A.; Ordentlich, A.; Barak, D.; Stein, D.; Ariel, N.; Velan, B. *Biochemical Journal* **1996**, *318*, 833.
(46) Mercey, G.; Verdelet, T.; Renou, J.; Kliachyna, M.; Baati, R.; Nachon, F.; Jean, L.; Renard, P.-Y. *Accounts of Chemical Research* **2012**, *45*, 756.
(47) Gray, P. J.; Dawson, R. M. *Toxicology and Applied Pharmacology* **1987**, *91*, 140.
(48) Luo, C.; Tong, M.; Chilukuri, N.; Brecht, K.; Maxwell, D. M.; Saxena, A. *Biochemistry* **2007**, *46*, 11771.
(49) Herkert, N. M.; Schulz, S.; Wille, T.; Thiermann, H.; Hatz, R. A.; Worek, F. *Toxicology and Applied Pharmacology* **2011**, *253*, 7.
(50) Luo, C.; Chambers, C.; Yang, Y.; Saxena, A. *Chemico-Biological Interactions* **2010**, *187*, 185.
(51) Carletti, E.; Colletier, J.-P.; Dupeux, F.; Trovaslet, M.; Masson, P.; Nachon, F. *Journal of Medicinal Chemistry* **2010**, *53*, 4002.
(52) Topczewski, J. J.; Quinn, D. M. *Organic Letters* **2013**, *15*, 1084.
(53) van Helden, H. P. M.; Busker, R. W.; Melchers, B. P. C.; Bruijnzeel, P. L. B. *Arch Toxicol* **1996**, *70*, 779.

(54) Ashani, Y.; Bhattacharjee, A. K.; Leader, H.; Saxena, A.; Doctor, B. P. *Biochemical Pharmacology* **2003**, *66*, 191.
(55) Hackley, B. E.; Steinberg, G. M.; Lamb, J. C. *Archives of Biochemistry and Biophysics* **1959**, *80*, 211.
(56) Childs, A. F.; Davies, D. R.; Green, A. L.; Rutland, J. P. *British Journal of Pharmacology and Chemotherapy* **1955**, *10*, 462.
(57) Wilhelm, C. M.; Snider, T. H.; Babin, M. C.; Jett, D. A.; Platoff Jr, G. E.; Yeung, D. T. *Toxicology and Applied Pharmacology* **2014**, *281*, 254.
(58) Ekström, F.; Hörnberg, A.; Artursson, E.; Hammarström, L.-G.; Schneider, G.; Pang, Y.-P. *PLoS ONE* **2009**, *4*, e5957.
(59) Wilson, I. B. *Journal of Biological Chemistry* **1952**, *199*, 113.
(60) Davies, D. R.; Green, A. L. *Biochemical Journal* **1956**, *63*, 529.
(61) Hackley, B. E.; Plapinger, R.; Stolberg, M.; Wagner-Jauregg, T. *Journal of the American Chemical Society* **1955**, *77*, 3651.
(62) Askew, B. M. *British Journal of Pharmacology and Chemotherapy* **1956**, *11*, 417.
(63) de Jong, L. P. A.; Verhagen, M. A. A.; Langenberg, J. P.; Hagedorn, I.; Löffler, M. *Biochemical Pharmacology* **1989**, *38*, 633.
(64) Clement, J.; Hansen, A.; Boulet, C. *Arch Toxicol* **1992**, *66*, 216.
(65) Wilson, I. B.; Ginsburg, S. *Biochimica et Biophysica Acta* **1955**, *18*, 168.
(66) Kliachyna, M.; Santoni, G.; Nussbaum, V.; Renou, J.; Sanson, B.; Colletier, J.-P.; Arboléas, M.; Loiodice, M.; Weik, M.; Jean, L.; Renard, P.-Y.; Nachon, F.; Baati, R. *European Journal of Medicinal Chemistry* **2014**, *78*, 455.
(67) Wei, Z.; Liu, Y.-q.; Zhou, X.-b.; Luo, Y.; Huang, C.-q.; Wang, Y.-a.; Zheng, Z.-b.; Li, S. *Bioorganic & Medicinal Chemistry Letters* **2014**, *24*, 5743.
(68) Radić, Z.; Dale, T.; Kovarik, Z.; Berend, S.; Garcia, E.; Zhang, L.; Amitai, G.; Green, C.; Radić, B.; Duggan, B. M.; Ajami, D.; Rebek, J.; Taylor, P. *The Biochemical journal* **2013**, *450*, 231.
(69) de Koning, M. C.; van Grol, M.; Noort, D. *Toxicology Letters* **2011**, *206*, 54.
(70) Askew, B. M. *British Journal of Pharmacology and Chemotherapy* **1957**, *12*, 340.
(71) O'Leary, J. F.; Kunkel, A. M.; Jones, A. H. *Journal of Pharmacology and Experimental Therapeutics* **1961**, *132*, 50.
(72) Harvey, B.; Sellers, D. J.; Watts, P. *Biochemical Pharmacology* **1984**, *33*, 3499.
(73) Wolthuis, O. L.; Cohen, E. M. *Biochemical Pharmacology* **1967**, *16*, 361.
(74) Shih, T.-M. *Arch Toxicol* **1993**, *67*, 637.
(75) Worek, F.; Wille, T.; Koller, M.; Thiermann, H. *Chemico-Biological Interactions* **2013**, *203*, 125.
(76) Worek, F.; Reiter, G.; Eyer, P.; Szinicz, L. *Arch Toxicol* **2002**, *76*, 523.
(77) Poziomek, E. J.; Hackley, B. E.; Steinberg, G. M. *The Journal of Organic Chemistry* **1958**, *23*, 714.
(78) Heilbronn, E.; Tolagen, B. *Biochemical Pharmacology* **1965**, *14*, 73.
(79) Inns, R. H.; Leadbeater, L. *Journal of Pharmacy and Pharmacology* **1983**, *35*, 427.
(80) Herkenhoff, S.; Szinicz, L.; Rastogi, V. K.; Cheng, T. C.; DeFrank, J. J.; Worek, F. *Arch Toxicol* **2004**, *78*, 338.
(81) Hackley Jr, B. E.; Steinberg, G. M.; Lamb, J. C. *Archives of Biochemistry and Biophysics* **1959**, *80*, 211.
(82) Kepner, L. A.; Wolthuis, O. L. *European Journal of Pharmacology* **1978**, *48*, 377.

(83) Kušic, R.; Boškovic, B.; Vojvodić, V.; Jovanović, D. *Fundamental and Applied Toxicology* **1985**, *5*, S89.
(84) Klimmek, R.; Eyer, P. *Arch Toxicol* **1986**, *59*, 272.
(85) Koplovitz, I.; Stewart, J. R. *Toxicology Letters* **1994**, *70*, 269.
(86) Wolthuis, O. L.; Clason-Van Der Wiel, H. J.; Visser, R. P. L. S. *European Journal of Pharmacology* **1976**, *39*, 417.
(87) Eyer, P.; Hagedorn, I.; Ladstetter, B. *Arch Toxicol* **1988**, *62*, 224.
(88) Eyer, P.; Hagedorn, I.; Klimmek, R.; Lippstreu, P.; Löffler, M.; Oldiges, H.; Spöhrer, U.; Steidl, I.; Szinicz, L.; Worek, F. *Arch Toxicol* **1992**, *66*, 603.
(89) Kuca, K.; Jun, D.; Cabal, J.; Musilova, L. *Basic & Clinical Pharmacology & Toxicology* **2007**, *101*, 25.
(90) Alberts, P. *European Journal of Pharmacology* **1990**, *184*, 191.
(91) Melchers, B. P. C.; Philippens, I. H. C. H. M.; Wolthuis, O. L. *Pharmacology Biochemistry and Behavior* **1994**, *49*, 781.
(92) Worek, F.; Thiermann, H. *Chemico-Biological Interactions* **2011**, *194*, 91.
(93) Kuca, K.; Jun, D. *Journal of Medical Toxicology* **2006**, *2*, 141.
(94) Kuca, K.; Cabal, J.; Kassa, J. *Journal of Toxicology and Environmental Health, Part A* **2005**, *68*, 677.
(95) Kuca, K.; Cabal, J.; Jun, D.; Koleckar, V. *Toxicology Mechanisms & Methods* **2008**, *18*, 329.
(96) Horn, G.; Wille, T.; Musilek, K.; Kuca, K.; Thiermann, H.; Worek, F. *Arch Toxicol* **2015**, *89*, 405.
(97) Berends, F.; Posthumus, C. H.; Sluỳs, I. v. d.; Deierkauf, F. A. *Biochimica et Biophysica Acta* **1959**, *34*, 576.
(98) Blumbergs, P.; Ash, A. B.; Daniher, F. A.; Stevens, C. L.; Michel, H. O.; Hackley, B. E.; Epstein, J. *The Journal of Organic Chemistry* **1969**, *34*, 4065.
(99) Qian, N.; Kovach, I. M. *FEBS Letters* **1993**, *336*, 263.
(100) Radić, Z.; Kalisiak, J.; Fokin, V. V.; Sharpless, K. B.; Taylor, P. *Chemico-Biological Interactions* **2010**, *187*, 163.
(101) Štalc, A.; Šentjurc, M. *Biochemical Pharmacology* **1990**, *40*, 2511.
(102) Dawson, R. M.; Crone, H. D.; Bladen, M. P.; Poretski, M. *Neurochemistry International* **1981**, *3*, 335.
(103) Puu, G. *Biochemical Pharmacology* **1988**, *37*, 969.
(104) Dawson, R. M. *Neuroscience Letters* **1989**, *100*, 227.
(105) Harris, L. W.; Heyl, W. C.; Stitcher, D. L.; Broomfield, C. A. *Biochemical Pharmacology* **1978**, *27*, 757.
(106) Johnson, J. L.; Cusack, B.; Hughes, T. F.; McCullough, E. H.; Fauq, A.; Romanovskis, P.; Spatola, A. F.; Rosenberry, T. L. *Journal of Biological Chemistry* **2003**, *278*, 38948.
(107) Topczewski, J. J.; Lodge, A. M.; Yasapala, S. N.; Payne, M. K.; Keshavarzi, P. M.; Quinn, D. M. *Bioorganic & Medicinal Chemistry Letters* **2013**, *23*, 5786.
(108) Marrs, T.; Rice, P.; Vale, J. A. *Toxicol Rev* **2006**, *25*, 297.
(109) Jokanović, M.; Maksimović, M.; Kilibarda, V.; Jovanović, D.; Savić, D. *Toxicology Letters* **1996**, *85*, 35.
(110) Hoskovcová, M.; Halámek, E.; Kobliha, Z.; Tušarová, I. *Toxicology mechanisms and methods* **2010**, *20*, 223.

(111) Ashani, Y.; Radic, Z.; Tsigelny, I.; Vellom, D. C.; Pickering, N. A.; Quinn, D. M.; Doctor, B. P.; Taylor, P. *Journal of Biological Chemistry* **1995**, *270*, 6370.
(112) Ordentlich, A.; Kronman, C.; Barak, D.; Stein, D.; Ariel, N.; Marcus, D.; Velan, B.; Shafferman, A. *FEBS Letters* **1993**, *334*, 215.
(113) Abass Askar, K.; Caleb Kudi, A.; John Moody, A. *The Journal of Toxicological Sciences* **2011**, *36*, 237.
(114) Costa, M. D.; Freitas, M. L.; Soares, F. A. A.; Carratu, V. S.; Brandão, R. *Toxicology in Vitro* **2011**, *25*, 2120.
(115) Bodor, N.; Shek, E.; Higuchi, T. *Journal of Medicinal Chemistry* **1976**, *19*, 102.
(116) Ellman, G. L.; Courtney, K. D.; Andres, V.; Featherstone, R. M. *Biochemical pharmacology* **1961**, *7*, 88.
(117) Rajapurkar, M. V.; Koelle, G. B.; Smart, P. *Journal of Pharmacology and Experimental Therapeutics* **1958**, *123*, 247.
(118) Skovira, J. W.; O'Donnell, J. C.; Koplovitz, I.; Kan, R. K.; McDonough, J. H.; Shih, T.-M. *Chemico-Biological Interactions* **2010**, *187*, 318.
(119) Fedorenko, V.; Genilloud, O.; Horbal, L.; Marcone, G. L.; Marinelli, F.; Paitan, Y.; Ron, E. Z. *BioMed Research International* **2015**, *2015*, 591349.
(120) Worthington, R. J.; Melander, C. *The Journal of Organic Chemistry* **2013**, *78*, 4207.
(121) Bassetti, M.; Merelli, M.; Temperoni, C.; Astilean, A. *Annals of Clinical Microbiology and Antimicrobials* **2013**, *12*, 1.
(122) Johnson, G.; Moore, S. *Current pharmaceutical design* **2006**, *12*, 217.
(123) Mallender, W. D.; Szegletes, T.; Rosenberry, T. L. *Biochemistry* **2000**, *39*, 7753.
(124) Doctor, B. P.; Taylor, P.; Quinn, D. M.; Rotundo, R. L.; Gentry, M. K. *Structure and function of cholinesterases and related proteins*; Springer Science & Business Media, 2013.
(125) Millard, C. B.; Kryger, G.; Ordentlich, A.; Greenblatt, H. M.; Harel, M.; Raves, M. L.; Segall, Y.; Barak, D.; Shafferman, A.; Silman, I. *Biochemistry* **1999**, *38*, 7032.